

**Pacific Northwest
National Laboratory**

Operated by Battelle for the
U.S. Department of Energy

**Treatability Study of In Situ
Technologies for Remediation of
Hexavalent Chromium in Groundwater
at the Puchack Well Field Superfund
Site, New Jersey**

V. R. Vermeul
J. E. Szecsody
M. J. Truex
C. A. Burns
D. C. Girvin
J. L. Phillips
B. J. Devary
A. E. Fischer
S-M. W. Li

October 2006



Prepared for the U.S. Department of Energy
under Contract DE-AC05-76RL01830

DISCLAIMER

This report was prepared as an account of work sponsored by an agency of the United States Government. Neither the United States Government nor any agency thereof, nor Battelle Memorial Institute, nor any of their employees, makes **any warranty, express or implied, or assumes any legal liability or responsibility for the accuracy, completeness, or usefulness of any information, apparatus, product, or process disclosed, or represents that its use would not infringe privately owned rights.** Reference herein to any specific commercial product, process, or service by trade name, trademark, manufacturer, or otherwise does not necessarily constitute or imply its endorsement, recommendation, or favoring by the United States Government or any agency thereof, or Battelle Memorial Institute. The views and opinions of authors expressed herein do not necessarily state or reflect those of the United States Government or any agency thereof.

PACIFIC NORTHWEST NATIONAL LABORATORY
operated by
BATTELLE
for the
UNITED STATES DEPARTMENT OF ENERGY
under Contract DE-AC05-76RL01830

Printed in the United States of America

Available to DOE and DOE contractors from the
Office of Scientific and Technical Information,
P.O. Box 62, Oak Ridge, TN 37831-0062;
ph: (865) 576-8401
fax: (865) 576-5728
email: reports@adonis.osti.gov

Available to the public from the National Technical Information Service,
U.S. Department of Commerce, 5285 Port Royal Rd., Springfield, VA 22161
ph: (800) 553-6847
fax: (703) 605-6900
email: orders@ntis.fedworld.gov
online ordering: <http://www.ntis.gov/ordering.htm>



This document was printed on recycled paper.

**Treatability Study of In Situ Technologies for
Remediation of Hexavalent Chromium in Groundwater
at the Puchack Well Field Superfund Site, New Jersey**

V. R. Vermeul
J. E. Szecsody
M. J. Truex
C. A. Burns
D. C. Girvin
J. L. Phillips
B. J. Devary
A. E. Fischer
S-M. W. Li

October 2006

Prepared for
the U.S. Department of Energy
under Contract DE-AC05-76RL01830

Pacific Northwest National Laboratory
Richland, Washington 99352

Summary

This treatability study was conducted by Pacific Northwest National Laboratory (PNNL), at the request of the U. S. Environmental Protection Agency (EPA) Region 2, to evaluate the feasibility of using in situ treatment technologies for chromate reduction and immobilization at the Puchack Well Field Superfund site in Pennsauken Township, New Jersey. In addition to in situ reductive treatments, which included the evaluation of both abiotic and biotic reduction of Puchack aquifer sediments, natural attenuation mechanisms were evaluated (i.e., chromate adsorption and reduction). Chromate exhibited typical anionic adsorption behavior, with greater adsorption at lower pH, at lower chromate concentration, and at lower concentrations of other competing anions. Competitive anions, sulfate in particular (at 50 mg/L), suppressed chromate adsorption by up to 50%. Chromate adsorption was not influenced by inorganic colloids.

Results from long-term experiments indicate that natural chromate reduction occurs in Puchack sediments. Sediment composites of seven different Puchack aquifer units showed either no reduction or very slow chromate reduction (0.3 to 3.1 year half-life). However, three selected sediments showed much more rapid reduction (half lives: 49 h to ~3000 h). Although the spatial variability in natural reductive capacity appears to be relatively large, experimental results indicate that chromate reduction can remain viable even in the presence of dissolved oxygen. Most sediments that showed some natural reduction of chromate had very small reductive capacities (average $2.76 \pm 1.02 \mu\text{mol/g}$), but one sediment had a large reductive capacity ($636 \mu\text{mol/g}$) with considerable amorphous ferrous iron and 2.25% organic carbon (i.e., contained clays, iron oxides, and possibly lignite). There was wide variability in the iron oxide content of Puchack sediments.

Results from chemical reduction experiments on Puchack sediments showed a considerable increase in the reductive capacity (average $60.2 \pm 25.6 \mu\text{mol/g}$, maximum of $390 \mu\text{mol/g}$), indicating that reductive treatment may be an effective approach when deployed at the field scale. The average measured reductive capacity, assuming typical site groundwater chemistry conditions, would result in a treatment zone longevity of 360 pore volumes or 39 years of treatment for a uniform treatment zone 40 ft wide and an average groundwater velocity of 1 ft/d. It was also shown that reductive capacity is a function of pH. The capacity of the sediment column to consume 2.0 mg/L chromate and 8.4 mg/L dissolved oxygen (saturated conditions) was estimated to be 310 pore volumes at pH 4.5 and 480 pore volumes at pH 7.0. Chromate reduction/immobilization was shown to be effective in four long-term column studies at pH 4.5 to 7.0. Chromate was removed in all columns initially, then partial chromate breakthrough occurred by 170 pore volumes for pH values of 4.5 and 5.3, 280 pore volumes at pH 6.2, and 340 pore volumes at pH 7.0. There was no evidence of mobile Cr(III) species at any pH. Iron (II) mobility increased under acidic pH with 3.6 to 10.5% of the Fe(II) mobilized at pH 4.5 compared with 0.1 to 0.35% at pH 7.0. Dithionite reduction of sediment, therefore, produced mainly immobile Fe(II) species in Puchack sediments; likely reduced structural iron in clays or mixed Fe(II/III) oxides. Trichloroethylene (TCE) contamination in portions of the Puchack aquifer system are also likely to be degraded by dithionite-reduced sediment and possibly by naturally reduced sediment with a high reductive capacity. Although TCE degradation was not investigated in Puchack sediments, dithionite reduction of other natural sediments resulted in TCE degradation to chloroacetylene, then acetylene, then ethylene, then ethane, so avoids toxic biodegradation intermediates cis-DCE and vinyl chloride.

Biostimulation of Puchack sediments would be difficult at the field scale, as iron-reducing bacteria were present in sediments at very low population densities of < 20 cells per gram of sediment and sulfate-reducing bacteria were only detected in one sediment sample. In contrast, aquifers in eastern and western Washington show population densities of 10^2 to 10^4 and greater, and are sufficient for biotic or coupled abiotic/biotic degradation.

In summary, the combination of natural chromate reduction (natural attenuation) and abiotic reduction (in situ redox manipulation treatment with dithionite) of specific aquifer zones shows promise as an effective remedy for chromate contaminated groundwater at the Puchack Well Field Site. Although these studies confirm the presence of mechanisms attributed to the natural attenuation of chromate in the Puchack subsurface environment, the field-scale effect of these mechanisms must be better quantified to determine the suitability of monitored natural attenuation (MNA) as a remedial alternative. Based on the EPA framework for the application of MNA (OSWER Directive 9200.4-17P), both bench and field-scale data should be used when evaluating the site-specific suitability of MNA as a remedy. In addition to chromate trend monitoring at the site, numerical groundwater flow and reactive transport models could be developed that incorporate the rate and treatment capacity data resulting from these studies. These models could be used to make predictions of long-term field-scale attenuation of the chromate plume and expected impact at potential receptor locations.

Acronyms

1,1-DCE	1,1-dichloroethene
1,1,1-TCA	1,1,1-trichloroethane
1,2-DCA	1,2-dichloroethane
1-D	one dimensional
ASTM	American Society for Testing and Materials
CDM	Camp Dresser and McKee
CERCLA	<i>Comprehensive Environmental Response, Compensation, and Liability Act</i>
DC-1	deep composite 1
DCB	dithionite-citrate-bicarbonate
DCE	dichloroethylene
DOT	U.S. Department of Transportation
DPC	1,5 diphenylcarbazide
EPA	U.S. Environmental Protection Agency
Fe(III)NTA	ferric nitrilotriacetic acetate
FTIR	Fourrier Transform Infra-Red Spectrometer
H ₂ S	hydrogen sulfide
ICP-MS	inductively coupled plasma/mass spectrometry
IR	infrared
IRB	iron-reducing bacteria
ISRM	in situ redox manipulation
MCL	maximum contaminant level
MNA	monitored natural attenuation
MPN	most probable number
NDMA	N-nitrosodimethylamine
NJDEP	New Jersey Department of Environmental Protection
NOM	natural organic matter
NPL	National Priorities List
OP	operable unit
PCE	tetrachloroethylene
PNNL	Pacific Northwest National Laboratory
PRM	Potomac-Raritan-Magothy
r _{sw}	soil-to-water ratio
SGL Chrome	SGL Modem Hard Chrome Service
SRB	sulfate-reducing bacteria
TCE	trichloroethylene
USGS	U.S. Geological Survey
VOC	volatile organic compound
XRD	x-ray diffraction

Contents

Summary	iii
Acronyms	v
1.0 Introduction	1.1
1.1 Site Description	1.1
1.2 Site History	1.2
1.3 Site Hydrogeology.....	1.3
1.4 Treatability Study Objectives	1.5
2.0 Background	2.1
2.1 Chromium Transport and Immobilization in the Subsurface	2.1
2.1.1 Cr Speciation.....	2.1
2.1.2 Cr(VI) Reduction and Precipitation.....	2.2
2.1.3 Chromium Adsorption.....	2.3
2.2 Abiotic Technology Description	2.4
2.2.1 Iron Reduction Mechanism	2.4
2.2.2 Sediment Oxidation and Chromate Reduction Mechanism	2.5
2.2.3 Trichloroethylene Reduction Mechanism	2.6
2.3 Biotic Technology Description	2.9
2.3.1 Direct Cr(VI) Reduction Approach	2.10
2.3.2 In Situ Reaction Zone Approach	2.10
2.3.3 Sulfate Reduction Process	2.11
2.3.4 Biotic Iron Reduction Process.....	2.11
3.0 Experimental Methods.....	3.1
3.1 Sampling	3.1
3.2 Sediment Physical Properties and Groundwater Analysis.....	3.1
3.2.1 Groundwater Analyses	3.1
3.3 Column Experiments.....	3.2
3.3.1 Sediment Reduction by Dithionite.....	3.2
3.3.2 Sediment Oxidation with Dissolved Oxygen.....	3.3
3.3.3 Chromium Transport in Untreated Sediments	3.4
3.3.4 Chromate Transport in Reduced Sediments	3.4
3.4 Batch Experiments	3.4
3.4.1 Chromate Adsorption Edge	3.4
3.4.2 Chromate Adsorption Isotherm.....	3.5
3.4.3 Natural Attenuation Studies	3.5
3.4.4 Iron Extractions of Treated and Untreated Sediments	3.6

3.5	Biotic Studies.....	3.6
3.5.1	Sediments	3.6
3.5.2	Microbial Batch Tests.....	3.6
4.0	Results.....	4.1
4.1	Sediment and Aqueous Sample Collection.....	4.1
4.1.1	Sediment Sample Collection	4.1
4.1.2	Sediment Physical Property Analysis.....	4.1
4.1.3	Groundwater Chemistry Analysis.....	4.9
4.2	Natural Attenuation of Chromate - Adsorption.....	4.12
4.2.1	Influence of Time and Solution Composition on Chromate Adsorption	4.12
4.2.2	Influence of pH on Chromate Adsorption	4.14
4.2.3	Adsorption Isotherm – Influence of Chromate Concentration on Adsorption	4.15
4.2.4	Influence of Sulfate on Chromate Adsorption	4.16
4.2.5	Influence of Colloids on Chromate Adsorption	4.18
4.3	Natural Attenuation of Chromate – Reduction/Immobilization by Natural Aquifer Sediments.....	4.18
4.3.1	Rate of Chromate Reduction by Natural Aquifer Sediments.....	4.18
4.3.2	Influence of Dissolved Oxygen on the Natural Chromate Reduction Rate	4.23
4.3.3	Influence of Natural Organic Matter on the Natural Chromate Reduction Rate	4.26
4.3.4	Redox Reactive Phases in Natural Puchack Sediments	4.27
4.4	Chromate Reactive Transport in Natural Puchack Sediments	4.30
4.5	Chemical Reduction of Puchack Sediments	4.32
4.5.1	Barrier Capacity and Longevity	4.32
4.5.2	Redox Reactive Phases Produced with Dithionite Reduction	4.35
4.5.3	Trace Metal Mobilization with Dithionite Reduction	4.36
4.6	Chromate Immobilization and Changes in Other Metals/Solutes in Dithionite- Reduced Sediments	4.38
4.6.1	Chromate Transport and Reduction	4.38
4.6.2	Trace Metal Mobility Changes During Reduced Sediment Oxidation	4.40
4.7	Biostimulation	4.47
5.0	Conclusions	5.1
5.1	Chromate Adsorption	5.1
5.2	Chromate Reduction in Natural Puchack Sediments	5.1
5.3	Chromate Reactivity in Dithionite-Reduced Sediments	5.2
5.4	Biostimulation of Iron-Reducing and Sulfate-Reducing Bacteria	5.3
5.5	Recommended Future Studies.....	5.4
6.0	References	6.1
	Appendix A – Physical Characterization of Puchack Sediments	A.1
	Appendix B – Chromate Adsorption to Natural Sediments.....	B.1

Appendix C – Chromate Reduction by Natural Attenuation	C.1
Appendix D – Sediment Reductive Capacity	D.1
Appendix E – Chromate Transport and Reduction	E.1
Appendix F – X-Ray Diffraction Spectra	F.1
Appendix G – Growth Media for Biotic Studies	G.1

Figures

1.1 Puchack Site with Approximate Location of Aquifer Chromate Plume	1.2
1.2 Five-Layer and Subdivided Interpretations of the Hydrostratigraphic Framework of the Potomac-Paritan-Magothy Aquifer System, Puchack Well Field Superfund Site, Pennsauken Township, New Jersey	1.4
2.1 Stability of Cr(VI) and Cr(III) Phases at Equilibrium at Different pH and Eh	2.1
2.2 Cr(III) Aqueous Speciation at Equilibrium without Additional Organic or Inorganic Ligands.....	2.1
2.3 Solubility of $(\text{Cr}, \text{Fe})(\text{OH})_3$ Precipitates with a) 1% Cr, and b) 69% Cr, Relative to Theoretical $\text{Cr}(\text{OH})_3$	2.2
2.4 Rate of Chromium Reduction by Aqueous Ferrous Iron as a Function of pH.....	2.3
3.1 Fraction Collection of Column Effluent into Anaerobic Vials	3.2
3.2 Sediment Column Oxidation System with Automated Calibration of Oxygen Electrodes.....	3.4
4.1 Sieve Analysis of Sediment from 162.5-ft Depth of MW-37S-C, Aquifer Unit C2AI	4.7
4.2 Sieve Analysis of Sediment from 171.5-ft Depth of MW-37S-F, Aquifer Unit C2AI.....	4.7
4.3 Sieve Analysis of Sediment from 190.5-ft Depth of MW-37S-G,.....	4.7
4.4 Time to Reach a Stable pH as Chromate Adsorption Equilibrium is Approached in a Suspension of the DC-1 Sediment after the Initial pH Adjustment to Approximately pH 8 and 4 and Addition of Chromate	4.14
4.5 Approach to Chromate Adsorption Equilibrium in Distilled Water and Synthetic Groundwater Suspensions of Deep Composite 1	4.14
4.6 Dependence of Chromate Adsorption on pH in Deionized Water.....	4.15
4.7 Chromate Adsorption Edge in Puchack Groundwater for Deep Composite 2 using Two Contact Times.....	4.15
4.8 Chromate Adsorption Isotherm for Deep Composite 2 in Synthetic Puchack Groundwater after 24-Hour Contact Time	4.16
4.9 Evaluation of Potential Interference of SO_4 with the DPC Analysis of 10 ppm CrO_4 in Distilled Water	4.17
4.10 Decrease in Chromate Adsorption with an Increase in Sulfate Concentration at pH 6.3.....	4.17
4.11 Reduction in the Chromate Distribution Coefficient (K_d) on Deep Composite 2 with Increasing Sulfate Concentration Corresponding to the Decline in the Percent Adsorption Shown in Figure 4.9	4.17

4.12 Evaluation of Chromate Adsorption to Colloids present in Deep Composite 1 Sediments using a Sequence of Membrane Filters to Separate Phases at the Termination of a 24-Hour Adsorption Experiment in Distilled Water and Synthetic Groundwater at pH 4 and 8.....	4.18
4.13 Reduction of Chromate by Selected Natural Aquifer Sediments.....	4.19
4.14 Pseudo-First Order Model Fits to Reduction of Chromate by Selected Natural Aquifer Sediments.....	4.20
4.15 Reduction of Chromate Under Anoxic Conditions by Untreated Sediment Composites of Wells MW 36 and 37.....	4.24
4.16 Comparison of Chromate Reduction for Natural Sediments with Oxygen: a) NRS-1, and b) NRS-3	4.25
4.17 Long-Term Chromate Reduction by a Reduced Sediment Column in which 2 mg/L Chromate, 8.4 mg/L O ₂ , and 60 mg/L Nitrate was Injected	4.26
4.18 FTIR Spectrum of the Base Soluble Components of NRS-1	4.27
4.19 Chromate Reduction Rate a) NRS-1 RSW 0.37 with 4.8388 mg/L Chromate and b) NRS-1 Base/Heat Treated	4.27
4.20 Evaluation of Chromate Adsorption at pH 4.8 and 3.85 During Reactive Transport in a 1-D Column Packed with a Shallow Sediment Composite	4.30
4.21 Evaluation of Chromate Adsorption at pH 7 during Reactive Transport in a 1-D Column Packed with a Shallow Sediment Composite	4.31
4.22 Comparison of K _d vs. pH for Deep Composite 2 Sediment from Batch Experiments to the K _d Derived from 1-D Column Experiments with the Shallow Composite Sediment	4.31
4.23 Oxidation of a Reduced Sediment Column with Dissolved Oxygen in Water	4.34
4.24 Chromate Transport in Reduced Sediment with 8.4 mg/L O ₂ and 2 mg/L CrO ₄ ⁻ at (a) pH 4.5, (b) pH 5.3, (c) pH 6.2, and (d) pH 7.0	4.39
4.25 Amount of Ferrous Iron in the Effluent of the Chromate Transport Experiments using Reduced Sediments at pH a) 4.5, b) 5.3, c) 6.2, and d) 7.0	4.40
4.26 Amount of Total Iron in Column Effluent during Injection of Puchack Oxic Groundwater into Reduced Sediments.....	4.41
4.27 Mobility of (a) Mercury and (b) Arsenic as a Function of Pore Volume during Sediment Oxidation at Different pH.....	4.47

Tables

4.1	Aquifer Core Samples for Well MW-36	4.2
4.2	Aquifer Core Samples for Well MW-37	4.3
4.3	Aquifer Core Samples for Well D-1	4.4
4.4	Aquifer Core Samples for Well D-2	4.5
4.5	Sediment Core General Physical Properties	4.6
4.6	List of Composite Sediments.....	4.8
4.7	Aqueous Samples Collected During Well Drilling.....	4.10
4.8	Field and Laboratory Analysis of Aqueous Samples.....	4.11
4.9	Water Quality Data from Three Monitoring Wells at the Puchack Site Sampled between September 2000 and February 2001	4.13
4.10	Composition of Synthetic Groundwater Used in Adsorption Experiments	4.13
4.11	Sediments Used in Studies of Chromate Reduction by Natural Aquifer Sediments	4.19
4.12	Natural Attenuation Pseudo-First Order Rates of Chromate Observed in Experiments	4.21
4.13	Carbon Analysis of Selected Sediments	4.21
4.14	Natural and Dithionite-Reduced Sediment Reductive Capacity and Iron Phases.....	4.22
4.15	Natural and Dithionite-Reduced Sediment Reductive Capacity and Iron Speciation	4.33
4.16	Metals Mobility during Sediment Reduction in Columns.....	4.37
4.17	Hg Mobility during Reduction and Oxidation	4.38
4.18	Metals Mobility during Sediment Oxidation in Columns at pH 4.5	4.42
4.19	Metals Mobility during Sediment Reduction in Columns at pH 5.3	4.43
4.20.	Metals Mobility during Sediment Oxidation in Columns at pH 6.2	4.44
4.21	Metal Mobility during Sediment Oxidation at pH 7.0.....	4.45
4.22	Iron Mobility during Reduced Sediment Oxidation	4.46
4.23	Puchack Sediment Cores Selected for Microbiology Studies	4.48
4.24	Summary of Iron-Reducing Bacteria Enumeration and Enrichment.....	4.49
4.25	Summary of Sulfate-Reducing Bacteria Enumeration and Enrichment	4.49
5.1	Influence of pH on Chromate Immobilization in Reduced Sediments	5.3

1.0 Introduction

This report describes results from bench scale laboratory experiments documented in a test plan entitled *Bench Scale Test Plan: Treatability Study of In Situ Technologies for the Remediation of Hexavalent Chromium in Groundwater* (Vermeul et al. 2004). These treatability studies were conducted using sediment and groundwater samples collected from the Puchack Well Field Superfund Site in Pennsauken Township, New Jersey. Results are reported for specific laboratory experiments that were conducted to evaluate mechanisms that could contribute to attenuation of the chromate plume and potential technologies for the remediation of chromate contaminated groundwater. Three general categories of technologies that were evaluated include: a) abiotic reduction of ferric oxides in sediments to create a reduced zone (in situ redox manipulation or ISRM), b) biostimulation (nutrient injection) of the natural microbial population to create a reduced zone, and c) natural attenuation of the chromate plume.

1.1 Site Description

The Puchack Well Field Superfund Site is located in a commercial/industrial and residential neighborhood of Pennsauken Township, Camden County, New Jersey. Because of the nature and complexity of the site, involving a large contaminant plume containing chromium and numerous volatile organic compounds, the U.S. Environmental Protection Agency (EPA) is handling the investigation and cleanup in two distinct phases, called operable units. Operable Unit 1 (OU1) deals solely with the investigation and cleanup of contaminated groundwater at the site. Operable Unit 2 (OU2) deals with the investigation and clean up of the source areas that contributed to the groundwater contamination.

Puchack Well Field Superfund Site OU1 (Puchack OU1, Figure 1.1) is defined by the location of the chromium contamination in groundwater, which is defined by the 100 microgram per liter ($\mu\text{g}/\text{L}$) chromium isoconcentration line. The 100 $\mu\text{g}/\text{L}$ chromium isoconcentration line was chosen because this is the EPA and the New Jersey Department of Environmental Protection (NJDEP) maximum contaminant level (MCL) for chromium. Since the shape of the chromium 100 $\mu\text{g}/\text{L}$ isoconcentration line may change over time in response to groundwater flow and other geochemical factors, the boundaries of OU1 may shift.

The Puchack Well Field is located within OU1 and consists of six public supply wells that are owned and were operated by the City of Camden. The six public water supply wells are referred to as Nos. 1, 2, 3 (also referred to as 3A), 5 (also referred to as 5A), 6, and 7. During operation, the six wells had a combined capacity of six million gallons per day (mgd). The area surrounding the well field is used for residential, commercial, and industrial purposes. Several hundred single and multi-family residential buildings, commercial buildings, and industrial facilities are located within a 2-mile radius of the site. One section of the Pennsauken Industrial Park is located approximately 0.5 mile to the northeast of the site while another section of the industrial park is located approximately 0.25 mile to the southwest. Conrail railroad tracks are situated approximately 500 ft to the northeast and southeast of the well field, and the tollgate for the Betsy Ross Bridge (Route 90) is located approximately 250 ft to the east.

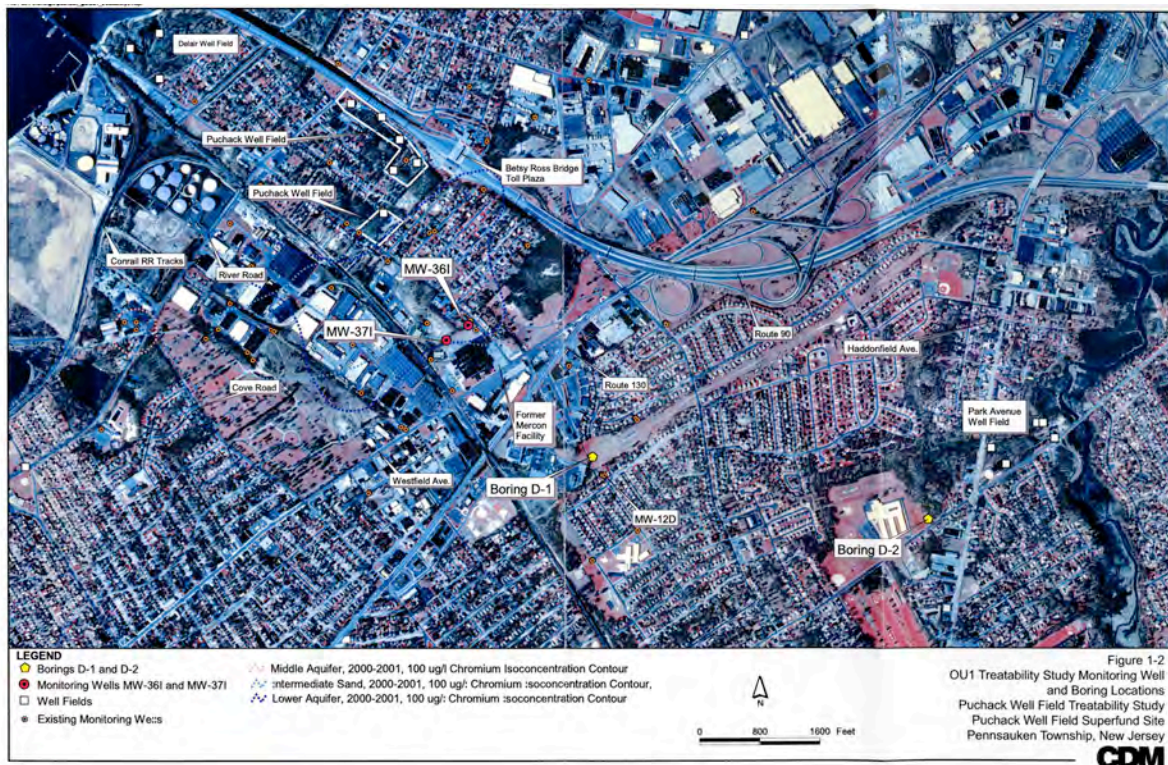


Figure 1.1. Puchack Site with Approximate Location of Aquifer Chromate Plume

1.2 Site History

Contamination was first detected at the Puchack Well Field in the early 1970s with the presence of trichloroethylene (TCE), 1,2-dichloroethane (1,2-DCA), tetrachloroethylene (PCE), and chromium compounds in Puchack Well No. 6. Further sampling indicated the presence of total and hexavalent chromium at concentrations above the U.S. Public Health Standards MCL, which resulted in the well being removed from service in 1975. In 1978, chromium was detected in Puchack Well No. 5. In 1982, chromium was detected in Puchack Well Nos. 2, 3, and 7. Historical chromium concentrations ranged from 1,500 to 3,000 µg/L. In 1984, general use of the Puchack Well Field was terminated, and all wells were removed from service, except for Well No. 1, which under permit, NJDEP allowed to be pumped at approximately 800,000 gallons per day, to help prevent the plume from spreading to other public supply wells. Well No. 1 was removed from service in March 1998. The area encompassed by the Puchack Well Field is approximately 450,000 square feet, or 10.33 acres.

In 1986, Camp Dresser and McKee (CDM) investigated the chromium contamination in the well field on behalf of the NJDEP. CDM found chromium concentrations up to 1,000 ppb, mercury concentrations up to 5.8 µg/L, and TCE concentrations up to 70 µg/L in the well field. However, according to NJDEP, in October 1989, the highest chromium concentration ever in a water supply well in New Jersey was detected in Puchack Well No. 3 at a concentration of 4,180 µg/L.

In March of 1996, NJDEP collected additional groundwater samples from the Puchack supply wells and monitoring wells. Samples were analyzed for volatile organic compounds (VOCs), total metals, and cyanide. Analytical results indicated the continued persistence of chromium, low concentrations of mercury, and TCE in all Puchack water supply wells. Detected chromium concentrations ranged from

46.6 µg/L in Well No. 1 to 1,410 µg/L in Well No. 7. Mercury concentrations ranged from 0.15 µg/L in Well No. 6 to 0.77 µg/L in Well No. 2. TCE concentrations ranged from 0.3 µg/L in Well No. 5A to 20 µg/L in Well No. 2 (Weston 1997).

Several contaminated sites were identified by NJDEP in Pennsauken Township in the early 1980s. Potentially contaminated sites located within or near the Puchack Well Field site include SGL Modern Hard Chrome Service (SGL Chrome), King Arthur, Mercon, and Supertire, among others. The SGL Chrome site was used for chromium plating and is currently a parking lot with no structural features remaining.

In 1997, the NJDEP and the United States Geological Survey (USGS) initiated an investigation of the groundwater contamination of the Pennsauken Township area. Groundwater contaminated with chromium was found in the Middle Aquifer in two isolated areas, one is located at the SGL Chrome property and one area located to the north that is not related to the site (associated with the Pennsauken Landfill). The SGL site is also the location of the highest chromium groundwater contamination in the Middle Aquifer at 8,000 µg/L. As a result, it is suspected that the SGL Chrome site is a major contributor to chromium contamination of the groundwater. It is suspected that chromium contamination migrated from the SGL Chrome site into the Middle Aquifer, then to the Intermediate Sand layer, and finally to the Lower Aquifer. There may be other potential chromium sources within the area that will be investigated during the OU2 Remedial Investigation. The chromium plume in the Intermediate Sand has migrated toward the east, while the chromium plume in the Lower Aquifer had been drawn back toward the north under the influence of the Puchack Well Field pumping. Chromium levels in the Middle Aquifer, Intermediate Sand, and Lower Aquifer generally range from 700 to 8,000 µg/L, 1,000 to 6,000 µg/L, and 200 to 1,500 µg/L, respectively.

VOC contamination is more widespread, with multiple sources, and is present in pockets near contaminant source areas. VOCs detected include PCE; TCE; 1,1-dichloroethene (1,1-DCE); 1,1,1-trichloroethane (1,1,1-TCA); dichloromethane; and benzene. VOC contamination in the three aquifer levels has commingled with the chromium plume and is generally larger in size. Total VOC levels in the Middle Aquifer, Intermediate Sand, and Lower Aquifer generally range from 3 to 700 µg/L, 5 to 140 µg/L, and 1 to 50 µg/L, respectively.

In 1997, the NJDEP recommended the Puchack Site be listed on the National Priorities List (NPL) and addressed under CERCLA as a Superfund Site. The Puchack Site was proposed for inclusion on the NPL in September of 1997. The Puchack well field became final on the NPL on March 6, 1998, and EPA became the lead agency for this site. NJDEP is the support agency.

1.3 Site Hydrogeology

The Puchack Well Field is situated in the outcrop area of the Potomac-Raritan-Magothy (PRM) aquifer system in the New Jersey Coastal Plain physiographic province. This aquifer system is the primary source of drinking water in northwestern Camden County. Groundwater is still being used for potable water in several nearby well fields including Morris and Delair well fields to the northwest, Park Avenue well field to the east, Marion and Woodbine well fields to the southeast, and Browning well field to the south. Some of these well fields are contaminated with volatile organic compounds (VOCs). As a result, water pumped from some of these well fields is treated to remove organic compounds prior to distribution for public use.

The PRM aquifer system is a high yielding formation with several stratigraphic layers. These include the Upper Aquifer, Upper/Middle Confining Unit, Middle Aquifer, Middle/Lower Confining Unit (which contains an intermediate sand layer), Lower Aquifer, and Lower Confining Unit (bedrock) (Figure 1.2). In the vicinity of the site, the major aquifer units include the Upper Aquifer (0 to 20 feet below ground surface (ft bgs)), Middle Aquifer (30 to 60 ft bgs), Intermediate Sand (100 to 120 ft bgs), and Lower Aquifer (160 to 250 ft bgs). These hydrostratigraphic layers dip to the east. The water table typically is encountered at 30 to 50 ft bgs and due to pumping from inland well fields, groundwater flow is generally towards the east, away from the Delaware River.



Figure 1.2. Five-Layer and Subdivided Interpretations of the Hydrostratigraphic Framework of the Potomac-Paritan-Magothy Aquifer System, Puchack Well Field Superfund Site, Pennsauken Township, New Jersey (prepared by the USGS, NJ)

1.4 Treatability Study Objectives

The primary objective of this study was to determine the feasibility of using an abiotic or biotic technology to create a subsurface reduced zone in the aquifer that will reduce and permanently immobilize Cr(VI) species. In addition, natural processes such as chromate adsorption and reduction were assessed with Puchack aquifer sediments for two reasons: 1) to determine how much Cr(VI) mass could be immobilized naturally in the subsurface with no treatment and 2) to quantify the effects of these natural processes on in situ reductive treatment. A secondary objective of the treatability study was to assess the technologies' effectiveness for the treatment of VOC contamination (i.e., TCE). Although EPA decided to eliminate this task from the treatability study, background information on reductive dechlorination of TCE is provided in Section 2.2.3.

The specific objectives of testing the abiotic technology included:

- a. determine whether a stable (immobile) reduced sediment barrier can be created in Puchack sediments at pH 4.5 to 7.0
- b. determine what the longevity of this barrier would be
- c. determine whether reduced sediments immobilize Cr(VI) species at pH 4.5 to 7.0.

The specific objectives of testing the biostimulation technology included:

- a. determine whether appropriate populations of microorganisms can be biostimulated within the Puchack sediments to catalyze either direct chromium (VI) reduction or reduction of iron and sulfate to establish a reduced sediment barrier
- b. quantify the relevant microbial reduction processes and determine appropriate amendments to stimulate these processes
- c. assess the stability of the reduced Cr(III) species within a biologically-reduced sediment at pH 4.5 to 7.0.

The specific objectives of the natural attenuation studies included:

- a. determine the influence of adsorption (i.e., how much Cr(VI) mass is on surfaces relative to in solution)
- b. determine whether there is any significant natural reduction of Cr(VI) species in the targeted aquifer units (primarily intermediate sand and lower aquifer units).

Experimental results provided in this report will provide the basis for developing an in situ treatment approach for the Puchack site, which may be subjected to pilot-scale field testing. Results from both the bench and pilot-scale testing would then be used, along with hydrogeologic and well field operational information, to determine locations for cost effective deployment alternatives.

2.0 Background

This section provides a discussion of the various elements that have been investigated to determine the efficacy of in situ treatment technologies for the remediation of hexavalent chromium in groundwater at the Puchack Well Field Superfund Site.

2.1 Chromium Transport and Immobilization in the Subsurface

In a reducing subsurface environment, whether natural or artificially created, hexavalent chromium contaminated groundwater can, under favorable pH and reducing (Eh) conditions, be reduced and permanently immobilized as a mixed Cr-Fe precipitate. As the dissolved hexavalent chromium in a toxic environment (Figure 2.1, high Eh) enters the reducing environment, it will react with reduced species including ferrous iron and sulfides (and also organic matter or microbial enzymes) and be reduced to the trivalent form (Figure 2.1, low Eh). Once Cr(III) precipitates form, they are extremely difficult to oxidize (and remobilize), even though under geochemical equilibrium conditions, Cr(VI) species should be formed. As a consequence, Cr(III) precipitates are permanently immobilized in subsurface systems at $4 < \text{pH} < 13$ even under highly oxidizing conditions. This activation barrier for Cr(III) oxidation is the basis for the success of in situ chromium immobilization.

2.1.1 Cr Speciation

Chromium occurs in the +2, +3, and +6 oxidation states in water, although only +3 and +6 are common. Aqueous hexavalent chromium (as Cr(VI) species) are toxic and highly mobile, exhibiting no sorption at a pH > 7 in most sediments. Cr(VI) species include

- HCrO_4^- ($\text{pH} < 6.5$) and CrO_4^{2-} ($\text{pH} > 6.5$) when $\text{Cr}_{\text{total}} < 0.1 \text{ mol liter}^{-1}$
- HCr_2O_7^- ($\text{pH} < 1$), $\text{Cr}_2\text{O}_7^{2-}$ ($1 < \text{pH} < 7.5$), CrO_4^{2-} ($\text{pH} > 7.5$) when $\text{Cr}_{\text{total}} > 0.1 \text{ mol liter}^{-1}$

Common Cr(III) species (Figure 2.2) include Cr(OH)_3 [aqueous and precipitate], Cr(OH)_4^- [$\text{pH} > 9$], CrOH^{2+} , Cr(OH)_2^+ , and $\text{Cr}_3(\text{OH})_4^{5+}$.

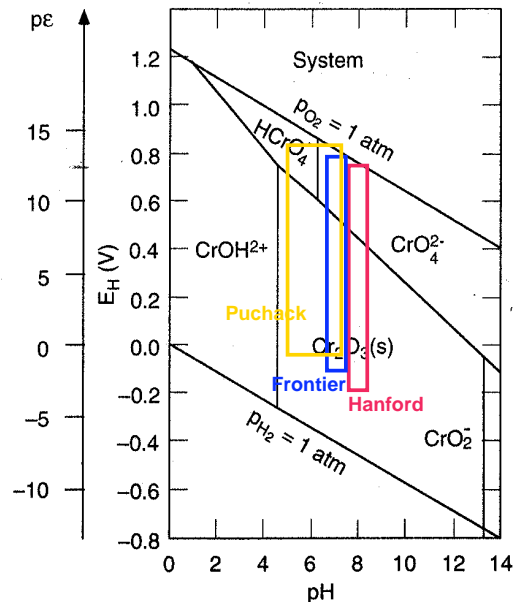


Figure 2.1. Stability of Cr(VI) and Cr(III) Phases at Equilibrium at Different pH and Eh (Stumm and Morgan 1996)

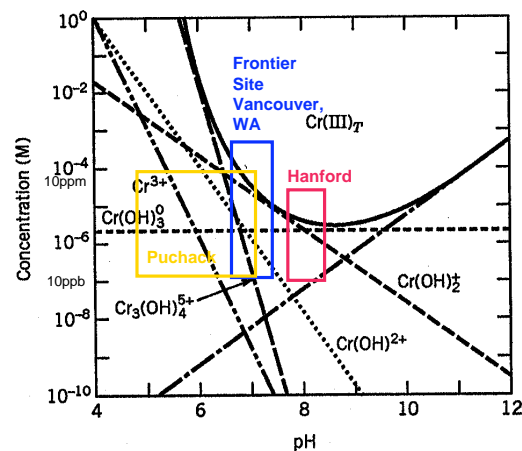


Figure 2.2. Cr(III) Aqueous Speciation at Equilibrium without Additional Organic or Inorganic Ligands (Stumm and Morgan 1996)

Although $\text{Cr}_3(\text{OH})_4^{5+}$ should dominate aqueous solubility at $\text{pH} < 8$, it is slow to form, and a state of nonequilibrium of this Cr(III) species can exist in natural waters. Cr(III) complexes with many inorganic ligands (including sulfate, oxalate, ammonia, and fluoride) and organic ligands in natural waters. In contrast to the few Cr(VI) aqueous species, there are thousands of synthetic Cr(III)-ligand complexes used in various industries, so natural and synthetic Cr(III) complexes can be found in contaminated groundwater. In addition, metals including Cr have been found associated with suspended clay and organic matter (i.e., colloids), indicating the need to filter samples to evaluate transport mechanisms. Because these aqueous Cr(III) species can be oxidized to Cr(VI) species, total chromium [Cr(VI) and Cr(III) species] is the basis of EPA water-quality standards, even though only Cr(VI) is considered toxic.

2.1.2 Cr(VI) Reduction and Precipitation

Cr(VI) species that exist under highly oxidizing conditions are rapidly reduced to Cr(III) species (rate described below). Over much of the pH range of natural waters, a $\text{Cr}(\text{OH})_3$ precipitate forms (Figure 2.1), where the low Cr(III) aqueous solubility is shown theoretically in Figure 2.2. An iron-reducing or sulfide environment (biotically or abiotically created) exhibits an order of magnitude less solubility than shown in Figure 2.2. This is because when trivalent chromium is precipitated as a mixed $(\text{Cr}, \text{Fe})(\text{OH})_3$ precipitated, it has lower solubility. This effect was demonstrated in a series of mixed solubility experiments (Figure 2.3), where a lower fraction of Cr in the precipitate has much lower solubility than pure $\text{Cr}(\text{OH})_3$. The solubility of Cr as a function of the ratio of Cr/Fe in precipitates has also been quantified (Early and Rai 1988; Loyaux-Lawniczak et al. 2000; Patterson and Fendorf 1997).

While the three example sites provided (Figures 2.1 and 2.2, two at the Hanford Site, Washington, and one at the Frontier Hard Chrome site in Vancouver, Washington) where the ISRM technology has been previously demonstrated cover a pH range from 6.5 to 8.3, evidence exists that aquifers at pH values as low as 4.1 will also reduce and form Cr(III) precipitates that remain immobile. Under highly acidic conditions, CrOH^{2+} and other aqueous Cr(III) species form; therefore, reduction results in both precipitated and aqueous species. For a pure laboratory system containing only Cr(VI), these mobile Cr(III) species form at a $\text{pH} < 4.3$ (Figure 2.2). As described in the preceding paragraph, the mixed (Cr, Fe) hydroxides that form have lower solubilities, so sediments with iron reducing conditions typically have a large excess of ferrous iron relative to the chromate. For example, the Frontier Hard Chrome site (Vancouver, Washington) with 10 ppm chromate has 2,500 times more ferrous iron ($46.1 \mu\text{mol/g}$ reducible iron), which illustrates why precipitates will typically contain a small Cr fraction. In a weathered shale (Jardine et al. 1999), natural ferrous iron present at pH 4.6 results in significant chromate reduction and permanent immobilization, based on long-term (10 month) one-dimensional (1-D) laboratory transport studies. At a landfill in northern France, ferrous iron in green clay at pH 4.1 has also resulted in the reduction and precipitation of Cr(VI) species (Loyaux et al. 2001). In contrast, at a pH of 3.0, Cr(III)

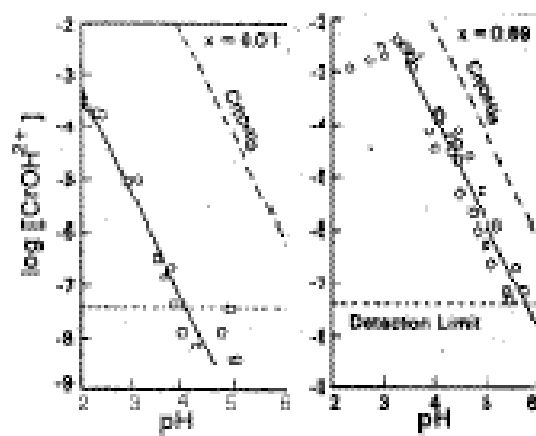


Figure 2.3. Solubility of $(\text{Cr}, \text{Fe})(\text{OH})_3$ Precipitates with a) 1% Cr, and b) 69% Cr, Relative to Theoretical $\text{Cr}(\text{OH})_3$ (Sass and Rai 1987)

species remained in aqueous solution in an aquifer (Seaman et al. 1999), possibly due to acetate or sulfate complexation. Reduction of Cr(VI) followed by precipitation of Cr(III) has also been demonstrated in the laboratory with amorphous iron sulfide from pH 5 to pH 8 (Patterson and Fendorf 1997), with mackinawite (FeS) at pH 5 (Boursiquot et al. 2002), and with hydrogen sulfide from pH 6.5 to pH 10 (Kim et al. 2001).

In a natural subsurface system, the redox environment is controlled largely by microbial reactions and to a small extent, abiotic reactions. Oxidation of natural organic matter occurs in the general order of energetic preference by dissolved oxygen, then nitrate, ferric iron, sulfate, and all microbial mediated. Adding carbon to an electron-donor-limited aquifer (i.e., oxidizing system - little organic matter) can stimulate microbial activity, driving the consumption of these electron acceptors, as described in further detail in Section 1.4. At sites with sufficient organic matter, such as the Puchack Well Field, localized zones of significant organic matter (lignite deposits, for example, Murphy et al. 1992) can create sufficiently reducing conditions to reduce Cr(VI) species.

The rate of Cr(VI) species reduction by ferrous iron has been extensively studied in a variety of geochemical conditions. In the pH range of 4.4 to 7.2, the Cr(VI) reduction rate decreases nearly three orders of magnitude from over a 1,000 seconds at pH 7.2 to just a few seconds by pH 4.4 (Figure 2.4; Buerge and Hug 1997). At a pH >10, and at lower pH values for solutions containing significant phosphate, chromate is less efficiently reduced by ferrous iron (Eary and Rai 1988). In a field system, both ferrous iron and organic matter appear to influence the rate of Cr(VI) reduction, and a faster rate was observed with lower pH in one case (Anderson et al. 1994). The rate of Cr(VI) reduction by hydrogen sulfide increases significantly with decreasing pH between pH 6.5 and pH 10, potentially due to the dependence of the reduction on the concentration of H_2S (Kim et al. 2001). Data describing the rate of Cr(VI) reduction by iron sulfide materials is limited.

2.1.3 Chromium Adsorption

At neutral and alkaline pH, chromate moves nearly unretarded in aquifers (Fruchter et al. 2000), whereas under acidic conditions, considerable chromate sorption has been observed (Zachara et al. 1987; Jardine et al. 1999; Seaman et al. 1999). At a pH of 4.6 in a weathered shale, nonlinear sorption with an affinity parameter of 15.6 was observed (S (sorbed mass) = $15.6 C^{0.61}$, where C = aqueous chromate mass). This sorption increased four fold with the addition of natural organic matter (NOM; $S = 65 C^{0.39}$), indicating in this case, it appears that sorption was dominated by organic matter. Interestingly, this same sediment also exhibited some reduction of chromate, which did not change with the addition of organic matter. Sediments from the Savannah River site (pH 5.3, 5.52) exhibited some sorption, but apparently not related to organic matter. At high NOM (0.76 g /100 g), little sorption was observed ($K_d = 0.1 \text{ cm}^3/\text{g}$), whereas at low NOM (0.02 g /100 g), moderate sorption was observed ($K_d = 1.5 \text{ cm}^3/\text{g}$; Seaman et al. 1999).

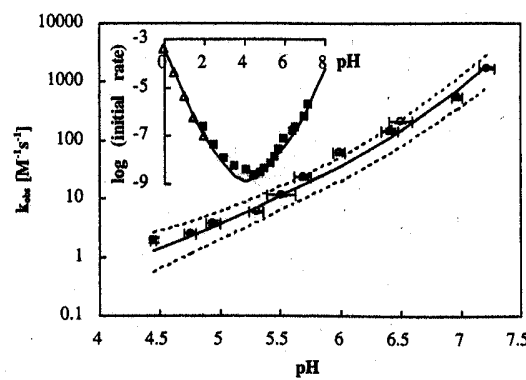


Figure 2.4. Rate of Chromium Reduction by Aqueous Ferrous Iron as a Function of pH (Buerge and Hug 1997)

2.2 Abiotic Technology Description

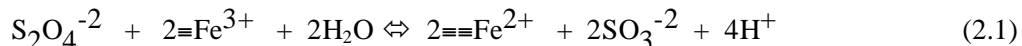
The ISRM approach involves the creation of a permeable treatment zone downstream of a contaminant plume or contaminant source through injection of a chemical reducing agent to alter the redox potential of aquifer fluids and sediments (Fruchter et al. 2000; Vermeul et al. 2002; Szecsody et al. 2004a, 2004b, 2005a, 2005b). Redox-sensitive contaminants migrating through this treatment zone are immobilized (metals) or transformed to less toxic intermediates or end products (organic solvents and energetics). Injected reagents create the zone through reactions that reduce iron naturally present in aquifer sediments from Fe(III) to Fe(II). Use of standard wells for treatment zone creation allows treatment of contaminants too deep for conventional trench-and-fill technologies.

This technology has been successfully demonstrated in two field tests at the Hanford Site in Washington State for the remediation of hexavalent chromium in the groundwater (Fruchter et al. 2000, Williams et al., 2000). One site is a single-well demonstration, whereas the other site is a 65-well subsurface barrier that is 2300 ft long and installed in a 15 to 30 ft thick aquifer located approximately 85 ft below ground surface. A third ISRM barrier has been installed to remediate hexavalent chromium in groundwater at the Frontier Hard Chrome Superfund Site, Vancouver, Washington (Vermeul et al. 2003). In all cases, mobile Cr(VI) species at circumneutral pH values (6.5 at Frontier, 7.5 to 8.3 at Hanford) have been reduced and immobilized to below detection limits.

The reducing agent used in these field and laboratory tests is sodium dithionite ($\text{Na}_2\text{S}_2\text{O}_4$). Sodium dithionite is a strong reducing agent, and it possesses a number of desirable characteristics for this type of application, including instability in the natural groundwater environment (~ days) with reaction and degradation products that ultimately oxidize to sulfate. A potassium carbonate/bicarbonate pH buffer is also added to the injection solution to enhance the stability of dithionite during the reduction of available iron.

2.2.1 Iron Reduction Mechanism

The dithionite chemical treatment dissolves and reduces amorphous and some crystalline Fe(III) oxides. The reduced Fe(II) created by the dithionite chemical treatment appears to be present in several different Fe(II) phases: adsorbed Fe(II), Fe(II)-carbonate (siderite), and FeS (iron sulfide), although adsorbed Fe(II) appears to be the dominant Fe(II) phase (surface Fe(III) and Fe(II) phases indicated by “=Fe”). There may be other, unidentified Fe(II) mineral phases produced. Although more than one iron (III) phase is likely reduced in natural sediment, it can be useful to determine how simple a chemical model is needed to generally describe the observations. The reaction that describes a single phase of iron that is reduced by sodium dithionite:



demonstrates that the forward rate is a function of the dithionite concentration and the square of the reducible iron concentration (rate is overall a third-order function of concentration). The third-order reduction rate was experimentally verified (Szecsody et al. 2004). The aqueous Fe(II) produced has a high affinity for surfaces at mid-to-high pH and low ionic strength, so is quickly adsorbed. Therefore, Fe(II) mobility is extremely limited under these conditions, and iron is not expected to leach significantly from sediments during the dithionite treatment. Aqueous iron measurements in previous studies have

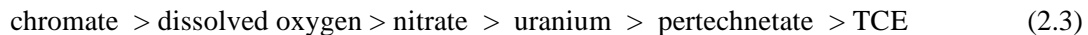
shown <1% iron leaching even after 600 pore volumes of groundwater through a sediment column. Corresponding solid iron measurements of sediments used in these columns showed 4 to 10% loss of iron. Iron mobility is somewhat higher during the actual dithionite injection because, at high ionic strength (~0.3 mol/L in this case), other cations compete for the same adsorption sites as Fe²⁺, resulting in some Fe²⁺ desorption. If the number of slowly reducing sites is small and the mass of iron is far in excess of the dithionite, reaction 1 can be reduced to a first-order reaction in which Fe³⁺ remains constant. Another reaction occurs in the system, which describes the disproportionation of dithionite in contact with sediment:



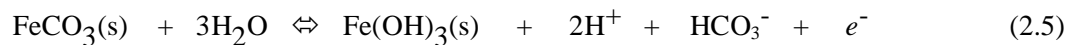
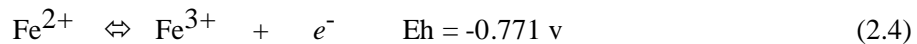
This reaction accounts for the mass loss of dithionite that cannot be used for iron reduction. Previous studies have shown that this reaction has a half-life of ~27 hours (basaltic sediments). This places a limit on the time available for dithionite to react with sediments in the field (i.e., minimum injection rate). If dithionite is injected too slowly, a significant amount of the mass is lost to disproportionation. Although iron(III) phases are the most significant phase that reacts with dithionite, other mineral phases present in natural sediments may also be reduced, and utilize some of the dithionite. Previous studies have shown that some Mn reduction occurs as a result of the dithionite treatment of Hanford sediment, although reduced Mn^{II} phases were only 3 to 4% relative to reduced iron phases. In the event that the reduced iron barrier is exhausted, previous laboratory studies with the Hanford 100-D and 100-H Area sediment have shown that sediment can be reduced with only a small (5% to 10%) loss in capacity (Szecsody et al. 2004).

2.2.2 Sediment Oxidation and Chromate Reduction Mechanism

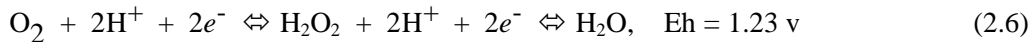
The oxidation of the adsorbed and structural Fe(II) in the sediments of the permeable redox barrier occurs naturally by the inflow of dissolved oxygen and other contaminants such as chromate, TCE, nitrate, uranium, or other electron acceptors (energetics, Szecsody et al. 2005b). If redox equilibrium completely defined the mechanism (i.e., no effects from activation energies or surface catalysis) and the following contaminants were present in equal molar concentrations, they would be reduced in the following order:



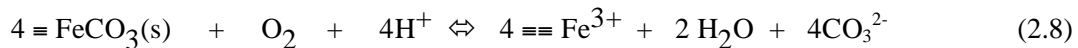
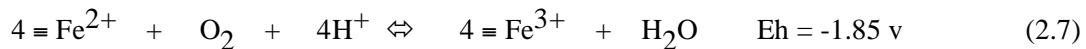
In most aquifers, dissolved oxygen in water is the dominant oxidant of reduced iron species, as contaminants are generally present in lower molar concentrations relative to dissolved oxygen. The oxidation of ferrous iron in siderite and on adsorption sites is described by the following reactions for dissolved oxygen and chromium. Fe(II) species that are known to exist in the dithionite-reduced sediments include adsorbed Fe(II) and siderite [Fe(II)CO₃]. A single mole of electrons is consumed as a mole of these species are oxidized:



The use of dissolved oxygen as an oxidant is generally divided into two electron sequences, which combined:

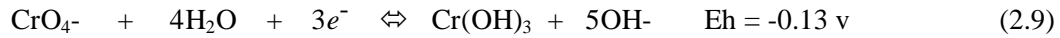


show that 4 moles of electrons are needed per mole of O₂ consumed (Stumm and Morgan 1996; Wehrli 1992). The rate of this reaction (aqueous ferrous iron oxidation by dissolved oxygen [2.4 + 2.6]) has generally been observed to be first-order at fixed pH and the rate increases 100 fold for a unit increase in pH. Experimental evidence during iron oxidation experiments indicates that two differing reduced iron species is present (adsorbed ferrous iron and siderite). Combining the two iron oxidation half reactions with oxygen reduction:



yields 4 moles of Fe(II) are oxidized and 4 moles of electrons transferred per mole of O₂ consumed. At oxygen-saturated conditions (8.4 mg L⁻¹ O₂, 1 atm, 25°C), 1.05 mmol L⁻¹ Fe(II) is consumed. Experimental evidence indicates that the oxygenation of Fe(II) in solution (pH > 5) is generally found to be first order with respect to the Fe(II) and O₂ concentrations and second-order with respect to OH⁻ concentration. The rate of oxidation (as a half-life) of aqueous Fe²⁺ by oxygen at pH 8 is a few minutes (Early and Rai 1988; Buerge and Hug 1997). In contrast, the oxidation rate observed in natural sediments [surface Fe(II) phases, mainly adsorbed Fe(II) and FeCO₃] was found to be 0.3 to 1.1 hours.

The reduction rate of Cr(VI) species by ferrous iron has been extensively studied under various geochemical conditions. For chromate:

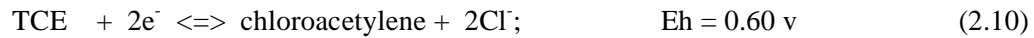


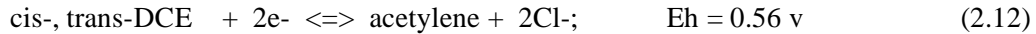
3 mole of electrons are consumed per mole of chromate reduced. The reduction of one mole of chromate oxidizes three mole of Fe(II), or 41 mg L⁻¹ chromate is needed to oxidize the equivalent mass of Fe(II) as water saturated with dissolved oxygen [1.05 mmol L⁻¹ Fe(II)].

In a pure laboratory system, the Cr(VI) reduction rate (by aqueous ferrous iron) at pH 7.0 (seconds to minutes) decreases about two orders of magnitude as the pH decreases to 4.5 (Buerge and Hug 1997). In natural aquifer sediments, however, the Cr(VI) reduction rate actually increases (Anderson et al. 1994) with lower pH, possibly due to both ferrous iron and organic matter.

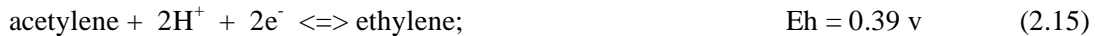
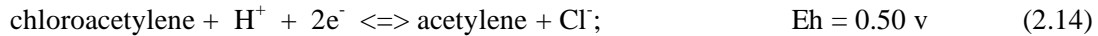
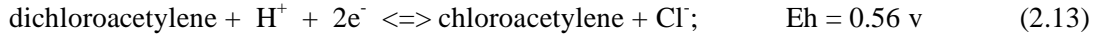
2.2.3 Trichloroethylene Reduction Mechanism

The degradation pathway of TCE by dithionite-reduced sediment has been previously investigated in two bench scale studies as well as at Ft. Lewis (Tacoma, Washington; Szecsody et al. 2000, 2004) in the field scale. Degradation pathways for most organic compounds including TCE are complex, involving multiple and potentially parallel reaction steps. Of four possible abiotic degradation pathways for TCE, the two considered most common are reductive elimination and hydrogenolysis. Reductive elimination has been shown to be the major pathway in other studies using zero-valent and ferrous iron (Sivavec et al. 1996; Orth and Gillham 1996). Reductive elimination reactions include (Roberts et al. 1996):

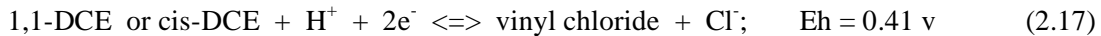
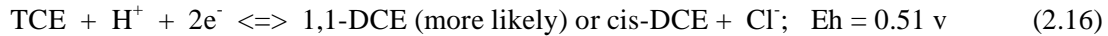




which describes the destruction of TCE and PCE to easily degraded (abiotically or biotically) chlorinated acetylene products. Abiotic degradation of these products by hydrogenolysis:



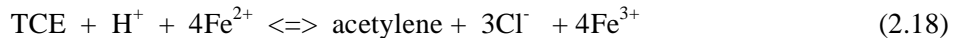
apparently proceeds rapidly as chlorinated acetylenes are unstable (Delavarenne and Viehe 1969). The degradation of TCE to ethylene by reductive elimination (or hydrogenolysis discussed below) involves the production of 6 moles of electrons, or 22 mg L⁻¹ TCE needed to oxidize the equivalent mass of Fe(II) as water saturated with dissolved oxygen [1.05 mmol L⁻¹ Fe(II)]. Hydrogenolysis reactions include:



which describes the degradation of TCE involving the production then destruction of dichloroethylene (DCE) and vinyl chloride intermediates (generally more difficult to degrade). These reduction potentials are lower than reductive elimination, indicating they are less likely to occur abiotically. Activation energies and the specific electron transfer mechanism, which does involve the Fe^{III} oxide surface, may also influence which reactions actually do occur. Studies of TCE degradation pathways using zero-valent iron and various Fe(II) minerals (Roberts et al. 1996; Sivavec and Horney 1995; Thornton et al. 1998) indicate that reductive elimination is the major pathway, with minor amounts of DCE isomers and vinyl chloride produced from the hydrogenolysis pathway. One study (Roberts et al. 1996) also indicates that the DCE isomers and vinyl chloride slowly degraded to ethylene.

2.2.3.1 TCE Dechlorination Rate in Reduced Sediment

The TCE reaction pathway can be used to model the observed rate of TCE degradation. Because acetylene is the main reaction product observed in previous studies, the combination of reactions (Equations 2.6, 2.10, and 2.14) described the major TCE degradation pathway:



The degradation rate equation for TCE:

$$\frac{\partial \text{TCE}}{\partial t} = -k_{f20} [\text{TCE}] [\text{H}^+] [\text{Fe}^{2+}]^4 - k_{b20} [\text{acetylene}] [\text{Cl}^-]^3 [\text{Fe}^{3+}]^4 \quad (2.19)$$

describes the TCE degradation rate (decreasing) as a function of each constituent concentration to each respective stoichiometric coefficient, and when integrated describes mass flux as a function of time. A set of differential equations for all redox reactions can be numerically solved (55 mixed equilibrium and kinetic reactions with 71 species described in Szecsody et al. 1998; Yeh et al. 1998), but this type of

detailed modeling is useful only if extensive knowledge of the reaction parameters exists. In the case of TCE degradation, not enough information is known about the reaction pathways and reaction parameters to justify this approach. Simpler models can be used to accurately describe the TCE degradation rate under specific conditions. The equation describing the TCE degradation rate can be greatly simplified assuming no backward mass flux (the reaction is irreversible) and that the pH is buffered:

$$\partial[\text{TCE}]/\partial t = -k'_{f20}[\text{TCE}][\text{Fe}^{2+}]^4 \quad (2.20)$$

which shows that the TCE degradation rate is a function of a rate coefficient (k'_{f20}), the TCE concentration, and the ferrous iron concentration (raised to a power >1 , as experimentally determined and described below). Therefore, as the sediment is slowly oxidized by both dissolved oxygen (Equation 2.7) and TCE (Equation 2.18), the observed overall TCE degradation rate ($\partial[\text{TCE}]/\partial t$) will decrease. Over a small number of pore volumes, the Fe^{2+} concentration can be assumed constant, and the TCE degradation rate simplifies to a first-order reaction that can be integrated:

$$\partial[\text{TCE}]/\partial t = -k''_{f20}[\text{TCE}] \quad (2.21)$$

$$[\text{TCE}] = [\text{TCE}]_{t=0} e^{-\lambda t} \quad (2.22)$$

Both the pseudo-first-order approach (Equation 2.21) and the fixed-pH approach (numerical solution to Equations 2.7 and 2.20) were used in this study to describe the TCE degradation data. Since the actual TCE degradation rate is a function of Fe^{2+} and decreases over time, the first-order half-life will appear to decrease at progressively later points in time. As the overall TCE degradation rate decreases, the relative concentrations of degradation products change during flow through a redox barrier in an aquifer. In general, final degradation products (ethylene, ethane) appear when all reactions are occurring at the fastest rates, and as reactions slow, intermediates (acetylene) and finally the initial degradation product of TCE dechlorination (chloroacetylene) appears.

The observed TCE degradation rate (reported as first-order half-life) varied over an order of magnitude from 0.013/hour (low iron content Hanford sediment) to 0.2/hour (high iron content Ft. Lewis sediment). Assuming a first-order dependence of Fe^{II} on the intrinsic TCE degradation rate, the rate variability was reduced by an average of 3x (range 0.0018 to 0.0054 (hour $\mu\text{mol Fe(II)}$) $^{-1}$), so is likely the correct dependence:

$$k_{f, \text{intrinsic}} = 0.0034 \pm 0.0014 \text{ 1/[h } \mu\text{mol Fe}^{\text{II}}] \quad (2.23)$$

Assuming a second-order dependence of Fe(II) , intrinsic rate values that varied 2.5 orders of magnitude, and assuming a third-order dependence of Fe(II) , intrinsic rate values that varied 4 orders of magnitude, so are most likely not the correct dependence of Fe(II) on the intrinsic TCE degradation rate. Therefore, although the theoretical rate dependence shows a fourth order dependence on ferrous iron concentration (Equation 2.20), observed rates in sediments are likely rate limited by other processes such as diffusion, and appear to be best fit with a first-order rate dependence on iron concentration (Equation 2.21).

2.2.3.2 Influence of Partial Iron Reduction on TCE Degradation Rate

The electron-transfer mechanisms of TCE dechlorination by surface Fe(II) phases are not completely understood, and as a consequence, there is a lack of ability to predict the TCE degradation rate with

sediment that is only partially reduced. Two aspects of the electron transfer reactions are known: abiotic dechlorination of TCE and other chlorinated organic compounds requires both available Fe(II) as an electron donor and the presence of an iron oxide or zero-valent iron surface. The surface is necessary for the electron transfer reaction as laboratory experiments have shown that TCE and carbon tetrachloride are not dechlorinated in the presence of only aqueous Fe(II). The role of the surface is not well understood, although it may act as a catalyst, a semiconductor, or provide the necessary surface coordination for the electron transfer reactions (Scherer et al. 1999).

The role of the iron oxide surface on TCE dechlorination was also experimentally investigated by developing a relationship between fraction-reduced iron and the resulting dechlorination ability of the sediment (Szecsody et al. 2004). In these experiments, sediment was reduced in batch systems and the mass of reduced iron measured by different types of iron extractions including oxygen breakthrough in columns. Batch time-course experiments were used to determine the resulting TCE dechlorination rate. Because TCE degradation requires both an electron donor (adsorbed Fe^{II}) and a surface (iron oxide or clay), the rate of dechlorination is not a simple function of the mass of reduced iron. This fact is significant at the field scale because sediments cannot be uniformly reduced, so studies were conducted to determine the rate of TCE degradation as the reduced iron mass was varied. The TCE degradation rate is highly dependent on the fraction of reduced iron in sediment and varied from >1,000 hours or 11% reduced to 1.2 hours for 100% reduced iron (Ft Lewis, Washington, sediment). The intrinsic TCE degradation rate varied two orders of magnitude, and there appeared to be a significant increase in the TCE degradation rate between 30% and 45% reduced sediment. The intrinsic degradation rate had a second-order dependence on the fraction of reduced iron, which may be caused by the influence of the surface on the TCE degradation rate. These results are consistent with a long-term (4-month) column study with Hanford sediments in which the TCE degradation rate decreased significantly when the sediment was <50% reduced.

2.2.3.3 Influence of Temperature on the TCE Degradation Rate

The potential role of the iron oxide surface as a catalyst for TCE dechlorination was investigated by batch TCE dechlorination time-course experiments over a distinct temperature range (Szecsody et al. 2000, 2004, 2006). In contrast to a simple chemical reaction, a chemical reaction that requires a surface catalyst will likely show a more complex relationship between reaction rate and temperature, because the catalyst may cease to function as the temperature decreases beyond a specific value. The ambient temperature of the Ft. Lewis (Tacoma, Washington) aquifer is unusually cold at 11°C to 12°C (compared with many aquifers in the 16°C to 19°C range). Batch experiments conducted from 2°C to 25°C showed a regular decrease ($2.67 \times /10^{\circ}\text{C}$) in TCE degradation rate with lower temperature. The activation energy (42 kJ/mole) indicated that the observed rate was chemically controlled and not diffusion controlled, and similar to that reported for reduction of vinyl chloride by Fe (Deng et al. 1999).

2.3 Biotic Technology Description

Biostimulation of indigenous bacteria can be applied to directly reduce Cr(VI) in situ or to reduce other species such as iron and sulfate to create an in situ reactive barrier capable of abiotically reducing Cr(VI). Biostimulation involves distributing an appropriate substrate (e.g., organic acid) in the subsurface that is subsequently metabolized by existing bacteria. Electron acceptors coupled to substrate metabolism include Cr(VI), Fe(III), and sulfate. The specific electron acceptor reduced during metabolism is dependent on the type and population of microorganisms in the aquifer, the concentration of each

potential electron acceptor, the type of substrate present, and the geochemical conditions such as pH that impact the metabolic rate of different microbial species in the subsurface.

2.3.1 Direct Cr(VI) Reduction Approach

Enzymatic reduction of Cr(VI) has been demonstrated in laboratory and field settings. Cr(VI) competes as an electron acceptor with other electron acceptors present in the groundwater. However, the enzymatic reduction of Cr(VI) can occur under a wide range of redox conditions including in the presence of small amounts of oxygen. Reduction of Cr(VI) has been demonstrated under aerobic conditions (e.g., Bopp and Ehrlich 1988; Horitsu et al. 1987; Ishibashi et al. 1990), by dissimilatory iron reducing bacteria, DIRB (e.g., Caccavo et al. 1992), under nitrate- or fumarate-reducing conditions (e.g., Viamajala et al. 2002), and by sulfate-reducing bacteria (SRB) (e.g., Lovley and Phillips 1994).

To apply direct Cr(VI) reduction as an in situ process, substrate must be distributed and mix with the Cr(VI) within the aquifer. This type of mixing typically requires a groundwater recirculation system. Contaminated groundwater is extracted, amended with substrate, and then re-injected to the aquifer. It is also possible to inject a substrate solution and rely on dispersive mixing of the substrate and Cr(VI), but this technique may not provide sufficient contact for effective direct Cr(VI) reduction.

2.3.2 In Situ Reaction Zone Approach

Fe(III) and sulfate can be biologically reduced because they are electron acceptors for microbial metabolism. Microorganisms that can use Fe(III) and sulfate as electron acceptors can be found in many different environments, however, they actively reduce Fe(III) or sulfate only under anaerobic conditions. While oxygen is generally present within the contaminated aquifer, addition of a microbial substrate will rapidly deplete the oxygen and create the anaerobic conditions conducive to Fe(III) and sulfate reduction.

The reduced iron and sulfide produced by microbial metabolism can be used to form an in situ reactive barrier for Cr(VI). The in situ reactive barrier is formed because the reduced iron and sulfide products are immobilized (dependent on pH) as either precipitates, mineral forms, or sorbed phases. The concept for implementing a reactive barrier involves biostimulation of a relatively small amount of in situ biomass to reduce sufficient iron and sulfate to enable long term reduction of Cr(VI) as it passes through the barrier. As with the abiotically produced barrier, the capacity of the biotically produced barrier depends on the number of moles of reduced iron and sulfide present in the barrier. Reduced iron processes are the same as those described above for the abiotic technology description. Amorphous iron sulfide produced by sulfate reduction has also been shown to reduce Cr(VI) (Patterson and Fendorf 1997). The dominant reaction appears to be:



whereby the reduction product is a mixed Cr, Fe precipitate that is also produced under reduced iron conditions. Compared to the rate of direct enzymatic reduction of Cr(VI), reduction by Fe(II) or sulfide appear to be significantly faster (Wielinga et al. 2001). However, microbial processes can play a key role in producing and maintaining reduced iron and sulfide in the aquifer.

2.3.3 Sulfate Reduction Process

Sulfate-reducing bacteria produce hydrogen sulfide (H_2S) by coupling the reduction of sulfate to the oxidation of organic compounds (e.g., lactate, acetate, ethanol) or hydrogen (Widdel 1988). Hydrogen sulfide is highly reactive, causing the reductive dissolution of some amorphous and poorly crystalline Fe(III) oxides (e.g., ferrihydrite) and the subsequent precipitation of the Fe(II) as amorphous FeS (Matsunaga et al. 1993). The reduction of structural Fe(III) in layer silicates without dissolution may also occur (Gan et al. 1992). These reduced phases store reductive capacity in sediments and subsequently can reduce soluble contaminants such as Cr(VI) to form insoluble precipitates (Amonette et al. 1994; Fredrickson and Gorby 1996; Deng and Stone 1996). Additionally, H_2S may directly reduce metallic contaminants such as Cr(VI) (Kim et al. 2001; Bidoglio et al. 1993).

The metabolic activity of sulfate reducers is not limited to the reduction of sulfate. Sulfate reducers may also directly reduce Cr(VI) (Lovley and Phillips 1994) resulting in formation of insoluble compounds. Structural Fe may also be reduced directly as an electron acceptor for sulfate reducers (Coleman et al. 1993; Lovley 1994) creating reactive sites for contaminant reduction. In this way, sulfate reducers perform the same function as other Fe(III) reducers such as *Shewanella* sp. or *Geobacter metallireducens*. Sulfate reduction and the direct reduction of Fe(III) can occur simultaneously depending on how labile the Fe(III) is to microbial reduction (Lovley and Phillips 1987).

In addition to possessing the capability for both direct and indirect metal reduction, sulfate reducing organisms have also shown a remarkable ability to withstand high concentrations of toxic heavy metals. The minimum inhibitory concentration of Cr(VI) on pure sulfate reducer cultures were observed to range from 0.7 to 1.4 mM (35 to 70 mg/L) (Karnachuk 1995) indicating that Cr(VI) concentrations in this range would have little to no effect on sulfide production. Sulfate reducer consortia have been shown to reduce Cr(VI) to Cr(III) as amorphous precipitates at concentrations up to 2,000 ppm and to simultaneously precipitate mixtures of Cr(VI) with U(VI) or Zn (Fude et al. 1994).

The pH of the aquifer will tend to increase during active sulfate reduction and decrease during sulfide oxidation. The extent of this change is related to buffering by carbonate-or hydroxide-containing minerals (Walter et al. 1994). Dissolution of iron sulfide will tend to increase the pH.

2.3.4 Biotic Iron Reduction Process

Some bacteria are able to couple oxidation of hydrogen or organic compounds to the reduction of Fe(III), thereby gaining energy for growth. Some of the common Fe(III) reduction reactions catalyzed by these organisms are outlined by Lovley (1994). These bacteria perform what is termed dissimilatory iron reduction and are comprised of species from several different genera, including *Geobacter*, *Desulfuromonas*, *Pelobacter*, *Shewanella*, *Ferrimonas*, *Geovibrio*, *Geothrix*, and *Bacillus* (Fredrickson and Gorby 1996). Also of note is that *Desulfovibrio* spp., may be important catalysts of Fe(III) reduction in the environment (Coleman et al. 1993). These bacteria, grouped together by their ability to perform dissimilatory iron reduction, have a broad spectrum of other metabolic capabilities. For instance, *Shewanella alga* can use O_2 , NO_3^- , U(VI), Mn(IV), and Fe(III) as electron acceptors. *Desulfovibrio desulfuricans* is a well-known sulfate reducing bacteria, but can also use Fe(III), U(VI), and Cr(VI) as electron acceptors (Lovley and Phillips 1992, 1994).

Dissimilatory iron reducing bacteria and other species such as *Desulfovibrio* sp. Have potential for use in bioremediation as a result of 1) the reduction of mineral-associated Fe(III) to produce reactive sites

within these minerals and 2) the direct reduction of contaminants such as U and Cr. The capability to reduce structure Fe(III) in minerals has been established for a number of species in the genera listed above. The Fe(III) in minerals such as amorphous and poorly crystalline Fe (e.g., ferrihydrite) (Lovley 1991, 1994; Coleman et al. 1993), crystalline Fe-oxides/hydroxides (e.g., hematite, goethite, and magnetite) (Arnold et al. 1988; DiChristina 1994; Roden and Zachara 1996; Kostka and Nealson 1995) can be microbially reduced and create the potential for subsequent Cr(VI) reduction.

3.0 Experimental Methods

3.1 Sampling

Sediment and aqueous samples were collected in accordance with requirements documented in the drilling statement of work and accompanying sampling and analysis plan. Due to the nature of the sediment samples being collected, special collection, handling, and preservation requirements were specified. Specifically, samples used for biologic analysis were collected using an aseptic sampling protocol and samples collected for the determination of naturally occurring reduced species were collected using an anoxic sampling protocol. All other samples were collected using similar methodologies, but with less stringent requirements for sample collection, handling, and preservation. Aqueous samples were collected for the determination of field parameters and a subset was submitted for laboratory analysis.

3.1.1 Sediment Physical Properties and Groundwater Analysis

The dry bulk density and porosity of Puchack sediments were measured on the intact cores, i.e., whole sediment properties. As the core samples were unpacked, the wet weight, dry weight, and core volume were used to calculate the dry bulk density and porosity. When necessary, glass beads or boiling chips were used to compensate for the “missing” volume of the sediment cores that were not fully packed which was corrected for when calculating the bulk density and porosity. The sediment samples were oven dried at 45°C until constant weight.

The sediment size fractions were determined by American Society for Testing and Materials (ASTM) sieve analysis (18 sediments) and additionally by hydrometer analysis to accurately determine the clay fraction (10 samples). The entire sediment size fraction was not used in laboratory experiments since large cobbles exhibit essentially no geochemical control (i.e., the surface area of gravels are extremely small relative to clays), and experiments of this scale would not be practical. For example, a sediment oxidation experiment (described below) requires 1,200 pore volumes and would take a considerable amount of time with a column containing the full sediment size fraction. Thus, only the <4 mm size fraction was used. Composite sediments were made from a range of different sediment cores. The composite sediments were analyzed using x-ray diffraction (XRD). The total carbon content, inorganic and organic (by difference), was also determined for some of the sediments used in this study.

3.1.2 Groundwater Analyses

Groundwater analyses were conducted in the field, these included hexavalent chrome using the HACH method 8023 and ferrous iron using HACH method 8146. Total chrome and organic compounds were analyzed for using inductively coupled plasma-mass spectrometry (ICP-MS) at off-site laboratories. In a previous EPA report (*Bench-Scale Tests for Evaluation of In Situ Technologies for Chromium and Volatile Organic Compounds in Groundwater* (Vermeul et al. 2004) a series of chemical analysis were carried out on Puchack groundwater and this data was used to design a synthetic groundwater.

The Ferrozine (Gibs 1976) colormetric method was used to analyze for Fe(II) at $\lambda=562$ in all of the Puchack groundwater samples received. This method is kinetically controlled, once initially formed (10 minutes) absorbance was measured (standards and samples) within 10 minutes.

3.2 Column Experiments

3.2.1 Sediment Reduction by Dithionite

Sediment reduction studies conducted in 1-D columns consisted of injecting a dithionite solution (0.09 mol/L dithionite and 0.36 mol/L K_2CO_3) at a steady rate into a sediment column for 120 hours. The flux rate was chosen to achieve a specific residence time of the dithionite solution in the column (≈ 5 hours) relative to the reduction rate. Dithionite was measured using an automated dilution/UV analysis system (Szecsody et al. 2004; Patent 6,706,527). The dry bulk density and porosity of the column were calculated from the dry and saturated column weight and column volume. The volumetric flow rate was calculated from the effluent volume and elapsed time. The electrical conductivity of the column effluent provided a second (dynamic) measure of the porosity, and was measured using a flow-through electrode and automatic data logging (Figure 3.1). While these experiments provide data of the mass of reduced iron in the sediments, the method is more complex and less accurate than oxidizing sediments with dissolved oxygen (described below). A maximum of five automated systems were operating simultaneously to reduce the sediments.

The process by which dithionite is manufactured (either zinc or formate process) impacts the concentration of metals in the dithionite. In general, the formate process produces more pure dithionite, and is used for field scale injection experiments. Dithionite produced with the zinc process was used for laboratory experiments, due to availability (from Fischer Scientific), as formate-process dithionite is generally only available in large quantities. A brief description of two processes for manufacturing dithionite is provided below.

There are two different processes to manufacture sodium dithionite, the zinc process and formate process. In the zinc process, one mole of powdered zinc is dissolved in water. This reacts with two moles of sulfur dioxide bubbling through the solution to produce one mole of zinc dithionite. Adding two moles of caustic will yield one mole of sodium dithionite plus one mole of zinc oxide precipitate plus one mole of water. A filter press is used to remove the zinc oxide. This process will yield about a 14% sodium dithionite solution. Because the powdered zinc usually contains small amounts of lead, sodium dithionite produced from the zinc process contains higher trace levels of lead and other heavy metals than the formate process.



Figure 3.1. Fraction Collection of Column Effluent into Anaerobic Vials

The electrical conductivity of the column effluent provided a second (dynamic) measure of the porosity, and was measured using a flow-through electrode and automatic data logging (Figure 3.1). While these experiments provide data of the mass of reduced iron in the sediments, the method is more complex and less accurate than oxidizing sediments with dissolved oxygen (described below). A maximum of five automated systems were operating simultaneously to reduce the sediments.

In the formate process, one mole of sodium formate is reacted with one mole of 50% caustic and two moles of sulfur dioxide to produce one mole of sodium dithionite plus one mole of water and one mole of carbon dioxide.



Typically methanol is added to make a water/methanol solution, which increases evaporation of the solution leaving solid sodium dithionite in a powder form.

This formate process produces the highest quality sodium dithionite solutions, formate produced sodium dithionite has been found to have the lowest trace metals content.

	MRL (ppm)	Typical		MRL (ppm)	Typical
Al	5	6	Fe	2	3
As	0.2	ND	Pb	0.02	ND
Ba	1	ND	Mn	1	ND
Cd	0.02	0.18	Ni	2	ND
Cr	0.1	0.4	Ag	1	ND
Cu	1	ND	Zn	1	ND

The solid or powder form of dithionite is classified spontaneously combustible, but if you handle it properly, it has excellent shelf life and can be transported safely and economically anywhere in the country. The liquid form of sodium dithionite is classified by U.S. Department of Transportation (DOT) as non-hazardous. It is, however, time and temperature sensitive. It is a very powerful reducing agent, which will react with the oxygen in the air. Therefore, a non-reactive gas (argon) is needed in the void space between the liquid surface and the top of the shipping container. The sodium dithionite solution is typically trucked at between 3.5°C to 4.5°C. If the temperature of the solution gets above 10°C, the sodium dithionite will start to decompose at a fairly rapid rate. If the solution temperature is allowed to rise above 15°C the decomposition rate is greatly accelerated until you lose all reactivity.

3.2.2 Sediment Oxidation with Dissolved Oxygen

Sediment oxidation studies were also conducted in 1-D columns to determine the rate at which the dithionite-reduced sediments are oxidized and to measure the mass of reduced iron (i.e., redox capacity). These experiments consisted of injecting oxygen-saturated (8.4 mg/L) water at a steady rate (typically 2 pore volumes per hour) into a reduced sediment column and measuring the concentration of dissolved oxygen over time in the effluent for 300 to 800 hours. The flux rate was chosen to achieve specific residence times of the dissolved oxygen in the column relative to the oxidation rate(s) of the sediment. A series of in-line micro-electrodes were used to monitor geochemical changes during oxidation and included dissolved oxygen (with 2 electrodes), pH, and electrical conductivity. Electrode measurements were continuously monitored, averaged, and data logged at 2 to 5 minute intervals using an automated fluid measurement and control system (U.S. Patent 6,438,501; J. Szecsody, M. Williams, V. Vermeul; Figure 3.2). A two-point calibration was conducted on the in-line oxygen electrodes at 4- to 8-hour intervals (oxygen-free and oxygen-saturated solutions) using the automated system. The electrode data from the calibrations were also data logged. The mass of reduced iron that was oxidized was calculated from the oxygen breakthrough curves. The difference in the total mass of dissolved oxygen injected minus dissolved oxygen in the effluent is that consumed by ferrous iron. This oxygen breakthrough

analysis assumes dynamic equilibrium, or that all of the reduced iron has been oxidized in the column. In many cases, there is a fraction of the sediment that has not been oxidized, so some error in estimating the un-reduced fraction is introduced.

To establish the mobility of trace metals during sediment reduction and oxidation, aqueous effluent samples from some of the reduction and oxidation column experiments were analyzed for trace metals by ICP-MS.

3.2.3 Chromium Transport in Untreated Sediments

Sediment transport studies of chromium (III/VI) were also conducted in 1-D columns as a function of pH. These experiments consisted of injecting pH adjusted tap water with a mixture of chromium (III/VI) into columns made from shallow composite 36/37 sediment at a steady rate with periodic sampling for several pore volumes (6-400PV/several days to 3 weeks). The effluent samples were then analyzed for total chromium by ICP-MS and Chrome(VI) using 1,5 diphenylcarbazide, (DPC), EPA Method 7196A for the low pH experiments and by DPC only for experiments where the pH > 6 (no aqueous chrome(III) in solution).

3.2.4 Chromate Transport in Reduced Sediments

Chromate transport studies of dithionite (see above) reduced shallow composite 36/37 sediment were also conducted in 1-D columns as a function of pH. The sediment columns were pH adjusted to the desired pH with either pipes or phthalate buffer. pH adjusted chromate-laden ($2 \mu\text{mol/L}$) deionized water was used as the injection solution, which was injected at a steady rate for 400 to 450 pore volumes (≈ 2 months). Samples were collected over 8 hours ($\approx 1\text{PV}$) every 24 hours and analyzed for chromate using DPC.

3.3 Batch Experiments

3.3.1 Chromate Adsorption Edge

The chromate adsorption was investigated as a function of pH, ionic strength and time on the untreated D1-H (220 ft), D2-H (271 ft), and deep composite 1 sediment (DC-1). The sediment was first equilibrated at the desired pH with a soil-to-water ratio (r_{sw}) of 0.25 and 0.5 (5g sediment/10 ml water) with either Puchack groundwater, synthetic Puchack groundwater or de-ionized water, and then the chromate was added. Samples were taken as a function of time, filtered through a $0.2\text{-}\mu\text{m}$ filter and analyzed for chromate using DPC. The potential effects of filtration were also investigated as a function of filter pore size.



Figure 3.2. Sediment Column Oxidation System with Automated Calibration of Oxygen Electrodes

The influence of SO_4 on chromate adsorption was also investigated on the MW36 and 37 composite sediment at pH 6.3 and a r_{sw} of 0.5. The sediment pH was allowed to equilibrate on a mechanical end-to-end mixer for several days before the addition of either sulfate or chromate. Sodium sulfate was then added at the desired concentration and allowed to equilibrate on the end-to-end mixer for 1 hour. Chromate was then added and allowed to mix for 3 hours, sampled and filtered with a 0.2 μm syringe filter then analyzed for chromate using DPC. The effect of SO_4 on the chromate analysis using DPC was investigated as a potential interference along with the presence of chromium(III).

3.3.2 Chromate Adsorption Isotherm

The adsorption isotherm of chromate at pH 5.6 was investigated using the deep composite sediment at a r_{sw} of 0.25. The initial pH of the sediment/chromate mixture was adjusted to 5.6 then readjusted at 2 and 4 hours. The sediment samples were then left to equilibrate for 24 hours. The pH was taken again and the samples were passed through a 0.2- μm syringe filter and analyzed for chromate using DPC.

3.3.3 Natural Attenuation Studies

The natural reduction ability of Puchack sediments was studied with a range of sediment and composite sediment samples under anoxic (purged with He) and oxic conditions. Chromate concentrations ranging from 1.8 to 5.5 mg/L, pH buffered to 7.5 with 0.01 M pipes buffer, with a r_{sw} of ≈ 0.08 , were used in this study. Sampling was carried out as a function of time with the aide of a needle tipped syringe, given that these experiments were carried out in rubber stopped septa bottles to control final O_2 concentrations, and then filtered though a 0.2 μm syringe tip filter. Samples were then analyzed for chromate using DPC.

The influence of organic carbon on chromate adsorption was also investigated on NRS-1 (D1-272 ft) under an anoxic environment (in a glove box). Approximately 17 g of NRS-1 sediment was added to 100 ml of 0.05 M NaNO_3 /0.132 M NaOH solution resulting in a suspension pH of 11.7. The suspension was then stirred while heating (85 to 90°C) for a period of 4 hours then left to cool overnight. A Bruker, Fourier Transform Infra-Red Spectrometer (FTIR), IFS66 was used to obtain an infrared spectrum to confirm the presence of NOM in the filtrate obtained from the base treatment process. The base treated sediment was washed several times over a period of 10 days with deionized water using a Sorvall RC5C centrifuge, the samples were allowed to mix on a mechanical end-to-end mixer between subsequent washes. After the final wash (supernatant was colorless) the sediment was transferred to a septa top bottle (to eliminate possible O_2 contamination) and weighed. Chromate (4.0688 mg/L, 4.8388 mg/L for the control), pH buffered to 7.5 with 0.01 M pipes buffer, with a dry sediment r_{sw} of 0.37 (0.31 for the control) was then added and allowed to equilibrate on the mechanical end-to-end mixer between samples. Samples were taken as a function of time with the aide of a needle tipped syringe and filtered with a 0.22 μm syringe tip filter then analyzed for chromate using DPC. Since the base treated sediment was wet after treatment the actual mass of sediment used was obtained upon completion of the batch experiment by determining the density of the residual soil suspension. This was obtained by determining the water content of the suspension, for both the base treated and the control, by oven drying at 45°C until constant weight (≈ 3 days). The intrinsic moisture of the sediment was also taken into account when calculating the mass of sediment present in the initial base treated suspension used for the chromate batch experiment. The initial chromate concentration was also adjusted to accommodate the presence of this excess water in the base treated sediment.

3.3.4 Iron Extractions of Treated and Untreated Sediments

Geochemical analysis of sediment samples was conducted to determine the amounts of various Fe(II/III) phases. These included five different methods of iron extraction (Heron et al. 1994): a) 0.5-M hydrochloric acid (HCl), b) ammonium oxalate, c) dithionite-citrate-bicarbonate (DCB), d) 5-M HCl, and e) 1-M CaCl₂. Ferrozine (Gibbs 1976) was used to quantify the aqueous Fe(II) and Fe_{total} from the extractions, where Fe_{total} (Fe(II) + Fe(III)) samples reduced aqueous Fe(III) to Fe(II) by 0.025-M NH₂OH, HCl. Extracted Fe(III) was obtained from the difference between Fe_{total} minus Fe(II). The ion exchangeable (adsorbed) Fe(II) was defined by the 1-M CaCl₂ extraction and FeCO₃/FeS phases were defined by the 0.5-M HCl extraction for 1 hour. Amorphous and poorly crystalline Fe(III) oxides were defined by the extraction using ammonium oxalate for 24 hours and crystalline Fe(III) oxides were defined by DCB extraction for 24 hours minus the ammonium oxalate extraction. Total Fe(II) and Fe(III) oxides were obtained by extraction with 5-M HCl for 3 weeks.

3.4 Biotic Studies

3.4.1 Sediments

The core samples used for biotic studies were from boreholes MW-36 and MW-37 at depths ranging from 151.5 to 211 feet. These samples were selected to represent the two hydrogeologic layers of interest, the Intermediate Sand and Lower Aquifer (upper zone).

3.4.2 Microbial Batch Tests

A modified Geobacter medium (Coates et al. 1996) with Fe(III)NTA (ferric nitrilotriacetic acetate) (10 mM) as the electron acceptor, was used for culturing iron-reducing bacteria (IRB; Appendix G). Fresh Fe(III)NTA medium has a clear amber color. The medium turns clear and colorless with whitish precipitates when Fe(III) is reduced to Fe(II) compounds, such as Fe(II) carbonate (gray, siderite) or Fe(II) orthophosphate (white/brown, vivianite). Postgate Medium B, as modified by us, was used for growing SRB (Appendix G). Presence of SRB is identified by the blackening of the medium due to iron sulfide produced from the reaction of iron with hydrogen sulfide that is produced when sulfate is reduced by SRB.

The most probable number (MPN) method (Alexander 1982) was employed to estimate IRB and SRB population densities using a 10-fold dilution (10⁻² to 10⁻⁷) with 5 tubes at each dilution. The MPN technique was applied for one sediment sample in the Intermediate Sand and one sediment sample in the Lower Aquifer. Initially, 10 g of sediments were transferred to 95 ml of homogenizing solution (0.1% pyrophosphate, pH 7.0) and shaken vigorously for 10 minutes. Subsequent 10-fold dilutions were prepared using phosphate-buffered-saline (Appendix G). All eight sediment samples were assayed in direct enrichment treatments with 1 g sediment per 10 ml culturing medium for IRB and SRB and with 30 g of sediment in 30 mL of culturing medium for SRB.

Pure cultures of *Geobacter metallireducens* GS-15 (ATCC 53774) and *Desulfovibrio vulgaris* (ATCC 29579) were used as positive controls for IRB and SRB, respectively. Their densities were determined by acridine orange direct count technique. Three levels of cell densities for these cultures (low, medium, and high cells) were used for the positive controls. All inoculation and transfers were performed inside an anaerobic glove box or using standard anaerobic culturing techniques (Coates et al. 1996). Stationary incubation was carried out at ambient temperature in the dark.

4.0 Results

4.1 Sediment and Aqueous Sample Collection

This section provides a brief description of the samples that were collected to support these treatability studies and a summary of the sediment physical property data and groundwater chemistry data that was collected. A detailed discussion of these sampling activities is provided in a treatability study sample collection report (CDM 2005).

4.1.1 Sediment Sample Collection

Aquifer core samples were collected during the installation of four characterization borings at the Puchack Well Field site, two of which were completed as monitoring wells 36 (MW-36 and MW-37). The other two downgradient borings (D-1 and D-2) were not completed as monitoring wells. In total, 157 sediment cores samples were collected. The aquifer unit and collection depth interval for each core sample are provided in Tables 4.1 through 4.4 along with the date collected and the planned analysis type (i.e., microbial, physical property, and geochemical). A detailed description of sampling locations, field activities, and operational procedures is provided in CDM (2005).

4.1.2 Sediment Physical Property Analysis

Physical property analysis was conducted on 37 of the core sediment samples obtained (Table 4.5), including characterization of the < 4-mm fraction, bulk density, and porosity. In addition, sediment particle size analysis was performed on 18 of the samples, three of which are shown in Figures 4.1 through 4.3. The remaining particle size analysis results are provided in Appendix A. Particle size distributions for monitoring well 37 have been used to highlight the variability in the particle size of the intermediate sand (C2AI) and the lower aquifer units (A3a). Particle-size distributions were not performed on the confining units between the intermediate sand and the lower aquifer units, i.e., clay. From the figures (Figure 4.1, 4.2, and 4.3), we can see that as we approach the aquitard the amount of clay and silt present in the intermediate sand increases (Figure 4.1 and 4.2) to approximately 20% and then tails off to about 5% for the upper portion of the lower aquitard (Figure 4.3). With the exception of one sample, all samples used in this study contained less than 16% silt and clay, with two of the four wells containing less than 5.5% silt and clay (D-1 and D-2). A representative sample from the sediments of all four wells contains less than 2% clay. Bulk density and porosity data are also given on Table 4.5, the average bulk density and porosity of all samples analyzed was $1.917 \pm 0.147 \text{ cm}^3/\text{g}$ and $28.6 \pm 8.6\%$, respectively.

Most of the clay and silty clay sample designations indicated in Table 4.5 are from depth intervals near the contact between aquifer and aquitard units. However, in some cases (e.g., sample MW-37S-I), a clay sample was obtained from within an aquifer unit (as designated by the field geologist logging the borehole) indicating that discontinuous clay lenses may be present within the delineated aquifer units. Detailed characterization of the spatial distribution of clay lenses within the various aquifer units was not within the scope of this study, and would likely require further characterization prior to pilot scale field testing of in situ technologies at the site.

Table 4.1. Aquifer Core Samples for Well MW-36

Borehole	Aquifer Unit	Start Depth (ft)	End Depth (ft)	Sample No.	Analysis (sample type)	Date Collected
MW-36	A2a	80.0	80.5	MW-36S-A	Micro	6/28/04
MW-36	A2b	108.5	109.0	MW-36S-B		
MW-36	A2b	109.0	109.5	MW-36S-B	Phys	6/28/04
MW-36	A2b	109.5	110.0	MW-36S-B	Micro	6/28/04
MW-36	C2AI	150.5	151.0	MW-36S-C	GeoChem	6/28/04
MW-36	C2AI	151.0	151.5	MW-36S-C	Phys	6/28/04
MW-36	C2AI	151.5	152.0	MW-36S-C	Micro	6/28/04
MW-36	C2AI	158.5	159.0	MW-36S-D	Phys	6/29/04
MW-36	C2AI	159.0	159.5	MW-36S-D	Micro	6/29/04
MW-36	C2AI	159.5	160.0	MW-36S-D	GeoChem	6/29/04
MW-36	C2AI	162.0	162.5	MW-36S-E	Micro	6/29/04
MW-36	C2AI	162.5	163.0	MW-36S-E	Phys	6/29/04
MW-36	C2AI	163.0	163.5	MW-36S-E	GeoChem	6/29/04
MW-36	C2AI	167.0	167.5	MW-36S-F	Micro	6/29/04
MW-36	C2AI	167.5	168.0	MW-36S-F	GeoChem	6/29/04
MW-36	C2AI	172.0	172.5	MW-36S-G	GeoChem	6/29/04
MW-36	C2AI	172.5	173.0	MW-36S-G	Micro	6/29/04
MW-36	A3a	189.0	189.5	MW-36S-H	Micro	6/30/04
MW-36	A3a	196.5	197.0	MW-36S-I	Phys	6/30/04
MW-36	A3a	197.0	197.5	MW-36S-I	GeoChem	6/30/04
MW-36	A3a	197.5	198.0	MW-36S-I	Micro	6/30/04
MW-36	A3a	200.5	201.0	MW-36S-J	GeoChem	6/30/04
MW-36	A3a	201.0	201.5	MW-36S-J	Micro	6/30/04
MW-36	A3a	204.5	205.0	MW-36S-K	GeoChem	7/6/04
MW-36	A3a	205.0	205.5	MW-36S-K	Micro	7/7/04
MW-36	A3a	205.5	206.0	MW-36S-K	Phys	7/6/04
MW-36	A3b	210.0	210.5	MW-36S-L	Phys	7/7/04
MW-36	A3b	210.5	211.0	MW-36S-L	Micro	7/7/04
MW-36	A3b	211.0	211.5	MW-36S-L	GeoChem	7/7/04
MW-36	A3b	220.0	220.5	MW-36S-M	GeoChem	7/7/04
MW-36	A3b	220.5	221.0	MW-36S-M	Micro	7/7/04
MW-36	A3b	221.0	221.5	MW-36S-M	Phys	7/7/04
MW-36	A3b	228.5	229.0	MW-36S-N	GeoChem	7/7/04
MW-36	A3b	229.0	229.5	MW-36S-N	Micro	7/7/04
MW-36	A3b	229.5	230.0	MW-36S-N	Phys	
MW-36	A3c	238.5	239.0	MW-36S-O	GeoChem	7/8/04
MW-36	A3c	239.0	239.5	MW-36S-O	Micro	7/8/04
MW-36	A3c	229.5	230.0	MW-36S-O	Phys	
MW-36	A3c	252.5	253.0	MW-36S-P	GeoChem	7/8/04
MW-36	A3c	253.0	253.5	MW-36S-P	Micro	7/8/04
MW-36	A3c	253.5	254.0	MW-36S-P	Phys	
MW-36	A3c	267.0	267.5	MW-36S-Q	GeoCChem	7/9/04
MW-36	A3c	267.5	268.0	MW-36S-Q	Micro	7/9/04

Table 4.2. Aquifer Core Samples for Well MW-37

Borehole	Aquifer Unit	Start Depth (ft)	End Depth (ft)	Sample No.	Analysis (sample type)	Date Collected
MW-37	A2a	80.5	81.0	MW-37S-A	GeoChem	6/9/04
MW-37	A2a	81.5	82.0	MW-37S-A	Phys	6/9/04
MW-37	A2a	81.5	82.0	MW-37S-A	Micro	6/9/04
MW-37	A2b	118.5	119.0	MW-37S-B	Micro	6/10/04
MW-37	A2b	119.0	119.5	MW-37S-B	GeoChem	6/10/04
MW-37	C2AI	153.0	153.5	MW-37S-A	Phys	6/14/04
MW-37	C2AI	154.0	154.5	MW-37S-C	GeoChem	6/14/04
MW-37	C2AI	161.5	162.0	MW-37S-D	GeoChem	6/15/04
MW-37	C2AI	162.0	162.5	MW-37S-C	Phys	6/15/04
MW-37	C2AI	167.5	168.0	MW-37S-E	Micro	6/15/04
MW-37	C2AI	168	168.5	MW-37S-E	Phys	6/15/04
MW-37	C2AI	168.5	169.0	MW-37S-E	GeoChem	6/15/04
MW-37	C2AI	171.0	171.5	MW-37S-F	Micro	6/22/04
MW-37	C2AI	171.5	172.0	MW-37S-F	GeoChem	6/22/04
MW-37	A3a	190.0	190.5	MW-37S-G	Micro	6/22/04
MW-37	A3a	190.5	191.0	MW-37S-G	GeoChem	6/22/04
MW-37	A3a	191.0	191.5	MW-37aS-G	Phys	6/22/04
MW-37	A3a	194.0	194.5	MW-37S-H	Micro	6/22/04
MW-37	A3a	194.5	195.0	MW-37S-H	GeoChem	6/22/04
MW-37	A3a	198.0	198.5	MW-37S-I	Micro	6/22/04
MW-37	A3a	199.0	199.5	MW-37S-I	GeoChem	6/22/04
MW-37	A3a	198.5	199.0	MW-37S-I	Phys	6/22/04
MW-37	A3a	204.0	204.5	MW-37S-J	GeoChem	6/23/04
MW-37	A3a	204.5	205.0	MW-37S-J	Micro	6/23/04
MW-37	A3a	205.0	205.5	MW-37S-J	Phys	6/23/04
MW-37	A3a	210.0	210.5	MW-37S-K	Phys	6/23/04
MW-37	A3a	210.5	211.0	MW-37S-K	GeoChem	6/23/04
MW-37	A3a	211.0	211.5	MW-37S-K	Micro	6/23/04
MW-37	A3a	216.5	217.0	MW-37S-L	GeoChem	6/23/04
MW-37	A3a	217.0	217.5	MW-37S-L	Phys	6/23/04
MW-37	A3a	217.5	218.0	MW-37S-L	Micro	6/23/04
MW-37	A3b	224.5	225.0	MW-37S-M	Micro	6/23/04
MW-37	A3b	225.0	225.5	MW-37S-M	GeoChem	6/23/04
MW-37	A3b	231.0	231.5	MW-37S-N	Micro	6/24/04
MW-37	A3b	231.5	232.0	MW-37S-N	GeoChem	6/24/04
MW-37	A3c	238.0	238.5	MW-37S-O	Phys	6/24/04
MW-37	A3c	238.5	239.0	MW-37S-O	GeoChem	6/24/04
MW-37	A3c	239.0	239.5	MW-37S-O	Micro	6/24/04
MW-37	A3c	247.0	247.5	MW-37S-P	GeoChem	6/24/04
MW-37	A3c	247.5	248.0	MW-37S-P	Micro	6/24/04
MW-37	A3c	257.0	257.5	MW-37S-Q	Micro	6/25/04
MW-37	A3c	257.5	258.0	MW-37S-Q	GeoChem	6/25/04
MW-37	A3c	266.5	267.0	MW-37S-R	Micro	6/25/04
MW-37	A3c	267.0	267.5	MW-37S-R	Phys	6/24/04
MW-37	A3c	267.5	268.0	MW-37S-R	GeoChem	6/25/04

Table 4.3. Aquifer Core Samples for Well D-1

Borehole	Aquifer Unit	Start Depth (ft)	End Depth (ft)	Sample No.	Analysis (sample type)	Date Collected
D-1	A2a	80.5	81.0	D-1S-A	Phys	7/24/04
D-1	A2a	81.0	81.5	D-1S-A	GeoChem	7/24/04
D-1	A2a	81.5	82.0	D-1S-A extra	GeoChem	7/24/04
D-1	A2b	105.0	105.5	D-1S-B extra	GeoChem	7/24/04
D-1	A2b	105.5	106.0	D-1S-B	GeoChem	7/24/04
D-1	A2b	106.0	106.5	D-1S-B	Phys	7/24/04
D-1	C-2AI	155.0	155.5	D-1S-C	Phys	7/25/04
D-1	C-2AI	155.5	156.0	D-1S-C	GeoChem	7/25/04
D-1	C-2AI	158.5	159.0	D-1S-D	GeoChem	7/25/04
D-1	C-2AI	159.0	159.5	D-1S-D	Microbial	7/25/04
D-1	C-2AI	161.5	162.0	D-1S-E	GeoChem	7/25/04
D-1	C-2AI	162.0	162.5	D-1S-E	Phys	7/25/04
D-1	C-2AI	162.5	163.0	D-1S-Eextra	GeoChem	7/25/04
D-1	C-2AI	164.5	165.0	D-1S-F	Phys	7/26/04
D-1	C-2AI	165.0	165.5	D-1S-F	GeoChem	7/26/04
D-1	A3a	205.0	205.5	D-1S-G	GeoChem	7/27/04
D-1	A3a	205.5	206.0	D-1S-G	Microbial	7/27/04
D-1	A3b	220.0	220.5	D-1S-H	GeoChem	8/2/04
D-1	A3b	220.5	221.0	D-1S-H	Phys	8/2/04
D-1	A3b	221.0	221.5	D-1S-H	Micro	8/2/04
D-1	A3b	221.5	222.0	D-1S-H extra	GeoChem	8/2/04
D-1	A3b	225	225.5	D-1SI extra	GeoChem	8/2/04
D-1	A3b	225.5	226.0	D-1S-I	GeoChem	8/2/04
D-1	A3c	226.0	226.5	D-1S-I	Phys	8/3/04
D-1	A3c	240.5	241.0	D-1S-J	Phys	8/4/04
D-1	A3c	241.0	241.5	D-1S-J extra	GeoChem	8/4/04
D-1	A3c	241.5	242.0	D-1S-J	Micro	8/4/04
D-1	A3c	242.0	242.5	D-1S-J	GeoChem	8/4/04
D-1	A3c	251.5	252.0	D-1S-K	GeoChem	8/4/04
D-1	A3c	252.5	253.0	D-1S-K	Phys	8/4/04
D-1	A3c	260.5	261.0	D-1S-L	Phys	8/4/04
D-1	A3c	261.0	261.5	D-1S-L	Micro	8/4/04
D-1	A3c	261.5	262.0	D-1S-L	GeoChem	8/4/04
D-1	A3c	270.0	270.5	D-1S-M	Phys	8/5/04
D-1	A3c	270.5	271.0	D-1S-M	GeoChem	8/5/04
D-1	A3c	272.0	272.5	D-1S-M extra	lignite/pyrite	8/5/04

Table 4.4. Aquifer Core Samples for Well D-2

Borehole	Aquifer Unit	Start Depth (ft)	End Depth (ft)	Sample No.	Analysis (sample type)	Date Collected
D-2	A2a	92.5	93.0	D-2S-A	Phys	7/12/04
D-2		93.0	93.5	D-2S-A	GeoChem	7/12/04
D-2	A2b	130.0	130.5	D-2S-B	Phys	7/13/04
D-2	A2a	130.5	131.0	D-2S-B	GeoChem	7/13/04
D-2	A2b	150.0	150.5	D-2S-C extra	Phys	7/13/04
D-2	A2b	151.0	151.5	D-2S-C	GeoChem	7/13/04
D-2	A2b	150.5	151.0	D-2S-C	Phys	7/14/04
D-2	C2AI	208.5	209.0	D-2S-D	GeoChem	7/14/04
D-2	C2AI	210.5	211.0	D-2S-E	GeoChem	7/14/04
D-2	C2AI	211.0	211.5	D-2S-E	Phys	7/14/04
D-2	C2AI	211.5	212.0	D-2S-E extra	Phys	7/14/04
D-2	A3a	260.0	260.5	D-2S-F		7/20/04
D-2	A3a	260.5	261.0	D-2S-F	GeoChem	7/20/04
D-2	A3a	261.0	261.5	D-2S-F	Phys	7/20/04
D-2	A3a	265.0	265.5	D-2S-G	GeoChem	7/20/04
D-2	A3a	265.5	266.0	D-2S-G	Micro	7/20/04
D-2	A3a	266.0	266.5	D-2S-G	Phys	7/19/04
D-2	A3a	270.0	270.5	D-2S-H	GeoChem	7/20/04
D-2	A3a	270.5	271.0	D-2S-H		7/20/04
D-2	A3a	271.0	271.5	D-2S-H	Phys	7/20/04
D-2	A3a	276.0	276.5	D-2S-I	Phys	7/20/04
D-2	A3a	276.5	277.0	D-2S-I	GeoChem	7/20/04
D-2	A3b	285.5	286.0	D-2S-J	GeoChem	7/21/04
D-2	A3b	286.0	286.5	D-2S-J	Phys	7/21/04
D-2	A3b	286.5	287.0	D-2S-J		7/21/04
D-2	A3b	291.0	291.5	D-2S-K	Micro	7/21/04
D-2	A3b	291.5	292.0	D-2S-K	GeoChem	7/21/04
D-2	A3b	295.0	295.5	D-2S-L extra	Micro	7/21/04
D-2	A3b	295.5	296.0	D-2S-L	Phys	7/21/04
D-2	A3b	296.0	296.5	D-2S-L	GeoChem	7/21/04
D-2	A3b	300.5	301.0	D-2S-M	GeoChem	7/22/04
D-2	A3b	301.0	301.5	D-2S-M	Phys	7/27/04
D-2	A3b	301.5	302.0	D-2S-M extra	Micro	7/22/04

Table 4.5. Sediment Core General Physical Properties

Sample Number	Depth (ft)	Grain Size Description, Color	Bulk Density (cm ³ /g)	Grain Size: Sieve/ Hydrometer	< 4 mm (fraction)	Porosity
MW-36S-B	109	gravely sand, orange/brown	1.638	sieve	0.9942	0.329
MW-36S-C	151	fine sand with some silt, orange	1.729			0.239
MW-36S-D	156	gravely sand with trace of silt, tan		sieve/hyd.	0.9551	
MW-36S-E	163	well-sorted sand with some silt and gravel, tan	1.930	sieve/hyd.	0.9864	0.304
MW-36S-F	168	gravely sand with trace of silt, orange/tan		sieve/hyd.	0.8428	
MW-36S-I	196	well sorted sand	1.865	sieve	0.9978	0.244
MW-36S-K	206	sandy gravel, tan	1.840	sieve/hyd.	0.4118	0.281
MW-36S-L	209	clay, grey	1.811			0.307
MW-36S-M	221	fine gravely sand with some silt, tan	1.813	sieve	0.9745	0.284
MW-36S-N	230	gravely sand, tan	1.967			0.170
MW-36S-P	254	well sorted sand with some gravel, grey	1.970	sieve	0.9829	0.224
MW-37S-Aa	81	red clay and silt	1.920			0.323
MW-37S-Ab	153	interbedded clay and silty sand, tan	1.804			0.348
MW-37S-C	162.5	medium to fine sand with trace of silt, grey	1.871	sieve/hyd.	1.0000	0.330
MW-37S-D	165	coarse sand, tan	1.857			0.308
MW-37S-E	168	well-sorted sand with some gravel, grey	1.879	sieve	0.9829	0.307
MW-37S-F	171.5	sand with some silt and gravel, tan		sieve/hyd.	1.0000	
MW-37S-G	190.5	medium to fine sand with trace of silt, tan	1.787	sieve/hyd.	1.0000	0.315
MW-37S-G	191	sand with trace of gravel and silt	1.787	sieve	0.9811	0.315
MW-37S-I	198	clay, grey	1.964			0.268
MW-37S-K	210	sand with some clay, grey	1.993			0.235
MW-37S-L	217	fine sand with trace of silt, tan	1.684	sieve/hyd.	1.0000	0.367
MW-37S-O	238	gravel, tan	2.157			0.644
MW-37S-R	267	gravel with some clay	2.096			0.222
D-2S-A	93	med. to coarse sand, tan	1.951			0.226
D-2S-C	151	sand with some silt, orange	1.987			0.226
D2S-E	211	silty clay				
D-2S-F	261	gravely sand with trace of silt, grey	2.073	sieve/hyd.	0.9612	0.209
D-2S-H	271	silty sand	1.718			0.347
D-2S-J	286	silty sand, grey	1.989			0.233
D-2S-M	301	sandy gravel	2.111	sieve	0.3155	0.179
D-1S-B	106	coarse to med. sand, orange	1.911			0.273
D-1S-F	165	coarse sand, tan	1.937			0.295
D-1S-H	220	coarse to med. sand with some gravel, brown	2.101	sieve	0.9279	0.241
D-1S-J	240	well sorted sand with some silt and gravel, brown	1.894	sieve/hyd.	0.9773	0.381
D-1S-K	253	sandy gravel	2.322			0.187
D1S-M	270	silty clay, grey				
		average:	1.917 ± 0.147			0.286 ± 0.086

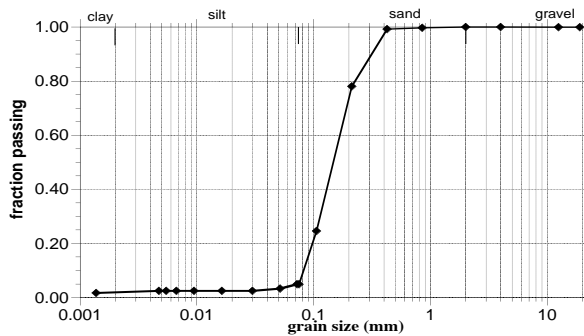


Figure 4.1. Sieve Analysis of Sediment from 162.5-ft Depth of MW-37S-C, Aquifer Unit C2AI

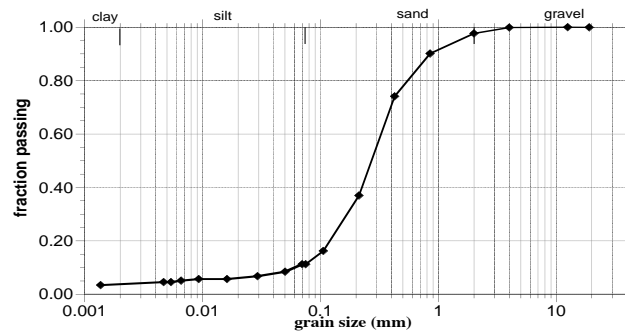


Figure 4.2. Sieve Analysis of Sediment from 171.5-ft Depth of MW-37S-F, Aquifer Unit C2AI

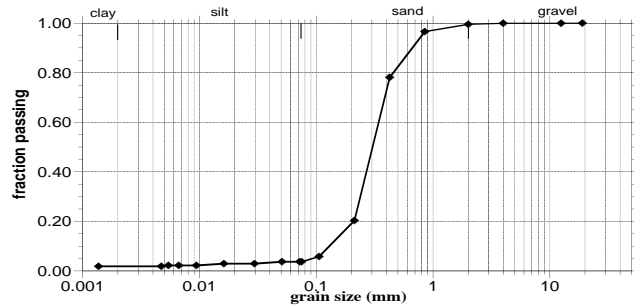


Figure 4.3. Sieve Analysis of Sediment from 190.5-ft Depth of MW-37S-G, Aquifer Unit A3a

Composite sediments were made from a range of different sediment cores in order to obtain a representative sample of the different aquifer units present at the Puchack Well Field. The compositions of the various composite sediments used in this study are given in Table 4.6. It is worth noting that the DC-1 and DC-2 sediments were used together to form composites since these wells are situated in an area that is considered uncontaminated. Sediments from MW-36 and MW-37 were combined to form composite sediment samples since both of these wells are located near the proposed site for pilot scale treatability testing of in situ technologies, which is known to be in a contaminated region of the Puchack site. Using this approach, representative samples of both uncontaminated and contaminated sediments were prepared.

Table 4.6. List of Composite Sediments

Deep composite 1 (DC-1)		Deep Composite 2 (DC-2)		MW36/37 composite		MW36/37 shallow composite		Equal parts		
equal parts		Equal parts		Equal parts		Equal parts				
D-1 & D-2		Aquifer units A3b-A3c		Aquifer units A2a-A3c		MW 36 & MW 37		Composite	MW 36	MW 37
Sample No.	Depth (ft)	Well	Depth (ft)	Sample No.	Depth (ft)	Sample No.	Depth (ft)	Name	Depth (ft)	Depth (ft)
D-1S-H	220.5-221'	D1	220-272.5'	MW 36		MW-36S-B	109-109.5'	A2a	80-80.5'	NA
D-1S-J	240.5-241'	D2	285-302'	MW 36S-A	80-80.5'	MW-36S-C	151-151.5'	A2b	108-108.5'	119-119.5'
D-1S-K	252.5-253'			MW-36S-B	108-108.5'	MW-36S-D	158.5-159'	C2AI	172-172.5'	168.5-169'
D-2S-F	260.5-261'			MW-36S-G	172-172.5'	MW-37S-C	154-154.5'	A3a	204.5-205'	199-199.5'
D-2S-H	270.5-271'			MW-36S-K	204.5-205'	MW-37S-C	162.5-163'	A3b	228.5-229'	217-217.5'
D-2S-J	285.5-286'			MW-36S-N	228.5-229'	MW-37S-F	171.5-172'	A3c	238.5-239'	267.5-268'
D-2S-M	300.5-301'			MW-36S-O	238.5-239'					
				MW 37						
				MW-37S-B	119-119.5'					
				MW-37S-E	168.5-169'					
				MW-37S-I	199-199.5'					
				MW-37S-L	217-217.5'					
				MW-37S-R	267.5-268'					

NA= sample from this aquifer was all clay, not used for the composite sediments

4.1.3 Groundwater Chemistry Analysis

A total of 40 aqueous samples were collected at various depths as the four boreholes were advance and are identified in Table 4.7. Selected field and laboratory analysis of these aqueous samples are tabulated in Table 4.8. A detailed description of samples collected, analytical methods, and analysis results is provided in a separate treatability study sample collection report (CDM 2005). Of particular interest are data from the targeted aquifer units, primarily the intermediate sands (C2AI) and the lower aquifer units (A3). There appears to have been some problems with the equipment used to obtain some of the field parameter data, in particular the dissolved oxygen (O_2 saturation is 8.4 mg/L at 25°C) and periodic malfunctioning and erroneous readings from the pH meter.

There is a considerable amount of variability in the pH range of the groundwater samples obtained ranging from 2.13 to 9.05. Monitoring well 36 appears to have the greatest variability in groundwater with the pH ranging from 2.13 to 7.36, while deep well 2 (D-2) and the second monitoring well (MW-37) appear to have circumneutral to basic groundwater (6.7 to 9.05). Given the observed problems with the pH meter, it is unclear how reliable the values obtained are. Deep well 1 (D-1) on the other hand appears to have circumneutral to acidic groundwater with a range of 2.71 to 6.79. The specific conductivity obtained for the aqueous samples is relatively uniform with an average of $0.236 \pm .097$ mS/cm. The average value obtained for the MW-36/37 monitoring wells was 0.248 ± 0.05 , while the average value for the two downgradient wells (D-1 and D-2) was 0.228 ± 0.116 mS/cm. There is a slightly more variability in the conductivity values obtained for the two downgradient wells, which showed a standard deviation twice that of the MW-36/37 monitoring wells, but over all the average value obtained was similar.

Consideration of the dissolved oxygen data in conjunction with the redox potentials provides, in some cases, corroborating evidence of the occurrence of naturally reducing conditions. For example, samples MW-37A-F, D-1A-G, D-1A-I, D-2A-D, and to a lesser extent MW-36A-A, D-1A-K, and D-2A-E show low dissolved oxygen concentrations and are well correlated with low (and sometimes negative) redox potentials. It should be noted that all of these samples also indicate high turbidity conditions during sample collection, so the reducing conditions observed may be caused in part by drilling induced effects (i.e., fresh mineral surfaces exposed during the drilling process). The amount of Fe(II) found in most of the aqueous samples is very low, <.005 mg/L, indicating that the majority of aquifer zones investigated are not highly reduced. One exception was noted deeper in the intermediate sand and lower aquifer at well D-1, where higher amounts of Fe(II) were observed. It should be noted that the dissolved oxygen and redox potentials over this depth interval are also indicative of more reducing conditions.

Groundwater samples were also analyzed for Fe(II) and Cr(VI) in the field by CDM personnel using a Hach field test kit. It should be noted that no sample dilutions were performed for these analyses, resulting in a maximum concentration detection limit of 0.66 mg/L. Comparison of these data with total chromium by ICP-MS (Table 4.8) indicates poor agreement for many of the samples. Although total chromium values can be slightly higher than Cr(VI) values due to the potential for small amounts of mobile Cr(III) in the aqueous samples (especially when not filtered), the differences observed in the collected data are not systematic and cannot be explained by this effect. Because no dilutions were performed for the Cr(VI) analysis on the higher concentration samples, a comparison of these values is not possible. Some of the low to moderate concentration samples do compare, although not very well, while others do not compare at all.

Table 4.7. Aqueous Samples Collected During Well Drilling

Borehole	Aquifer Unit	Sample Depth (ft)	Sample No.	Analysis (sample type)	Date Collected
MW-36	A2a	80	MW-36A-A	aqueous	6/28/04
MW-36	A-2b	109	MW-36A-B	aqueous	6/28/04
MW-36	C2AI	158	MW-36A-C	aqueous	6/29/04
MW-36	C2AI	170	MW-36A-D	aqueous	6/30/04
MW-36	A3a	196	MW-36A-E	aqueous	6/30/04
MW-36	A3a	204	MW-36A-F	aqueous	7/6/04
MW-36	A3b	220	MW-36A-G	aqueous	7/7/04
MW-36	A3c	252	MW-36A-H	aqueous	7/9/04
MW-40	A3c	252	MW-40A-Z	aqueous	7/9/04
MW-37	A2a	80	MW-37A-A	aqueous	6/10/04
MW-37	A2b	118	MW-37A-B	aqueous	6/10/04
MW-37	C2AI	153	MW-37A-C	aqueous	6/14/04
MW-37	C2AI	161	MW-37A-D	aqueous	6/15/04
MW-37	C2AI	167	MW-37A-E	aqueous	6/16/04
MW-37	A3a	190	MW-37A-F	aqueous	6/22/04
MW-37	A3a	198	MW-37A-G	aqueous	6/23/04
MW-37	A3a	210	MW-37A-H	aqueous	6/23/04
MW-37	A3b	224	MW-37A-I	aqueous	6/24/04
MW-37	A3c	256	MW-37A-J	aqueous	6/25/04
MW-40	C2AI	167	MW-40A-Y	aqueous	6/16/04
D-1	A2C1	80	D-1A-A	aqueous	7/24/04
D-1	A2b	105	D-1A-B	aqueous	7/24/04
D-1	C2AI	155	D-1A-C	aqueous	7/25/04
D-1	C2AI	161	D-1A-D	aqueous	7/26/04
D-1	A3a	200	D-1A-E	aqueous	7/26/04
D-1	A3b	210	D-1A-F	aqueous	7/27/04
D-1	A3b	220	D-1A-G	aqueous	8/2/04
D-1	A3b	230	D-1A-H	aqueous	8/3/04
D-1	A3c	240	D-1A-I	aqueous	8/4/04
D-1	A3c	260	D-1A-J	aqueous	8/5/04
D-1	A3c	270	D-1A-K	aqueous	8/5/04
D-2	A2a	94	D-2A-A	aqueous	7/13/04
D-2	A2C1	132	D-2A-B	aqueous	7/13/04
D-2	A2b	152	D-2A-C	aqueous	7/13/04
D-2	C2AI	209	D-2A-D	aqueous	7/14/04
D-2	C2AI	221	D-2A-E	aqueous	7/19/04
D-2	A3a	266	D-2A-F	aqueous	7/20/04
D-2	A3a	276	D-2A-G	aqueous	7/20/04
D-2	A3b	286	D-2A-H	aqueous	7/21/04
D-2	A3b	296	D-2A-I	aqueous	7/22/04

Table 4.8. Field and Laboratory Analysis of Aqueous Samples

Sample No.	PNNL Lab		CDM Supplied Field and Laboratory Data						
	Fe(II) mg/L	Cr(VI) mg/L	Cr(total) mg/L	Field pH	Spec. Cond. mS/cm ³	Turbidity	Dissolved O ₂ (mg/L)	Temp °C	Redox Potential
MW-36A-A	<DL	0	<DL	7.36	0.238	off scale	4.16	22.8	63
MW-36A-B	<DL	0.03	<DL	5.75	0.239	500	(194)	23	366
<i>MW-36A-C</i>	<DL	0.38	0.463	6.86	0.22	8.9	(18.58)	20.0	551
<i>MW-36A-D</i>	<DL	>0.66	1.37	2.13	0.196	4	6.14	18.2	369
MW-36A-E	<DL	0.16	0.228	3.51	0.286	50	(11.02)	19.5	397
MW-36A-F	<DL	>0.66	1.65	3.63	0.287	5.1	7.6	18.6	568
MW-36A-G	<DL	>0.66	1.31	(-8.22)	0.148	aq 80	5.73	24.2	596
MW-36A-H	0.012	0	<DL	6.34	0.301	47.8	5.1	18.8	363
MW-40A-Z	0.009	0	<DL						
 MW-37A-A	0.001	0	<DL						
MW-37A-B	0	0	<DL						
<i>MW-37A-C</i>	<DL	0	<DL						
<i>MW-37A-D</i>	0.047	0.01	<DL						
<i>MW-37A-E</i>	0.002	0	<DL	7.59	0.308	off scale	(13.21)	20.8	215
MW-37A-F	0.161	0	<DL	6.69	0.222	off scale	0.3	23.8	-248
MW-37A-G	0.002	0.05	0.192						
MW-37A-H	0.002	0.06	0.809						
MW-37A-I	0.002	0							
MW-37A-J	0.003	0	<DL	7.47	0.289	off scale	8.47	20.9	427
MW-40A-Y	0.002	0	<DL						
 D-1A-A	0.060	0	<DL	5.94	0.187	2.94	7.9	18.6	278
D-1A-B	<DL	0	<DL	6.79	0.213	6.54	8.63	22.9	426
<i>D-1A-C</i>	0.028	0	<DL	6.22	0.177	47	7.82	20.5	141
<i>D-1A-D</i>	0.067	0	<DL	5.67	0.154	25.1	6.89	18.7	240
D-1A-E	<DL	0	<DL	6.13	0.18	3.16	(12.71)	18.5	177
D-1A-F	0.107	0	<DL	5.89	0.131	176	3.76	20.2	283
D-1A-G	0.048	0	<DL	4.89	0.216	563	0.09	23.6	-347
D-1A-H	0.062	0	<DL	5.02	0.184	10.7	5.77	21.9	192
D-1A-I	0.278	0	<DL	4.91	0.149	off scale	0.96	20.8	-36
D-1A-J	0.102	0	<DL	5.84	0.31	off scale	4.4	18.9	222
D-1A-K	0.120	0	<DL	2.71	0.065	off scale	1.04	17.3	107
 D-2A-A	0.014	0	<DL	6.59	0.231	off scale	(14.5)	20.8	-57.5
D-2A-B	0.201	0	<DL	MNW	0.218	off scale	7.17	22.4	443
D-2A-C	0.041	0	<DL	MNW	0.156	52.9	4.21	22.5	149
<i>D-2A-D</i>	<DL	0	<DL	7.77	0.57	off scale	2.3	24.2	16.9
<i>D-2A-E</i>	0.006	0	<DL	MNW	0.159	off scale	4.51	18.3	131
D-2A-F	<DL	0	<DL	6.48	0.377	229	(9.27)	22.2	483
D-2A-G	<DL	0.28	<DL	6.64	0.434	69.2	4.68	25.0	566
D-2A-H	<DL	0	<DL	7.19	0.236	10.11	8.55	23.9	482
D-2A-I	<DL	0	<DL	9.05	0.222	14.7	8.04	18.8	253

mean:

0.236 9.38 20.98

std. deviation:

0.097 6.92 2.22

MNW= Meter not working

< DL= Less than detection limit

() not included

4.2 Natural Attenuation of Chromate - Adsorption

Chromate attenuation in the natural subsurface environment associated with abiotic geochemical processes in Puchack aquifer materials has been examined. These include batch studies of a) chromate adsorption, i.e., how much Cr(VI) mass is on surfaces relative to in solution (Section 4.2); and b) the natural reductive capacity of sediments from the targeted aquifer units (i.e., intermediate sand and lower aquifer) to provide an estimate of its potential for natural reduction of mobile chromate to immobile Cr(III) phases (Section 4.3). In addition, adsorption of chromate by sediments in 1-D columns was evaluated to confirm batch observations under flow conditions (Section 4.4).

Chromate adsorption-desorption results in a lag in the migration of the chromate plume through the aquifer. This lag depends on the amount of adsorption which is dependent on many factors including solution pH, chromate concentration, ionic strength and sulfate concentration in the aquifer groundwater and contact time of chromate with sediments. The influence of these factors on chromate adsorption by deep composite sediments are described in the following section. These sediments designated ‘DC-1’ and ‘DC-2’ are described in Section 4.1 and Table 4.6.

4.2.1 Influence of Time and Solution Composition on Chromate Adsorption

The time required for the deep composite sediment, DC1, to reach adsorption equilibrium, (equilibration time) was determined in both distilled water and a synthetic groundwater. Water quality data from three monitoring wells at the Puchack site (Table 4.9) for seven major constituents were averaged and this average determined the composition of the synthetic Puchack groundwater used in this study (Table 4.10). The ionic strength of the synthetic groundwater was 4.3 mM, which is typical of groundwater. Because adsorption of anions like CrO_4^{2-} are known to depend on solution pH, the pH of sediment suspensions was typically adjusted from its natural pH to a target value in the range $4 < \text{pH} < 9$ prior to the addition of chromate and the start of adsorption experiments. Once started, a stable suspension pH was approached for DC1 within 10 to 15 hours in both distilled water and synthetic groundwater (Figure 4.4). This was also true for DC2; however, up to 2 to 3 days were required for the individual deep core samples NRS-1, -2, and -3 (data not shown; see Section 4.3.1 for sample description) used in the natural reduction experiments discussed in Section 4.3 and 4.4. The relatively good agreement between the distilled water and synthetic groundwater cases indicates that pH equilibration times were not affected by solution composition (ionic strength) for any of the sediments examined at low ionic strength (<4.3 mM).

The time dependence of chromate adsorption in this experiment (Figure 4.5) demonstrates that the initial adsorption was fast (minutes) and that within 10 to 15 hours equilibrium was approached at pH values near 4 and 8 for both distilled water and groundwater. Thus, contact times of 18 to 24 hours were typically used in the adsorption experiments described below, unless otherwise noted. At equilibrium more chromate is adsorbed at both pH values from distilled water suspensions than from synthetic groundwater suspensions (Figure 4.5), indicating that solution composition and ionic strength affect chromate adsorption. This is consistent with previous studies of chromate adsorption (Zachara et al. 1987, 1989) and will be examined in more detail in the sections that follow.

Table 4.9. Water Quality Data from Three Monitoring Wells at the Puchack Site Sampled between September 2000 and February 2001

parameter	units	MW-1S	MW-1S	MW-251
Depth	feet	51 - 56		144 - 154
sampling date		2/15/05	5/8/02	11/1/2000
DO	mg/L	3.48	0.6	0.43
pH		5.17	5.2	4.94
Cr(VI)	ug/L	9420	11540	8740
Tot Cr	ug/L	8010	-	6310
Eh	MV	320.5	-	369
specific conductance	uS/cm	514	570	203
alkalinity as CaCO ₃	mg/L	17.2	-	10.4
Ca	mg/L	22.5	-	9.68
Mg	mg/L	11	-	6.38
Na	mg/L	59.3	-	10.4
K	mg/L	8.65	-	2.94
Cl	mg/L	61.2	-	13.3
SO ₄	mg/L	111	-	37.5
NH ₃	mg/L	1.2	-	0.77
NO ₂	mg/L	0.074	-	0.091
NO ₃ /NO ₂	mg/L	<0.1	-	0.91
PO ₄	mg/L	0.12	-	0.17
Tot P	mg/L	0.26	-	0.035
TOC	mg/L	1.2	-	0.58
Al	ug/L	27.1	-	47.6
Ba	ug/L	41.4	-	94.6
Tot Fe	ug/L	<100	9.3	<100
Mn	ug/L	607	-	87.4

Table 4.10. Composition of Synthetic Groundwater Used in Adsorption Experiments

Composition	Concentration
	mmol/L
*CaCO ₃	0.14
Ca	0.42
Mg	0.35
Na	1.22
K	0.13
Cl	1.31
SO ₄	0.66
pH	4.94 - 5.17

* Alkalinity as CaCO₃

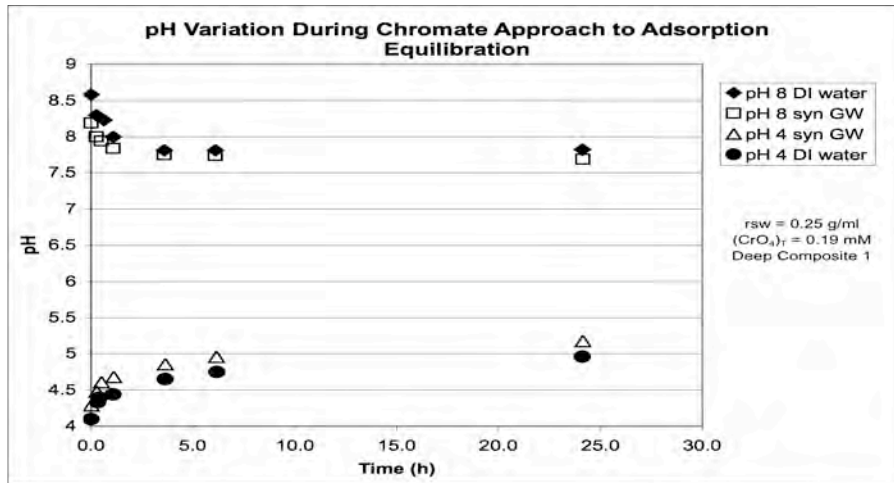


Figure 4.4. Time to Reach a Stable pH as Chromate Adsorption Equilibrium is Approached in a Suspension of the DC-1 Sediment after the Initial pH Adjustment to Approximately pH 8 and 4 and Addition of Chromate

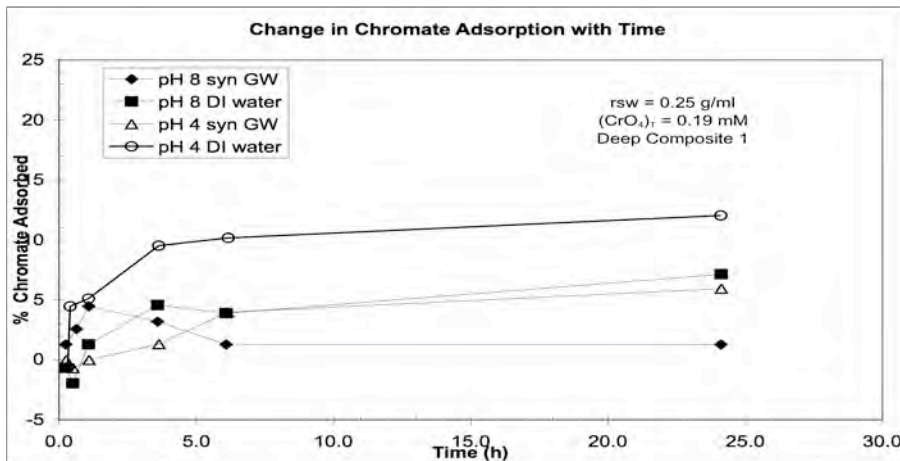


Figure 4.5. Approach to Chromate Adsorption Equilibrium in Distilled Water and Synthetic Groundwater Suspensions of Deep Composite 1

4.2.2 Influence of pH on Chromate Adsorption

Chromate adsorption by deep composite sediments DC1 in distilled water (Figure 4.4) and DC2 in actual Puchack ground water containing sulfate (a maximum of 50 mg/L) (Figure 4.5) was highly dependent on the pH. These pH edges are typical for anions such as CrO₄²⁻ (Zachara et al. 1987, 1989, 2004) and show more adsorption at low pH (pH < 7 to 8.5) and decreasing adsorption under increasingly alkaline conditions. The adsorption ‘edge’ refers to the pH region over which adsorption is rapidly changing as a function of pH. Although different sediment composites were used for the distilled water and the Puchack ground water adsorption edges, these experiments do show that more chromate is adsorbed from distilled water than from the groundwater. This is apparent from the displacement of the groundwater edge to lower pHs relative of that of the distilled water edge (compare Figures 4.6 and 4.7). This is most likely due to the presence of SO₄ in the groundwater (Zachara et al. 1987), which is

examined in Section 4.2.4. The difference between the 3-hour and 18-hour groundwater edges (Figure 4.7) is consistent with sorption equilibrium requiring 10 to 15 hours as described in the previous section.

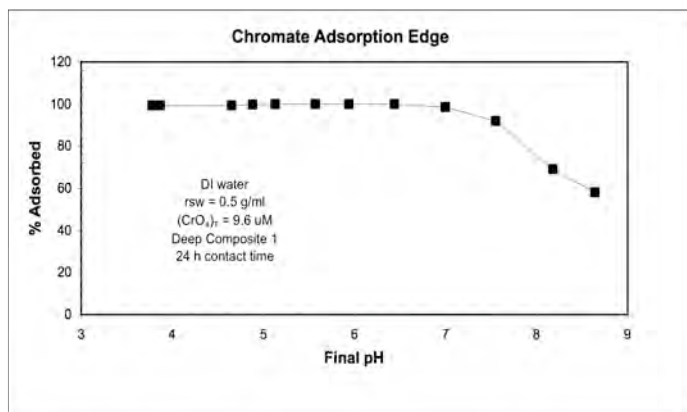


Figure 4.6. Dependence of Chromate Adsorption on pH in Deionized Water

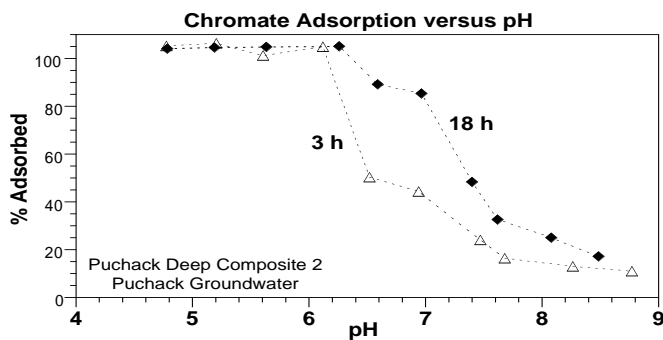


Figure 4.7. Chromate Adsorption Edge in Puchack Groundwater for Deep Composite 2 using Two Contact Times

4.2.3 Adsorption Isotherm – Influence of Chromate Concentration on Adsorption

Aquifer sediments have an adsorption maximum or “loading” capacity for chromate, sulfate, and other adsorbing constituents in solution. The adsorption maximum occurs when the surface sites, to which CrO_4^{2-} coordinates, have been completely occupied. This loading capacity will depend on the surface area and/or surface functional groups at the sediment-solution interface. This maximum loading capacity for the DC2 sediment at pH 5.6 (in the pH region where adsorption is the strongest) in synthetic Puchack groundwater (soil water ratio, $r_{sw} = 0.25 \text{ g/mL}$) was evaluated by varying the initial chromate concentration in separate suspensions from 0 to 0.96 mmol/L. Suspensions were equilibrated for 24 hours, and the final chromate solution concentration in the $0.1 \mu\text{m}$ filtrate was measured. The concentration of adsorbed chromate was determined from the difference in the initial concentration and the measured final solution concentration. A plot of the adsorbed concentration, normalized to the grams of sediment, $S(\mu\text{mol/g})$, versus the final equilibrium solution concentration, $C(\mu\text{mol/L})$, is referred to as an adsorption isotherm (Figure 4.8). For sediment DC-2 chromate adsorption is linear at low concentrations,

but as the solution concentration increases the incremental increase in adsorption diminishes and eventually reaches a plateau, the adsorption maximum.

As the adsorption maximum is approached the percentage of the total chromate that is adsorbed decreases. Under these high loading conditions the adsorption edge is suppressed over the entire pH range and at low pH adsorption would not approach 100% as it did in Figures 4.6 and 4.7. This occurs because the loading of surface sites has reached the limit for that particular sediment. The isotherm in Figure 4.8 has been fit with both Langmuir and Langmuir-Freundlich equations from which the adsorption maximum, M, and an affinity constant, K, were derived. These can be used in chromate transport calculations in groundwater systems. At the Puchack site where a continuous influx of chromate from the source area may occur the adsorption maximum may eventually be reached and adsorption will no longer retard the advancement of the chromate plume.

As the adsorption maximum is approached the percentage of the total chromate that is adsorbed decreases. Under these high loading conditions the adsorption edge is suppressed over the entire pH range and at low pH adsorption would not approach 100% as it did in Figures 4.6 and 4.7. This occurs because the loading of surface sites has reached the limit for a particular sediment. The isotherm in Figure 4.8 has been fit with both Langmuir and Langmuir-Freundlich equations from which the adsorption maximum, M, and an affinity constant, K, were derived. These can be used in chromate transport calculations in groundwater systems. At the Puchack site where a continuous influx of chromate from the source area may occur the adsorption maximum may eventually be reached and adsorption will no longer retard the advancement of the chromate plume.

4.2.4 Influence of Sulfate on Chromate Adsorption

The influence of SO_4^{2-} on CrO_4^{2-} adsorption by deep composite sediments DC2 was examined to determine if competition by another adsorbing oxyanion for available surface sites results in a significant reduction in chromate adsorption. Sulfate additions to separate distilled water suspensions of DC2 at pH 6.3 covered a range of 0.5 to 50 ppm (1.04 to 521 μM), which has been observed in well water from the Puchack site. After mixing with SO_4^{2-} for 1-hour suspensions were spiked with chromate (9.6 μM) and then mixed for an additional 3 hours before being filtered and analyzed for chromate.

The presence of sulfate in the concentration range examined did not interfere with the DPC analysis of chromate as shown in Figure 4.9. Chromate adsorption was suppressed by sulfate (Figure 4.10), which was alluded to above and is consistent with prior observations under similar conditions for amorphous

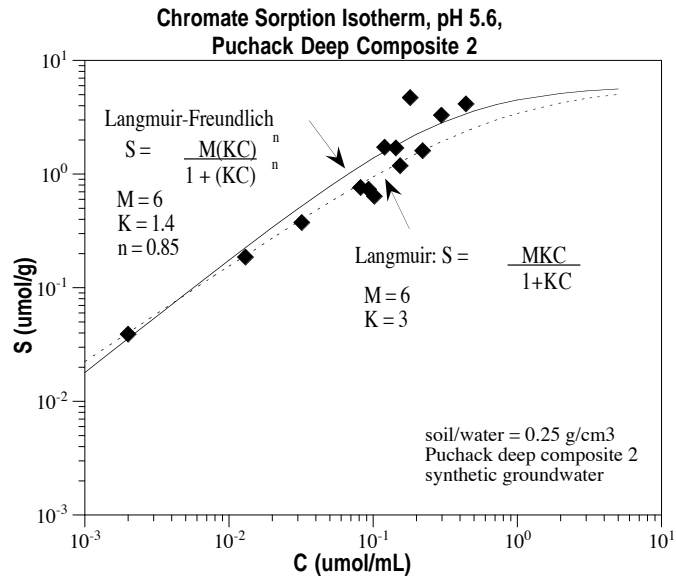


Figure 4.8. Chromate Adsorption Isotherm for Deep Composite 2 in Synthetic Puchack Groundwater after 24-Hour Contact Time

iron oxides (Zachara et al. 1987) and subsurface soils (Zachara et al. 1989). This suppression increased with increasing sulfate concentration resulting in a 15% drop in chromate adsorption. Thus, chromate disposal and migration in the presence of SO_4^{2-} and other anions (e.g., HCO_3^{2-} and CO_3^{2-}) in the contaminant plume will decrease chromate adsorption relative to adsorption which would occur in their absence. However, with only a factor of 2 decrease in the K_d values derived from these experiments (Figure 4.11), the effect of sulfate on chromate migration in the concentration range found at Puchack is relatively small.

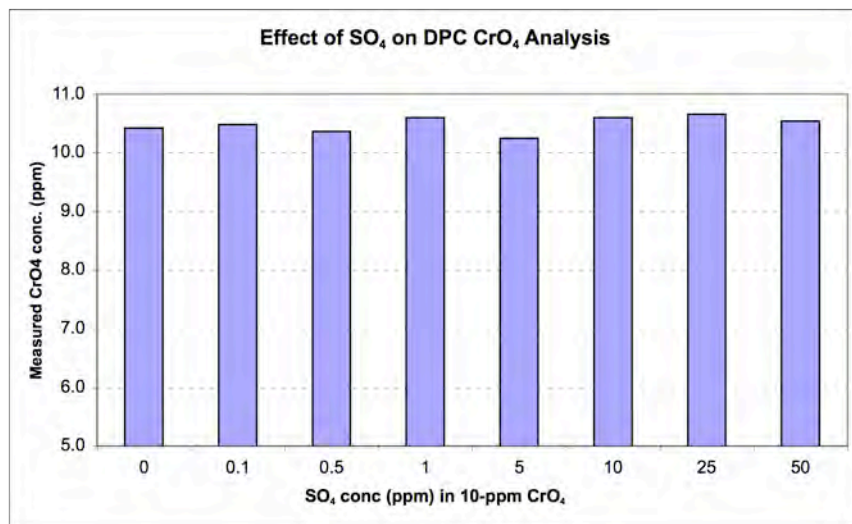


Figure 4.9. Evaluation of Potential Interference of SO_4 with the DPC Analysis of 10 ppm CrO_4 in Distilled Water

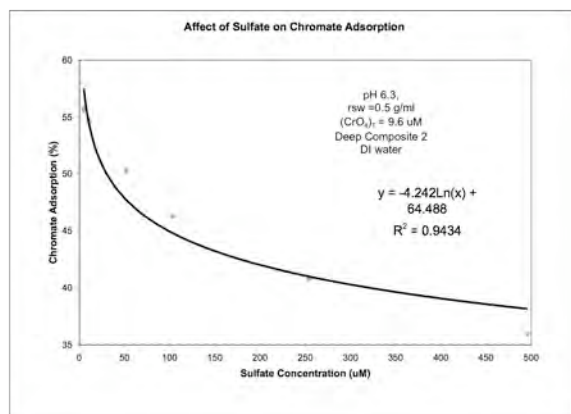


Figure 4.10. Decrease in Chromate Adsorption with an Increase in Sulfate Concentration at pH 6.3

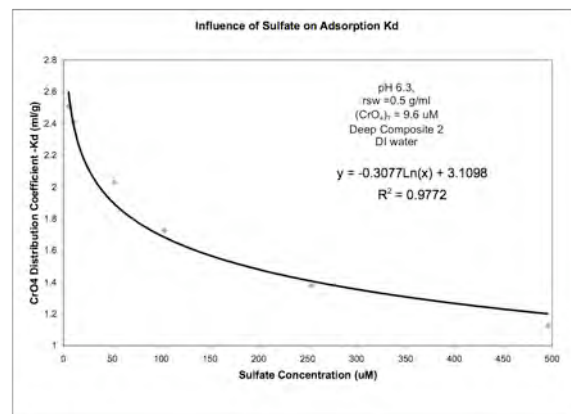


Figure 4.11. Reduction in the Chromate Distribution Coefficient (K_d) on Deep Composite 2 with Increasing Sulfate Concentration Corresponding to the Decline in the Percent Adsorption Shown in Figure 4.9

4.2.5 Influence of Colloids on Chromate Adsorption

Adsorbed chromate on colloidal particles could possibly be a mode of chromium transport in subsurface aquifers. To evaluate the possibility of colloidal chromate present in Puchack composite sediment DC-1, chromate was adsorbed to this sediment at pH 4.6 and 7.7 in distilled water and synthetic Puchack groundwater. After a 24-hour equilibration time, aqueous samples were filtered with 0.45, 0.2, 0.1 and 0.01 um membrane filters and the filtrates analyzed for CrO₄ (Figure 4.12). If significant colloidal chromate were present, chromate concentration should decrease with successive decreases in filter pore size. No consistent variation in chromate concentration with filter pore size was observed. Although this does not prove that inorganic colloids are totally absent, we can conclude that either there is no generation of inorganic colloids in Puchack sediments and/or the small fraction of total chromate present on these colloids is of negligible importance for chromate mobility.

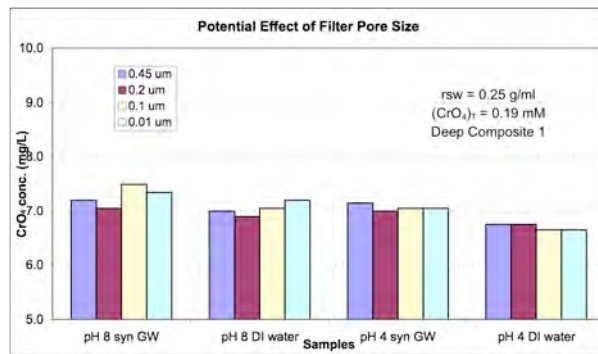


Figure 4.12. Evaluation of Chromate Adsorption to Colloids present in Deep Composite 1 Sediments using a Sequence of Membrane Filters to Separate Phases at the Termination of a 24-Hour Adsorption Experiment in Distilled Water and Synthetic Groundwater at pH 4 and 8

4.3 Natural Attenuation of Chromate – Reduction/Immobilization by Natural Aquifer Sediments

Chromate adsorption not only results in a lag in the plume as indicated in Section 4.2, but also facilitates or catalyzes chromate reduction to Cr(III) by sediment surfaces containing electron donors , e.g., sorbed or mineral Fe(II) phases resulting from chemical or microbial reduction of Fe(III) oxides. Mineral surfaces facilitate the three electron transfer required in chromate reduction. If there is some degree of naturally occurring reductive capacity in the sediments, some fraction of the Cr(VI) species can be reduced to Cr(III) species and form insoluble mixed Cr, Fe precipitates. It is critical to quantify this reductive capacity because, if the amount of natural reductive treatment is significant, credit can be taken for treatment of a substantial mass of the chromate plume. To address this possibility untreated Puchack sediments were used in long-term (2 to 9 months) batch studies to determine: a) the degree to which chromate is reduced by untreated Puchack sediments, b) the influence of oxygen on the rate of chromate reduction, c) the reactive phase(s) responsible for chromate reduction.

4.3.1 Rate of Chromate Reduction by Natural Aquifer Sediments

To address whether chromate can be reduced in the natural Puchack aquifer and at what rate, long-term chromate batch reduction studies were conducted with four sediments (Table 4.11). The first was a deep composite sediment (DC-2) suspected of having little reductive capacity. The three other sediments were not composites but were representative of the deep aquifer units that were visually judged to have

some reductive capacity. These latter sediments were designated “natural reduced sediments,” NRS-1, -2, and -3. In anoxic reduction experiments the loss of chromate from solution was followed over time (Figure 4.13) and interpreted as chromate reduction based on the fact that adsorption equilibrium is obtained within 10 to 15 hours (Section 4.2). After adsorption equilibrium is reached the continued loss from solution over the remaining 1,500 to 6,600 hours of the experiments was due to the reduction of the adsorbed Cr(VI) to Cr(III). As reduction occurred with time, adsorption equilibrium was reestablished with the accompanying decrease in aqueous chromate. This interpretation is supported by the fact that 0.1% or less of the total chromate initially added to NRS-1 in three separate 1,500-hour experiments could be recovered by raising the suspension pH to 12, to desorb chromate, mixing the suspension for 24 hours and analyzing the filtrate for chromate. This lack of recovery is consistent with reduction of the adsorbed Cr(VI) to Cr(III) which then precipitates to form $\text{Cr}(\text{III})(\text{OH})_3$ or as a mixed $(\text{Cr}, \text{Fe})(\text{OH})_3$ solid, both of which are very insoluble. Thus, the continued loss of chromate from solution after 15 hours was interpreted as surface catalyzed chromate reduction.

Table 4.11. Sediments Used in Studies of Chromate Reduction by Natural Aquifer Sediments

Sample Name	Sample No.	Well	Depth	OC (wt %)	Fe(II)	Characterization
DC2	see Table 4.8	D1 and D2	220 - 302.5'	nd	nd	Deep composite 2 (DC2)
NRS - 1	D-1S-M extra	D1	272- 272.5'	2.25	P	dark clay
NRS - 2	MW37S-C	MW-37	154-154.5'	0.01	nd	sand < 1% with black dposits
NRS - 3	MW37S-L	MW-37	217-217.5'	0.01	nd	sand < 1% with black dposits

nd : no data available

P : indicates that sediment possibly contains Fe(II) and/or lignite (see text)

The observed chromate reduction rates for these sediments varied considerably (Figures 4.13 and 4.14) from a relatively short reduction half-life of 49.5 hours for NRS-1 (a dark clay sample) to considerably longer and relatively consistent half-lives for DC2, NRS-2 and NRS-3 (aquifer sediments) of 2,570, 2,900, and 2,900 hr, respectively (Table 4.11). It is important to note however, that for all of these natural untreated sediments significant chromate reduction occurred. With NRS-1 essentially 100% reduction of the initial chromate (10.6 micromoles) occurred within 120 hours, whereas for the other sediments nearly 77% of the chromate was reduced after 6,600 hr. This would indicate that chromate reduction could occur in the natural untreated sediments through which the Puchack chromate plume migrates.

The mineral and/or organic phases within these sediments responsible for the observed chromate reduction remain the subject of investigation (Table 4.12). The organic phase of NRS-1 has been

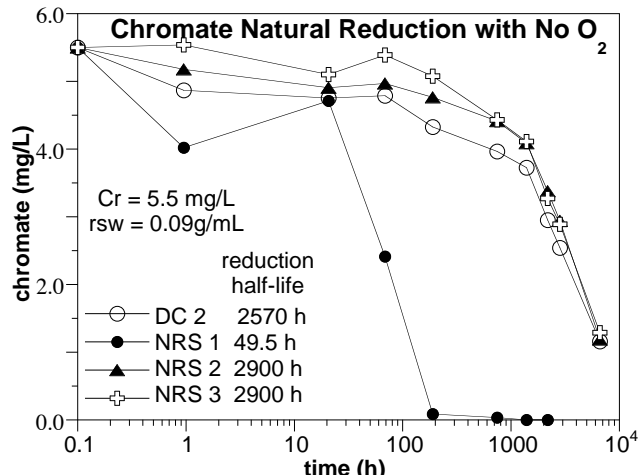


Figure 4.13. Reduction of Chromate by Selected Natural Aquifer Sediments

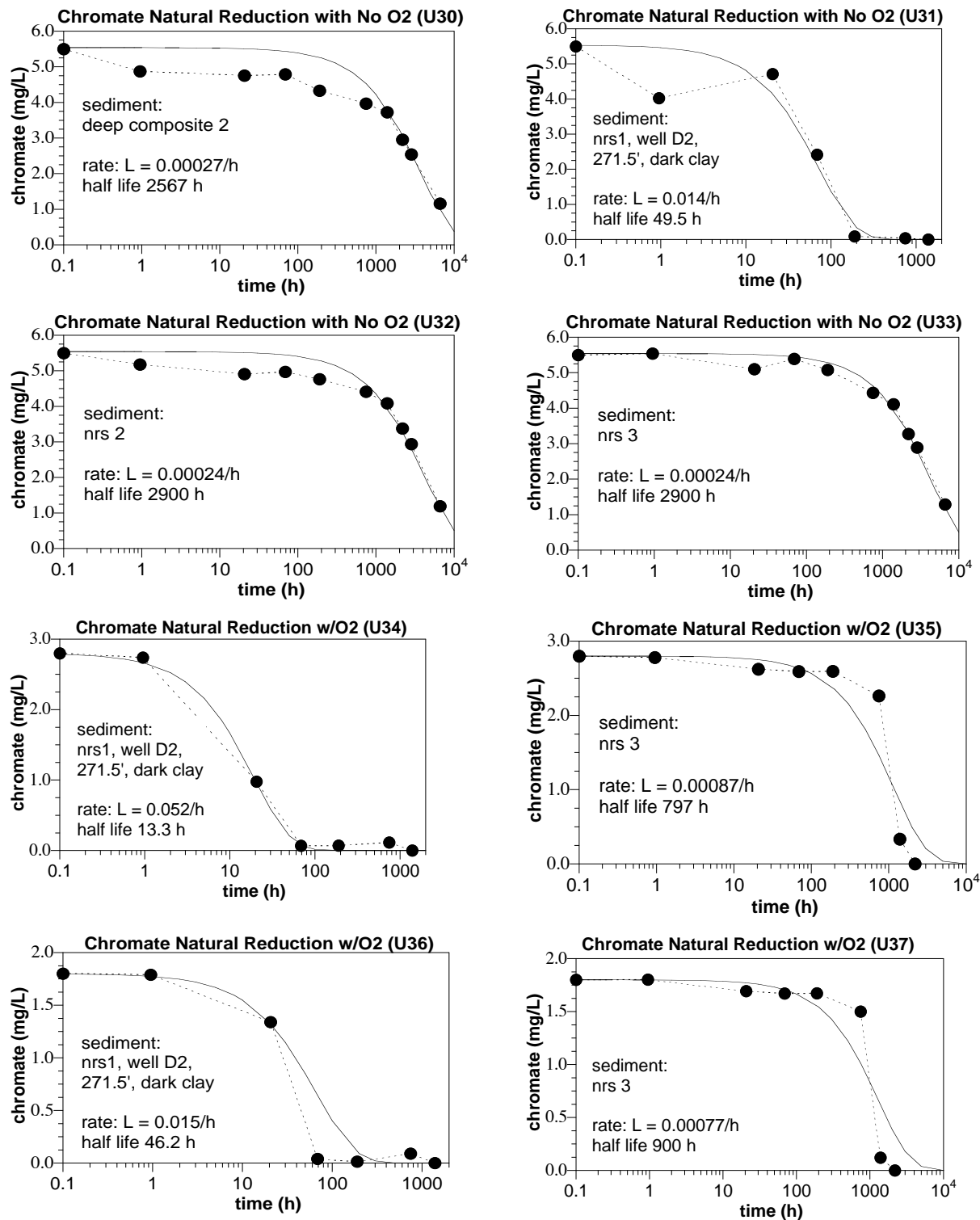


Figure 4.14. Pseudo-First Order Model Fits to Reduction of Chromate by Selected Natural Aquifer Sediments

investigated and will be considered in Section 4.3.3. However, there are some clues regarding possible reactive phases in sediment NRS-1 for which rapid reduction occurred. NRS-1 the dark clay material, was the only sediment to contain significant organic carbon (2.25 wt%), which based on sediment color was thought to contain lignite (Table 4.11). The other sediments contained very little organic carbon (< 0.01%, Table 4.13). The absence of detectable inorganic carbon (Table 4.13) places an upper limit of 5- μ mol FeCO₃ per gram of sediment that could be present assuming a detection limit of 50- μ g inorganic carbon per gram of sediment.

Table 4.12. Natural Attenuation Pseudo-First Order Rates of Chromate Observed in Experiments. For sediment descriptions, see Tables 4.10 and 4.6.

Sediment	Depth (ft)	Chromate, O ₂ conc.	e- acceptor ratio (O ₂ /Cr)	Experiment Longevity (h)	Reduction Rate (1/h)	Reduction Half-Life (h)	Total e-acceptor (meq)
<i>Sediments from specific depths chosen for reductive properties:</i>							
DC 2	220-302.5	5.5 mg/L Cr, no O ₂	0/1	6600	2.70E-04	2570	0.038
NRS-2	154-154.5	5.5 mg/L Cr, no O ₂	0/1	6600	2.40E-04	2900	0.038
NRS-1	272-272.5	5.5 mg/L Cr, no O ₂	0/1	1500	0.014	49.5	0.038
NRS-1	272-272.5	2.8mg/L Cr, 2.2 mg/L O ₂	1.7/1	1500	0.052	13.3	0.053
NRS-1	272-272.5	1.7mg/L Cr, 2.2 mg/L O ₂	2.8/1	1500	0.015	46.2	0.046
NRS-3	217-217.5	5.5 mg/L Cr, no O ₂	0/1	6600	2.40E-04	2900	0.038
NRS-3	217-217.5	2.8mg/L Cr, 2.2 mg/L O ₂	1.7/1	2400	8.70E-04	797	0.053
NRS-3	217-217.5	1.7mg/L Cr, 2.2 mg/L O ₂	2.8/1	1500	7.70E-04	900	0.046
<i>Composite sediments representative of aquifer units:</i>							
A2a	80-110	2.0 mg/L Cr, no O ₂	0/1	2900	6.50E-05	10,700	0.014
A2b	108-120	2.0 mg/L Cr, no O ₂	0/1	2900	none	--	0.014
C2Al	165-172	2.0 mg/L Cr, no O ₂	0/1	2900	2.50E-05	27,700	0.014
A3a	199-204	2.0 mg/L Cr, no O ₂	0/1	2900	2.50E-05	27,700	0.014
A3b	215-230	2.0 mg/L Cr, no O ₂	0/1	2900	none	--	0.014
A3c	238-267	2.0 mg/L Cr, no O ₂	0/1	2900	none	--	0.014
MW36/37	80-267	2.0 mg/L Cr, no O ₂	0/1	2900	none	--	0.014

Table 4.13. Carbon Analysis of Selected Sediments

Sediment	Organic Carbon (%)	Inorganic Carbon (%)	Total Carbon (%)
NRS-1, D1m, 272'	2.25	0.00	2.25
NRS-2, MW 37c	0.011	0.00	0.011
NRS-3, MW37L	0.010	0.00	0.010
DC-2, composite	0.020	0.00	0.020

Fe(II) analyses of water in well D1 as a function of depth (Table 4.7) (where the NRS-1 sediment was taken) shows Fe(II) concentration increasing with depth from 0.05 ppm at 155 ft to 0.12 ppm at 253 ft (Table 4.8). This trend may have extended downward in this aquifer unit to a depth of 273 ft where the NRS-1 sediment was collected. If so, this would surely indicate the presence of Fe(II) or other electron donor in the NRS-1 sediment. In addition, the dissolved O₂ concentrations in well D1 decreased with depth (Table 4.8) indicating an increasingly reduced environment with depth in which Fe(II) would persist. Iron characterization of the NRS-1 sediment (Table 4.13, D1-M, 272.5 ft) indicates very large reductive capacity (636 μ mol/g, measured by O₂ consumption). The 1-hour 0.5-M HCl extraction of this

sediment indicated the presence of 2.4 $\mu\text{mol Fe(II)}/\text{g}$, possibly present as Fe(II) adsorbed + FeCO₃ + FeS (Table 4.14). Possible reductive phases that are not ruled out include lignite and structurally reduced iron in 2:1 smectite clays, as this sediment contains considerable high plasticity clay. In addition to the measured extractable Fe(II), the presence of clays with structural ferrous iron (not determined in iron extractions) and/or lignite in the NRS-1 sediment would provide additional suitable electron donors capable of the rapid ‘natural’ chromate reduction observed for this sediment. For the NRS-2 and -3 sediments, no extractions or O₂ column reductive capacity measurements were performed. Thus, a similar conjecture (line of evidence) for these sediments is not justified because they contained no significant organic carbon, and well waters (well MW37, Table 4.8) at depths in the vicinity where these sediments were obtained contained high dissolved O₂ and very low aqueous Fe(II) concentrations. The Fe(II) concentrations at depth in well MW37 were 400 times lower than those in well D1 where sediment NRS-1 was obtained. This is consistent with the very slow reduction rates observed for these two sediments, but as already noted significant reduction did occur in NRS-2 and -3 over a period of 9 months.

Table 4.14. Natural and Dithionite-Reduced Sediment Reductive Capacity and Iron Phases (Selective sediment extractions were used to determine the distribution of iron among Fe(II) and Fe(III) phases. The ferrozine method was used to measure Fe(II) and Fe(total) after sample reduction by hydroxylamine hydrochloride; Fe(III) was calculated by difference.)

borehole, depth	treat- ment	O ₂ column reductive capacity ($\mu\text{mol/g}$)	Fe ^{II} phases			Fe ^{III} phases			Fe ^{II} +Fe ^{III} total ($\mu\text{mol/g}$) [7]	
			Fe ^{II} CO ₃ +FeS ($\mu\text{mol/g}$) [1]	other Fe ^{II} ($\mu\text{mol/g}$) [2]	adsorbed Fe ^{II} ($\mu\text{mol/g}$) [8]	total Fe ^{II} ($\mu\text{mol/g}$) [3]	amorphous Fe ^{III} oxides ($\mu\text{mol/g}$) [4]	crystalline Fe ^{III} oxides ($\mu\text{mol/g}$) [5]		
MW36C, 151'	none	4.10	8.63	1290		631	528	168	245	876
MW37I, 197.5'	none	2.56	2.28	3.64		14.9	2.17	91.7	41.3	56.3
D1-H, 220.5'	none		2.81	10.4		16.2	6.11	196	66.7	82.9
D1-M, 272.5'	none	636	2.38	237	2.26	8.37	25.0	222	22.2	30.5
D2-E, 211	none	1.63	3.10	2.90		30.5	0.87	99.4	22.3	52.8
D2-H, 271'	none	2.77	1.75	6.01		9.62	3.32	96.5	39.6	49.2
average natural sediments:		129 \pm 283	3.49 \pm 2.56			118 \pm 251			72.8 \pm 85.9	210 \pm 281
		2.76 \pm 1.02 (no D1-M)								
composite, pH 4.5 reduced		54.5								
composite, pH 5.3 reduced		62.2								
composite, pH 6.2 reduced		106								
composite, pH 7.0 reduced		84.8								
MW-36C, 151'	reduced	390	1210		3.54	7.04			535	542
MW-36F, 167.5'	reduced		41.8		0.20	21.5			7.47	29.0
MW-36I, 197.5'	reduced	23.9	63.8		0.23	35.3			5.29	40.6
MW-36M, 221'	reduced		27.1		0.46	2.15			26.7	28.9
MW-37C, 154'	reduced	80.5	52.7		0.40	2.23			44.3	46.6
MW-37F, 171.5'	reduced		40.20		0.54	2.39			39.5	41.9
MW-37I, 199'	reduced		172.4		2.20	2.26			37.5	39.7
D1-B, 106'	reduced	52.4			0.34					
D1-F, 164'	reduced	54.7			0.39					
D1-H, 220.5'	reduced	58.5	71.2		1.02	2.75			143	145.4
D2-C, 151'	reduced	23.9			0.54					
D2-H, 271'	reduced		50.2		1.31	1.16			63.2	64.4
average reduced sediments:		90.1 \pm 102	192 \pm 384		0.93 \pm 1.0	3.31 \pm 12.0			100 \pm 168	109 \pm 166
		60.2 \pm 25.6 (no MW36C)								

[1] From 1 h, 0.5 M HCl extraction.

[2] Amorphous Fe^{II} from 24 h, 0.18 M ammonium oxalate extraction at pH 3.4.

[3] From 21 day, 5 M HCl extraction

[4] From 24 h, 0.18 M ammonium oxalate extraction at pH 3.4.

[5] From DCB extraction and subtraction of the amorphous Fe^{III}.

[6] From 21 day, 5 M HCl extraction, and hydroxylamine hydrochloride reduction of filtrate.

[7] The sum of Fe^{II} and Fe^{III} columns.

[8] From 24 h, 1 M CaCl₂ extraction

An additional group of composite sediments was used in batch anoxic experiments to evaluate chromate reduction, which could occur in individual aquifer units intersecting monitoring wells MW 36 and 37. Composites were designed to approximate an average composition within each aquifer units and were given the name of that unit, namely A2a, A2b, C2A1, A3a, A3b, A3c (Table 4.6). The observed reduction of chromate in these composites (Figure 4.15) was significantly less after 2900 hours than observed for the NRS sediments that were specifically selected for their potential reductive capacity (Table 4.14). Four of these composites showed no reduction of chromate (A2b, A3a, A3c and MW36/37, Figure 4.15). Three others composites (A2a, C2A1 and A3b, Figure 4.15) showed only slight reduction with estimated half-lives of 10,700; 27,700; and 27,700 hours, respectively (1 to 3 years; Table 4.11). At the field scale, the combination of the geochemistry and flow determine the amount of reduction/immobilization of the chromate plume that would occur.

Shallow aquifer composites show that slow chromate reduction occurred in half of the samples, although these rates were vary slow (1 year to 3 year half-life), based on only a few samples of the aquifer system with wide ranging properties. A deep aquifer composite showed about 10 times more rapid chromate reduction (108-day half-life), and selected sediments (typically finer grain sediments from interbedded clays) showed rapid chromate reduction with a 46-hour half-life. Clearly, these results show that natural chromate reduction can occur in the Puchack aquifer system, and as will be shown in Section 4.3.2, chromate reduction does not appear to be adversely effected by the presence of dissolved oxygen. Given the amount of variability observed in the samples analyzed in this study, predicting the expected chromate reduction rate in a complex aquifer system, based on the eight composite sediments and the three individual sediments examined, would result in a relatively high degree of uncertainty. With this additional data, simulations using a reactive transport model could track the chromate plume through the aquifer system using ranges of natural reduction rates. Thus, residence times could be determined in specific aquifer units/zones in which reduction rate data had been determined.

4.3.2 Influence of Dissolved Oxygen on the Natural Chromate Reduction Rate

Specific Puchack sediments have been shown to be highly effective in reducing chromate under anoxic conditions. Thermodynamically, dissolved O₂ should be reduced before chromate in suspensions of these sediments. Thus, chromate reduction by naturally reduced sediments should be slowed in the presence of dissolved O₂, often present in groundwater. A recent study found that nitrate reduction by dithionite reduced sediments was not affected when the electron acceptors equivalents of nitrate present in suspension were comparable to the equivalents of either dissolved O₂ or chromate (Szecsody et al. 2005b). This is contrary to the thermodynamic sequence that dissolved O₂ and chromate should be reduced before nitrate. The lack of any observed affect was attributed to the overwhelming excess of electron donor equivalents supplied by the reduced sediments in that study.

The influence of dissolved O₂ was examined with 10 g suspensions of NRS-1 and NRS-3 with 2.2 mg/L of dissolved O₂ (0.033 meq of electron acceptors) and 1.7 and 2.8 mg/L of Cr(VI) (0.0125 and 0.0194 meq) resulting in O₂: Cr electron acceptor ratios 2.8:1 and 1.7:1, respectively (Table 4.11). For these sediments no extractions for Fe(II) were performed so no estimate of electron donor equivalents is available, however using an average extractable Fe(II) (see next section) the electron donor capacity in these experiments may have been > 3.5 meq/g. Rather than decreasing or remaining the same in the presence of dissolved O₂ the rate of chromate reduction increased by a factor of 3 in three out of four experiments relative to rates in anoxic experiments. This is shown clearly by comparing chromate loss for anoxic and oxic conditions (Figure 4.16). The explanation for the acceleration of chromate reduction

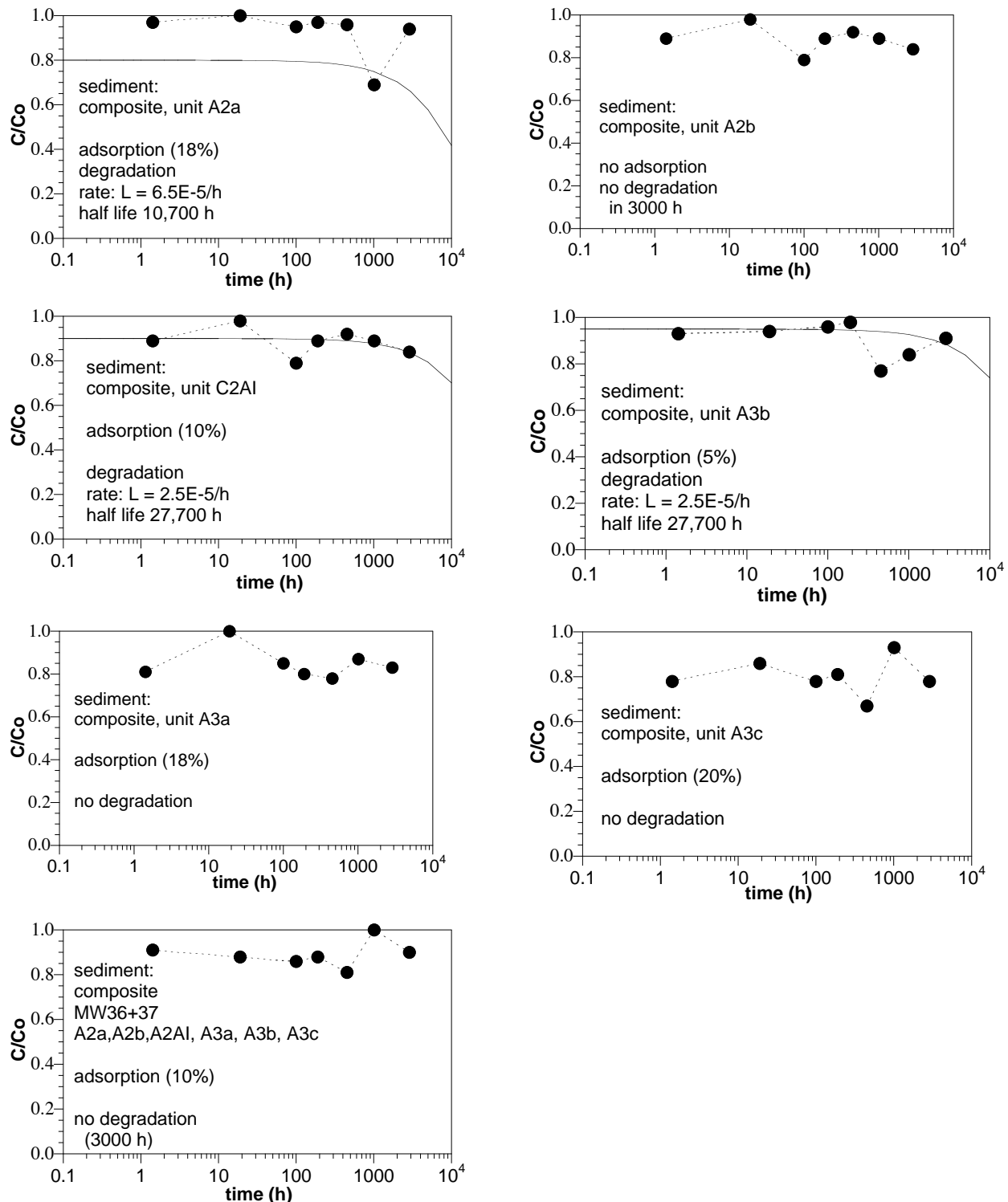


Figure 4.15. Reduction of Chromate Under Anoxic Conditions by Untreated Sediment Composites of Wells MW 36 and 37. Initial conditions were 4.6 mg/L chromate and 0.00 mg/L dissolved oxygen.

is presently unclear, but may possibly be attributed to sediment heterogeneity in sub-samples used for either the anoxic or oxic experiments. In the fourth experiment (NRS-1 with electron acceptor ratio of 2.8:1), no change in reduction rate was observed. Thus, the effect of dissolved oxygen on the rate of chromate reduction in these batch experiments is currently unresolved. However, the most important result derived from all of these experiments is that the amount of chromate reduced by the end of the experiments was approximately the same with and without the presence of dissolved oxygen. Thus, oxygen at the concentration considered did not appear to diminish the ultimate extent of chromate reduction by the NRS-1 and NRS-3 sediments.

However, in these experiments the initial concentration of O₂ was not constantly replenished as it would be in a naturally reduced aquifer with an oxygenated Cr(VI) plume moving through it. A recent study with dithionite reduced Hanford 100-D Area sediments addressed this case (Szecsody et al. 2005b). In that study, a series of five column experiments were conducted where 250 pore volumes of O₂ saturated solution (8.4 mg/L O₂) containing 2 mg/L chromate and 60 mg/L of nitrate were pumped through the sediment column at a flow rate to achieve an 8-hour residence time (Figures 4.17a though c). Periodic measurements of N-compounds, oxygen, and chromate were made to determine reaction rate changes. During the first 125 pore volumes (hours) O₂ was consumed by the reduced sediment (Figure 4.17a and b) and the sediment's capacity to reduce Cr(VI) was not significantly affected as the effluent chromate data shows (Figure 4.17c). Beyond 125 pore volumes (hours) chromate reduction is diminished as a result of the consumption of the sediments electron donor capacity by the presence of dissolved O₂, nitrate and chromate. Note that this sediment was highly reduced and the flow rate used in this experiment was greater than in typical groundwater flow conditions. Thus, with a less reduced Puchack sediment, and slower flow the time scale for dissolved O₂ to impact chromate reduction may be different. Nevertheless, this demonstrates the effect that dissolved O₂ in groundwater may have on chromate reduction by natural reduced Puchack sediments. Additional column studies with composites of

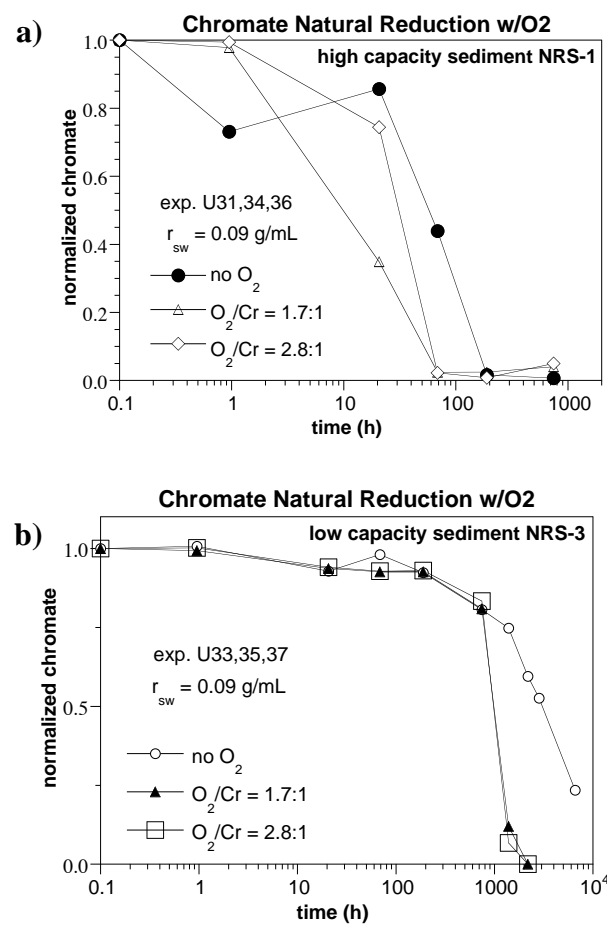


Figure 4.16. Comparison of Chromate Reduction for Natural Sediments with Oxygen:
a) NRS-1, and b) NRS-3

natural reduced Puchack sediments and typical groundwater composition and flow would be required to resolve the time-distance scale over which O₂ and other electron acceptors present in Puchack groundwater impact natural chromate reduction.

4.3.3 Influence of Natural Organic Matter on the Natural Chromate Reduction Rate

As discussed in the previous section, 2.25% organic carbon and hence NOM was found in one of the natural reducing sediments used in this study, NRS-1 (D1, 273 ft).

Experiments were conducted to determine if the NOM or abiotic mineral phases were reducing chromate. These experiments were conducted by comparison of the chromate reduction rate with the NOM removed (base/heat treatment) to untreated sediment under anoxic conditions. The FTIR spectrum of the organic matter present in the filtrate resulting from the base/heat treatment of the sediment (Figure 4.18) was used to identify the organic phases removed. Though it is difficult to identify discrete compounds from a complex mix such as NOM, it is possible to identify the chemical nature of some of the components present in the NOM. The spectrum obtained is consistent with organic compounds such as humic substances (Nardi et al. 2005) and lignites (Burns et al. 2005). The characteristic

broad bands of the O-H stretching vibrations of carboxylic acid functional groups can be seen around 2,810 cm⁻¹ and aromatic ring stretching band (C=C) at 1567 cm⁻¹. The presence of other oxygen containing functional groups also found in NOM such as alcohols and ethers are indicated with the presence of the strong C-O stretches at 1,105 and 1,000 cm⁻¹ with the O-H stretch from the alcohols incorporated in the broad peak centered around 2,810 cm⁻¹ of the carboxylic acids along with any C-H stretch bands from alkanes, alkyls and alkenes, all of which are found either to the left or right of 3,000 cm⁻¹.

If NOM is responsible for the reduction of chromate, the removal or decrease of the NOM in the sediment should result in a decrease in the rate of chromate reduction. From the results given in Figure 4.19 it can be seen that the rate of chromate reduction did not change due to the removal of the organic matter. This observed slight increase in rate could be due to an increase in surface area of the treated sediment due to the removal of the organic matter opening up internal pore networks previously

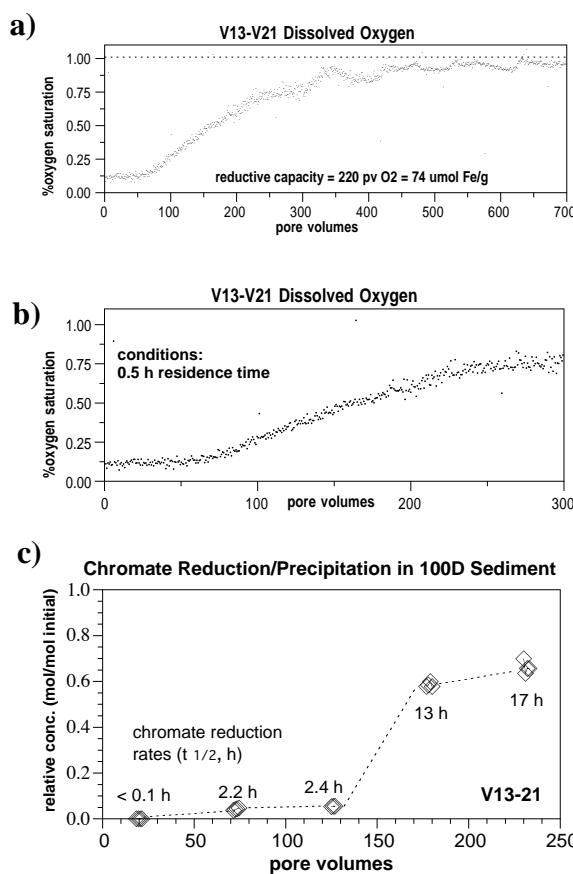


Figure 4.17. Long-Term Chromate Reduction by a Reduced Sediment Column in which 2 mg/L Chromate, 8.4 mg/L O₂, and 60 mg/L Nitrate was Injected (Influent and effluent concentration of dissolved oxygen (a, b), and chromate (c))

unavailable for chromate reduction. From these results we can conclude that chromate is reduced abiotically by mineral phases present in the sediment and not by NOM. The relatively high pH of 11.7 used to extract the NOM from the sediment would likely have killed most of the microbial population, so direct biotic chromate reduction for this sediment is highly unlikely. However, indirect evidence obtained for sediment NRS-1 suggests that this sediment contains bacteria that could aid either indirectly or directly with chromate reduction. This untreated sediment is able to mineralize N-nitrosodimethylamine (NDMA), which requires microbes. Unfortunately this particular sediment was not chosen for the biotic study given in Section 4.7. These bacteria could indirectly contribute to the ability of this particular sediments ability to reduce chromate by reducing iron present in the sediment, which would consequently be available to reduce chromate.

4.3.4 Redox Reactive Phases in Natural Puchack Sediments

Estimation of the total reductive capacity of natural (untreated) and/or chemically reduced sediments is central to the prediction of the longevity of these sediments as barriers capable of reducing chromate to its insoluble form, namely Cr(III) or mixed (Cr, Fe) hydroxides. Two approaches have been taken to estimate the reductive capacity of Puchack sediments. First, by measuring the consumption of dissolved O₂ from effluent waters pumped through sediment columns (data shown in Appendix C), mass balance calculations yield O₂ consumption as moles of O₂ consumed per gram of sediment (Table 4.13). This provides a defacto measure of the net reductive capacity due to ferrous iron, organic carbon and other possible sources and is described in more detail in Section 4.5.1. For the untreated sediments (Table 4.13) the average reductive capacity from O₂ measurements was $2.76 \pm 1.02 \mu\text{mol}$ of O₂ consumed per g of sediment. This average excluded the value for borehole sediment D1-M, which was a black clay with a reductive capacity over 200 standard deviations greater than the average for the remaining five sediments.

Although this O₂ column approach measures the net reductive capacity, it does not quantify the individual constituents contributing to this capacity, e.g., ferrous iron as structural or surface species, organic matter or sulfides. Thus, the second approach was to estimate the reactive/accessible Fe(II) in

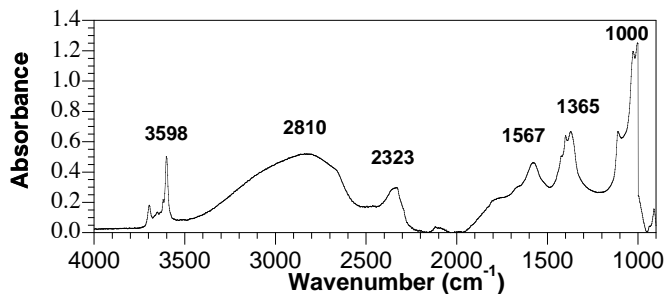


Figure 4.18. FTIR Spectrum of the Base Soluble Components of NRS-1

This untreated sediment is able to mineralize N-nitrosodimethylamine (NDMA), which requires microbes. Unfortunately this particular sediment was not chosen for the biotic study given in Section 4.7. These bacteria could indirectly contribute to the ability of this particular sediments ability to reduce chromate by reducing iron present in the sediment, which would consequently be available to reduce chromate.

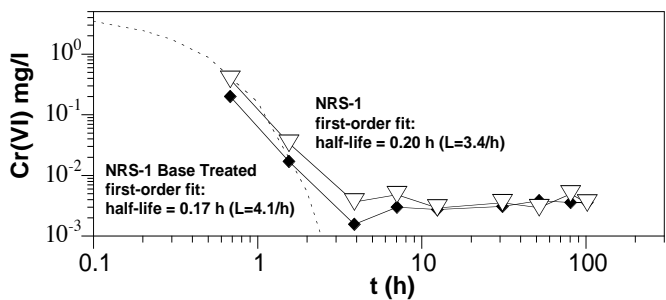


Figure 4.19. Chromate Reduction Rate a) NRS-1 RSW 0.37 with 4.8388 mg/L Chromate (triangles) and b) NRS-1 Base/Heat Treated (RSW 0.31 g/mL with 4.0688 mg/L of chromate (diamonds) both pH 7.5 in 0.01 M PIPES buffer.)

sediments. Ferrous iron is the primary reductant (electron donor) in the majority of naturally or chemically reduced sediments. It is present structurally in primary minerals (magnetite), secondary clay-sized minerals (smectites and illites) or adsorbed to mineral surfaces and coordinated by soil organic matter (Amonette et al. 2000). The rate of chromate reduction by ferrous iron has been extensively studied in a variety of geochemical conditions (Eary and Rai 1988; Anderson et al. 1994; Buerge and Hug 1997, 1999; Szecsody et al. 2004a, 2005c, 2006). The iron phases were examined in selected sediments using well-established extraction procedures (Heron et al. 1994). These extractions operationally estimate the distribution of ferrous and ferric iron in sediments (Table 4.13). The most accessible and/or reactive Fe(II) phase acting as a reductant for mobile pollutants has typically been estimated using a short (1 to 24 hour) 0.5-M HCl extraction of sediments (Heron et al. 1994). For selected Puchack sediments, the quantities of Fe(II) measured in 1 hour 0.5-M HCl extractions are typically less than the operational estimate of total Fe(II) as measured in 21-day 5-M HCl extractions (compare column 3 and 5 in Table 4.13). This is to be expected because much of the structural Fe(II) is not accessible to the short 0.5-M extraction. The average 0.5-M HCl measure of Fe(II) was $3.49 \pm 2.56 \mu\text{mol}$ per gram of sediment. This estimate of the reductive capacity was in remarkably close agreement to the average obtained by the O₂ column approach (Table 4.13), suggesting that for these sediments either estimate of reductive capacity could be used to estimate the longevity of these sediments as a natural barrier for chromate reduction.

In estimating the longevity for chromate reduction of the untreated Puchack sediments, the following assumptions were made: the average of 3.5- μmol Fe(II)/g of sediment is representative and Fe(II) is the dominant electron donor present; nitrate and other major electron acceptors are absent. The average sediment bulk density (1.92 g/cm³) and porosity (0.286), measured in this study (Table 4.5), will be used in this calculation. It is also assumed that a range of chromate (0.005 to 2 mg/L as Cr(VI)) and O₂ (0, 2, and 8.4 mg/L) concentrations could be present to derive a range in possible treatment capacities. These Cr(VI) concentrations represent the range observed in monitoring wells MW36/37 and borehole D-2; concentrations in borehole D-2 were below the detection limit of approximately 5 $\mu\text{g}/\text{L}$. The moles of Fe(II) electron donors per unit volume of pore space liquid divided by the moles of electron acceptors per unit pore volume represents the longevity in units of pore volumes (for the volume element of sediment being considered). A representative calculation is as follows for the highest Cr(VI) concentration observed in boreholes (2 mg/L) and O₂ at 2 mg/L, approximately 1/4 saturation of 8.4 mg/L at 25°C (Szecsody et al. 2005a):

electron donor: moles of electrons per cm³ liquid from the Fe(II):

$$(3.5 \mu\text{mol Fe}^{2+}/\text{g})(1 \text{ e}^-/\text{Fe}^{2+})(1.92 \text{ g sed./cm}^3)(\text{cm}^3/0.29 \text{ cm}^3 \text{ liquid}) \\ \times (\text{mol}/10^6 \mu\text{mol})(10^3 \text{ cm}^3/\text{L}) \\ = 23.2 \text{ mmol e}^-/\text{L liquid}$$

electron acceptors: moles of electrons per cm³ liquid from 2 mg/L dissolved oxygen and CrO₄²⁻

$$(2 \text{ mg/L O}_2)(\text{g}/1,000 \text{ mg})(\text{mol O}_2/32 \text{ g}) (4 \text{ mol e}^-/\text{mol O}_2) \\ = 2.5 \times 10^{-4} \text{ mol e}^-/\text{L}$$

$$(2.0 \text{ mg/L Cr(VI)})(\text{g}/1,000 \text{ mg})(\text{mol Cr(VI)}/52 \text{ g}) (3 \text{ mol e}^-/\text{mol CrO}_4^{2-}) \\ = 1.2 \times 10^{-4} \text{ mol e}^-/\text{L}$$

$$\text{total electron acceptors} = 2.5 \times 10^{-4} + 1.2 \times 10^{-4} = 3.7 \times 10^{-4} \text{ mol e}^-/\text{L}$$

barrier longevity (BL): electron donors/electron acceptors (number of pore volumes barrier will last)

for 2 mg/L O₂, 2.0 mg/L Cr(VI)

$$BL = 23.2 \times 10^{-3} \text{ mol e}^-/\text{L} / 3.7 \times 10^{-4} \text{ mol e}^-/\text{L}$$

$$BL = 63 \text{ pore volumes}$$

Thus, 63 pore volumes of groundwater containing the highest observed chromate concentration could pass through the *average* untreated Puchack sediment before its reductive capacity is exhausted. The aquitard sample NRS-1 from D1-M at 272.5 ft (i.e., dark clay) with a reductive capacity of 636 μmol/g would last an estimated 11,000 pore volumes, although little groundwater would pass through this clay unit, but would pass next to it, so some dissolved oxygen and chromate would be reduced.

With zero and 8.4 mg/L of O₂ present in the average aquifer sediments (3.5 μmol/g) longevity would vary between 193 and 20 pore volumes, respectively. If, on the other hand, the chromate concentration was near the low end of the observed concentrations, 0.1 mg/L, the barrier longevity for 0, 2 and 8.4 mg/L O₂ would be 3,866, 91, and 22 pore volumes, respectively. These calculations suggest that naturally reduced sediments can play a meaningful role in the attenuation of the chromate plume at the Puchack site even at the higher chromate concentrations as long as groundwater velocities and O₂ concentrations are not too high. On the other hand, looking back at the iron extraction data (Table 4.13) the ferrous phase designated as “other,” namely the Fe(II) which was oxalate extractable from amorphous iron phases, was highly variable (spatially). For sediment D1-M, this variability showed up in the O₂ column reductive capacity as an outlier (200 standard deviation), which we disregarded in deriving an average. This variability did not show up in the 0.5-M HCl extraction data. The observed spatial variability indicates that the chromate reduction rate would be expected to vary considerably from zone to zone in the subsurface.

Although these studies confirm the presence of mechanisms contributing to the natural attenuation of chromate in the Puchack subsurface environment, the field-scale effect of these mechanisms must be better quantified to determine the suitability of MNA (OSWER Directive 9200.4-17P), both bench and field scale data should be used when evaluating the site-specific suitability of MNA as a remedy. In addition to chromate trend monitoring at the site, numerical groundwater flow and reactive transport models could be developed that incorporate the rate and treatment capacity data resulting from these studies. These models could be used to make predictions of long-term field-scale attenuation of the chromate plume and expected impact at potential receptor locations.

The x-ray diffraction analysis of selected Puchack sediments identified quartz as the dominant mineral phase in deep composite sediment DC-2 and individual sediments NRS-1, -2, and -3. The x-ray diffraction data is provided in Appendix F. However, identification of redox reactive mineral phases, possibly containing Fe(II) (e.g., magnetite, illite, smectite, hematite) did not yield any useful information because these phases were not present at high enough weight percentages (0.5%) to produce identifiable diffraction patterns.

4.4 Chromate Reactive Transport in Natural Puchack Sediments

Adsorption of chromate by sediments in 1-D columns were evaluated to confirm that parameters determined in batch experiments were in general agreement with adsorption parameters determined for flow conditions approximating those found in the field. Columns were packed with the shallow composite sediment from monitoring well MW36/37 (Table 4.6) resulting in a dry bulk density (ρ_b) and porosity (θ) of 1.65 g/cm^3 and 0.30, respectively. Two separate flow experiments were conducted under slightly different conditions. In each, the unbuffered chromate solution was injected during the first portion of the experiment to allow chromate adsorption, then the chromate concentration was reduced to zero to allow the subsequent desorption of chromate. In the first experiment the influent contained 2.7 mg/L of Cr(VI) (as chromate) and had a flow velocity through the column of 10 cm/h resulting in a 1-hour residence time. The average effluent pH for the adsorption and desorption portion of the experiment was 4.8 and 3.8, respectively (Figure 4.20). The retardation factors (R_f) (and K_d) for the adsorption and desorption phases were 37.2 (6.6) and 18.6 (3.2), respectively. The influent solution in the second experiment contained 2 mg/L Cr(VI), as chromate, with a flow velocity of 5.75 cm/hour and a residence time of 8.25 hours (Figure 4.20). For both the adsorption and desorption portions of this experiment, the average effluent pH was 7 with a R_f (K_d) of 16.5 (2.8). The retardation factors in these experiments were derived by converting the vertical axis of Figures 4.20 and 4.21 to C/C_0 , integrating the area in front of these breakthrough curves and normalizing the areas with the porosity of each column. The adsorption mass (K_d values) were calculated from the relation $R_f = 1 + \rho/\theta K_d$. The flow velocities in these experiments were higher than the upper end of the typical groundwater flows seen in field situations (0.013 to 1.3 cm/hour), however they were in the range of velocities typically observed near a pumping well.

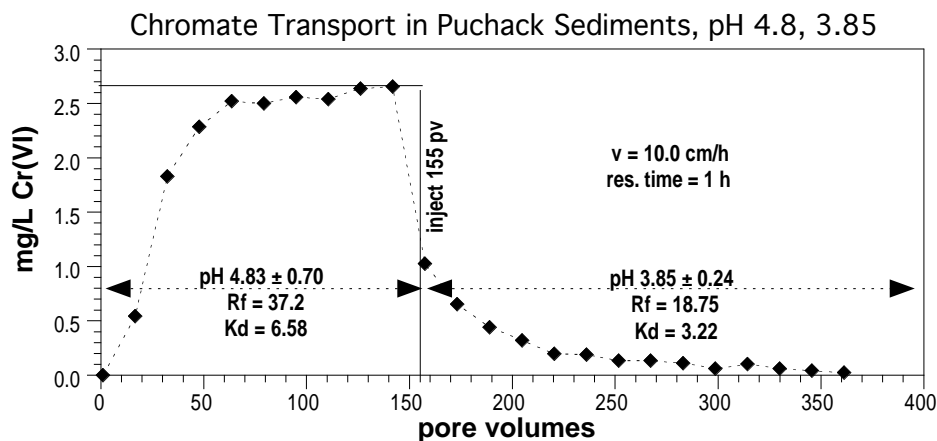


Figure 4.20. Evaluation of Chromate Adsorption at pH 4.8 and 3.85 During Reactive Transport in a 1-D Column Packed with a Shallow Sediment Composite

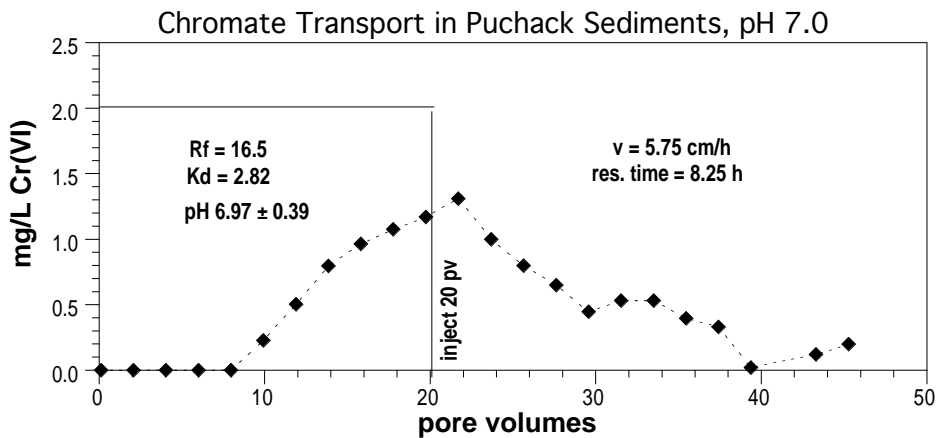


Figure 4.21. Evaluation of Chromate Adsorption at pH 7 during Reactive Transport in a 1-D Column Packed with a Shallow Sediment Composite

In both experiments the attenuation of chromate was mainly due to adsorption with greater lag (retardation due to adsorption) at low pH (pH 4.8, $K_d = 6.6$) and less lag at high pH (pH 7, $K_d = 2.8$). This is consistent with batch experiment pH edges for the deep composite sediment DC2 (Figure 4.14) where adsorption is greater at low pH. The K_d values calculated for $pH > 6$ from this adsorption edge for 3- and 18-hour batch experiments are shown in Figure 4.22. Below pH 6, adsorption was essentially 100% resulting in aqueous concentrations being below detection limits, which precluded the calculation of accurate K_d values. With adsorption equilibrium requiring between 10 to 15 hours (Section 4.2.1) the increase in K_d between 3 and 18 hours represent the approach to equilibrium. The equilibrium K_d from the 8.25-hour resident time column experiments is shown in Figure 4.22 for comparison. The agreement

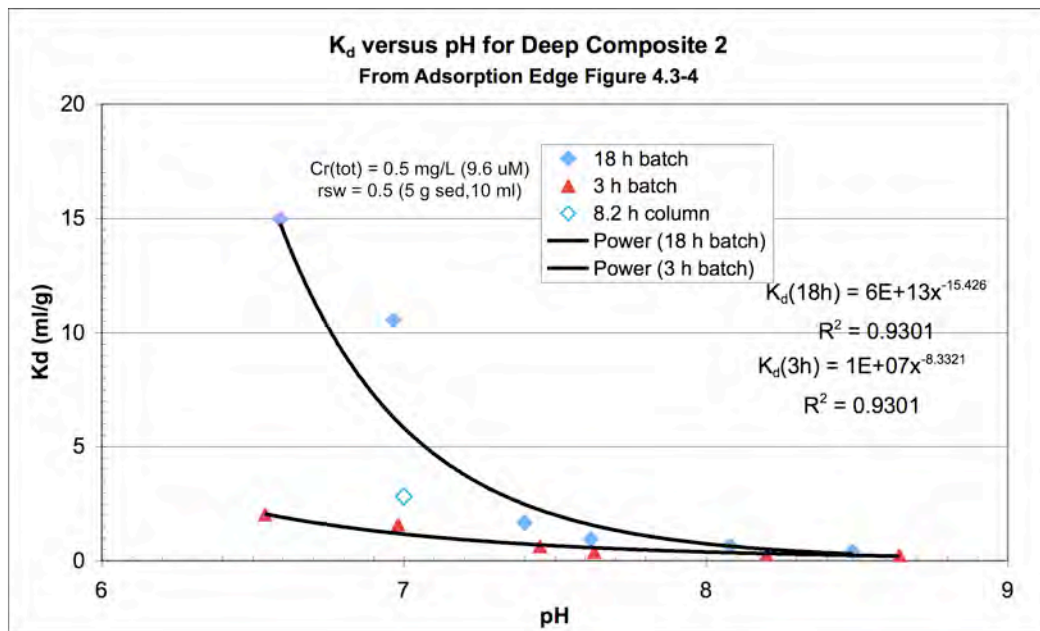


Figure 4.22. Comparison of K_d vs. pH for Deep Composite 2 Sediment from Batch Experiments to the K_d Derived from 1-D Column Experiments with the Shallow Composite Sediment

between this batch and column K_d is worth noting, with the column K_d being lower, which would be expected based on the shorter residence time in the column. The fact that different sediment composites were used also may have contributed to this difference. A comparison between batch and the column K_d values at pH 4.8 is not possible because batch K_d values at this pH could not be calculated. Although only a single point comparison, this would suggest that adsorption parameters (e.g., K_d as a function of pH and/or sulfate concentration [Figure 4.11]), measured in batch experiments, which are easier to perform than column experiments, are adequate for use in Cr(VI) reactive transport modeling.

4.5 Chemical Reduction of Puchack Sediments

4.5.1 Barrier Capacity and Longevity

Column experiments were conducted to determine the amount of reducible iron and the oxidation rate of Puchack sediments using a dithionite/pH buffer solution (reduction) and oxygen-saturated water (oxidation). The natural reductive capacity of Puchack sediments was discussed in Section 4.2 while this section will focus on the reductive capacity of dithionite-reduced sediments. The mechanism for sediment reduction using dithionite was discussed previously in Section 2.2.1. Dithionite reduction dissolves and reduces amorphous and some of the crystalline Fe(III) oxides present in sediments. This method produces many different Fe(II) phases some of which have been identified and quantified in Table 4.15, for comparative purposes the natural sediment data has also been included. Eleven reduction/oxidation experiments were carried out on both the shallow composite MW36/37 sediment and sediment samples from all four wells used in this study. The reduced sediment columns were then oxidized with oxygen-saturated water to simulate what would occur naturally in the field. Oxidizing species in groundwater i.e., dissolved oxygen, contaminants like chromate, nitrate or other electron acceptors flow through sediment under natural gradient conditions which are best simulated using columns in the laboratory.

The most accurate method for determining the mass of reduced iron in sediments is considered to be the column O_2 oxidation method. This is because actual electron transfer from iron oxidation reactions (Equations 2.7 and 2.8, Section 2.2.2) are measured by the O_2 consumption from the O_2 saturated influent solution. This is in contrast to the 0.5-M HCl extraction method of measuring Fe(II), where all acid soluble Fe(II) phases are measured regardless of the electron transfer efficiency of the dissolved phase. During the O_2 column oxidation experiments two oxygen probes continuously monitor the oxygen concentration of the effluent. The oxidation experiments were continued until most of the reduced iron was oxidized and the end point was determined by the amount of oxygen in the effluent. An ideal oxidation end point would be achieved when the measured effluent O_2 approaches 95 to 100% of the influent value. Because this condition is difficult to achieve experimentally, the end point was typically when the measured effluent O_2 was found to be > 80% of the influent value. This calibration data was used to calculate the oxygen-free (0) and oxygen-saturated (1) lines shown on Figure 4.23 (results from all experiments are provided in Appendix C). The reductive capacity in μmol pf Fe(II)/g of sediment reported in Table 4.14 are average values of the two probes. The size and shape of oxygen breakthrough curves are used to calculate the mass of reduced iron and provide oxidation rate information.

Results from one oxidation experiment using Puchack sediment are shown in Figure 4.23. Although oxygen saturated water is injected into the column, the effluent is oxygen free for approximately the first 18 pore volumes due to oxygen consumption by ferrous iron. At this point in the experiment, rapid oxygen breakthrough is observed (not all O_2 added is consumed) and a change in slope results from

Table 4.15. Natural and Dithionite-Reduced Sediment Reductive Capacity and Iron Speciation

borehole, depth	treat ment	O ₂ column reductive capacity (μmol/g)	Fe ^{II} phases				Fe ^{III} phases			Fe ^{II} +Fe ^{III} total (μmol/g) [7]
			Fe ^{II} CO ₃ +FeS (μmol/g) [1]	other Fe ^{II} (μmol/g) [2]	adsorbed Fe ^{II} (μmol/g) [8]	total Fe ^{II} (μmol/g) [3]	amorphous Fe ^{III} oxides (μmol/g) [4]	crystalline Fe ^{III} oxides (μmol/g) [5]	total Fe ^{III} (μmol/g) [6]	
MW36C, 151'	none	4.10	8.63	1290		631	528	168	245	876
MW37I, 197.5'	none	2.56	2.28	3.64		14.9	2.17	91.7	41.3	56.3
D1-H, 220.5'	none		2.81	10.4		16.2	6.11	196	66.7	82.9
D1-M, 272.5'	none	636	2.38	237	2.26	8.37	25.0	222	22.2	30.5
D2-E, 211	none	1.63	3.10	2.90		30.5	0.87	99.4	22.3	52.8
D2-H, 271'	none	2.77	1.75	6.01		9.62	3.32	96.5	39.6	49.2
average natural sediments:		129 ± 283 2.76 ± 1.02 (no D1-M)	3.49 ± 2.56			118 ± 251			72.8 ± 85.9	210 ± 281
composite, pH 4.5 reduced										
composite, pH 5.3 reduced		54.5								
composite, pH 6.2 reduced		62.2								
composite, pH 7.0 reduced		106								
MW-36C, 151'	reduced	84.8								
MW-36F, 167.5'	reduced	390	1210		3.54	7.04			535	542
MW-36I, 197.5'	reduced		41.8		0.20	21.5			7.47	29.0
MW-36I, 197.5'	reduced	23.9	63.8		0.23	35.3			5.29	40.6
MW-36M, 221'	reduced		27.1		0.46	2.15			26.7	28.9
MW-37C, 154'	reduced	80.5	52.7		0.40	2.23			44.3	46.6
MW-37F, 171.5'	reduced		40.20		0.54	2.39			39.5	41.9
MW-37I, 199'	reduced		172.4		2.20	2.26			37.5	39.7
D1-B, 106'	reduced	52.4			0.34					
D1-F, 164'	reduced	54.7			0.39					
D1-H, 220.5'	reduced	58.5	71.2		1.02	2.75			143	145.4
D2-C, 151'	reduced	23.9			0.54					
D2-H, 271'	reduced		50.2		1.31	1.16			63.2	64.4
average reduced sediments:		90.1 ± 102 60.2 ± 25.6 (no MW36C)	192 ± 384		0.93 ± 1.0	31 ± 12.0			100 ± 168	109 ± 166

[1] From 1 h, 0.5 M HCl extraction.

[2] Amorphous Fe^{II} from 24 h, 0.18 M ammonium oxalate extraction at pH 3.4.

[3] From 21 day, 5 M HCl extraction

[4] From 24 h, 0.18 M ammonium oxalate extraction at pH 3.4.

[5] From DCB extraction and subtraction of the amorphous Fe^{III}.

[6] From 21 day, 5 M HCl extraction, and hydroxylamine hydrochloride reduction of filtrate.

[7] The sum of Fe^{II} and Fe^{III} columns.

[8] From 24 h, 1 M CaCl₂ extraction

partial consumption of the added O₂. After an initial steep increase in O₂ concentration, the slope gently tails off to a saturation of approximately 0.90. These slope changes are indicative of Fe(II) phases being oxidized at different rates, hence for the oxidation reaction of the sediment shown in Figure 4.23, there are at least two different Fe(II) phases present. Other studies have shown that adsorbed ferrous iron (Table 4.14) is quickly oxidized and may represent the majority of the reduced iron in sediments, while the slowly oxidizing Fe(II) phases are thought to represent siderite (FeCO₃).

The average reductive capacity of the untreated sediments in Table 4.15 is greater than that of the reductive capacity of the dithionite reduced sediments. Upon closer inspection of the data it is apparent that this value is skewed due to the reductive capacity from one untreated sediment (D-1S-M) having an appreciably greater reductive capacity (two orders of magnitude) than all of the other untreated sediments tested. A similar observation can be made for sample, MW-36S-C, from the reduced sediments. Given the heterogeneous nature of natural samples it is not uncommon to have samples that behave differently and are not representative of more typical reductive capacities. In order to minimize the impact of non-representative samples on the overall quality of the data set, greater sample numbers are needed, within practical limitations of laboratory experiments (time constraints, cost etc). Considering the reductive

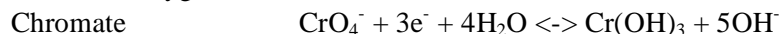
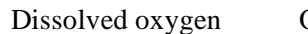
capacity data, excluding the aforementioned samples, there is a decrease in the standard deviation for both the natural and treated sediments and the reduced sediments show a significant increase in reductive capacity. The average reductive capacity of the dithionite reduced sediments increased by an order of magnitude to $60.2 \pm 25.6 \mu\text{mol/g}$ from a naturally occurring reductive capacity of $2.76 \pm 1.02 \mu\text{mol/g}$. Similar results were obtained from Fe(II) extraction by 0.5-M HCl, again the higher values have been disregarded, resulting in average reductive capacity values of $64.9 \pm 45.6 \mu\text{mol/g}$ for the reduced sediment and $3.49 \pm 2.56 \mu\text{mol/g}$ for the untreated sediment.

In Section 4.2.3, the longevity of the naturally occurring reductive capacity of the sediments was estimated to be 63 pore volumes for 2 mg/L O_2 and 2.0 mg/L CrO_4^- . The barrier longevity of the dithionite reduced sediment can be estimated using the same approach. Assuming the same conditions as above (2 mg/L O_2 , and 2 mg/L CrO_4^- , average dry bulk density of 1.917 g/cm^3 , porosity of $0.286 \text{ cm}^3 \text{ liquid/cm}^3 \text{ solid}$, and an average reductive capacity from the O_2 columns and Fe(II) extraction data $(60.2 + 64.9)/2 = 62.55 \mu\text{mol/g}$) we obtain:

electron donor: moles of electrons per cm^3 liquid from the Fe(II):

$$(62.55 \mu\text{mol Fe}^{2+}/\text{g})(1 \text{ e}^-/\text{Fe}^{2+})(1.92 \text{ g sed./cm}^3)(\text{cm}^3/0.29 \text{ cm}^3 \text{ liquid})(\text{mol}/10^6 \mu\text{mol})(10^3 \text{ cm}^3/\text{L}) \\ = 414.124 \text{ mmol e}^-/\text{L}$$

electron acceptors: moles of electrons per cm^3 liquid from 2 mg/L dissolved oxygen and CrO_4^- :



$$(8.4 \text{ mg/L O}_2)(\text{g}/1,000 \text{ mg})(\text{mol O}_2/32 \text{ g})(4 \text{ mol e}^-/\text{mol O}_2) \\ = 1.050 \text{ mmol e}^-/\text{L}$$

$$(2 \text{ mg/L CrO}_4^-)(\text{g}/1,000 \text{ mg})(\text{mol CrO}_4^-/52 \text{ g})(3 \text{ mol e}^-/\text{mol CrO}_4^-) \\ = 0.115 \text{ mmol e}^-/\text{L}$$

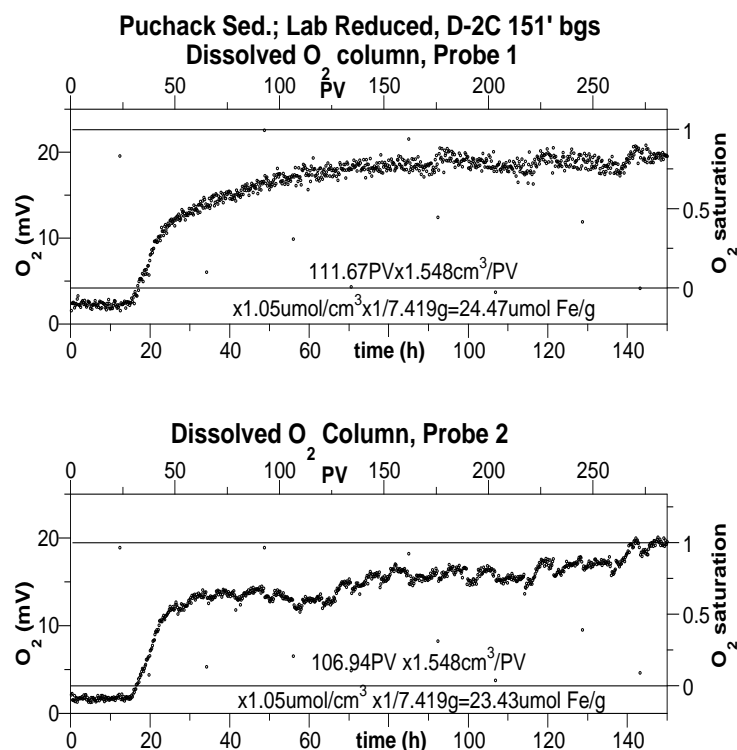


Figure 4.23. Oxidation of a Reduced Sediment Column with Dissolved Oxygen in Water

Total electron acceptors = **1.050 + 0.115 = 1.165 mmol e⁻/L**

barrier longevity: electron donors/electron acceptors (number of pore volumes the acceptor can be passed through the donor region to oxidize it):

for 8.4 mg/l O₂, 2.0 mg/L CrO₄⁻

414.124/1.165

Barrier Longevity = 355.4 pore volumes

Thus, 355 pore volumes of groundwater containing the highest observed chromate concentration could pass through the average fully reduced Puchack sediment at the upper O₂ limit i.e., the saturation point of the natural dissolved O₂ concentration (8.4 mg/L at 25°C) before the reductive capacity of the barrier would be depleted. For a 40-ft-wide barrier and an average groundwater velocity of 1 ft/day, 355 pore volumes of treatment would result in a barrier longevity of 39 years. Comparing this value to the natural reducing sediments under the same conditions we observe a significant increase in barrier longevity, 355 pore volumes as opposed to 20 pore volumes. Assuming an O₂ concentration on the low end of the observed range (3 mg/L), the barrier longevity would increase to 845 pore volumes (or a longevity of 92 years), in comparison to 193 pore volumes for the natural sediment. This suggests that the reduced sediments would be considerably more effective in the attenuation of chromate at the Puchack site for at high chromate and oxygen concentrations than the naturally reduced sediments. Reconsidering the iron extraction data provided in Table 4.15, the outlier MW-36C, which was disregarded when deriving the average reduction capacity for both the O₂ column and ferrous iron extraction data, gives an indication of the spatial variability of iron present at the Puchack site. If this sediment were to be included in the average reductive capacity the value increases from 68.5 to 141.1 µmol/g of sediment and our barrier longevity range increases accordingly. Therefore, due to the spatial variability of iron present at the Puchack site, some degree of variability in the chromate reduction capacity will occur from zone to zone in the subsurface.

4.5.2 Redox Reactive Phases Produced with Dithionite Reduction

Sediment reduction with dithionite solution (dithionite and potassium carbonate) dissolves and reduces amorphous and some crystalline Fe(III) oxide phases producing several different Fe(II) phases. Reducing the Puchack sediments (Table 4.15) has resulted in an increase in the amount of ferrous iron phases present. The reductive capacity obtained ($64.9 \pm 45.6 \mu\text{mol/g}$) from the ferrous iron phases (Fe(II)_(ads.), Fe(II)CO₃, FeS) extracted from the reduced sediments are comparable to the average reductive capacity obtained from O₂ column oxidation. The iron extraction data obtained in this study does not permit designation of particular ferrous iron phases responsible for the reduction capacity observed. Possible phases produced during reduction include adsorbed Fe(II), siderite, FeS, and reduced structural iron in clay present within the sediments. If the predominate phase produced from the reduction of Puchack sediment was adsorbed Fe(II) chromate reduction at low pH (pH<5) would not be possible using the reduced sediments. The adsorption edge for ferrous iron typically occurs between pH 4 and 5 and is not adsorbed at low pH. Thus, adsorbed Fe(II) resulting from sediment reduction would be mobile and easily washed out of the system at low pH and unavailable as an electron donor for chromate reduction. It has been demonstrated (Section 4.6.1) that even at pH values from 4.5 to 7, appreciable amounts of chromate can be treated with reduced Puchack sediment, indirectly implying that not all the ferrous iron

present is adsorbed and thus, is present as other ferrous iron phases. This is consistent with the low adsorbed Fe(II) data given on Table 4.15 from the 1-M CaCl₂ extraction.

4.5.3 Trace Metal Mobilization with Dithionite Reduction

The mobility of major and trace metals during sediment reduction was measured in effluent samples by ICP-MS during reduction for 24.7 pore volumes (Table 4.16) to assess the potential migration of heavy metals that could occur as the natural (oxic) sediment is reduced. Total metal concentrations were measured by ICP-MS. The data shown in Table 4.16 is the product of two column reduction experiments, the pore volumes associated with the first column experiment have been made bold for identification purposes. Slight variations in the data can be seen between the two different experiments characteristic of heterogeneous samples.

The dithionite solution injected into the sediments during reduction is comprised of Na₂S₂O₄ (0.09 mol/L) and K₂CO₃ (0.36 mol/L) at pH 10.5 and Eh 560 mV. It only takes a few pore volumes for the effluent concentrations to reach the concentrations of the injection solution. Major and trace metals found in the chemical compounds used to make the dithionite solution and other trace elements present (due to manufacturing processes) in the unreacted dithionite solution (Table 4.15) have been marked with an asterisk. The dithionite injection solution used in this study contains appreciable amounts of Cr, V, Se, Br, Rb, Zn and Hg (Tables 4.16 and 4.17). There are two different manufacturing process for dithionite one uses a zinc process and the other a formate process. The zinc process produces higher amounts of trace metals in the final product than the formate process. The dithionite used in all of the laboratory experiments was made by the zinc process resulting in the presence of trace amounts of zinc and the other elements mentioned above. Appendix G gives a brief outline on the manufacturing process of dithionite by both processes along with the typical trace metal analysis of the formate process from the manufacturer.

Metals that were mobilized due to the reducing conditions created include Fe, Mn, and As, as the reduced species of these metals are more mobile under low Eh conditions. There is no effect on the concentration of Ti, Se, and Ni, which leach out at a constant rate from the sediment regardless of Eh. The concentration of Pb, Co, Ni, Mo, Sb, Cs, I, Ba, and Sr initially increase then decrease most probably due to ion exchange and would have also leached out of the sediment regardless of Eh. Metals that decrease due to the reducing conditions include Mg and U. All of these changes are not considered significant because the highly reducing conditions that mobilize these metals are only produced during the dithionite injection in the treatment zone and only occur over a period of 2 to 3 days of treatment until the dithionite degrades. It has been previously demonstrated that the metal mobilization is not widespread and that Fe/Mn/As mobilization does not extend beyond the treatment radius (20 to 25 ft)

Table 4.16. Metals Mobility during Sediment Reduction in Columns

pore volumes	Li $\mu\text{g/l}$	Be $\mu\text{g/l}$	*Na g/l	Mg mg/l	Al mg/l	Si mg/l	*K g/l	Ca mg/l	Sc $\mu\text{g/l}$	Ti $\mu\text{g/l}$	*V $\mu\text{g/l}$	*Cr $\mu\text{g/l}$	Mn $\mu\text{g/l}$	Fe mg/l	Co $\mu\text{g/l}$	Ni $\mu\text{g/l}$	Cu $\mu\text{g/l}$
Dithionite inj. Soln.																	
<1000	<100	7.10	<2	<2	<200	>20	<700	<1000	<100	262	967	<100	<10	<5	<300	<200	
0.9	<100	<10	2.37	46.3	<0.2	<20	>2	107	<100	30.7	48.9	<50	612.2	3.5	110.7	268.7	<20
1.9	<100	<10	>3.5	2.0	0.2	<20	>2	<70	<100	23.0	<10	<50	351.1	3.5	18.7	326.0	<20
2.9	<100	<10	>3.6	1.5	<0.2	<20	>2	<70	<100	20.7	<10	<50	444.7	<1	5.7	182.5	<20
3.9	<100	<10	>3.7	1.3	<0.2	<20	>2	<70	<100	27.4	<10	<50	638.6	4.3	5.1	300.6	<20
4.9	<100	<10	>3.8	1.1	<0.2	<20	>2	<70	<100	32.9	<10	<50	731.7	15.1	3.1	277.8	<20
6.9	<100	<10	>3.5	0.5	<0.2	<20	>2	<70	<100	28.6	<10	<50	248.5	<1	15.5	194.6	<20
9.7	<100	<10	>3.6	0.2	<0.2	<20	>2	<70	<100	25.0	<10	<50	226.5	<1	7.2	197.3	<20
19.7	<100	<10	>3.7	0.2	0.3	<20	>2	<70	<100	26.3	22.8	<50	106.7	<1	4.6	204.9	<20
24.7	<100	<10	>3.8	<0.2	0.3	<20	>2	<70	<100	20.2	24.3	<50	108.6	<1	3.5	268.2	<20
Dithionite inj. Soln.																	
pore volumes	*Zn $\mu\text{g/l}$	Ga $\mu\text{g/l}$	Ge $\mu\text{g/l}$	As $\mu\text{g/l}$	*Se $\mu\text{g/l}$	*Br mg/l	*Rb mg/l	Sr $\mu\text{g/l}$	Y $\mu\text{g/l}$	Zr $\mu\text{g/l}$	Nb $\mu\text{g/l}$	Mo $\mu\text{g/l}$	Ru $\mu\text{g/l}$	Pd $\mu\text{g/l}$	Ag $\mu\text{g/l}$	Cd $\mu\text{g/l}$	In $\mu\text{g/l}$
<1000	898	<10	21	59	620	3.6	2.5	<40	<3	38	<5	<100	<10	88	<200	<10	<1
0.9	<50	1.1	<1	33.7	38.3	0.7	0.9	1000.0	97.5	104.4	<0.5	230.4	<1	<1	<20	1.3	<0.1
1.9	72.2	2.6	2.3	163.8	37.5	1.9	2.3	185.8	187.7	96.2	<0.5	150.0	<1	67.4	<20	<1	<0.1
2.9	92.5	<1	1.8	214.5	36.2	1.9	2.2	129.8	3.3	92.6	<0.5	79.9	<1	47.6	<20	<1	<0.1
3.9	79.7	<1	1.1	302.9	38.7	1.9	2.3	125.1	89.8	26.8	<0.5	63.0	<1	31.5	<20	<1	<0.1
4.9	80.5	<1	<1	512.2	<20	1.9	2.3	119.8	141.5	28.0	<0.5	82.8	<1	<1	<20	<1	<0.1
6.9	117.6	<1	1.2	847.5	27.7	1.8	2.3	95.8	1.5	77.8	<0.5	96.0	<1	488.0	<20	<1	<0.1
9.7	65.6	<1	<1	770.1	24.9	1.9	2.2	77.5	3.5	53.8	<0.5	67.4	<1	177.2	<20	<1	<0.1
19.7	74.5	4.9	<1	217.3	30.6	1.8	2.2	45.4	42.4	107.9	<0.5	17.4	<1	92.5	<20	<1	<0.1
24.7	60.8	4.6	1.2	215.6	24.1	1.8	2.2	45.6	38.6	109.8	<0.5	11.3	<1	68.5	<20	<1	<0.1
Dithionite inj. Soln.																	
pore volumes	Sn $\mu\text{g/l}$	Sb $\mu\text{g/l}$	Te $\mu\text{g/l}$	I $\mu\text{g/l}$	Cs $\mu\text{g/l}$	Ba $\mu\text{g/l}$	La $\mu\text{g/l}$	Ce $\mu\text{g/l}$	Pr $\mu\text{g/l}$	Nd $\mu\text{g/l}$	Sm $\mu\text{g/l}$	Eu $\mu\text{g/l}$	Gd $\mu\text{g/l}$	Tb $\mu\text{g/l}$	Dy $\mu\text{g/l}$	Ho $\mu\text{g/l}$	Er $\mu\text{g/l}$
<1000	<10	<100	<1000	<1	<100	2	3	1	3	3	1	<1	<1	<1	<1	<1	<1
0.9	<10	27.5	<10	245.8	15.4	342.4	3.6	12.4	2.7	18.1	5.6	1.8	7.8	1.6	11.1	2.8	10.5
1.9	<10	11.1	<10	198.7	13.0	137.6	15.3	57.6	12.4	78.5	26.4	6.4	28.5	4.9	25.6	5.9	17.2
2.9	<10	4.5	<10	138.9	2.5	47.1	<0.1	0.4	<0.1	0.4	<0.1	<0.1	0.2	<0.1	0.3	0.1	0.3
3.9	<10	7.8	<10	109.2	1.1	125.7	9.5	36.4	7.4	43.4	16.3	3.4	15.7	2.6	13.2	2.7	7.6
4.9	<10	12.6	<10	<100	0.8	128.3	13.1	53.2	10.3	65.2	20.7	5.3	23.0	3.8	21.7	4.3	12.1
6.9	<10	12.4	<10	738.1	0.7	28.6	<0.1	0.3	<0.1	0.1	0.1	<0.1	<0.1	<0.1	0.1	<0.1	0.1
9.7	<10	11.9	<10	285.4	0.4	49.0	<0.1	0.5	<0.1	0.2	0.3	<0.1	0.1	<0.1	0.2	<0.1	0.3
19.7	<10	1.7	<10	191.3	0.2	44.7	4.2	16.8	3.1	19.8	5.9	1.5	6.5	1.0	6.5	1.3	3.8
24.7	<10	2.1	<10	157.2	0.3	44.1	3.4	13.6	2.5	16.7	5.2	1.2	5.5	1.0	5.6	1.2	3.9
Dithionite inj. Soln.																	
pore volumes	Tm $\mu\text{g/l}$	Yb $\mu\text{g/l}$	Lu $\mu\text{g/l}$	Hf $\mu\text{g/l}$	Ta $\mu\text{g/l}$	W $\mu\text{g/l}$	Re $\mu\text{g/l}$	Os $\mu\text{g/l}$	Pt $\mu\text{g/l}$	Au $\mu\text{g/l}$	Hg $\mu\text{g/l}$	Tl $\mu\text{g/l}$	Pb $\mu\text{g/l}$	Bi $\mu\text{g/l}$	Th $\mu\text{g/l}$	U $\mu\text{g/l}$	
<1	<1	<1	<1	<1	<20	<1	<2	<300	65	<200	<1	<10	<300	15	<1		
0.9	1.7	13.2	2.5	2.5	<0.1	7.8	<0.1	<0.2	<30	<0.2	<20	<0.1	9.4	<30	54.5	157.8	
1.9	2.4	19.4	3.3	1.6	<0.1	17.0	<0.1	<0.2	<30	24.1	<20	<0.1	1.1	<30	35.1	47.6	
2.9	<0.1	0.4	<0.1	0.8	<0.1	10.4	<0.1	<0.2	<30	18.2	<20	<0.1	<1	<30	0.2	14.2	
3.9	1.0	6.8	1.1	0.3	<0.1	2.9	<0.1	<0.2	<30	12.3	<20	<0.1	<1	<30	7.6	24.6	
4.9	1.8	11.9	1.9	0.5	<0.1	2.4	<0.1	<0.2	<30	0.3	<20	<0.1	<1	<30	41.0	38.5	
6.9	<0.1	<0.1	<0.1	1.2	<0.1	2.9	<0.1	<0.2	<30	116.0	91.4	<0.1	<1	<30	<0.1	17.5	
9.7	<0.1	0.5	<0.1	0.6	<0.1	<2	<0.1	<0.2	<30	50.0	36.8	<0.1	<1	<30	<0.1	20.1	
19.7	0.5	4.3	0.6	1.7	<0.1	2.2	<0.1	<0.2	<30	30.0	24.9	<0.1	<1	<30	57.4	34.2	
24.7	0.6	4.3	0.7	1.8	<0.1	<2	<0.1	<0.2	<30	24.4	25.1	<0.1	<1	<30	48.7	35.4	

Table 4.17. Hg Mobility during Reduction and Oxidation

Dithionite Reduction		Oxidation pH=4.5		Oxidation pH=5.3		Oxidation pH=6.2		Oxidation pH=7	
Pore Volumes	Hg ng/L	Pore Volumes	Hg ng/L	Pore Volumes	Hg ng/L	Pore Volumes	Hg ng/L	Pore Volumes	Hg ng/L
0.38 1.38 2.38 3.38 4.38	35	1	<12	1	10635	1	743	2	22865
	4235	3	18	3	40	3	<12	3	154
	4877	5	18	5	57	5	<12	5	18
	58	7	48	7	<12	7	<12	7	<12
	4129	9	<12	9	17	9	<12	9	16
		18	16	18	12	18	<12	18	<12
		26	12	26	<12	26	<12	26	<12
		44	28	44	<12	44	<12	44	<12
		52	13	52	<12	52	<12	52	<12
		150	<12	150	15	150	<12	150	<12
		265	<12	265	<12	263.6	<12	265	<12
		415	<12	415	<12	413	<12	415	<12
		565	<12			563	<12	565	<12
matrix Dble DI H ₂ O	19970 <12	matrix Dble DI H ₂ O	<12 <12						

4.6 Chromate Immobilization and Changes in Other Metals/Solutes in Dithionite-Reduced Sediments

4.6.1 Chromate Transport and Reduction

Column experiments investigating the transport of chromate (CrO_4^-) as a function of the pH range found in Puchack groundwater (4.5 to 7.0) were conducted on dithionite-reduced sediments (Figures 4.24a through d). As previously discussed, dithionite reduction creates a range of different ferrous iron surface phases and sufficient amounts of immobile ferrous iron are produced to immobilize chromate for a considerable length of time i.e., hundreds of pore volumes or tens of years. The significance of these experiments is that dithionite treatment of Puchack sediments can produce an effective barrier to immobilize chromate, even under acidic conditions. It was hypothesized that under acidic conditions: a) ferrous iron phases produced could be mobile (aqueous), and b) Cr(III) species produced could be mobile. Ferrous iron mobility is described in this section and total Cr (III + VI) is described in the following section.

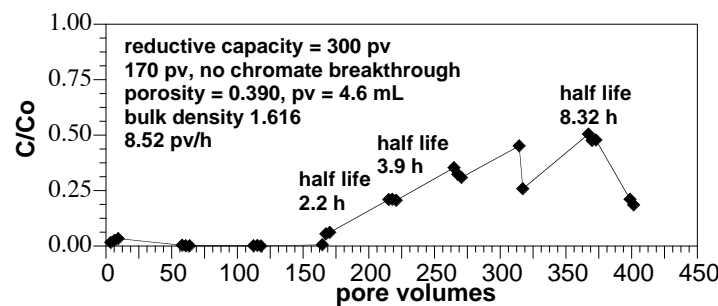
Under acidic conditions adsorbed ferrous iron is mobile so the capacity of reduced sediments to immobilize chromate may be less at low pH than at neutral pH. Reduced structural iron in clay on the other hand is not mobilized at low pH and could be a source of immobile ferrous iron. If the only ferrous phase produced during sediment reduction was adsorbed, rapid Fe(II) chromate breakthrough would occur during transport experiments due to the washing out of the adsorbed Fe(II). Complete removal of chromate is observed in Figures 4.24a) through d) for the first 160 pore volumes over the pH range 4.5 to 7.0. After this time, the partial chromate breakthrough is observed in the lower pH columns (Figure 4.24a and 4.24b). This would suggest that there is less reductive capacity at lower pH either due to less initial

reduction or some of the Fe(II) has washed out at low pH. All sediment columns were reduced with potassium carbonate under similar alkaline conditions (pH 10).

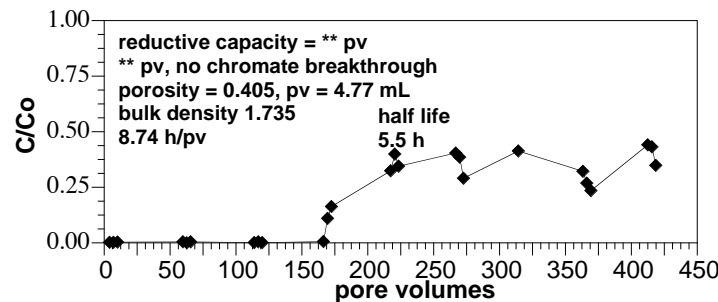
The minimum reductive capacity of these four sediment columns was calculated from the chromate consumption in these experiments and dissolved oxygen breakthrough for an additional 200 pore volumes after the end of these chromate experiments. At pH 6.2 and 7.0, since there was only partial chromate break through, the capacity was higher than this calculated value. Results (Table 4.14) indicate a reductive capacity of 54.5 $\mu\text{mol/g}$ (pH 4.5), 62.2 $\mu\text{mol/g}$ (pH 5.5), 106 $\mu\text{mol/g}$ (pH 6.2), and 84.8 $\mu\text{mol/g}$ (pH 7.0). For all four columns, most of the reductive capacity (> 90%) was due to oxygen consumption. The reductive capacity (i.e., presumed to be ferrous iron in one or more surface phases) was compared with the amount of ferrous iron eluted from the columns.

The column effluent was analyzed for ferrous iron (Figure 4.25). The lower pH columns had a much higher initial release of Fe(II) with initial concentrations of 240 and 78 mg/L for the 4.5 and 5.3 pH columns respectively, whereas < 5 mg/L Fe(II) was eluted in the first sample at pH 6.2 or 7.0. In all cases, the ferrous iron elution was brief (typically only the first sample), so the total mass of ferrous iron removed from the column was small. The amount of ferrous iron eluted from each column was determined from integrating the area under the Fe(II) data (Figure 4.25), which was 0.037 mmol Fe(II) at pH 4.5,

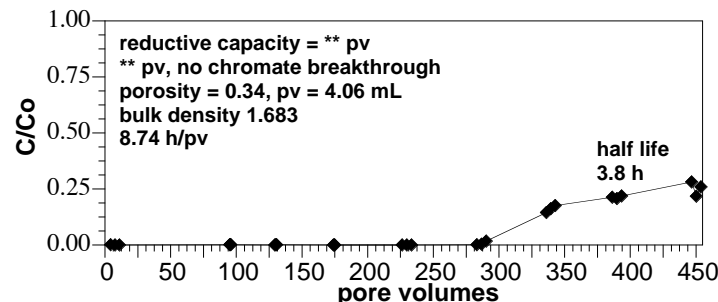
a) pH 4.5



b) pH 5.3



c) pH 6.2



d) pH 7.0

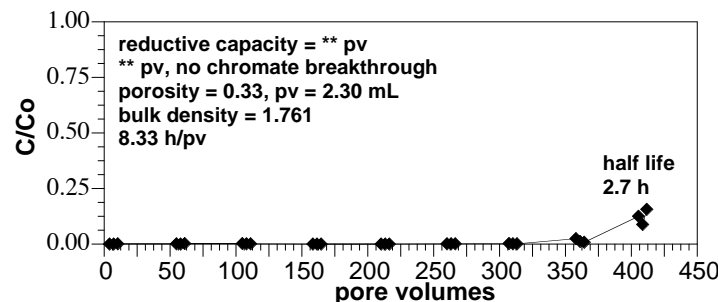


Figure 4.24. Chromate Transport in Reduced Sediment with 8.4 mg/L O₂ and 2 mg/L CrO₄⁻ at (a) pH 4.5, (b) pH 5.3, (c) pH 6.2, and (d) pH 7.0

0.016 μmol Fe(II) at pH 5.3, 0.0034 mmol Fe(II) at pH 6.2, and 0.0035 mmol Fe(II) at pH 7.0, or 10 times more at pH 4.5 compared with pH 7.0. The total ferrous iron in each column was calculated from the reductive capacity and weight of sediment in the column (12 to 20 g), which was 1.0 to 2.1 mmol Fe(II). Therefore, the ferrous iron eluted from the pH 4.5 column was 3.6% of the total reductive capacity, 1.3% (pH 5.3), 0.16% (pH 6.2), and 0.35% (pH 7.0). The significance of these findings is that dithionite reduction of Puchack sediments results in mainly immobile ferrous iron phases, and not significant amounts of adsorbed Fe(II), which would wash down gradient during flow in column (and field) experiments. Based on these findings, only a small percentage (<4%) of the ferrous iron phases produced could be adsorbed Fe(II).

Experiments were carried out in an attempt to measure the surface phases of chromium present on the sediment surface. It was found that small amounts of Cr(VI) could be extracted from the surface of the naturally reduced sediments by increasing the pH of the sediment to pH 12 for 24 hours. Permanganate extraction and oxidation of surface Cr(III) was also carried out on the sediments with some success. Most of the Cr(III) on the surface was recovered by these studies.

4.6.2 Trace Metal Mobility Changes During Reduced Sediment Oxidation

The mobility of major and trace metals were measured in effluent samples by ICP-MS (total concentration) during sediment oxidation at the four different pH values (pH 4.5, 5.3, 6.2, and 7.0) in parallel experiments to those described in the previous section (Tables 4.18 – 4.21). In these experiments, four sediment columns were reduced with sodium dithionite/potassium carbonate for 120 hours, and the metals mobility leaching during reduction was previously reported (Section 4.5.3). Oxic Puchack groundwater was then equilibrated to different pH values (pH 4.5, 5.3, 6.2, and 7.0) and used as the injection solution. This groundwater contained 11.7 ppb total Cr (as chromate, described in Section 4.2.1), along with a variety of other trace metals. As described in Section 4.6.1, chromate injection into dithionite-

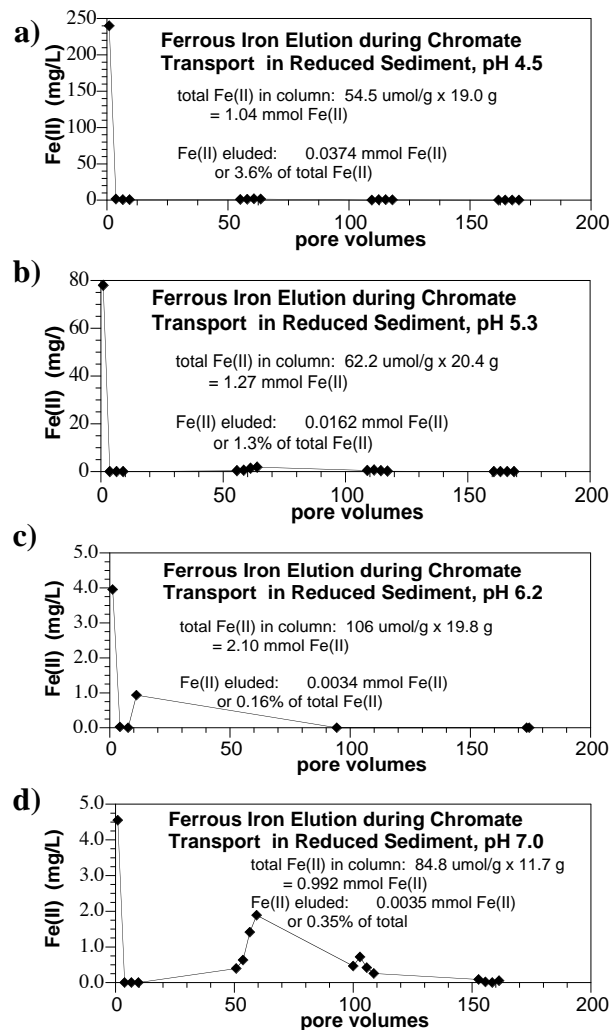


Figure 4.25. Amount of Ferrous Iron in the Effluent of the Chromate Transport Experiments (8.14 mg/L O_2 and 2 mg/L CrO_4^-) using Reduced Sediments at pH a) 4.5, b) 5.3, c) 6.2, and d) 7.0

reduced sediments at pH 4.5, 5.3, 6.2, and 7.0 is reduced and apparently immobilized (Figure 4.24) and only a small fraction of ferrous iron was washed out of the sediment columns at low pH (i.e., 3.6% at pH 4.5 versus 0.35% at pH 7.0, Figure 4.25) and total iron (Figure 4.26). Because only chromate (and ferrous iron) analysis was conducted in those experiments, the question remains as to whether chromate was reduced to immobile or mobile Cr(III) species. Under acidic conditions at equilibrium, there are significant concentrations of aqueous Cr(III) species (Figure 2.2), but it should also be noted that there are significant kinetic issues associated with the dissolution of Cr(III) species, so nonequilibrium phases may exist (i.e., departure from equilibrium phase diagrams).

Injection of Puchack groundwater with 11.7 ppb chromate at pH 4.5, 5.3, 6.2, and 7.0 for 580 pore volumes apparently does not result in the formation of aqueous Cr(III) species (Tables 4.17 through 4.20). Because the dithionite solution contains significant Cr (967 ppb), within the first pore volume of oxidation, there is some elution of Cr. At pH 4.5 and 5.3, there were total Cr values of 0.5 to 4.1 ppb from 2 through 14 pore volumes. All other samples from 14 through 580 pore volumes at all pH values showed < 0.5 ppb total Cr. Because the injection solutions were oxic and dissolved oxygen is the main oxidant, as the reductive capacity of the sediment is consumed, the injected chromate should be eluted from the column. Based on the reductive capacities (54.5 $\mu\text{mol/g}$; pH 4.5, 62.2 $\mu\text{mol/g}$; pH 5.5, 106 $\mu\text{mol/g}$; pH 6.2, and 84.8 $\mu\text{mol/g}$; pH 7.0), the capacity to remove chromate is expected to last 310 pore volumes (pH 4.5) to 600 pore volumes (pH 7.0). The trace metals analysis shows no total Cr breakthrough at later times (> 50 pore volumes), so at a minimum several hundred pore volumes of capacity was achieved for chromate reduction/immobilization, and it appears that the reduced Cr(III) species produced are immobile.

The column effluent was also analyzed for total iron (Figure 4.26). Both pH 4.5 and 5.3 showed increasing total iron after 100 pore volumes, and pH 6.5 data showed total iron increasing after 200 to 300 pore

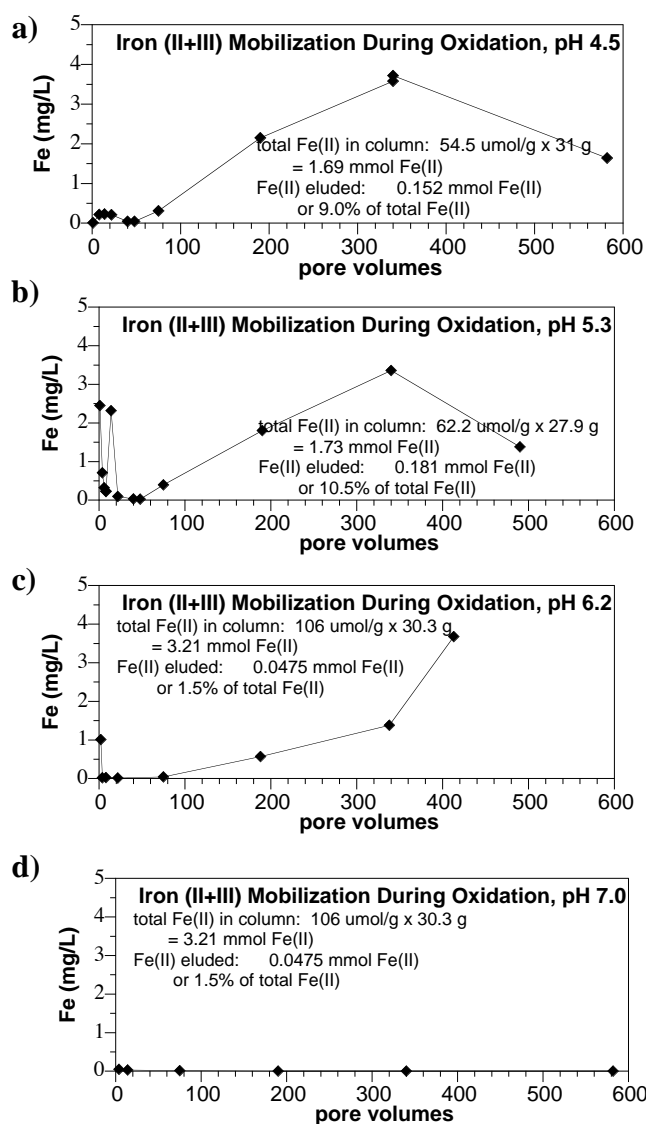


Figure 4.26. Amount of Total Iron in Column Effluent during Injection of Puchack Oxic Groundwater (with 11.7 ppb CrO_4^{2-}) into Reduced Sediments

Table 4.18. Metals Mobility during Sediment Oxidation in Columns at pH 4.5 (* = present in dith. solution, ** = present in oxidation solution)

pore volumes	Li $\mu\text{g/l}$	Be $\mu\text{g/l}$	*Na $\mu\text{g/l}$	**Mg $\mu\text{g/l}$	Al $\mu\text{g/l}$	**Si mg/l	*K mg/l	Ca mg/l	Sc $\mu\text{g/l}$	Ti $\mu\text{g/l}$	*V $\mu\text{g/l}$	*Cr $\mu\text{g/l}$	Mn $\mu\text{g/l}$	Fe $\mu\text{g/l}$	Co $\mu\text{g/l}$	Ni $\mu\text{g/l}$	Cu $\mu\text{g/l}$	*Zn $\mu\text{g/l}$	Ga $\mu\text{g/l}$	Ge $\mu\text{g/l}$	*As $\mu\text{g/l}$	*Se $\mu\text{g/l}$	*Br $\mu\text{g/l}$	
dithionite	<1000	<100	7,100	<2000	<2000	<200	>2000	<700	<1000	<100	262	967	<100	<10000	<5	<300	<200	898	<10	21	59	620	3,630	
oxidation inj. Soln.	12	<0.1	5.3	1,440	<2	12.5	2.7	6.3	1	0.7	2.3	11.7	15.0	<10	4.03	6.7	2.4	30.5	0.01	0.47	1.97	2.4	81	
0	<100	<10	>3500	368	784	<20	>2000	<70	127	<59	463	<50	92	<1000	<0.5	205	<20	721	12	2	177	36	1,240	
2	<1	<0.1	>35	8	916	5.4	>20	<0.7	<1	0.9	0.4	1.8	1.0	<10	0.025	4.5	1.4	13.9	8.70	0.47	39.7	1.2	122	
4	1	<0.1	>35	6	884	4.9	>20	<0.7	<1	0.7	<0.1	<0.5	0.6	<10	0.021	1.3	<0.2	0.7	6.48	0.19	12.9	<0.2	89	
6	1	<0.1	32.7	5	716	5.1	>20	<0.7	<1	0.6	<0.1	<0.5	0.5	<10	0.023	0.7	<0.2	<0.5	4.34	0.14	8.86	<0.2	77	
8	2	<0.1	20.5	11	676	5.2	>20	<0.7	<1	5.1	3.6	0.6	4.6	218	0.277	0.9	0.4	2.3	3.15	0.11	6.40	0.3	72	
14	3	<0.1	14.3	10	493	4.9	>20	<0.7	<1	4.4	3.2	<0.5	3.6	231	0.249	0.7	0.4	2.1	1.89	0.08	4.44	<0.2	68	
22	6	<0.1	8.5	24	293	5.4	42.3	<0.7	<1	3.7	2.7	<0.5	3.0	213	0.257	0.3	0.4	1.2	0.74	0.06	2.30	<0.2	66	
40	14	<0.1	6.6	510	48	5.6	21.0	3.1	<1	0.8	0.4	<0.5	2.8	43	0.079	<0.3	1.2	1.5	0.11	0.02	0.57	<0.2	61	
48	14	<0.1	6.6	513	80	5.8	20.9	3.3	<1	1.7	0.5	<0.5	2.8	41	0.067	<0.3	0.6	1.1	0.12	0.02	0.56	<0.2	64	
75	14	<0.1	5.9	1,640	6	6.5	4.2	7.3	<1	0.4	<0.1	<0.5	149	308	0.009	<0.3	0.3	<0.5	0.01	0.02	0.10	<0.2	65	
190	12	<0.1	5.8	1,470	4	6.8	2.3	6.1	<1	0.3	<0.1	<0.5	94.5	2,150	0.016	<0.3	<0.2	<0.5	<0.01	0.02	0.19	<0.2	68	
340	13	<0.1	5.5	1,570	5	7.9	1.9	6.8	<1	0.3	<0.1	<0.5	124	3,580	0.542	0.4	<0.2	<0.5	0.02	0.02	0.22	0.3	72	
340	13	<0.1	5.7	1,610	5	8.2	2.0	7.1	<1	0.4	<0.1	<0.5	128	3,720	0.581	0.4	<0.2	<0.5	0.02	0.03	0.31	<0.2	74	
582.8	12	0.5	5.4	1,450	62	8.8	1.8	6.6	<1	0.5	0.2	<0.5	49.2	1,640	24.8	186	7.7	22.4	0.02	0.05	0.13	0.3	71	
pore volumes	*Rb $\mu\text{g/l}$	**Sr $\mu\text{g/l}$	Y $\mu\text{g/l}$	Zr $\mu\text{g/l}$	Nb $\mu\text{g/l}$	Mo $\mu\text{g/l}$	Ru $\mu\text{g/l}$	Pd $\mu\text{g/l}$	Ag $\mu\text{g/l}$	Cd $\mu\text{g/l}$	In $\mu\text{g/l}$	Sn $\mu\text{g/l}$	Sb $\mu\text{g/l}$	Te $\mu\text{g/l}$	I $\mu\text{g/l}$	Cs $\mu\text{g/l}$	Ba $\mu\text{g/l}$	La $\mu\text{g/l}$	Ce $\mu\text{g/l}$	Pr $\mu\text{g/l}$	Nd $\mu\text{g/l}$	Sm $\mu\text{g/l}$	Eu $\mu\text{g/l}$	
dithionite	2,450	<40	<3	38	<5	<100	<10	88	<200	<10	<1	<100	<10	<1000	<1	<100	<1	<100	2	3	1	3	1	1
oxidation inj. Soln.	3.05	85.7	0.008	<0.01	<0.005	<0.1	<0.01	<0.01	<0.2	0.07	<0.001	<0.1	0.08	<0.1	52	0.178	17.5	0.003	0.002	<0.001	0.005	<0.001	0.001	
0	1,650	35	78.99	307	<0.5	59	<1	<1	<20	<1	<0.1	<10	2	<10	159	0.2	26	3.48	14.69	2,908	18.6	7,465	1,810	
2	78.4	2.55	0.26	0.43	<0.005	2.3	<0.01	0.14	<0.2	<0.01	<0.001	<0.1	0.13	59	0.008	0.3	0.02	0.13	0.009	0.064	0.023	0.005		
4	28.8	2.34	0.06	0.02	<0.005	1.1	<0.01	0.03	<0.2	<0.01	<0.001	<0.1	0.08	<0.1	48	0.003	0.2	0.01	0.04	0.003	0.026	0.008	0.002	
6	17.3	1.54	0.03	0.01	<0.005	0.6	<0.01	0.02	<0.2	<0.01	<0.001	<0.1	0.08	<0.1	44	0.001	0.1	0.01	0.03	0.003	0.014	0.003	0.002	
8	11.9	1.97	1.73	0.62	0.016	0.3	<0.01	<0.01	<0.2	<0.01	<0.002	<0.1	0.03	<0.1	40	0.003	0.8	2.19	6.17	0.842	3.37	0.939	0.190	
14	8.50	1.55	1.17	0.44	0.008	0.3	<0.01	<0.01	<0.2	<0.01	<0.001	<0.1	0.02	<0.1	50	0.003	0.5	1.63	5.11	0.620	2.45	0.697	0.144	
22	5.44	2.08	0.78	0.38	0.008	<0.1	<0.01	<0.01	<0.2	<0.01	<0.001	<0.1	0.01	<0.1	45	0.003	0.4	1.12	3.25	0.397	1.65	0.430	0.096	
40	6.76	30.7	0.11	0.10	<0.005	<0.1	<0.01	<0.01	<0.2	<0.01	<0.001	<0.1	0.03	<0.1	38	0.001	1.1	0.14	0.49	0.056	0.251	0.068	0.016	
48	6.54	30.9	0.12	0.08	<0.005	<0.1	<0.01	<0.01	<0.2	<0.01	<0.001	<0.1	0.02	<0.1	37	0.002	1.1	0.15	0.36	0.041	0.164	0.042	0.012	
75	4.96	90.8	0.01	<0.005	<0.1	<0.01	<0.01	<0.2	<0.01	<0.001	<0.1	<0.01	<0.1	52	0.001	4.3	0.01	0.01	<0.001	0.009	0.003	0.005		
190	3.34	87.6	0.02	<0.01	<0.005	<0.1	<0.01	<0.01	<0.2	<0.01	<0.001	<0.1	<0.01	<0.1	40	0.005	14.4	0.02	0.02	0.003	0.015	0.003	0.003	
340	3.81	95.6	0.03	<0.01	<0.005	<0.1	<0.01	<0.01	<0.2	<0.01	<0.001	<0.1	<0.01	<0.1	40	0.011	34.2	0.02	0.02	0.004	0.024	0.005	0.008	
340	3.92	98.8	0.03	<0.01	<0.005	<0.1	<0.01	<0.01	<0.2	<0.01	<0.001	<0.1	<0.01	<0.1	44	0.010	36.2	0.02	0.03	0.004	0.026	0.004	0.006	
582.8	3.53	92.2	0.44	0.01	<0.005	<0.1	<0.01	<0.01	<0.2	0.73	<0.001	<0.1	<0.01	<0.1	40	0.079	26.1	0.28	0.73	0.082	0.414	0.121	0.036	

pore volumes	Gd $\mu\text{g/l}$	Tb $\mu\text{g/l}$	Dy $\mu\text{g/l}$	Ho $\mu\text{g/l}$	Er $\mu\text{g/l}$	Tm $\mu\text{g/l}$	Yb $\mu\text{g/l}$	Lu $\mu\text{g/l}$	Hf $\mu\text{g/l}$	Ta $\mu\text{g/l}$	W $\mu\text{g/l}$	Re $\mu\text{g/l}$	Os $\mu\text{g/l}$	Pt $\mu\text{g/l}$	Au $\mu\text{g/l}$	Hg $\mu\text{g/l}$	Tl $\mu\text{g/l}$	Pb $\mu\text{g/l}$	Bi $\mu\text{g/l}$	Th $\mu\text{g/l}$	U $\mu\text{g/l}$	
dithionite	<1	<1	<1	<1	<1	<1	<1	<1	<1	<1	<20	<1	<2	<0.2	<30	2.2	<20	<1	<1	<30	91.5	89.8
oxidation inj. Soln.	0.002	<0.001	<0.001	<0.001	<0.001	<0.001	<0.001	<0.001	<0.001	<0.001	<0.001	0.08	0.001	<0.002	<0.3	<0.002	<0.2	0.074	0.05	<0.3	<0.001	7.18
0	9.6	1.8	12.4	2.6	7.3	0.9	6.9	1.07	9.48	<0.1	2	<0.1	<0.2	<0.002	<0.3	<0.002	<0.2	0.074	0.05	<0.3	<0.001	7.18
2	0.029	0.005	0.034	0.007	0.018	0.002	0.014	0.002	0.008	<0.001	0.12	<0.001	0.02	<0.002	<0.3	<0.002	<0.2	0.016	<0.01	<0.3	0.006	0.021
4	0.009	0.001	0.008	0.002	0.004	<0.001	0.003	<0.001	0.002	<0.001	0.07	<0.001	<0.002	<0.3	<0.002	<0.2	0.006	0.01	<0.3	0.001	0.007	
6	0.006	<0.001	0.004	0.001	0.003	<0.001	0.004	<0.001	<0.001	<0.001	0.04	<0.001	0.004	<0.001	<0.002	<0.3	<0.002	<0.2	0.005	0.03	<0.3	0.002
8	0.751	0.098	0.405	0.065	0.184	0.021	0.141	0.019	0.035	<0.001	<0.02	<0.001	<0.002	<0.3	<0.002	<0.2	0.004	0.39	<0.3	0.107	0.191	
14	0.545	0.072	0.303	0.049	0.134	0.016	0.104	0.014	0.024	<0.001	<0.02	<0.001	<0.002	<0.3	<0.002	<0.2	0.004	0.29	<0.3	0.073	0.158	
22	0.358	0.04																				

Table 4.19. Metals Mobility during Sediment Reduction in Columns at pH 5.3 (* = present in dith. solution, ** = present in oxidation solution)

pore volumes	Li $\mu\text{g/l}$	Be $\mu\text{g/l}$	*Na $\mu\text{g/l}$	**Mg $\mu\text{g/l}$	Al $\mu\text{g/l}$	*Si mg/l	K mg/l	Ca mg/l	Sc $\mu\text{g/l}$	Ti $\mu\text{g/l}$	*V $\mu\text{g/l}$	*Cr $\mu\text{g/l}$	Mn $\mu\text{g/l}$	Fe $\mu\text{g/l}$	Co $\mu\text{g/l}$	Ni $\mu\text{g/l}$	Cu $\mu\text{g/l}$	*Zn $\mu\text{g/l}$	Ga $\mu\text{g/l}$	Ge $\mu\text{g/l}$	*As $\mu\text{g/l}$	*Se $\mu\text{g/l}$	*Br $\mu\text{g/l}$	
dithionite	<1000	<100	7100	<2	<2000	<200	>2000	<700	<1000	<100	262	967	<100	<10000	<5	<300	<200	898	<10	21	59	620	3600	
oxidation																								
inj. soln.	12	<0.1	5.3	1,440	<2	12.5	2.7	6.3	1	0.7	2.3	11.7	15.0	<10	4.03	6.7	2.4	30.5	0.01	0.47	1.97	2.4	81	
0	<10	<1	>350	620	635	<2	>200	<7	206	59	382	47	119	2,450	2.36	407	99	47	7.4	1.2	317	<2	>2,000	
2	<100	<10	469.0	<200	632	<20	>2000	<70	<100	<10	<50	<10	<1000	<0.5	<30	<20	65	10	<1	55	<20	<300		
4	<1	0.2	32.0	16	1,050	3.9	>20	<0.7	1	8.0	2.0	9.6	710	0.581	1.8	0.8	3.2	8.33	0.24	18.4	0.4	80		
6	<1	<0.1	17.6	12	785	4.1	>20	<0.7	<1	7.5	4.6	0.9	5.5	324	0.328	0.7	0.4	2.8	4.97	0.15	11.6	0.4	73	
8	<1	<0.1	12.6	9	609	4.2	>20	<0.7	<1	4.5	3.4	0.7	3.8	220	0.247	0.6	0.3	2.2	3.28	0.10	8.54	0.5	69	
8	<1	<0.1	13.1	10	639	4.4	>20	<0.7	<1	4.4	3.5	0.5	3.9	232	0.248	0.5	0.3	2.3	3.36	0.10	9.02	0.3	71	
14	2	0.2	9.3	20	521	4.6	>20	<0.7	1	5.4	10.9	4.1	11.7	2,320	1.28	3.1	3.0	3.8	2.11	0.08	6.79	0.2	67	
22	7	<0.1	7.1	185	47	36.5	<0.7	<1	1.5	1.1	<0.5	1.4	98	0.135	<0.3	0.4	0.9	0.67	0.04	3.00	0.5	63		
40	15	<0.1	5.8	708	53	5.3	16.1	3.1	<1	1.6	<0.1	<0.5	7.2	29	0.034	<0.3	0.5	0.8	0.09	0.02	0.60	0.4	61	
48	15	<0.1	5.8	698	35	5.2	15.8	3.1	<1	1.3	<0.1	<0.5	7.0	28	0.033	<0.3	0.6	1.7	0.09	0.02	0.64	0.6	62	
75	14	<0.1	5.4	1,690	9	6.1	2.9	6.6	<1	0.6	<0.1	<0.5	168	397	0.015	<0.3	<0.2	<0.5	0.02	0.02	0.14	0.2	61	
190	13	<0.1	5.2	1,400	4	6.2	1.8	5.7	<1	0.4	<0.1	<0.5	96.2	1,800	0.012	<0.3	<0.2	<0.5	0.01	0.02	0.08	0.4	60	
340	13	<0.1	5.5	1,390	3	6.8	1.8	5.7	<1	0.5	<0.1	<0.5	81.6	3,360	0.015	<0.3	<0.2	2.3	0.01	0.03	0.21	<0.2	64	
490	13	0.1	5.5	1,370	2	6.8	1.7	5.5	1	0.4	<0.1	<0.5	52.1	1,380	30.9	57.8	0.3	9.1	<0.01	0.02	0.19	0.4	63	
oxidation																								
pore volumes	*Rb $\mu\text{g/l}$	**Sr $\mu\text{g/l}$	Y $\mu\text{g/l}$	Zr $\mu\text{g/l}$	Nb $\mu\text{g/l}$	Mo $\mu\text{g/l}$	Ru $\mu\text{g/l}$	*Pd $\mu\text{g/l}$	Ag $\mu\text{g/l}$	Cd $\mu\text{g/l}$	In $\mu\text{g/l}$	Sn $\mu\text{g/l}$	Sb $\mu\text{g/l}$	Te $\mu\text{g/l}$	I $\mu\text{g/l}$	Cs $\mu\text{g/l}$	Ba $\mu\text{g/l}$	La $\mu\text{g/l}$	Ce $\mu\text{g/l}$	Pr $\mu\text{g/l}$	Nd $\mu\text{g/l}$	Sm $\mu\text{g/l}$	Eu $\mu\text{g/l}$	
dithionite	2500	<40	<3	38	<5	<100	<10	88	<200	<10	<1	<100	<10	<1000	<1	<100	2	3	1	3	1	1	3	1
oxidation																								
inj. soln.	3.05	85.7	0.01	<0.01	<0.005	<0.1	<0.01	<0.01	<0.2	0.07	<0.001	<0.1	0.08	<0.1	52	0.178	17.5	0.003	0.002	<0.001	0.005	<0.001	0.001	
0	>2,000	59.5	137.32	479	0.203	67	0.2	29.1	3	0.4	0.02	2	5.3	<1	470	0.23	37	8.50	33.6	5.31	32.1	11.2	2.95	
2	187	<4	<0.3	9	<0.5	42	<1	2	<20	<1	<0.1	<10	<1	<10	<100	<0.1	<10	0.5	0.2	<0.1	0.4	<0.1	<0.1	
4	17.5	2.54	2.41	0.82	0.015	23.5	<0.01	<0.01	<0.2	0.04	0.003	<0.1	0.06	<0.1	42	0.006	1.3	1.83	5.59	0.780	3.48	1.02	0.250	
6	10.6	2.39	1.51	0.51	0.014	19.7	<0.01	<0.01	<0.2	0.04	0.002	<0.1	<0.01	<0.1	44	0.004	1.1	1.46	4.23	0.576	2.34	0.655	0.161	
8	7.64	2.01	0.96	0.47	0.008	16.9	<0.01	<0.01	<0.2	0.03	0.001	<0.1	<0.01	<0.1	42	0.002	0.7	1.03	2.94	0.380	1.60	0.422	0.111	
8	7.90	2.07	1.06	0.33	0.008	15.6	<0.01	<0.01	<0.2	0.02	0.002	<0.1	<0.01	<0.1	44	0.002	0.7	1.10	3.18	0.402	1.61	0.433	0.116	
14	5.87	2.18	1.72	0.12	<0.005	10.7	<0.01	<0.01	<0.2	0.03	0.005	<0.1	<0.01	<0.1	74	0.012	1.3	2.04	6.04	0.830	3.70	1.00	0.227	
22	4.30	1.16	0.26	0.11	<0.005	5.3	<0.01	<0.01	<0.2	<0.01	<0.001	<0.1	<0.02	<0.1	44	0.001	0.3	0.306	0.926	0.115	0.480	0.133	0.029	
40	5.96	32.2	0.05	0.25	<0.005	1.0	<0.01	<0.01	<0.2	<0.01	<0.001	<0.1	<0.02	<0.1	64	0.002	1.6	0.059	0.165	0.015	0.065	0.020	0.005	
48	5.94	32.2	0.03	0.10	<0.005	0.9	<0.01	<0.01	<0.2	<0.01	<0.001	<0.1	<0.01	<0.1	68	<0.001	1.6	0.038	0.157	0.012	0.049	0.014	0.004	
75	4.14	88.1	0.01	<0.01	<0.005	0.4	<0.01	<0.01	<0.2	<0.01	<0.001	<0.1	<0.01	<0.1	58	0.002	5.1	0.013	0.044	0.004	0.022	0.004	0.006	
190	3.50	93.2	0.01	<0.01	<0.005	1.1	<0.01	<0.01	<0.2	<0.01	<0.001	<0.1	<0.01	<0.1	45	0.001	16.5	0.009	0.025	0.004	0.017	0.003	0.006	
340	3.83	94.8	0.01	0.02	<0.005	0.3	<0.01	<0.01	<0.2	<0.01	<0.001	<0.1	<0.01	<0.1	41	0.002	34.0	0.012	0.018	0.002	0.011	<0.001	0.008	
490	3.88	91.5	0.03	0.03	<0.005	4.2	<0.01	<0.01	<0.2	0.12	<0.001	<0.1	<0.01	<0.1	42	0.026	26.9	0.026	0.041	0.005	0.023	0.003	0.009	
oxidation																								
pore volumes	Gd $\mu\text{g/l}$	Tb $\mu\text{g/l}$	Dy $\mu\text{g/l}$	Ho $\mu\text{g/l}$	Er $\mu\text{g/l}$	Tm $\mu\text{g/l}$	Yb $\mu\text{g/l}$	Lu $\mu\text{g/l}$	Hf $\mu\text{g/l}$	Ta $\mu\text{g/l}$	W $\mu\text{g/l}$	Re $\mu\text{g/l}$	Os $\mu\text{g/l}$	Pt $\mu\text{g/l}$	Au $\mu\text{g/l}$	Hg $\mu\text{g/l}$	Tl $\mu\text{g/l}$	Pb $\mu\text{g/l}$	Bi $\mu\text{g/l}$	Th $\mu\text{g/l}$	U $\mu\text{g/l}$			
dithionite	<1	<1	<1	<1	<1	<1	<1	<1	<1	<1	<20	<1	<2	<300	65	<200	<1	<10	<300	15	<1			
oxidation																								
inj. soln.	0.002	<0.001	<0.001	<0.001	<0.001	<0.001	<0.001	<0.001	<0.001	<0.001	0.08	0.001	<0.002	<0.3	<0.002	<0.2	0.074	0.05	<0.3	<0.001	7.18			
0	15.3	2.83	17.8	4.06	12.4	1.83	12.7	2.08	13.8	0.14	14.7	<0.01	<0.02	<3	2.89	2	0.01	1.2	<3	250	202			
2	<0.1	<0.1	<0.1	<0.1	<0.1	<0.1	<0.1	<0.1	<0.1	0.3	<0.1	3	<0.1	<0.2	<30	1.7	<20	<0.1	<30	<0.1	0.9			
4	0.928	0.125	0.542	0.088	0.240	0.029	0.192	0.027	0.032	0.04	0.014	<0.001	<0.002	<0.3	<0.002	<0.2	0.001	0.66	<0.3	0.192	0.588			
6	0.596	0.077	0.329	0.055	0.154	0.018	0.122	0.014	0.019	0.001	0.19	<0.001	<0.002	<0.3	<0.002	<0.2	<0.001	0.39	<0.3	0.101	0.311			
8	0.387	0.049	0.220	0.036	0.101	0.011	0.083	0.009	0.020	<0.001	0.17	<0.001	<0.002	<0.3	<0.002	<0.2	<0.001	0.21	<0.3	0.074	0.235			
8	0.395	0.053	0.221	0.038	0.107	0.012	0.08																	

Table 4.20. Metals Mobility during Sediment Oxidation in Columns at pH 6.2 (* = present in dithionite solution, ** = present in oxidation solution)

pore volumes	Li $\mu\text{g/l}$	Be $\mu\text{g/l}$	*Na mg/l	**Mg $\mu\text{g/l}$	Al $\mu\text{g/l}$	**Si mg/l	*K mg/l	Ca mg/l	Sc $\mu\text{g/l}$	Ti $\mu\text{g/l}$	*V $\mu\text{g/l}$	Cr $\mu\text{g/l}$	Mn $\mu\text{g/l}$	Fe $\mu\text{g/l}$	Co $\mu\text{g/l}$	Ni $\mu\text{g/l}$	Cu $\mu\text{g/l}$	*Zn $\mu\text{g/l}$	Ga $\mu\text{g/l}$	Ge $\mu\text{g/l}$	As $\mu\text{g/l}$	*Se $\mu\text{g/l}$	*Br $\mu\text{g/l}$	
dithionite	<1000	<100	7100	<2	<2000	>20000	<700	<1000	<100	262	967	<100	<10000	<5	<300	<200	898	<10	21	59	620	3600		
oxidation inj. Soln.	12	<0.1	5.3	1,440	<2	12.5	2.7	6.3	1	0.7	2.3	11.7	15.0	<10	4.03	6.7	2.4	30.5	0.01	0.47	1.97	2.4	81	
0	<100	<10	>3500	446	595	<20	>2000	<70	<100	59	303	<50	85	1,010	1.0	113	<20	<50	7	1	122	32	1,380	
2	<1	<0.1	>35	4	1,790	6.3	>20	0.8	<1	1.0	<0.1	<0.5	0.8	18	0.030	2.3	<0.2	3.1	11.7	0.30	22.6	<0.2	136	
4	<1	<0.1	16.1	2	1,370	6.4	>20	<0.7	1	0.7	<0.1	<0.5	0.3	<10	0.030	0.3	0.5	4.9	5.99	0.17	8.06	0.4	113	
6	<1	<0.1	11.2	<2	906	5.9	>20	<0.7	<1	0.5	<0.1	<0.5	0.2	27	0.025	<0.3	<0.2	<0.5	3.06	0.11	5.31	0.3	109	
8	<1	<0.1	9.1	<2	635	5.6	>20	<0.7	<1	0.5	<0.1	<0.5	0.1	<10	0.018	<0.3	<0.2	2.9	1.85	0.08	3.86	0.4	110	
14	<1	<0.1	7.5	<2	379	4.8	>20	<0.7	<1	0.4	<0.1	<0.5	0.2	13	0.013	<0.3	<0.2	<0.5	0.98	0.05	2.73	0.5	105	
22	3	<0.1	6.3	6	167	4.5	38.9	<0.7	<1	0.3	<0.1	<0.5	0.1	<10	0.037	<0.3	0.3	2.6	0.38	0.04	1.47	0.4	101	
40	15	<0.1	6.1	40	4.7	24.3	<0.7	<1	0.4	<0.1	<0.5	0.8	<10	0.020	0.4	<0.2	0.7	0.08	0.02	0.44	0.7	99		
40	15	<0.1	6.3	66	42	4.8	25.0	<0.7	<1	0.5	<0.1	<0.5	0.9	<10	0.022	0.4	0.2	1.1	0.09	0.02	0.48	0.4	103	
48	15	<0.1	6.1	64	49	4.8	24.3	<0.7	<1	0.4	<0.1	<0.5	0.9	<10	0.027	0.3	0.4	2.1	0.08	0.03	0.42	0.4	101	
75	13	<0.1	5.0	1,510	10	5.3	3.1	7.5	<1	0.3	<0.1	<0.5	16.3	43	0.010	<0.3	1.0	2.9	0.02	0.02	0.22	0.4	99	
188.6	13	<0.1	5.1	1,480	4	5.8	2.4	7.0	<1	0.3	<0.1	<0.5	72.9	568	0.015	<0.3	0.6	1.4	<0.01	0.02	0.07	0.4	103	
338.6	13	<0.1	5.0	1,490	3	6.7	1.8	6.8	1	0.4	<0.1	<0.5	82.5	1,380	0.019	<0.3	0.4	2.4	<0.01	0.02	0.21	0.4	85	
413	13	0.1	5.1	1,390	4	7.5	2.1	6.1	1	0.5	<0.1	<0.5	64.2	3,680	2.10	<0.3	0.2	0.6	<0.01	0.03	0.56	0.4	83	
4.44																								
pore volumes	*Rb $\mu\text{g/l}$	**Sr $\mu\text{g/l}$	Y $\mu\text{g/l}$	Zr $\mu\text{g/l}$	Nb $\mu\text{g/l}$	Mo $\mu\text{g/l}$	Ru $\mu\text{g/l}$	Pd $\mu\text{g/l}$	Ag $\mu\text{g/l}$	Cd $\mu\text{g/l}$	In $\mu\text{g/l}$	Sn $\mu\text{g/l}$	Sb $\mu\text{g/l}$	Te $\mu\text{g/l}$	I $\mu\text{g/l}$	Cs $\mu\text{g/l}$	Ba $\mu\text{g/l}$	La $\mu\text{g/l}$	Ce $\mu\text{g/l}$	Pr $\mu\text{g/l}$	Nd $\mu\text{g/l}$	Sm $\mu\text{g/l}$	Eu $\mu\text{g/l}$	
dithionite	2500	<40	<3	38	<5	<100	<10	88	>200	<10	<1	<100	<10	<1000	<1	<100	2	3	1	3	3	1		
oxidation inj. Soln.	3.05	85.7	0.008	<0.01	<0.005	<0.1	<0.01	<0.1	<0.2	0.07	<0.001	<0.1	0.08	<0.1	52	0.178	17.5	0.003	0.002	<0.001	0.005	<0.001	0.001	
0	1,590	38	48.8	275	<0.5	11	<1	3	<20	<1	<0.1	<10	<1	<100	0.2	20	3.7	15.1	2.9	17.5	7.5	1.7		
2	27.3	1.01	0.120	0.07	<0.005	0.6	<0.01	0.02	<0.2	<0.01	0.002	<0.1	0.22	<0.1	<1	0.003	0.1	0.035	0.126	0.016	0.075	0.024	0.006	
4	9.31	0.35	0.027	<0.01	<0.005	0.3	<0.01	0.04	<0.2	<0.01	0.001	<0.1	0.03	<0.1	61	<0.001	0.2	0.016	0.055	0.008	0.033	0.012	0.004	
6	7.24	0.25	0.012	<0.01	<0.005	0.4	<0.01	0.01	<0.2	<0.01	<0.001	<0.1	0.01	<0.1	47	<0.001	0.1	0.012	0.039	0.005	0.026	0.004	0.001	
8	6.26	0.20	0.006	<0.01	<0.005	0.4	<0.01	0.01	<0.2	<0.01	<0.001	<0.1	0.01	<0.1	49	<0.001	<0.1	0.006	0.018	0.002	0.014	<0.001	<0.001	
14	5.47	0.14	<0.003	<0.01	<0.005	0.4	<0.01	<0.1	<0.2	<0.01	<0.001	<0.1	0.03	<0.1	45	<0.001	<0.1	0.005	0.011	0.001	0.007	<0.001	<0.001	
22	4.26	0.19	<0.003	<0.01	<0.005	0.2	<0.01	<0.1	<0.2	<0.02	<0.001	<0.1	0.02	<0.1	117	<0.001	<0.1	0.004	0.009	<0.001	0.001	<0.001	<0.001	
40	4.82	2.43	0.008	0.02	<0.005	<0.1	<0.01	<0.1	<0.2	<0.01	<0.001	<0.1	0.03	<0.1	44	<0.001	0.2	0.015	0.025	0.004	0.016	0.002	0.002	
40	4.90	2.50	0.004	<0.01	<0.005	<0.1	<0.01	<0.1	<0.2	<0.01	<0.001	<0.1	0.03	<0.1	47	<0.001	0.2	0.021	0.031	0.005	0.012	0.002	<0.001	
48	4.80	2.45	<0.003	0.03	<0.005	<0.1	<0.01	<0.1	<0.2	<0.01	<0.001	<0.1	0.02	<0.1	43	<0.001	0.2	0.012	0.029	0.003	0.013	0.004	<0.001	
75	5.80	70.2	0.004	<0.01	<0.005	<0.1	<0.01	<0.1	<0.2	<0.01	<0.001	<0.1	0.03	<0.1	80	<0.001	2.0	0.003	0.004	0.001	0.003	0.001	0.001	
188.6	3.32	89.9	<0.003	<0.01	<0.005	<0.1	<0.01	<0.1	<0.2	<0.03	<0.001	<0.1	0.01	<0.1	69	0.001	7.6	0.005	0.007	<0.001	0.010	<0.001	0.002	
338.6	3.87	97.1	<0.003	<0.01	<0.005	<0.1	<0.01	<0.1	<0.2	<0.01	<0.001	<0.1	<0.01	<0.1	41	0.003	10.7	0.002	0.004	<0.001	0.003	<0.001	0.002	
413	3.73	91.7	<0.003	<0.01	<0.005	<0.1	<0.01	<0.1	<0.2	0.01	<0.001	<0.1	<0.01	<0.1	43	0.011	39.1	0.002	0.005	<0.001	0.004	<0.001	0.002	

Table 4.21. Metal Mobility during Sediment Oxidation at pH 7.0 (* = present in dithionite solution, ** = present in oxidation solution)

pore volumes	Li $\mu\text{g/l}$	Be $\mu\text{g/l}$	*Na mg/l	**Mg mg/l	Al $\mu\text{g/l}$	*Si mg/l	*K mg/l	Ca mg/l	Sc $\mu\text{g/l}$	Ti $\mu\text{g/l}$	*V $\mu\text{g/l}$	*Cr $\mu\text{g/l}$	Mn $\mu\text{g/l}$	Fe $\mu\text{g/l}$	Co $\mu\text{g/l}$	Ni $\mu\text{g/l}$	Cu $\mu\text{g/l}$	*Zn $\mu\text{g/l}$	Ga $\mu\text{g/l}$	Ge $\mu\text{g/l}$	*As $\mu\text{g/l}$	*Se $\mu\text{g/l}$	*Br $\mu\text{g/l}$	
dithionite inj. soln.	<1000	<100	7100	<2	<2000	<200	>20000	<700	<1000	<100	262	967	<100	<10000	<5	<300	<200	898	<10	21	59	620	3600	
oxidation inj. soln.	12	<0.1	5.3	1.4	<2	12.5	2.7	6.3	1	0.7	2.3	11.7	15.0	<10	4.03	6.7	2.4	30.5	0.01	0.47	1.97	2.4	81	
0	<100	<10	>3500	1.4	281	<20	>2000	<70	156	53	432	<50	193	<1000	1.2	321	<20	702	4	1	91	26	2,010	
0	<100	<10	>3500	1.4	309	<20	>2000	<70	158	55	443	<50	201	<1000	1.4	278	<20	111	5	1	92	23	2,070	
2	<100	<10	733.0	<0.2	452	<20	>2000	<70	<100	<10	<10	<50	10	<1000	<0.5	36	<20	123	4	<1	15	<20	<300	
4	6	<0.1	25.5	0.0	146	4.8	>20	<0.7	<1	0.7	15.4	<0.5	2.4	47	0.176	4.9	3.6	70.6	1.19	0.08	7.83	<0.2	89	
6	8	<0.1	17.7	0.1	45	5.0	>20	1.7	<1	0.6	8.2	<0.5	3.0	<10	0.091	2.2	0.5	5.8	0.59	0.05	4.28	<0.2	83	
9	9	<0.1	15.2	0.4	30	5.2	>20	2.9	<1	0.6	6.0	<0.5	2.2	<10	0.059	1.7	0.3	4.2	0.40	0.04	3.06	<0.2	76	
14	10	<0.1	13.8	0.7	27	5.1	45.8	3.5	<1	0.7	3.6	<0.5	2.3	33	0.069	1.5	0.3	3.6	0.29	0.04	2.09	<0.2	73	
22	11	<0.1	12.5	1.0	13	5.4	30.3	4.2	<1	0.4	2.4	<0.5	3.2	<10	0.063	0.9	<0.2	2.3	0.21	0.03	1.30	<0.2	72	
40	11	<0.1	11.2	1.4	13	6.2	16.4	5.5	<1	0.7	2.5	<0.5	4.2	<10	0.094	0.6	0.4	2.7	0.19	0.02	0.75	<0.2	69	
48	11	<0.1	11.1	1.4	10	6.1	16.4	5.4	<1	0.4	2.5	<0.5	4.2	<10	0.085	0.5	0.3	2.6	0.20	0.03	0.73	0.3	66	
75	12	<0.1	10.5	1.6	12	7.4	9.0	6.5	1	0.7	1.3	<0.5	11.0	17	0.175	0.7	0.6	4.8	0.11	0.04	0.44	<0.2	67	
190	12	<0.1	10.4	1.7	19	8.4	4.9	7.0	1	0.9	0.8	<0.5	27.0	<10	0.575	3.1	2.5	10.4	0.05	0.06	0.31	<0.2	67	
190	13	<0.1	10.8	1.7	20	8.7	5.1	7.2	1	0.9	0.8	<0.5	28.2	<10	0.615	3.2	2.6	11.3	0.05	0.06	0.29	<0.2	69	
340	12	<0.1	9.1	1.7	7	3.6	7.1	1	0.8	0.4	<0.5	36.0	<10	2.31	4.7	1.3	10.7	0.02	0.08	0.22	<0.2	61		
582.8	12	<0.1	9.0	1.7	5	8.9	2.9	7.3	1	0.7	<0.1	<0.5	38.3	<10	6.67	6.2	0.7	6.3	<0.01	0.07	0.13	<0.2	65	
pore volumes	*Rb $\mu\text{g/l}$	**Sr $\mu\text{g/l}$	Y $\mu\text{g/l}$	Zr $\mu\text{g/l}$	Nb $\mu\text{g/l}$	Mo $\mu\text{g/l}$	Ru $\mu\text{g/l}$	Pd $\mu\text{g/l}$	Ag $\mu\text{g/l}$	Cd $\mu\text{g/l}$	In $\mu\text{g/l}$	Sn $\mu\text{g/l}$	Sb $\mu\text{g/l}$	Tc $\mu\text{g/l}$	I $\mu\text{g/l}$	Cs $\mu\text{g/l}$	Ba $\mu\text{g/l}$	La $\mu\text{g/l}$	Ce $\mu\text{g/l}$	Pr $\mu\text{g/l}$	Nd $\mu\text{g/l}$	Sm $\mu\text{g/l}$	Eu $\mu\text{g/l}$	
dithionite inj. soln.	2500	<40	<3	38	<5	<100	<10	88	<200	<10	<1	<100	<10	<1000	<1	<100	2	3	1	3	3	1		
oxidation inj. soln.	3.05	85.7	0.008	<0.01	<0.005	<0.1	<0.01	<0.01	<0.2	0.07	<0.001	<0.1	0.08	<0.1	52	0.178	17.5	0.003	0.002	<0.001	0.005	<0.001	0.001	
0	2,340	77	61.1	439	<0.5	19	<1	<1	<20	<1	<0.1	<10	6	<10	<100	0.3	50	10.1	37.7	6.4	36.2	12.4	2.6	
0	2,360	79	62.5	469	<0.5	19	<1	<1	<20	<1	<0.1	<10	6	<10	<100	0.3	52	10.5	39.5	6.7	37.6	12.1	3.2	
2	294	6	0.3	12	<0.5	<10	<1	<1	<20	<1	<0.1	<10	<1	<10	<100	<1	<10	<1	<1	0.3	0.1	<0.1	<0.1	
4	14.4	0.74	0.036	0.39	<0.005	5.3	<0.01	<0.01	<0.2	0.10	0.002	0.5	0.53	<0.1	<1	0.010	0.6	0.033	0.093	0.012	0.041	0.013	0.002	
6	9.99	5.19	0.027	0.13	<0.005	2.5	<0.01	<0.01	<0.2	0.04	0.001	<0.1	0.20	<0.1	<1	0.005	0.9	0.012	0.030	0.004	0.020	0.004	<0.001	
9	7.65	16.5	0.015	0.07	<0.005	1.7	<0.01	<0.01	<0.2	0.02	0.001	<0.1	0.12	<0.1	<1	0.003	1.1	0.010	0.020	0.002	0.014	0.003	<0.001	
14	6.39	28.7	0.015	0.05	<0.005	1.1	<0.01	<0.01	<0.2	<0.01	<0.01	<0.1	0.07	<0.1	<1	0.003	0.8	0.016	0.031	0.004	0.021	0.005	<0.001	
22	5.48	38.2	0.011	0.04	<0.005	0.6	<0.01	<0.01	<0.2	<0.01	<0.01	<0.1	0.05	<0.1	<1	0.002	1.3	0.003	0.005	<0.001	0.002	<0.001	<0.001	
40	4.41	55.5	0.006	0.02	<0.005	0.3	<0.01	<0.01	<0.2	<0.01	<0.01	<0.1	0.06	<0.1	<1	0.013	1.2	0.003	0.004	<0.001	0.003	<0.001	<0.001	
48	4.35	54.4	0.006	0.03	<0.005	0.2	<0.01	<0.01	<0.2	<0.01	<0.01	<0.1	0.06	<0.1	<1	0.014	1.1	0.002	0.003	<0.001	0.002	<0.001	<0.001	
75	3.84	70.4	0.009	0.01	<0.005	<0.1	<0.01	<0.01	<0.2	<0.01	<0.01	<0.1	0.05	<0.1	<1	0.030	1.0	0.004	0.006	0.001	0.003	<0.001	<0.001	
190	3.73	78.9	0.009	0.01	<0.005	<0.1	<0.01	<0.01	<0.2	<0.02	<0.01	<0.1	0.05	<0.1	<1	0.085	9.5	0.007	0.010	0.001	0.003	0.001	<0.001	
190	3.85	82.7	0.009	0.02	<0.005	<0.1	<0.01	<0.01	<0.2	<0.04	<0.01	<0.1	0.05	<0.1	<1	0.093	9.6	0.008	0.010	0.002	0.004	0.002	0.002	
340	3.61	85.8	0.005	0.03	<0.005	<0.1	<0.01	<0.01	<0.2	<0.02	<0.01	<0.1	0.03	<0.1	<1	0.135	15.8	0.010	0.011	0.002	0.006	<0.001	0.002	
582.8	3.42	86.5	0.006	0.03	<0.005	<0.1	<0.01	<0.01	<0.2	<0.01	<0.01	<0.1	0.02	<0.1	<1	0.145	18.6	0.005	0.006	<0.001	0.001	<0.001	0.003	

pore volumes	Gd $\mu\text{g/l}$	Tb $\mu\text{g/l}$	Dy $\mu\text{g/l}$	Ho $\mu\text{g/l}$	Er $\mu\text{g/l}$	Tm $\mu\text{g/l}$	Yb $\mu\text{g/l}$	Lu $\mu\text{g/l}$	Hf $\mu\text{g/l}$	Ta $\mu\text{g/l}$	W $\mu\text{g/l}$	Re $\mu\text{g/l}$	Os $\mu\text{g/l}$	Pt $\mu\text{g/l}$	Au $\mu\text{g/l}$	Hg $\mu\text{g/l}$	Tl $\mu\text{g/l}$	Pb $\mu\text{g/l}$	Bi $\mu\text{g/l}$	Th $\mu\text{g/l}$	U $\mu\text{g/l}$		
dithionite inj. soln.	<1	<1	<1	<1	<1	<1	<1	<1	<1	<20	<1	<2	<300	65	<200	<1	<10	<300	15	<1			
oxidation inj. soln.	0.002	<0.001	<0.001	<0.001	<0.001	<0.001	<0.001	<0.001	<0.001	0.08	0.001	<0.002	<0.3	<0.002	<0.2	0.074	0.05	<0.3	<0.001	7.18			
0	13.0	2.3	11.8	2.1	5.6	0.7	4.7	0.8	10.0	<0.1	2	<0.1	<0.2	<30	1.7	<20	<1	2	<30	124	95.1		
0	13.6	2.2	12.2	2.1	5.5	0.8	5.6	0.8	10.7	<0.1	3	<0.1	<0.2	<30	1.3	<20	<1	2	<30	131	97.6		
2	<0.1	<0.1	0.1	<0.1	<0.1	<0.1	<0.1	<0.1	0.2	<0.1	<2	<0.1	<0.2	<30	1.0	<20	<1	<1	<30	0.2	0.3		
4	0.013	0.002	0.006	<0.001	0.002	<0.001	0.002	<0.001	0.004	<0.001	0.22	0.002	<0.002	<0.3	<0.002	<0.2	0.005	0.28</td					

volumes (none at pH 7.0). The amount of iron eluted from each column was determined from integrating the area under the iron data and compared with the previous iron mobility versus pH data (Table 4.20). These results differ from the previous set (Figure 4.25), which showed only very large initial ferrous iron mobility. If the high values of total iron observed (4 mg/L or 71 μ mol/L) were Fe(III) this solution would be highly over saturated even at pH 4.5. Thus, it is reasonable to assume that this total iron is Fe(II). The difference may be due to particulate Fe measured by ICP-MS in Figure 4.25.

The mobility of major and trace metals was also measured in the effluent samples during sediment oxidation. For this study the effects of metal migration during oxidation were investigated using the same pH values as those used for the chromate transport experiments in Section 4.6.1 (4.5, 5.3, 6.2, 7.0) over the range of 418- 582 pore volumes. This groundwater (“oxidation injection solution” in Tables 4.17 through 4.20) contained 11.7 ppb total Cr (as chromate), along with a variety of other trace metals. The analysis of metal mobility during sediment oxidation shows which metals are mobile under reduced conditions and which metals are immobile under oxic conditions. Metals that were present in the dithionite solution (Na, K, V, Zn, Se, Ba, Cr, Br, Rb, As), marked with a single asterisk on Tables 4.17 through 4.20, decrease in concentration during oxidation as species are advected out of the column. Metals that were present in the oxidation solution (uncontaminated Puchack groundwater), including Mg, Ca, Si, and Sr (double asterisk on Tables 4.17 through 4.21) all decrease initially in concentration and then start to increase up to the injection concentration well before the partial breakthrough point of chromate (Section 4.6.1) for all pH values investigated. This initial decrease, followed by an increase in concentration occurs during approximately the first 20 pore volumes of oxidation and may be ascribed to an increase in ionic strength during dithionite reduction. The sediment could, therefore, be in the process of approaching ion exchange equilibrium, which could explain why the metal concentrations slowly increase back up to concentrations found in the injection solution.

Table 4.22. Iron Mobility during Reduced Sediment Oxidation

pH	reductive capacity (μ mol//g)	2 mg/L Cr Injection*			0.012 mg/L Cr Injection**		
		Fe(II) eluted (mg)	Fe(II) in sediment (mg)	Fe(II) eluted (%)	Fe(II) eluted (mg)	Fe(II) in sediment (mg)	Fe(II) eluted (%)
4.5	54.5	0.037	1.04	3.6	0.152	1.69	9.0
5.3	62.2	0.016	1.27	1.3	0.181	1.73	10.5
6.2	106	0.0034	2.10	0.16	0.0475	3.21	1.5
7	84.8	0.0035	0.994	0.35	0.0033	3.26	0.10

* experiments U120-123

**experiments U112-115

The redox reactive metals Mn and Fe (as described earlier) are known to mobilize under extreme geochemical conditions and they also appear to decrease initially and then increase at lower pH values (4.5, 5.3, and 6.2). At pH 7, however, there appears to be very little Fe mobilization and Mn also appears to be less mobile. Arsenic, on the other hand, also considered a redox reactive metal, decreases with oxidation across the pH range investigated (Figure 4.27b). Although arsenic species were not determined, As(III) species are known to be mobile in reducing environments (i.e., such as during dithionite treatment), but As(V) species form precipitate(s) during oxic water injection or co-precipitates with iron oxides. Arsenic data (Figure 4.27b) showed a steady decrease over 600 pore volumes, with main leaching in the first 10 pore volumes, and no change with different pH. Other metals, such as Al, K, V, Zn and U, all decrease with oxidation. U(VI) species are mobile under oxic conditions, but U(IV) precipitates form under reducing conditions. There was no difference in U leaching with pH. The initial concentration of mercury, observed at pH values of 5.3 and above, were high (Table 4.17 and Figure 4.27a) but decreased within the first few pore volumes of oxidation. This can be explained by the amount of Hg present in the

dithionite solution (Table 4.17) leaching out of the sediment in the first few pore volumes. At pH 4.5 almost all of the Hg appears to be immobilized by the reduced sediment.

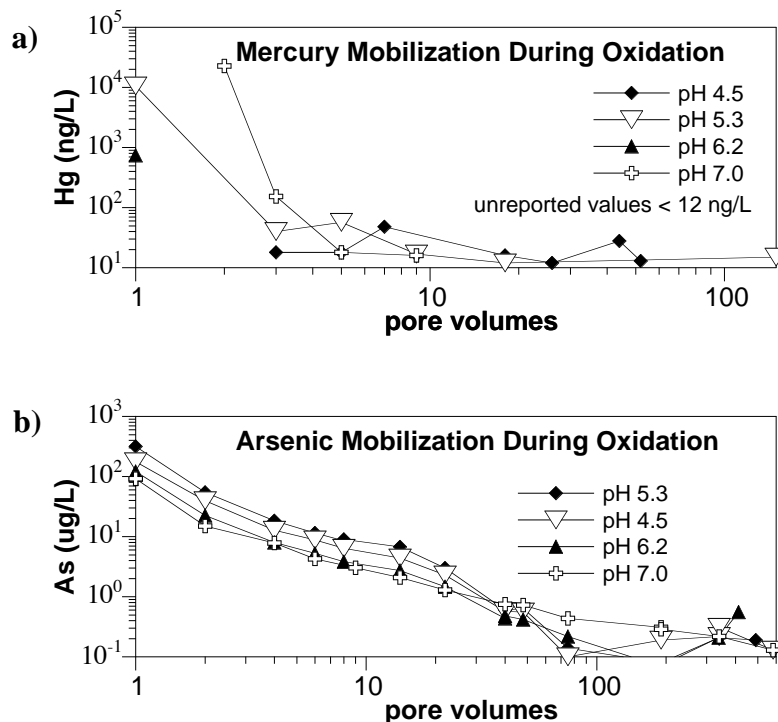


Figure 4.27. Mobility of (a) Mercury and (b) Arsenic as a Function of Pore Volume during Sediment Oxidation at Different pH

4.7 Biostimulation

The potential for creating a permeable reactive barrier in the Puchack aquifer using biotic processes is explored in this section. This assessment includes laboratory studies focused on determining the indigenous population of IRB and SRB in the aquifer. These bacteria can catalyze in situ formation of a permeable reactive barrier by using an amended substrate (e.g., lactate) to either directly or indirectly reduce sediment-associated iron. Barrier performance would be further enhanced by the presence of sulfide compounds with the use of sulfate-reducing bacteria. Both of these bacteria are primarily active under reducing geochemical conditions and while they are generally widely distributed in many aquifers, their populations may be low enough in some aquifers that they cannot be readily stimulated even with addition of appropriate substrates.

As the first step in assessing the viability of biotic processes for in situ formation of a permeable reactive barrier, available sediment core material was assayed to enumerate the indigenous populations of these bacteria. Eight aquifer sediment samples from boreholes MW-36 and MW-37 were chosen for this study and are given in Table 4.23. Enumeration and enrichment techniques were used to assess the population of viable iron-reducing and sulfate-reducing bacteria in the samples.

MPN enumeration of both the IRB and SRB was performed in replicates, on two sediments (PNNL ID # 1 and 2) with inoculants encompassing 10^{-2} to 10^{-7} dilutions. After incubation for 6 weeks, none of

the MPN tubes showed positive growth, implying that SRB and IRB were either not present, or in the best case, was present at a population of less than 20 cells per gram of sediment. All positive controls showed growth to demonstrate that the culturing media were suitable for inducing growth of IRB or SRB.

Direct enrichments could not be used to enumerate the bacterial population, but provided an indication of whether any viable bacteria are present in the sediment sample. In treatments with 1 g of sediment and 10 mL of culturing media, growth of IRB was observed in the majority of sediment samples (PNNL ID #5, 6,2,7,4,8), Table 4.23. No growth of SRB was detected in any of the sediments tested at this inoculum level, Table 4.24. In direct enrichments with 30 g sediment per 30 mL SRB medium, only one sample (PNNL ID #7) indicated potential SRB growth. Growth of IRB and SRB was observed in positive controls for direct enrichments. These positive control results indicate that the sediments are not toxic or inhibitory to iron/sulfate reducing microorganisms under the experimental conditions for the direct enrichments.

Table 4.23. Puchack Sediment Cores Selected for Microbiology Studies

Station Location	Hydrogeologic Layer ^(a)	Depth, ft	PNNL ID #	Sediment Description	pH	% moisture ^(b)
MW-36S-C	C-2A1	151.5 to 152	5	Yellow clay w. light gray sand	5.6	14.5
MW-37S-A	C-2A1	153.5 to 154	1	Light gray sand	6.4	21.1
MW-36S-D	C-2A1	159 to 159.5	3	Light gray silty sand	6.8	12.4
MW-37S-G	A-3a	190 to 190.5	6	Light gray fine sand	7.1	18.3
MW-37S-H	A-3a	194 to 194.5	2	Beige clay	5.5	17.9
MW-36S-J	A-3a	201 to 201.5	7	Whitish silty fine sand	6.8	17.3
MW-37S-J	A3-a	204 to 204.5	4	Beige clay	5.4	19.3
MW-37S-K	A3-a	210.5 to 211	8	Pale white clay & small gravels	5.5	15.7

(a) C-2A1=Intermediate Sand, A-3a=Lower Aquifer, upper zone.
(b) Dry weight base.

Tables 4.24 and 4.25 summarized the enumeration and direct enrichment results. In conclusion, IRB are present in the Puchack sediment samples tested, but at low population densities of <20 cells per g sediment. All of the samples from the Lower Aquifer showed the presence of IRB in the direct enrichments, though with varying degrees of growth intensity. Only one sample of three showed presence of IRB in direct enrichments but with a low growth intensity over the incubation period. Based on these results, stimulation of IRB through amendments to the subsurface may be possible but the response may be slow and the non uniform. Potentially, there are areas in the subsurface that contain higher populations of IRB than were observed in the sediment samples that would act as “seed populations” to enhance the response to amendments.

The SRB were detected in only one sediment sample from the Lower Aquifer in direct enrichments. If the SRB are present, their population is <20 cells per g of sediment. It is likely that the population of viable SRB in the aquifer is very low and may not be readily stimulated through amendments to the

subsurface. However, with long subsurface incubation times SRB may become active. Assessing the viability of SRB-catalyzed processes for in situ formation of a permeable reactive barrier will need to consider whether a long incubation period is possible.

Table 4.24. Summary of Iron-Reducing Bacteria Enumeration and Enrichment

			Treatment				
Sample ID	Depth, ft	PNNL ID #	1g ^(a)	10 ⁻² g to 10 ⁻⁷ g ^(b)	1g+low cells ^(c)	1g+med. Cells ^(d)	1g+high cells ^(e)
MW-36S-C C-2A1	151.5 to 152	5	+/+	not done	+/++	+/+	+/++
MW-37S-A C-2A1	153.5 to 154	1	- / -	- / - / - / -	- / -	- / ++	- / -
MW-36S-D C-2A1	159 to 159.5	3	- / -	not done	- / -	- / -	- / -
MW-37S-G A-3a	190 to 190.5	6	++/++	not done	++/++	++/++	++/++
MW-37S-H A-3a	194 to 194.5	2	+/+	- / - / - / -	++/+	+/+	+/++
MW-36S-J A-3a	201 to 201.5	7	-/+	not done	+/-	++/-	+/++
MW-37S-J A-3a	204 to 204.5	4	+/+	not done	+/+	++/++	++/++
MW-37S-K A-3a	210.5 to 211	8	+/+	not done	+/++	++/+	+/+

Growth assessment: growth medium clear colorless: ++, pale brown/cloudy: +, clear brown: -

(a) 1 g sediments per 10 ml IRB medium, 2 replicates, 4 weeks incubation.

(b) MPN, 5 replicates per each of 5 dilutions, 2 replicates per sediments tested, 6 weeks incubation.

(c) 1 g sediment plus 2E+3 cells (*G.metallireducens*) per 10 ml IRB medium, 2 replicates, 4 weeks incubation.

(d) 1 g sediment plus 2E+5 cells (*G.metallireducens*) per 10 ml IRB medium, 2 replicates, 4 weeks incubation.

(e) 1 g sediment plus 2E+7 cells (*G.metallireducens*) per 10 ml IRB medium, 2 replicates, 4 weeks incubation.

Table 4.25. Summary of Sulfate-Reducing Bacteria Enumeration and Enrichment

			Treatment					
Sample ID	Depth, ft	PNNL ID #	30 g ^(a)	1g ^(b)	10 ⁻² g to 10 ⁻⁷ g ^(c)	1g+low cells ^(d)	1g+med. Cells ^(e)	1g+high cells ^(f)
MW-36S-C C-2A1	151.5 to 152	5	-	-/-	not done	+/+	+/+	+/+
MW-37S-A C-2A1	153.5 to 154	1	-	-/-	- / - / - / -	+/+	+/+	+/+
MW-36S-D C-2A1	159 to 159.5	3	-	-/-	not done	+/+	+/+	+/+
MW-37S-G A-3a	190 to 190.5	6	-	-/-	not done	+/+	+/+	+/+
MW-37S-H A-3a	194 to 194.5	2	-	-/-	- / - / - / -	+/+	+/+	+/+
MW-36S-J A-3a	201 to 201.5	7	+	-/-	not done	+/+	+/+	+/+
MW-37S-J A-3a	204 to 204.5	4	-	-/-	not done	+/+	+/+	+/+
MW-37S-K A-3a	210.5 to 211	8	-	-/-	not done	+/+	+/+	+/+

Growth assessment: growth medium blackened: +, color not changed: -

(a) 30 g sediments per 30 ml SRB medium, no replicates, 2 weeks incubation.

(b) 1 g sediments per 10 ml SRB medium, 2 replicates, 4 weeks incubation.

(c) MPN, 5 replicates per each of 5 dilutions, 2 replicates per sediments tested, 6 weeks incubation.

(d) 1 g sediment plus 2E+3 cells (*D.vulgaris*) per 10 ml SRB medium, 2 replicates, 4 weeks incubation.

(e) 1 g sediment plus 2E+5 cells (*D.vulgaris*) per 10 ml SRB medium, 2 replicates, 4 weeks incubation.

(f) 1 g sediment plus 2E+7 cells (*D.vulgaris*) per 10 ml SRB medium, 2 replicates, 4 weeks incubation.

5.0 Conclusions

This report describes results from bench-scale laboratory experiments documented in a test plan entitled *Bench Scale Test Plan: Treatability Study of In Situ Technologies for the Remediation of Hexavalent Chromium in Groundwater* (Vermeul et al. 2004). These treatability studies were conducted using sediment and groundwater samples collected from the Puchack Well Field Superfund Site in Pennsauken Township, New Jersey. Results are reported for specific laboratory experiments that were conducted to evaluate mechanisms that could contribute to attenuation of the chromate plume and potential technologies for the remediation of chromate contaminated groundwater. Three general categories of technologies that were evaluated include:

- Abiotic reduction of ferric oxides in sediments to create a reduced zone (ISRM).
- Biostimulation (nutrient injection) of the natural microbial population to create a reduced zone.
- Natural attenuation of the chromate plume (adsorption and reduction).

5.1 Chromate Adsorption

Chromate adsorption was evaluated in order to accurately predict chromate transport, which would lag due to the reversible chromate adsorption (confirmed in column experiments) and result in an apparent lag that could be mistakenly attributed to chromate reduction and subsequent immobilization. Chromate adsorption by deep composite sediments was highly dependent on the pH, with greater adsorption at low pH (typical anion behavior). The initial chromate adsorption was fast (minutes), but there was continued adsorption for 24 hours, so there was some contact time dependence for chromate adsorption. As an anion, the amount of chromate adsorption was also dependent on the chromate and other anion concentrations. The adsorption maxima for a Puchack composite sediment was about 6 $\mu\text{mol/g}$, and chromate adsorption was shown to decrease with increasing concentration. The sulfate, at a concentration of 50 mg/L, was shown to suppress chromate adsorption by up to 50%. Thus, chromate disposal and migration in the presence of SO_4^{2-} and other anions (e.g., HCO_3^{2-} and CO_3^{2-}) in the contaminant plume will decrease chromate adsorption relative to adsorption which would occur in their absence. However, with only a factor of 2 decrease in the K_d values derived from these experiments (Figure 4.11), the effect of sulfate on chromate migration in the concentration range found at Puchack is relatively small. The influence of inorganic colloids on chromate mobility was studied with sequential filtration of aqueous samples with 0.45, 0.2, 0.1 and 0.01 micron filters. No consistent variation in chromate concentration with filter pore size was observed. Although this does not prove that inorganic colloids are totally absent, we can conclude that either there is no generation of inorganic colloids in Puchack sediments and/or the small fraction of total chromate present on these colloids is of negligible importance for chromate mobility.

5.2 Chromate Reduction in Natural Puchack Sediments

Chromate reduction by natural Puchack sediments was studied for time periods ranging from hours to 11 months. Results show that natural chromate reduction can occur in the Puchack sediments. At the field scale a combination of the geochemical mechanisms evaluated in this study and hydrogeologic conditions at the site determine the amount of reduction/immobilization of the chromate plume that would occur. Composite sediments from specific aquifer units showed no reduction of chromate for four

composites (A2b, A3a, A3c), and slow reduction for three composites (A2a, C2A1 and A3b with half-lives of 1, 3, and 3 years, respectively (Table 4.11). A deep aquifer composite showed approximately a ten-fold increase in chromate reduction rate (2600 hours or 108-day half-life), and selected sediments (typically finer grain sediments from interbedded clays) showed rapid chromate reduction with a 46-hour half-life. Experimental results indicate that chromate reduction can remain viable in the presence of dissolved oxygen. Given the amount of variability observed in the samples analyzed in this study, predicting the expected chromate reduction rate in a complex aquifer system, based on the eight composite sediments and the three individual sediments examined, would result in a relatively high degree of uncertainty. To better quantify the spatial variability within selected aquifer units, additional natural chromate reduction geochemical studies would be required. In addition, groundwater flow and reactive transport models could be used to evaluate various scenarios of groundwater flow and chromate plume transport through the aquifer system. These models would incorporate the type of rate and capacity data generated by this study to evaluate the impacts of the identified mechanisms on chromate plume attenuation.

Most sediments that showed some natural reduction of chromate had very small reductive capacities (average $2.76 \pm 1.02 \mu\text{mol/g}$), but one sediment with considerable amorphous ferrous iron and 2.25% organic carbon had a large reductive capacity ($636 \mu\text{mol/g}$). While some Puchack sediments have been shown to be redox reactive with chromate, the reactive surface phases at such low concentrations, in general, were not identified. These natural reductive capacities show that on average, 63 pore volumes of water containing the highest observed chromate concentration would be reduced (although the silt/clay sample with high reductive capacity would last an estimated 11,000 pore volumes).

5.3 Chromate Reactivity in Dithionite-Reduced Sediments

Chemical reduction of Puchack sediments resulted in a considerable increase in the reductive capacity, which averaged $60.2 \pm 25.6 \mu\text{mol/g}$ with an additional sample with very large capacity ($390 \mu\text{mol/g}$). This average reductive capacity would result in a reduced sediment barrier longevity of 355 pore volumes or 39 years (assuming a 40-ft-wide barrier and a groundwater velocity of 1.0 ft/day), with greater longevity for slower flow and less longevity for faster flow such as near pumping wells. While this reductive capacity is sufficient to consider dithionite-reduction of sediment a viable remediation technology, there was considerable variability in reductive capacity of sediments. Therefore, additional geochemical characterization of a specific aquifer zone of interest should be completed to determine the average reductive capacity that would result in that specific location.

In addition, of significance for applicability to the Puchack aquifer system is the influence of pH on the barrier longevity, as the Puchack aquifer system has pH values ranging from 4.5 to 7.0. It was hypothesized that under acidic conditions: a) ferrous iron phases produced *could* be mobile (aqueous), and b) Cr(III) species produced *could* be mobile. Surprisingly, chromate reduction/immobilization was very effective in four long-term column studies at pH 4.5, 5.3, 6.2, and 7.0, showing that most ferrous iron phases were immobile and aqueous Cr(III) species were not produced. These results indicate that most of the ferrous iron phases produced by dithionite reduction of Puchack sediments remained immobile, so were composed of structurally reduced iron in 2:1 clays, or other iron oxides, and not adsorbed Fe(II). Under acidic conditions, adsorbed ferrous iron is mobile so the capacity of reduced sediments to immobilize chromate may be less at low pH than at neutral pH. Column studies did show

the reductive capacity was a function of pH (Table 5.1), with a small amount of Fe(II) mobilization (3.6% to 9.0%) at pH 4.5 compared with less Fe(II) mobilization (0.1% to 0.35%) at pH 7.0.

Table 5.1. Influence of pH on Chromate Immobilization in Reduced Sediments

pH	reductive capacity (umol/g)	Chromate Breakthrough			Cr(total) Breakthrough		
		rapid Cr red. capacity (pv)	total capacity (pore vol.)	Fe(II) eluted (%)*	initial elution (pore vol.)	total capacity (pore vol.)	Fe(tot) eluted (%)*
4.5	54.5	170	310	3.6	8	> 583	9.0
5.3	62.2	170	350	1.3	14	> 490	10.5
6.2	106	280	601	0.16	1	> 413	1.5
7	84.8	340	480	0.35	1	> 583	0.10

* percent of reductive capacity (umol/g) x sediment (g)

Column studies also show chromate was initially reduced/immobilized in reduced sediment at all pH values at a rapid rate (reduction half-life > 0.1 hour). By 170 pore volumes at pH 4.5 and 5.3, partial chromate breakthrough was observed, indicating slower chromate reduction rates (half life 3 to 5 hours). In contrast, partial chromate breakthrough was not observed until 280 pore volumes at pH 6.3 and 340 pore volumes at pH 7.0. The ultimate capacity of the sediment column to consume 2.0 mg/L chromate plus 8.4 mg/L dissolved oxygen (saturated conditions) was about 310 pore volumes at pH 4.5 and 480 pore volumes at pH 7.0.

To address the question of mobile Cr(III) species, total Cr analysis (ICP-MS) was conducted during separate experiments. These results showed no indications of Cr breakthrough for 413 to 582 pore volumes (Table 5.1). Trace metal analysis during sediment reduction and oxidation experiments showed some mobilization of Hg, As, and Fe(II) during reduction, and a small amount of Hg and As mobilization during the first few pore volumes (of 400) during sediment oxidation. There was some Fe(II) mobilization observed, which was greater at lower pH, but still resulted in < 5% of the iron in the sediment column being mobilized. Therefore, aqueous ferrous iron data and total iron data both indicated a small amount of iron mobilization at pH 4.5 and 5.3, with less at pH 6.2 and 7.0.

5.4 Biostimulation of Iron-Reducing and Sulfate-Reducing Bacteria

The iron reducing bacteria (IRB) are present in the Puchack sediment samples tested, but at low population densities of <20 cells per g sediment. In comparison, cell densities in the Ft. Lewis, Washington, aquifer (60-ft depth) are 5×10^6 CFU/g, and Hanford, Washington, 100-N Area shallow aquifer (30-ft depth) range from 10^3 CFU/g to 10^6 CFU/g.

All of the samples from the Lower Puchack Aquifer showed the presence of IRB in the direct enrichments, though with varying degrees of growth intensity. Only one sample of three showed presence of IRB in direct enrichments but with a low growth intensity over the incubation period. Based on these results, stimulation of IRB through amendments to the subsurface may be possible but the response may be slow and the non-uniform. Potentially, there are areas in the subsurface that contain higher populations of IRB than were observed in the sediment samples that would act as “seed populations” to enhance the response to amendments.

The SRB were detected in only one sediment from the Lower Aquifer in direct enrichments. If SRB are present, their population is <20 cells per gram of sediment. It is likely that the population of viable

SRB in the aquifer is very low and may not be readily stimulated through amendments to the subsurface. However, with long subsurface incubation times, SRB may become active. Assessing the viability of SRB-catalyzed processes for in situ formation of a permeable reactive barrier would need to consider whether a long incubation period is possible.

5.5 Recommended Future Studies

Field-scale implementation of any process to manipulate the subsurface (i.e., chemical reduction of sediment or bio-stimulation) would require some additional geochemical/microbial characterization in the specific field site chosen for in situ remediation to define the spatial distribution of reducible iron and/or microbial population. Similarly, the use of MNA also requires additional characterization of the spatial distribution of the reduced phases that are reducing chromate. The current study has clearly shown that chromate reduction does occur for specific natural untreated sediments or sediment composites from the Puchack aquifer system. In addition, if the observed rates of reduction for these sediments are applicable over a large volume of the aquifer, natural attenuation could make a significant contribution to chromate remediation at the Puchack site. However, because the major focus of the current study was dithionite treated sediments a limited number of natural untreated sediments were examined. Additional research focused on natural attenuation is needed to establish its role and quantify its contribution to remediation of chromate in Puchack groundwater. A follow-on study outlined in the following paragraphs would focus on mapping the natural reductive potential of regions surrounding core samples shown to have significant reductive capacity in the current study. That is, it would establish the spatial distribution of sediments exhibiting measurable reduction rates. This would yield a quantitative estimate of the reductive capacity and the longevity of chromate reduction by sediments within this region.

Additional information identifying the mineral and/or organic phases acting as chromate reductants will be obtained. Finally, methods used in the current study to quantify the reductive capacity of sediments in terms of the moles of electrons available for chromate reduction per gram of sediment would be refined and expanded to all relevant reductants phases. With the limited but encouraging information on natural attenuation resulting from the current study, reliable estimates of the spatial extent of natural attenuation cannot be made. However, with additional information from the follow-on study outlined below together with groundwater flow maps of the target aquifer zone and knowledge of the aqueous concentrations of other electron acceptors in Puchack groundwater (e.g., O₂, TCE) reactive transport modeling could provide a far more reliable estimate of natural attenuation of chromate remediation at the Puchack site.

1. Determine the spatial extent and variability of chromate reduction for sediments in those aquifer zones where natural chromate reduction has been observed.

The deep aquifer regions would be of particular interest because there is significant groundwater flow through these zones. This would include measurement of chromate reduction rates and the sediment reductive capacity in selected core samples from wells MW36, MW37, D1 and D2 at the Puchack site. These core samples are currently in cold storage in the PNNL laboratory. A map of rates and reductive capacities for the zones examined is essential for prediction of the effectiveness and longevity of sediments over a significant spatial volume to act as a natural barrier within which chromate is reduced to insoluble Cr(III) or mixed (Cr, Fe) hydroxides.

2. Resolve differences in estimating sediment reductive capacities by the two methods employed in the current study.

The reductive capacity is defined as the moles electrons available for chromate reduction per gram of sediment. One measure was determined from the consumption of dissolved O₂ from effluent waters pumped through sediment columns. The net reductive capacity thus determined does not quantify the individual constituents contributing to the reductive capacity, e.g., ferrous iron as structural or surface species, NOM or sulfides. The second measure targeted ferrous iron, considered to be a primary reductant (electron donor) in a majority of natural reduced sediments; however, this ignores both NOM and bacterial populations as electron donors. The most accessible and/or reactive Fe(II) phases were estimated by measurement of Fe(II) extracted by a short 0.5-M HCl treatment of the sediment. For many of the natural sediments examined the average reductive capacity (moles e⁻/g of sediment) for both methods were in remarkably close agreement (Table 4.12). However, for other sediments the two methods disagreed by factors of 1.5 to 3, and for one natural sediment the methods differed by a factor of 265. The consistency of these two measures of reduction capacity and the reason(s) for the observed discrepancy should be understood before a reliable method for estimating reductive capacity can be established as a predictor of the longevity of sediments to act as natural barriers to chromate migration.

3. Identify reactive constituents in the natural sediments responsible for chromate reduction.

Identification of the Fe(II) mineral phases and/or NOM acting as electron donors, and understanding the role native bacteria play in zones where natural chromate reduction was observed, either directly (respiration) or indirectly as iron reducers, is important to defining the mechanisms of chromate reduction in natural sediments. Knowledge of the reactive phases is important because identification of the presence of these phases in other sediments can be used to predict potential effectiveness of the other sediments as a natural chromate reduction barrier without extensive characterization of the other sediments. Selective chemical extraction methods combined with spectroscopic techniques, including ⁵⁷Fe Mossbauer spectroscopy and electron microscopy, could be used to identify reactive mineral phases. Reactive NOM phases could be examined with appropriate chemical extraction and spectroscopic techniques. The role bacteria may be playing will be examined primarily by including sterilized controls or controls containing bactericides.

4. Simulate chromate transport in the aquifer system with natural reduction.

Given a reasonably accurate description of flow in the Puchack aquifer system and measurements of natural chromate reduction in the different aquifer units (i.e., including clay lenses), the extent of chromate transport and reduction could be quantified. Although the current study clearly demonstrated that natural sediments *could* reduce chromate, the extent of chromate reduction that would occur in the field depends on the flow hydrodynamics as well as the reduction processes. For example, most aquifer units exhibited slow to no chromate reduction, but a clay lens exhibited a very rapid chromate reduction rate. Although little water flows through the clay lens, there may be sufficient surface contact of aquifer fluids to cause significant chromate reduction, if the clay lens is laterally continuous.

6.0 References

- Amonette J, D Workman, D Kennedy, J Fruchter, and Y Gorby. 2000. "Dechlorination of Carbon Tetrachloride by Fe(II) Associated with Goethite." *Environmental Science and Technology* 34(21):4606-4613.
- Amonette JE, JE Szecsody, HT Schaefer, JC Templeton, YA Gorby, and JS Fruchter. 1994. "Abiotic Reduction of Aquifer Materials by Dithionite: A Promising In-Situ Remediation Technology," in *In-Situ Remediation: Scientific Basis for Current and Future Technologies*, p. 851-881, GW Gee and NR Wing (eds.), Battelle Press, Columbus, Ohio.
- Anderson LD, DB Kent, and JA Davis. 1994. "Batch Experiments Characterizing the Reduction of Cr(VI) Using Suboxic Material from a Mildly Reducing Sand and Gravel Aquifer." *Environmental Science and Technology* 28(1):178-185.
- Arnold RG, TJ DiChristina, and MR Hoffman. 1988. "Reductive Dissolution of Fe(III) Oxides by *Pseudomonas* sp 200." *Biotechnol. Bioeng.* 32:1081-1096.
- Bidoglio G, PN Gibson, M O'Gorman, and KJ Roberts. 1993. "X-Ray Absorption Spectroscopy Investigation of Surface Redox Transformations of Thallium and Chromium on Colloidal Mineral Oxides." *Geochemica et Cosmochimica Acta*. 57:2389-2394.
- Bopp LH and HL Ehrlich. 1988. "Chromate Resistance and Reduction in *Pseudomonas fluorescens* strain LB300." *Arch. Microbiol.* 150:426-431.
- Boursiquot S, M Mullet, and J Ehrrhardt. 2002. "XPS Study of the Reaction of Chromium (VI) with Mackinawite (FeS)." *Surface and Interface Analysis* 34:293-297.
- Buerge IJ and SJ Hug. 1997. "Kinetics and pH Dependence of Chromium (VI) Reduction by Iron (III)." *Environmental Science and Technology* 31:1426-1432.
- Buerge I and S Hug. 1999. "Influence of Mineral Surfaces on Chromium (VI) Reduction by Iron (II)." *Environmental Science and Technology* 33(23):4285-4291.
- Burns CA, J-F Boily, RJ Crawford, and IH Harding. 2005. "Cd(II) Sorption onto Chemically Modified Australian Coals." *Fuel* 84:1653-1660.
- Caccavo F Jr., RP Blakemore, and DR Lovley. 1992. "A Hydrogen Oxidizing, Fe(III)-Reducing Microorganism from the Great Bay Estuary, New Hampshire." *Appl. Environ. Microbiol.* 58:3211-3216.
- CDM - Camp, Dresser, and McGee. 2005. *Operable Unit 1, Treatability Study Sample Collection Report*. Puchack Well Field Superfund Site, Remedial Investigation/Feasibility Study (RI/FS), Pennsauken Township, New Jersey. Work assignment No.: 102-RICO-02JL.
- Coates C. 1996. "Geobacter Species of Sedimentary Environments." *Applied and Environmental Microbiology* 62(5):1531-1536.

- Chao TT and L Zhou. 1983. "Extraction Techniques for Selective Dissolution of Amorphous Iron Oxides from Soils and Sediments." *Soil Science Society of America Journal* 47:225-232.
- Coleman ML, DB Hedrick, DR Lovley, DC White, and K Pye. 1993. "Reduction of Fe(III) in Sediments by Sulphate-Reducing Bacteria." *Nature* 361:436-438.
- Delavarenne S and H Viehe. 1969. *Chemistry of Acetylenes*. p. 651-750, Marcel Dekker, New York.
- Deng B, DR Burris, and TJ Campbell. 1999. "Reduction of Vinyl Chloride in Metallic Iron - Water Systems." *Environmental Science and Technology* 33(15):2651-2656.
- Deng B and AT Stone. 1996. "Surface-Catalyzed Chromium(VI) Reduction: Reactivity Comparisons of Different Organic Reductants and Different Oxide Surfaces." *Environmental Science and Technology* 30:2484-2494.
- DiChristina TJ. 1994. "Bioextraction (reductive dissolution) of Iron from Low-Grade Iron Ores." *Ann. NY Acad. Sci.* 721:440-449.
- Eary LE and D Rai. 1988. "Chromate Removal from Aqueous Wastes by Reduction with Ferrous Ion." *Environmental Science and Technology* 22(8):972-977.
- EPA - U.S. Environmental Protection Agency. 1995. *Determination of Hexavalent Chromium by Ion Chromatography*. EPA 821/R/95/029; U.S. EPA Office of Water Engineering and Analysis Division, Washington, D.C.
- Fredrickson JK and YA Gorby. 1996. "Environmental Processes Mediated by Iron-Reducing Bacteria." *Current Opinion in Biotechnology* 7:287-294.
- Fruchter J, C Cole, M Williams, V Vermeul, J Amonette, J Szecsody, J Istok, and M Humphrey. 2000. "Creation of a Subsurface Permeable Treatment Barrier Using In Situ Redox Manipulation." *Ground Water Monitoring Review* 1:66-77.
- Fude L, B Harris, MM Urrita, and TJ Beveridge. 1994. "Reduction of Cr(VI) by a Consortium of Sulfate Reducing Bacteria (SRB III)." *Appl. Environ. Microbiol.* 60(5):1525-1531.
- Gan H, JW Stucki, and GW Bailey. 1992. "Reduction of Structural Iron in Ferruginous Smectite by Free Radicals." *Clays and Clay Minerals* 40(6):659-665.
- Gibbs CR. 1976. "Characterization and Application of Ferrozine Iron Reagent as a Ferrous Iron Indicator." *Analytical Chemistry* 48(8):1197-1200.
- Heron G, C Crouzet, AC Bourg, and TH Christensen. 1994. "Speciation of Fe(II) and Fe(III) in Contaminated Aquifer Sediments Using Chemical Extraction Techniques." *Environmental Science and Technology* 28:1698-1705.
- Horitsu H, S Futo, Y Miyazawa, S Ogai, and K Kawai. 1987. "Enzymatic Reduction of Hexavalent Chromium by Hexavalent Chromium Tolerant (*Pseudomonas ambigua*) G-1." *Agric. Biol. Chem.* 51:2417-2420.

- Ishibashi Y, C Cervantes, and S Silver. 1990. "Chromium Reduction in *Pseudomonas putida*." *Appl. Environ. Microbiol.* 56:2268-2270.
- Jardine PM, SE Fendorf, MA Mayes, IL Larsen, SC Brooks, and WB Bailey. 1999. "Fate and Transport of Hexavalent Chromium in Undisturbed Heterogeneous Soil." *Environmental Science and Technology* 33(17)2939-2944.
- Johnson T, W Fish, Y Gorby, and P Tratnyek. 1998. "Degradation of Carbon Tetrachloride: Complexation Effects on the Oxide Surface." *J. Cont. Hyd.* 29:379-398.
- Kanachuk OV. 1995. "Influence of Hexavalent Chromium on Hydrogen Sulfide Formation by Sulfate-Reducing Bacteria." *Mikrobiologiya* 64(3)315-319.
- Kim C, Q Zhou, B Deng, E Thornton, and H Xu. 2001. "Chromium (VI) Reduction by Hydrogen Sulfide in Aqueous Media: Stoichiometry and Kinetics." *Environmental Science and Technology* 35:2219-2225.
- Kostka JE and KH Nealson. 1995. "Dissolution and Reduction of Magnetite by Bacteria." *Environmental Science and Technology* 29:2535-2540.
- Lovley DR. 1991. "Dissimilatory Fe(III) and Mn(IV) Reduction." *Microbiology Review* 55:259-287.
- Lovley DR. 1994. "Microbial Reduction of Iron, Manganese, and Other Metals," in *Advances in Agronomy*, Vol. 54, DL Sparks (ed.), pp. 175-231, Academic Press, Inc., New York.
- Lovley DR and EJP Phillips. 1994. "Reduction of Chromate by *Desulfovibrio Vulgaris* (Hildenborough) and Its c₃ Cytochrome." *Applied Environmental Microbiology* 60:726-728.
- Lovley DR and EJP Phillips. 1992. "Reduction of Uranium by *Desulfovibrio Desulfuricans*." *Applied Environmental Microbiology* 58:850-856.
- Lovley DR and EJP Phillips. 1987. "Competitive Mechanisms for Inhibition of Sulfate Reduction and Methane Reduction in the Zone of Ferric Iron Reduction in Sediments." *Applied Environmental Microbiology* 53:2636-2641.
- Loyaux-Lawniczak S, P Refait, JJ Ehrhardt, P Lacomte, and JR Genin. 2000. "Trapping of Cr by Formation of Ferrihydrite During the Reduction of Chromate Ions by Fe(II)-Fe(III) Hydroxysalt Green Rusts." *Environmental Science and Technology* 34(3)438-443.
- Loyaux-Lawniczak S, P Lecomte, and J Ehrhardt. 2001. "Behavior of Hexavalent Chromium in a Polluted Groundwater: Redox Processes and Immobilization in Soils." *Environmental Science and Technology* 35(7):1350-1357.
- Matsunaga T, G Karametaxas, HR von Gunten, and PC Lichtner. 1993. "Redox Chemistry of Iron and Manganese Minerals in River-Recharged Aquifers: A Model Interpretation of a Column Experiment." *Geochemica et Cosmochimica Acta* 57:1691-1704.

- Murphy E, J Schramke, J Fredrickson, H Bedsoe, A Francis, D Sklarew, and J Linehan. 1992. "Influence of Microbial Activity and Sedimentary Organic Carbon on the Isotope Geochemistry of the Middendorf Aquifer." *Water Resources Research* 28(3):723-740.
- Nardi S, M Tosoni, D Pizzeghello, MR Provenzano, A Cilenti, A Sturaro, A Rella, and A Vianello. 2005. "Chemical Characteristics and Biological Activity of Organic Substances Extracted from Soils by Root Exudates." *Soil Sci. Soc. Am. J.* 69:2012-2019.
- Orth W and R Gillham. 1996. "Dechlorination of Trichloroethene in Aqueous Solution Using Fe⁰." *Environmental Science and Technology* 30(1):66-71.
- Patterson RR and S Fendorf. 1997. "Reduction of Hexavalent Chromium by Amorphous Iron Sulfide." *Environmental Science and Technology* 31:2039-2044.
- Roberts A, L Totten, W Arnold, D Burris, and T Campbell. 1996. "Reductive Elimination of Chlorinated Ethylenes by Zero-Valent Metals." *Environmental Science and Technology* 30(8):2654-2659.
- Roden EE and JM Zachara. 1996. "Microbial Reduction of Crystalline Fe(III) Oxides: Influence of Oxide Surface Area and Potential for Cell Growth." *Environmental Science and Technology* 30:1618-1628.
- Sass BM and D Rai. 1986. "Solubility of Amorphous Chromium(III)-Iron(III) Hydroxide Solid Solutions." *Inorganic Chemistry* 26(14):2228-2232.
- Seaman JC, PM Bertsch, and L Schwallie. 1999. "In Situ Cr(VI) Reduction Within Coarse-Textured, Oxide-Coated Soil and Aquifer Systems Using Fe(II) Solutions." *Environmental Science and Technology* 33(6):938-944.
- Scherer M, B Balko, and P Tratnyek. 1999. "The Role of Oxides in Reduction Reactions at the Metal-Water Interface, in Kinetics and Mechanisms of Reactions at the Mineral/Water Interface." D Sparks and T Grundl (eds.), ACS Symposium Series #715, p 301-322, American Chemical Society, Atlanta, Georgia.
- Sivavec T and D Horney. 1995. "Reductive Dechlorination of Chlorinated Ethenes by Iron Metal and Iron Sulfide Minerals," in *Emerging Technologies in Hazardous Waste Management VII*, p. 42-45. American Chemical Society, Atlanta, Georgia.
- Sivavec T, P Mackenzie, D Horney, and S Baghel. 1996. *Redox-Active Media for Permeable Reactive Barriers*. p. 753-759, General Electric Research and Development Center, Schenectady, New York.
- Stumm W and J Morgan. 1996. *Aqueous Chemistry*. Third edition, J Wiley and Sons, New York.
- Szecsody J, J McKinley, J Fruchter, V Vermeul, H Fredrickson, and K Thompson. 2006. *In Situ Chemical Reduction of Sediments for TCE, Energetics, and NDMA Remediation, Remediation of Chlorinated and Recalcitrant Compounds*, Monterey, California, May 2006.
- Szecsody J, J Fruchter, VR Vermeul, M Williams, and B Devary. 2005a. "In Situ Reduction of Aquifer Sediments to Create a Permeable Reactive Barrier to Remediate Chromate: Bench-Scale Tests to

Determine Barrier Longevity," Chapter 9, J Jacobs (ed.), *Groundwater Remediation of Chromate*, CRC Press.

Szecsody J, VR Vermeul, J Fruchter, M Williams, B Devary, J Phillips, M Rockhold, and Y Liu. 2005b. *Effect of Geochemical and Physical Heterogeneity on the Hanford 100D Area In Situ Redox Manipulation Barrier Longevity*. PNNL-15499, Pacific Northwest National Laboratory, Richland, Washington.

Szecsody J, J Phillips, V Vermeul, J Fruchter, and M Williams. 2005c. *Influence of Nitrate on the Hanford 100D Area In Situ Redox Manipulation Barrier Longevity*. PNNL-15262, Pacific Northwest National Laboratory, Richland, Washington.

Szecsody J, B Devary, D Girvin, J Campbell, and M McKinley. 2004a. "Fate and Transport of the Explosive CL-20 in Soils and Subsurface Sediments." *Chemosphere* 56:593-610.

Szecsody J, M Williams, J Fruchter, V Vermeul, and D. Sklarew. 2004b. "In Situ Reduction of Aquifer Sediments: Enhancement of Reactive Iron Phases and TCE Dechlorination." *Environmental Science and Technology* 38:4656-4663.

Szecsody J. 2004c. Patent issued, #6,706,527 on March 16, 2004. Automated Fluid Analysis Apparatus and Techniques, Battelle Memorial Institute.

Szecsody J, M Williams, and V Vermeul. 2002. Flow through Electrode with Automated Calibration, U.S. Patent 6,438,501.

Szecsody JE, JS Fruchter, DS Sklarew, and JC Evans. 2000. *In Situ Redox Manipulation of Subsurface Sediments from Fort Lewis, Washington: Iron Reduction and TCE Dechlorination Mechanisms*. PNNL-13178, Pacific Northwest National Laboratories, Richland, Washington.

Szecsody J, A Chilikapati, J Zachara, P Jardine, and A Ferrency. 1998. "Importance of Flow and Particle-Scale Heterogeneity on CoII/IIIEDTA Reactive Transport." *J. Hydrology* 209(1-4):112-136.

Thornton E, J Szecsody, K Cantrell, C Thompson, J Evans, J Fruchter, and A Mitroshkov. 1998. "Reductive Dechlorination of TCE by Dithionite," in *Physical, Chemical, and Thermal Technologies for Remediation of Chlorinated and Recalcitrant Compounds*, G Wickromanayake and R Hinchee (eds.), p. 335-340.

Vermeul VR, MD Williams, JE Szecsody, JS Fruchter, CR Cole, and JE Amonette. 2002. "Creation of a Subsurface" in *Groundwater Remediation of Trace Metals, Radionuclides, and Nutrients, with Permeable Reactive Barriers*, Academic Press.

Vermeul VR, JE Szecsody, and MJ Truex. 2004. *Bench Scale Test Plan: Treatability Study of In Situ Technologies for the Remediation of Hexavalent Chromium in Groundwater*. Prepared by Pacific Northwest National Laboratory for the U.S. Environmental Protection Agency, Washington, D.C.

Viamajala S, BM Peyton, WA Apel, and JN Petersen. 2002. "Chromate Reduction in *Shewanella oneidensis* MR-1 is an Inducible Process Associated with Anaerobic Growth." *Biotechnol. Prog.* 18:290-295.

Walter AL, EO Frind, DW Blowes, CJ Ptacek, and JW Molson. 1994. "Modeling of Multicomponent Reactive Transport in Groundwater 2. Metal Mobility in Aquifers Impacted by Acid Mine Drainage." *Water Resources Research* 30(11):3149-3158.

Wehrli B. 1992. "Redox Reactions of Metal Ions at Mineral Surfaces," in *Aquatic Chemical Kinetics*, W Stumm (ed.), Wiley Interscience, New York.

Weston RF, Jr. 1997. *Hazard Ranking System Documentation Package, Puchack Well Field, Pennsauken Township, Camden County, New Jersey*. Prepared for the U. S. Environmental Protection Agency, West Chester, Pennsylvania.

Wielinga B, Mizuba MM, Hansel CM and Fendorf S. 2001. "Iron promoted reduction of chromate by dissimilatory iron-reducing bacteria." *Environmental Science & Technology* 35 (3): 522-527

Widdel F. 1988. "Microbiology and Ecology of Sulfate- and Sulfur-Reducing Bacteria," in *Biology of Anaerobic Microorganisms*, pp. 469-586, AJB Zehnder (ed.), John Wiley and Sons, Inc., New York.

Williams M, V Vermeul, J Szecsody, and J Fruchter. 2000. *100D Area In Situ Redox Treatability Test for Chromate-Contaminated Groundwater*. PNNL-13349, Pacific Northwest National Laboratory, Richland, Washington.

Yeh G, G Iskra, J Zachara, and J Szecsody. 1998. "Development and Verifications of a Mixed Chemical Kinetic and Equilibrium Model." *Advances in Water Resources* 2(1):24-56.

Zachara J, C Ainsworth, C Cowan, and C Resch. 1989. "Adsorption of Chromate by Subsurface Soil Horizons." *Soil Science Society of America Journal* 53:418-428.

Zachara J, D Girvin, R Schmidt, and C Resch. 1987. "Chromate Adsorption on Amorphous Iron Oxyhydroxide in the Presence of Major Groundwater Ions." *Environmental Science and Technology* 21:589-594.

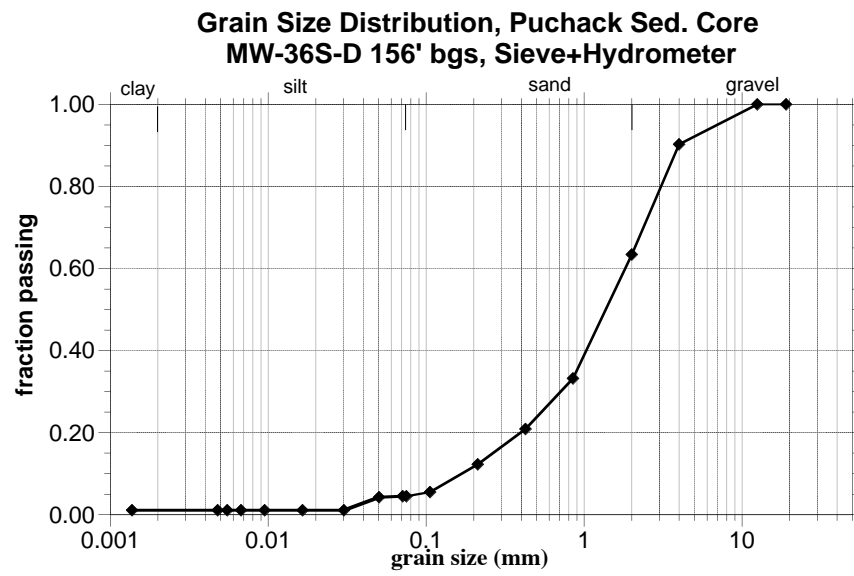
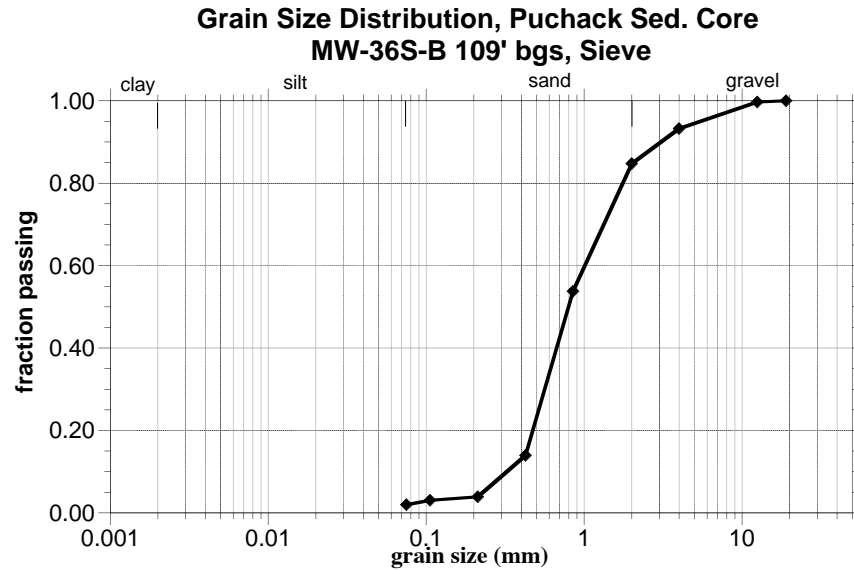
Zachara J, C Ainsworth, G Brown, J Catalano, J McKinley, O Qafoku, S Smith, J Szecsody, S Traina, and J Warner. 2004. "Chromium Speciation and Mobility in a High Level Nuclear Waste Vadose Zone Plume." *Geochimica et Cosmochimica Acta*, 68(1):13-30.

Appendix A

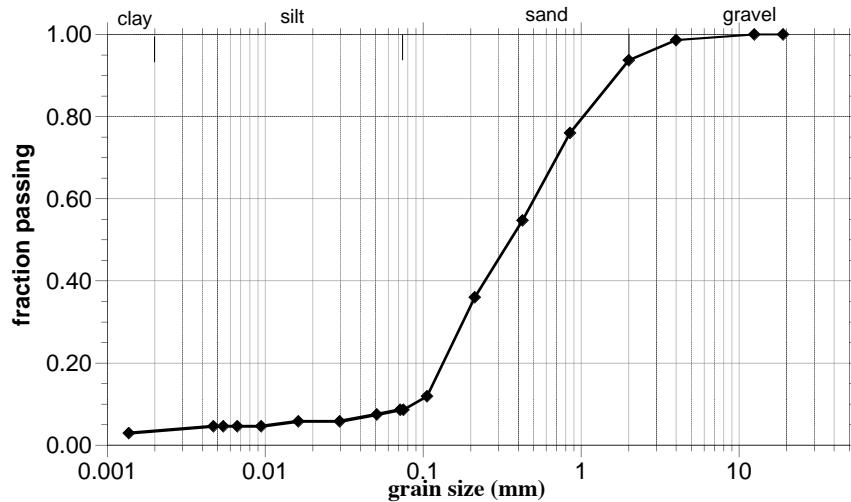
Physical Characterization of Puchack Sediments

Appendix A

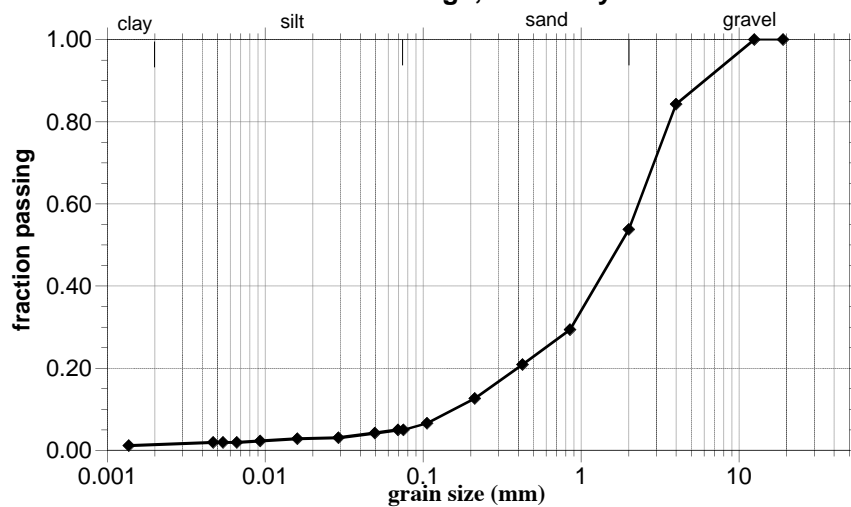
Physical Characterization of Puchack Sediments



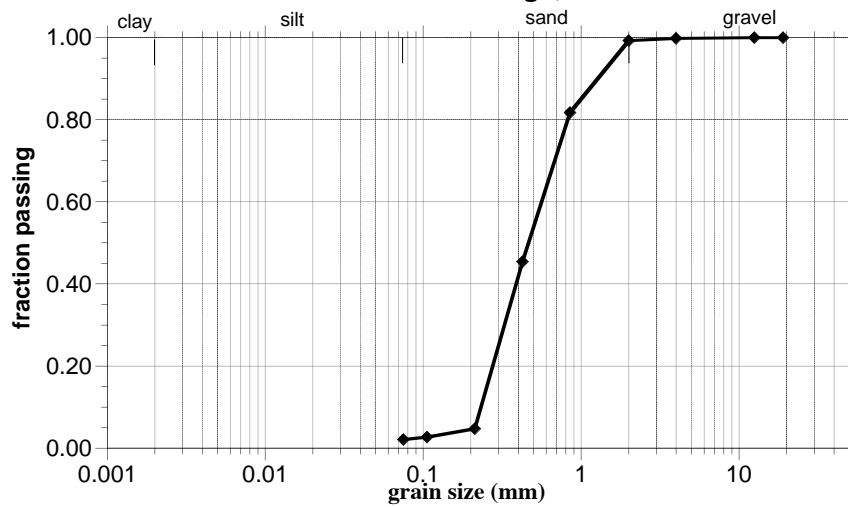
**Grain Size Distribution, Puchack Sed. Core
MW-36S-E 163' bgs, Sieve+Hydrometer**



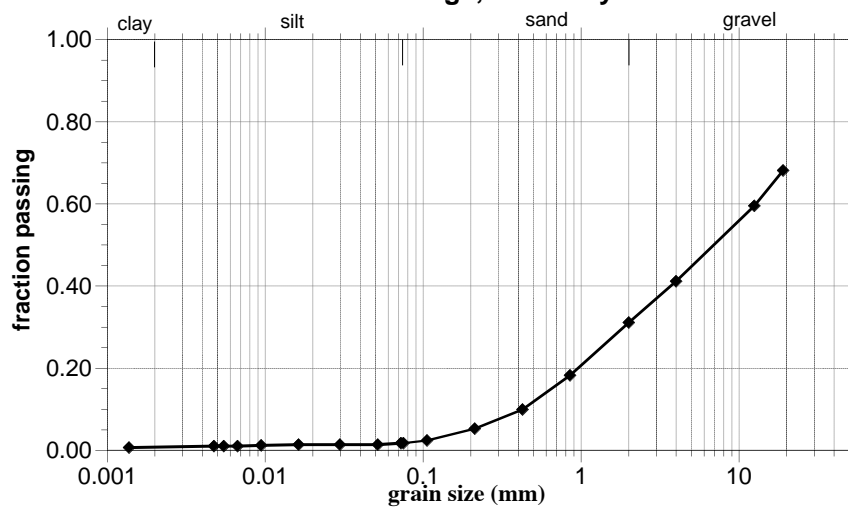
**Grain Size Distribution, Puchack Sed. Core
MW-36S-F 168' bgs, Sieve+Hydrometer**



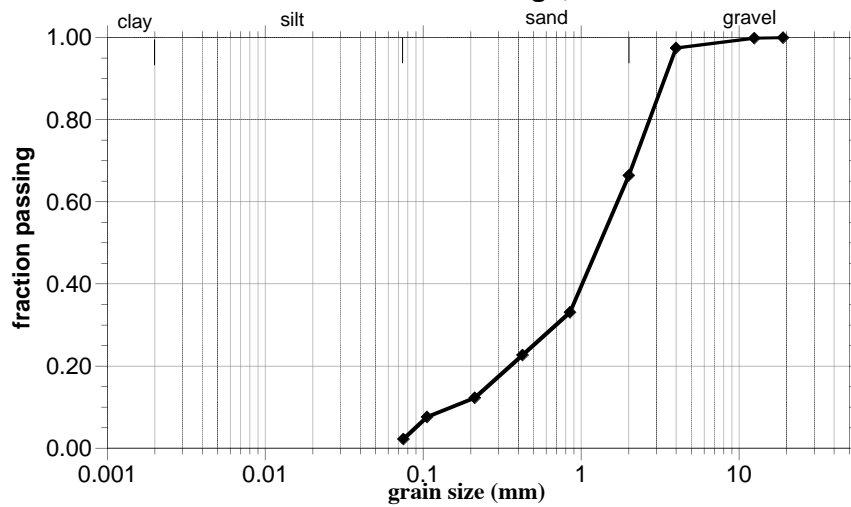
**Grain Size Distribution, Puchack Sed. Core
MW-36S-I 196' bgs, Sieve**



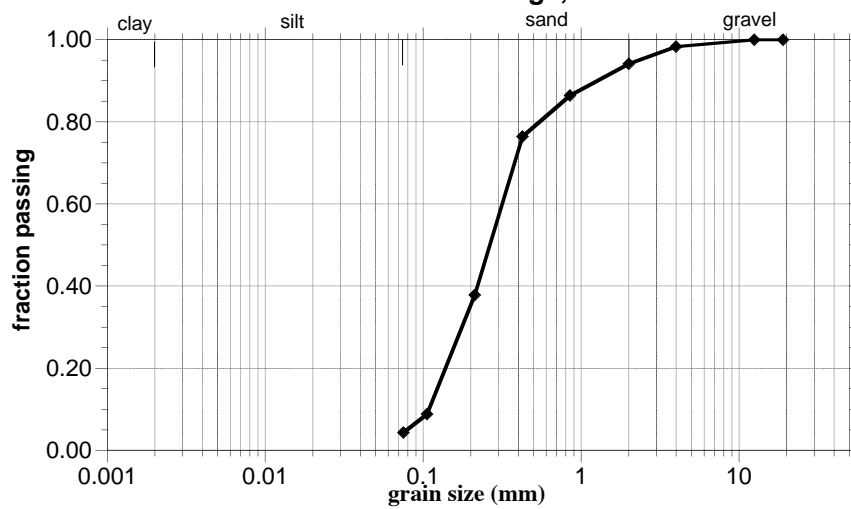
**Grain Size Distribution, Puchack Sed. Core
MW-36S-K 206' bgs, Sieve+Hydrometer**



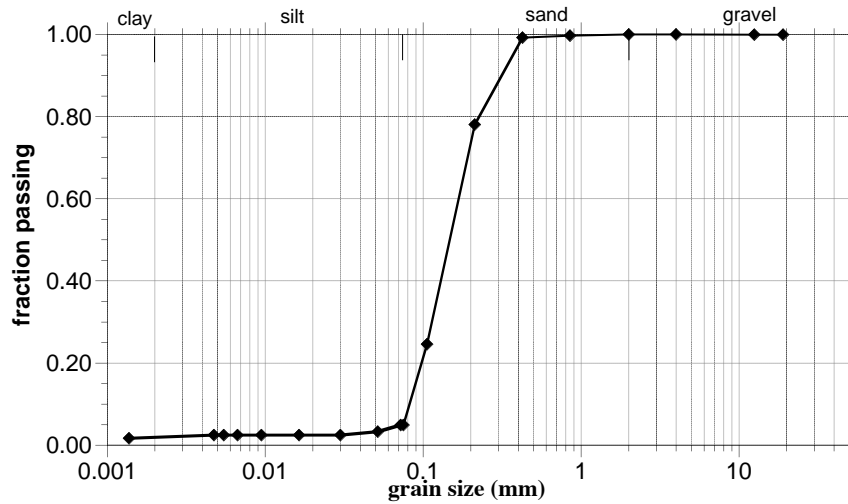
**Grain Size Distribution, Puchack Sed. Core
MW-36S-M 221' bgs, Sieve**



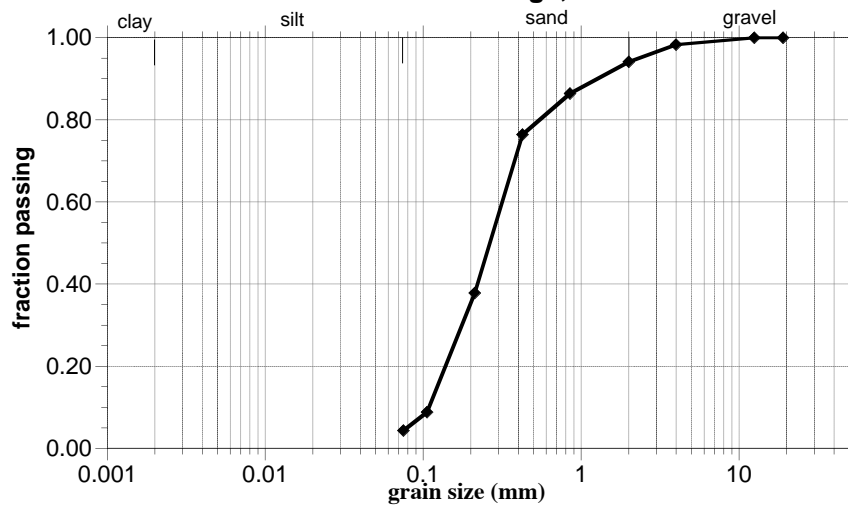
**Grain Size Distribution, Puchack Sed. Core
MW-36S-P 254' bgs, Sieve**



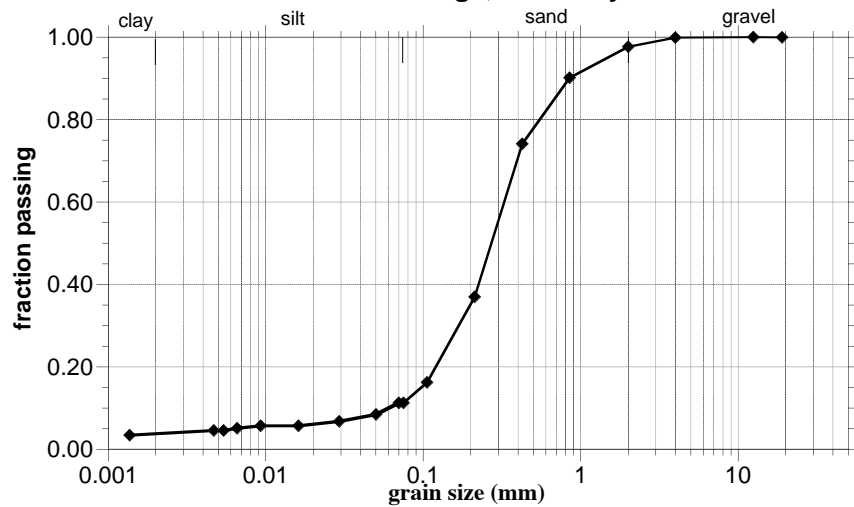
**Grain Size Distribution, Puchack Sed. Core
MW-37S-C 162.5' bgs, Sieve+Hydrometer**



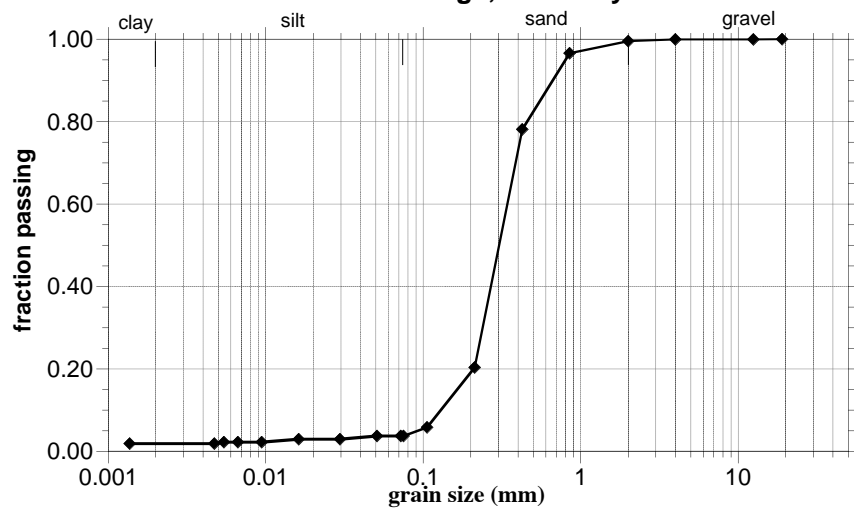
**Grain Size Distribution, Puchack Sed. Core
MW-37S-E 168' bgs, Sieve**



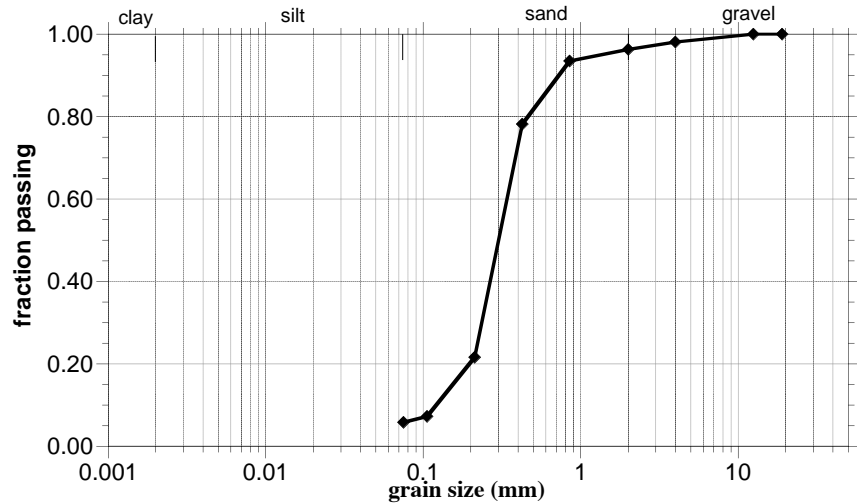
**Grain Size Distribution, Puchack Sed. Core
MW-37S-F 171.5' bgs, Sieve+Hydrometer**



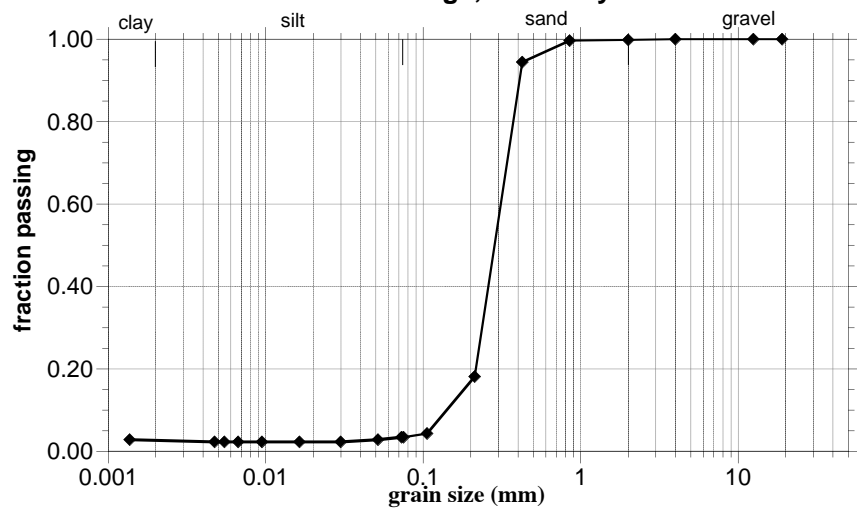
**Grain Size Distribution, Puchack Sed. Core
MW-37S-G 190.5' bgs, Sieve+Hydrometer**



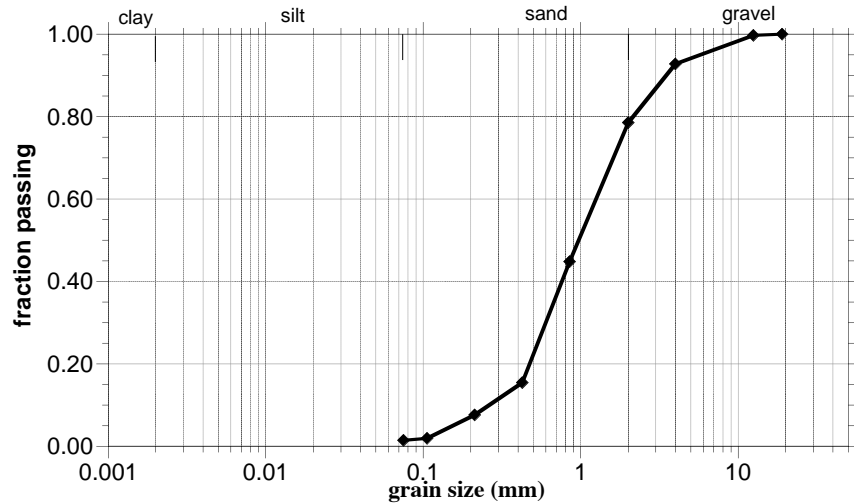
**Grain Size Distribution, Puchack Sed. Core
MW-37S-G 191' bgs, Sieve**



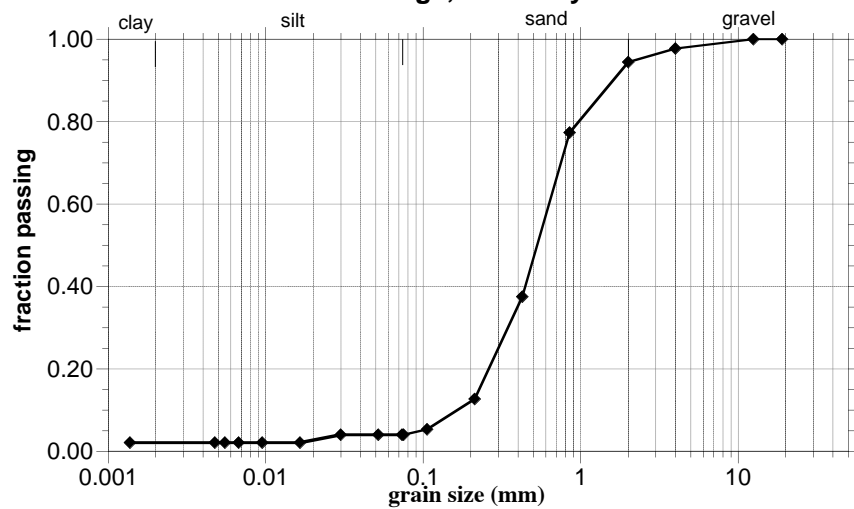
**Grain Size Distribution, Puchack Sed. Core
MW-37S-L 217' bgs, Sieve+Hydrometer**



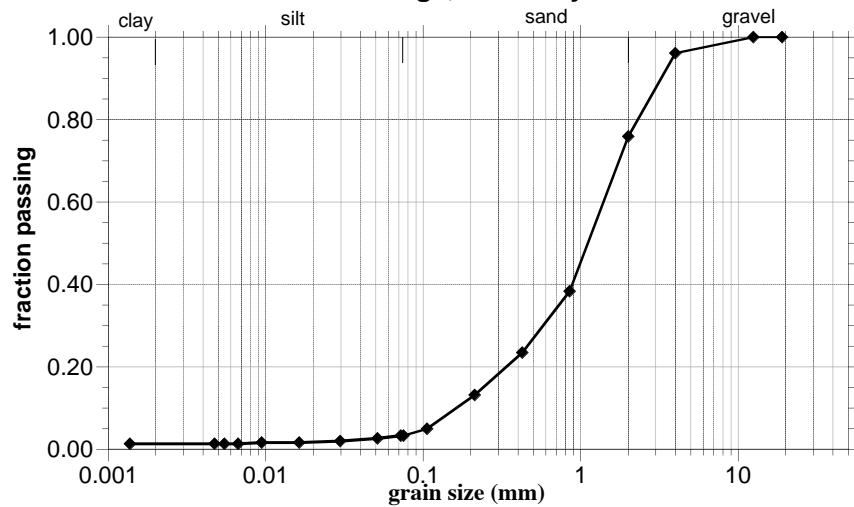
**Grain Size Distribution, Puchack Sed. Core
D1S-H 220' bgs, Sieve**



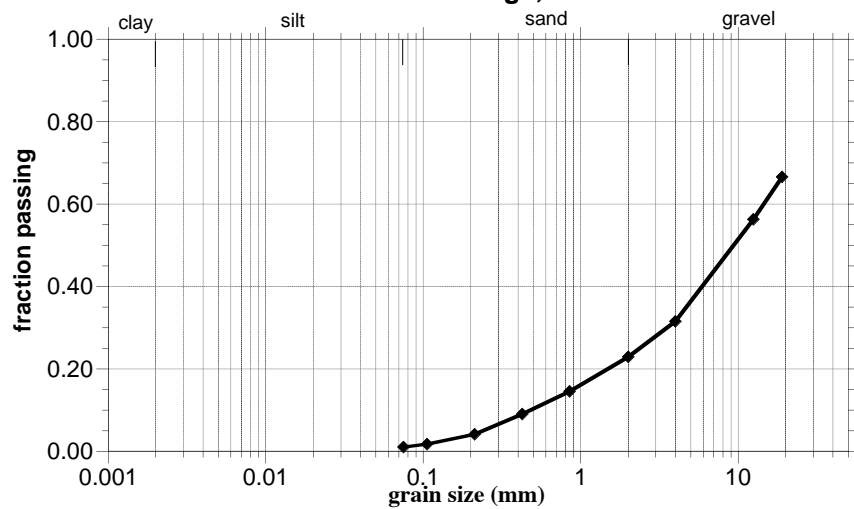
**Grain Size Distribution, Puchack Sed. Core
D1S-J 240' bgs, Sieve+Hydrometer**



**Grain Size Distribution, Puchack Sed. Core
D2S-F 261' bgs, Sieve+Hydrometer**



**Grain Size Distribution, Puchack Sed. Core
D2S-M 301' bgs, Sieve**

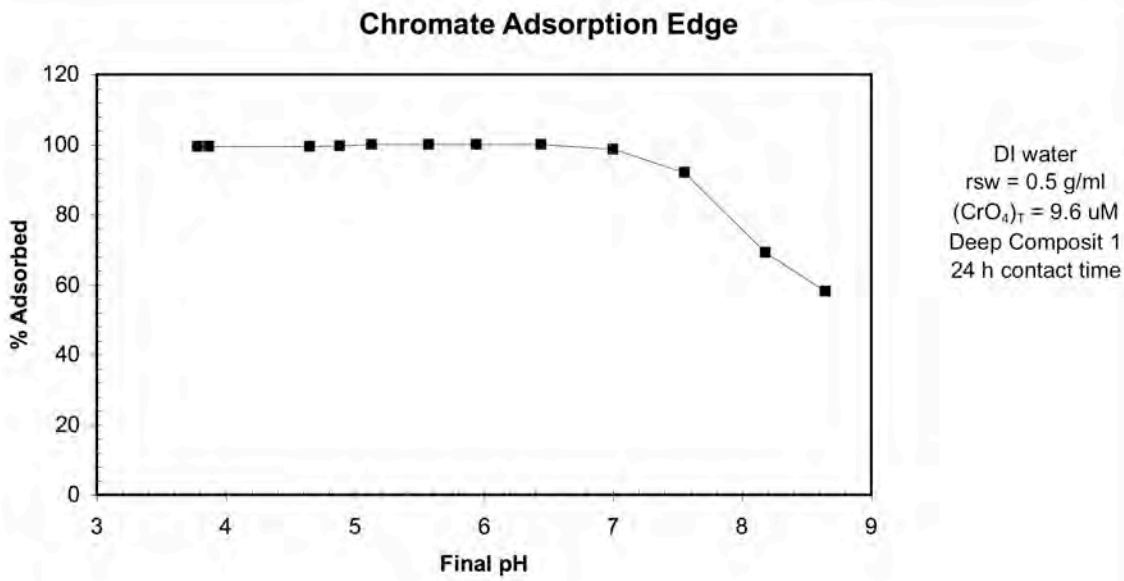
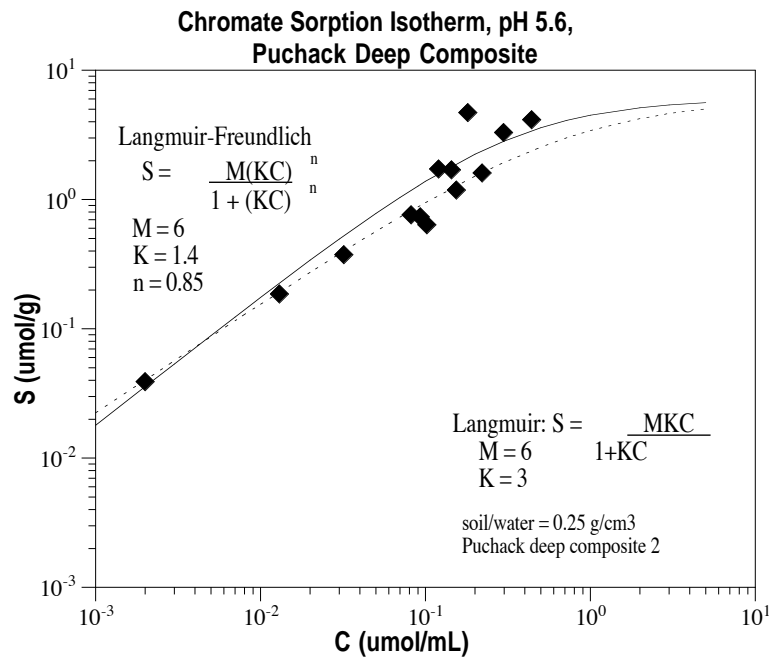


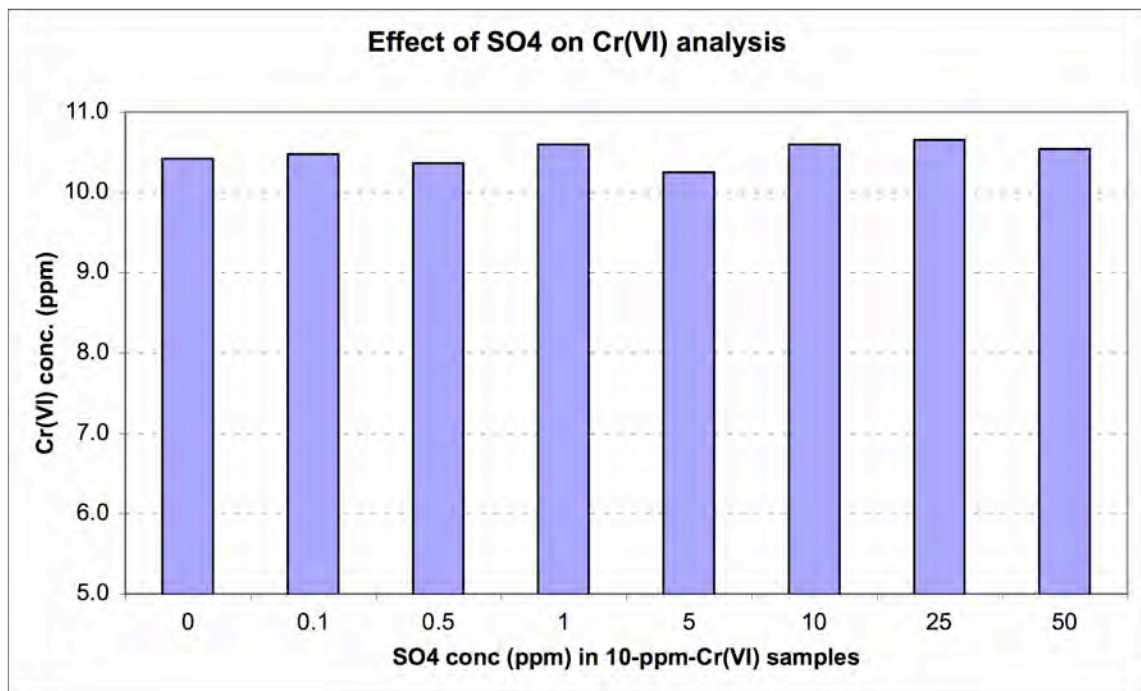
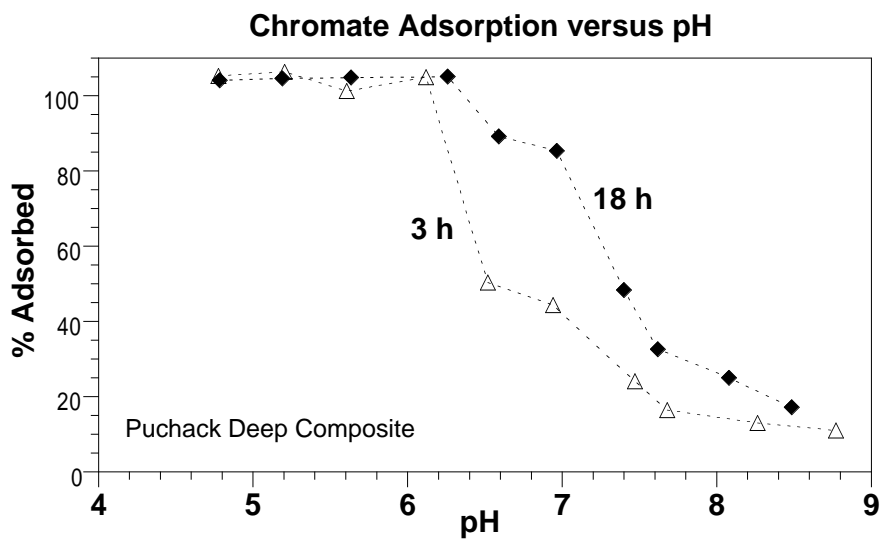
Appendix B

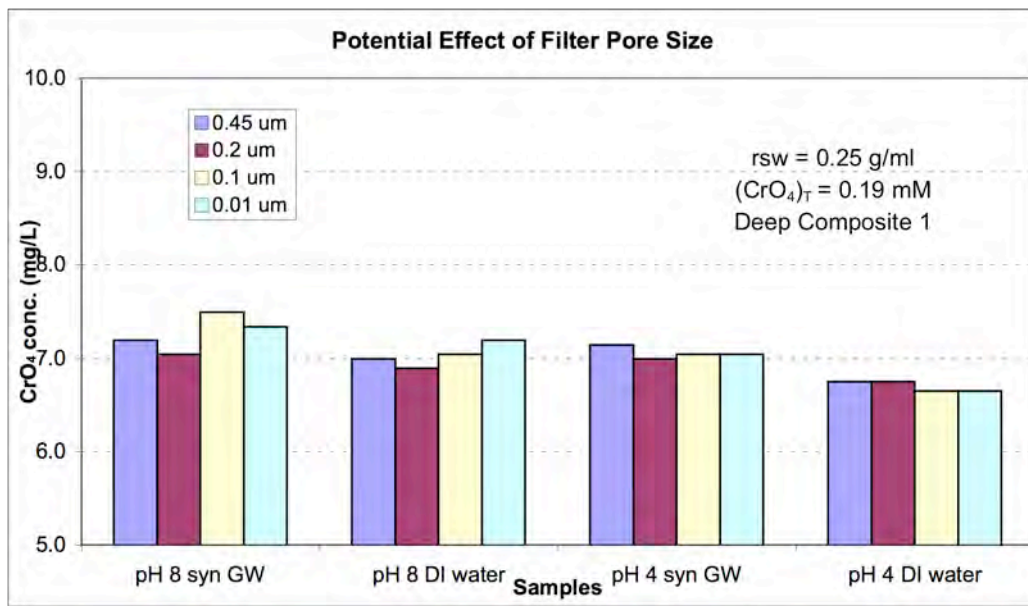
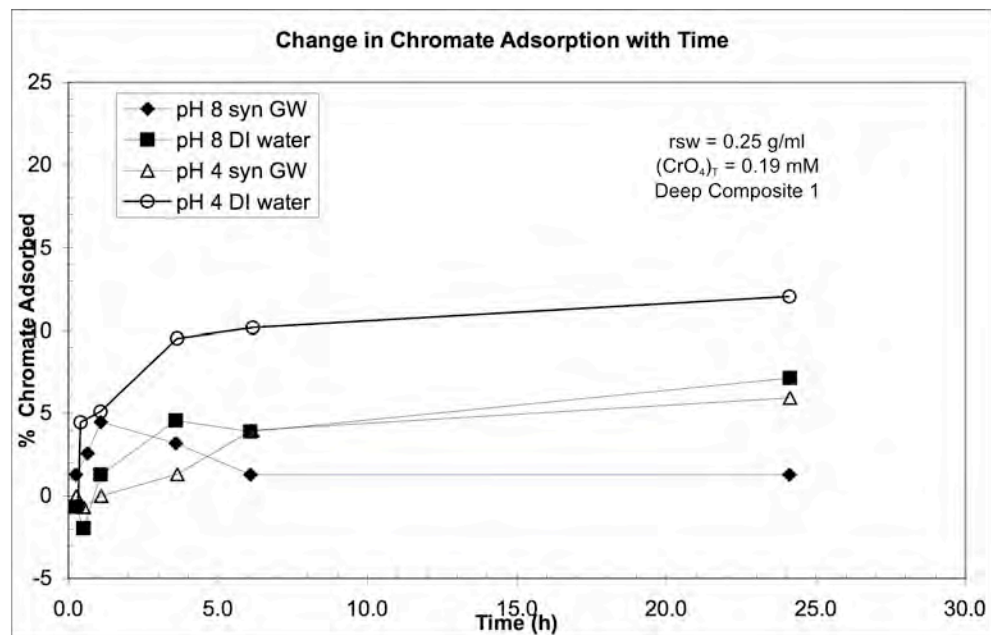
Chromate Adsorption to Natural Sediments

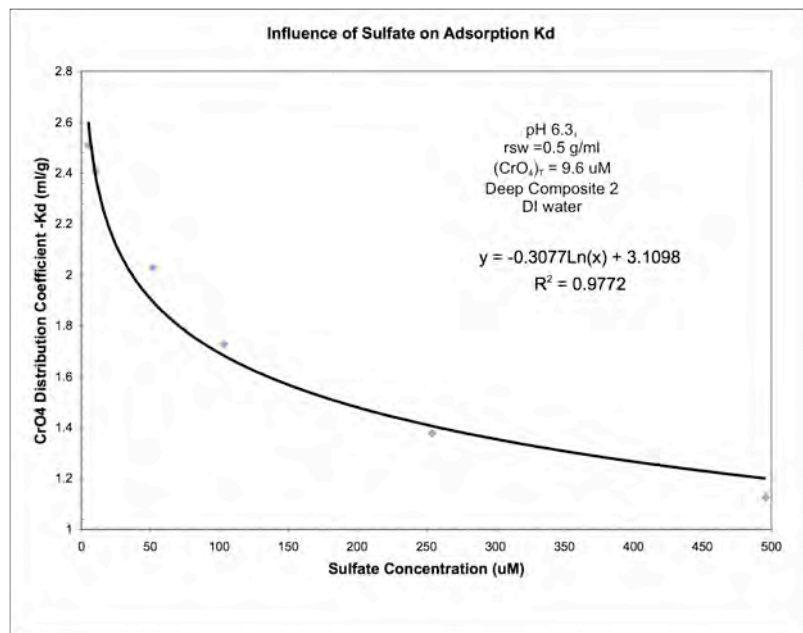
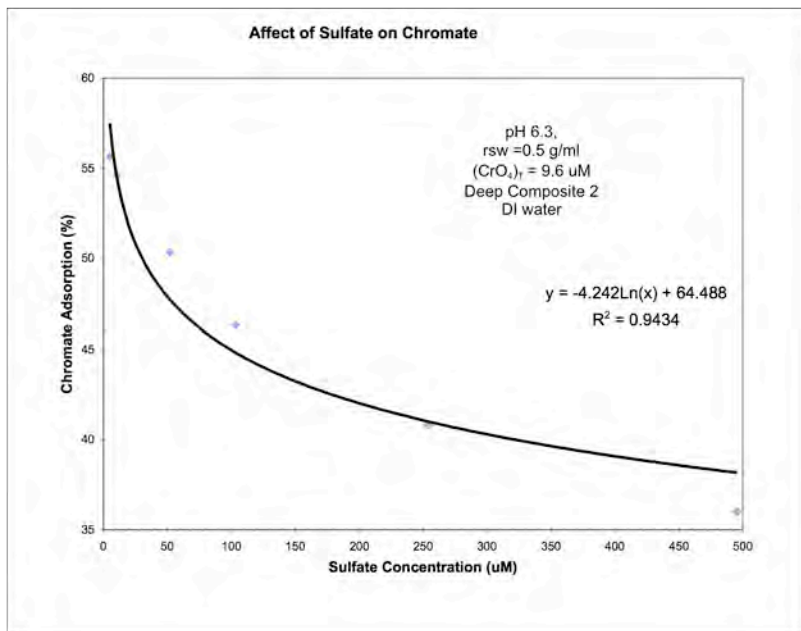
Appendix B

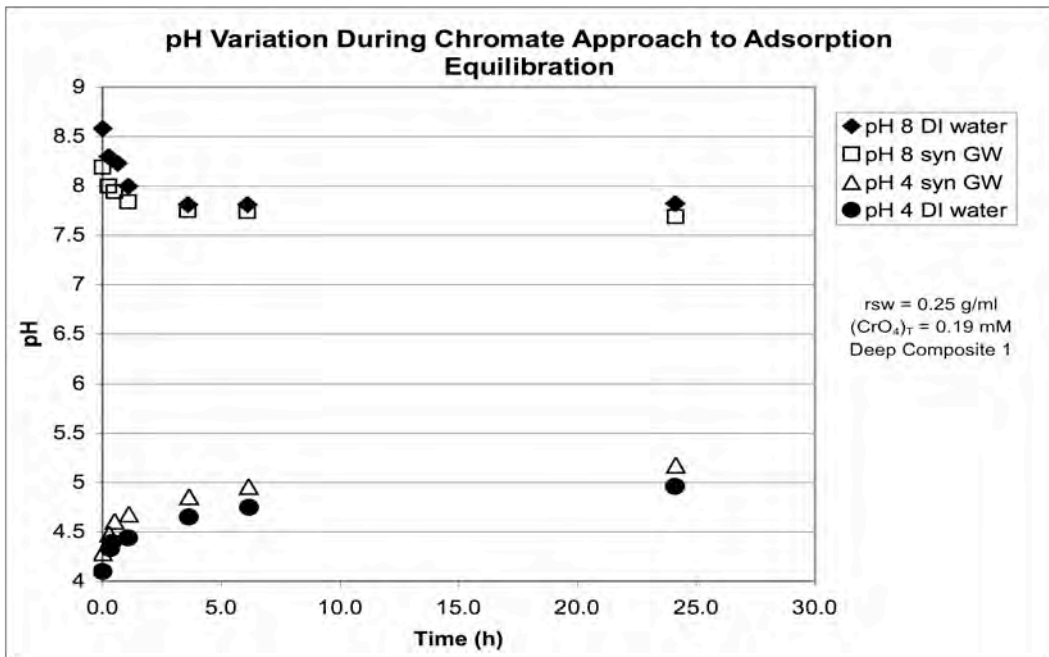
Chromate Adsorption to Natural Sediments











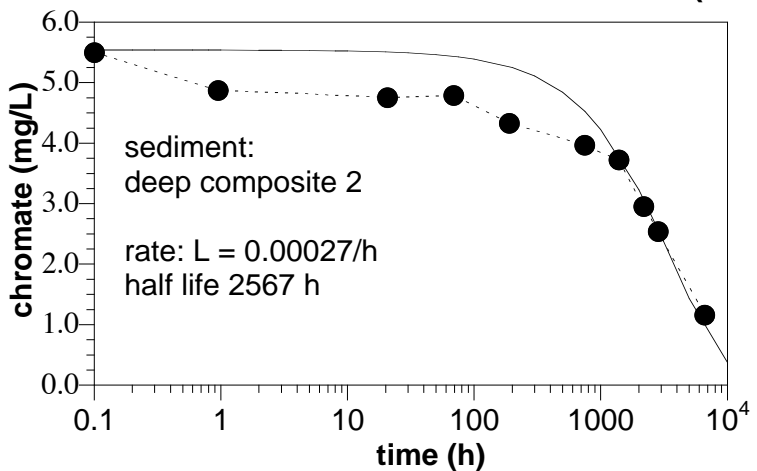
Appendix C

Chromate Reduction by Natural Attenuation

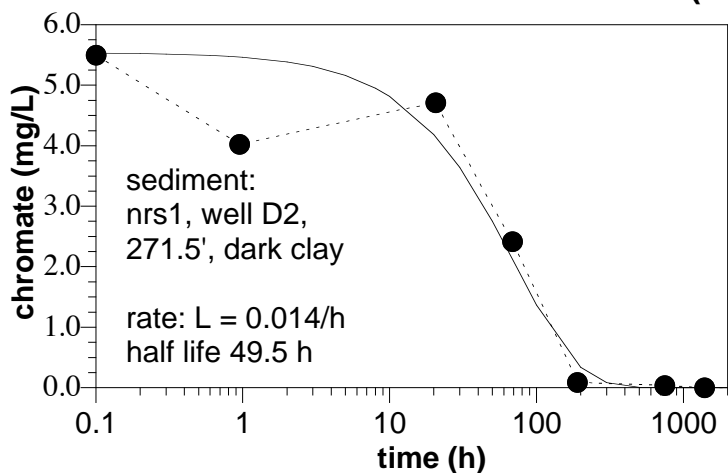
Appendix C

Chromate Reduction by Natural Attenuation

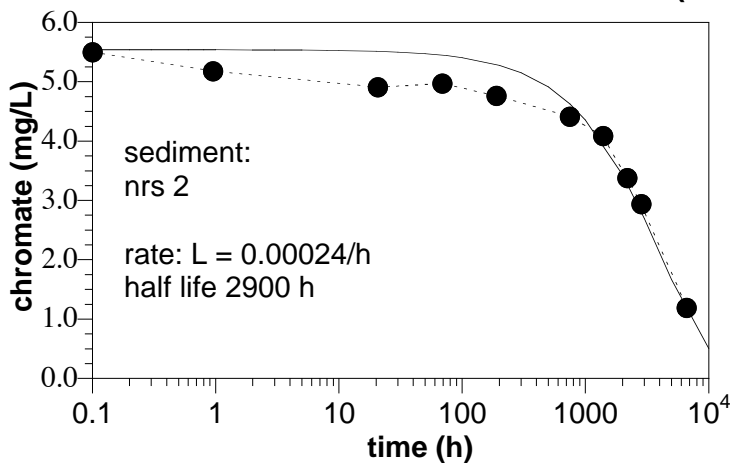
Chromate Natural Reduction with No O₂ (U30)



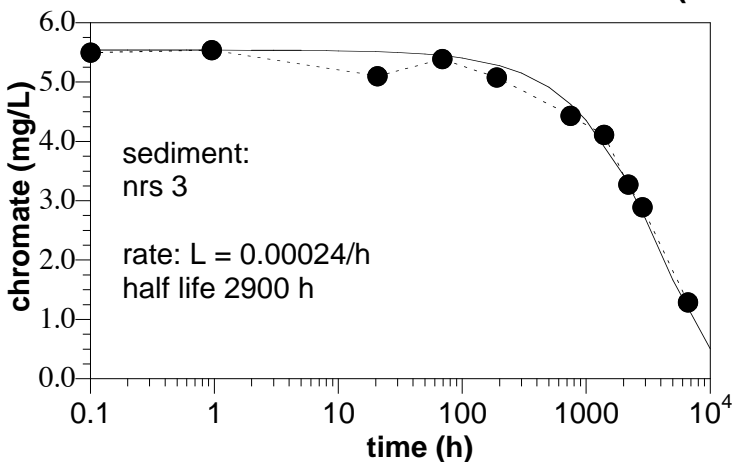
Chromate Natural Reduction with No O₂ (U31)



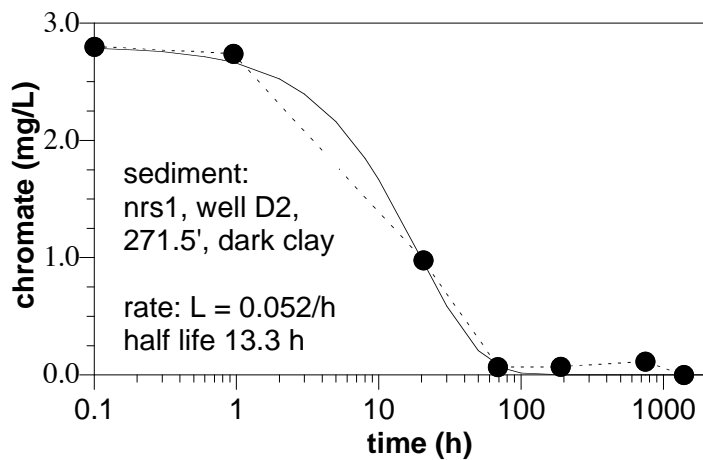
Chromate Natural Reduction with No O₂ (U32)



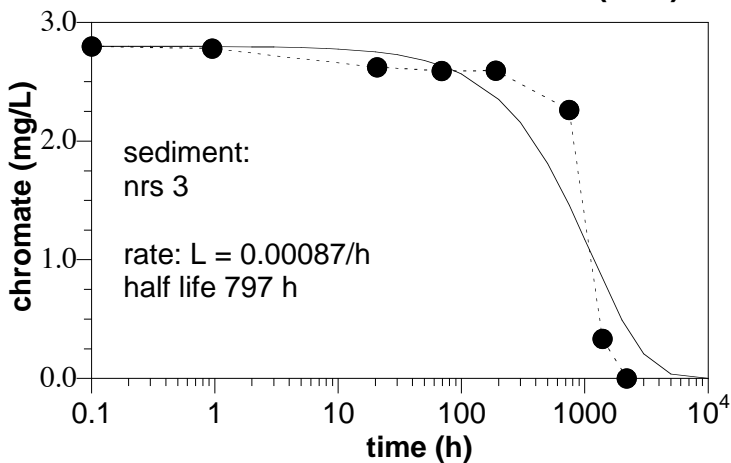
Chromate Natural Reduction with No O₂ (U33)



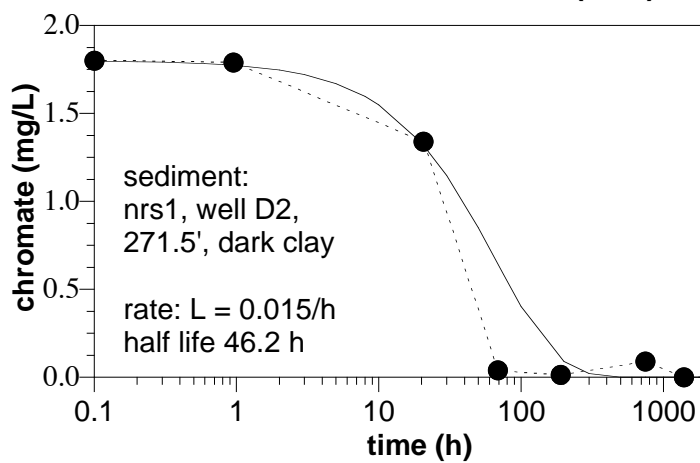
Chromate Natural Reduction w/O₂ (U34)



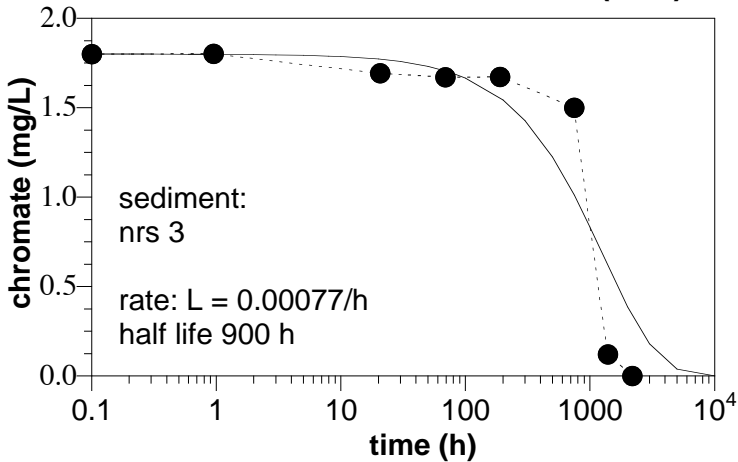
Chromate Natural Reduction w/O₂ (U35)



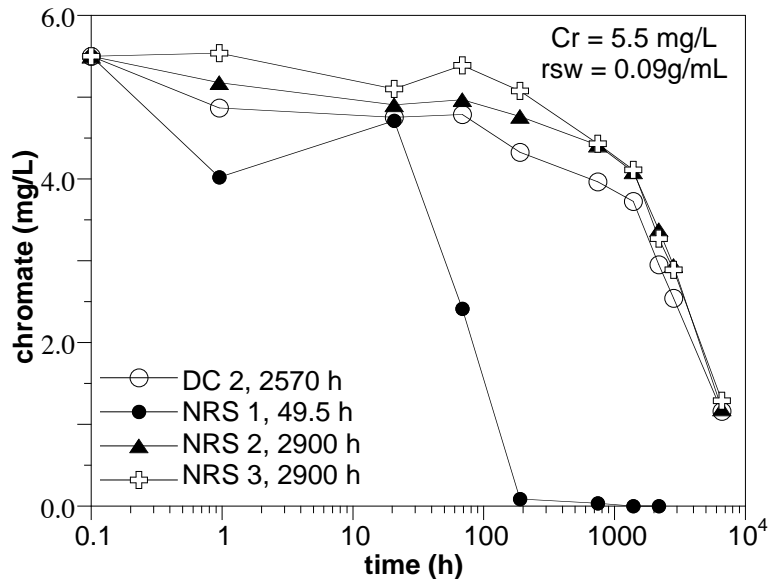
Chromate Natural Reduction w/O₂ (U36)



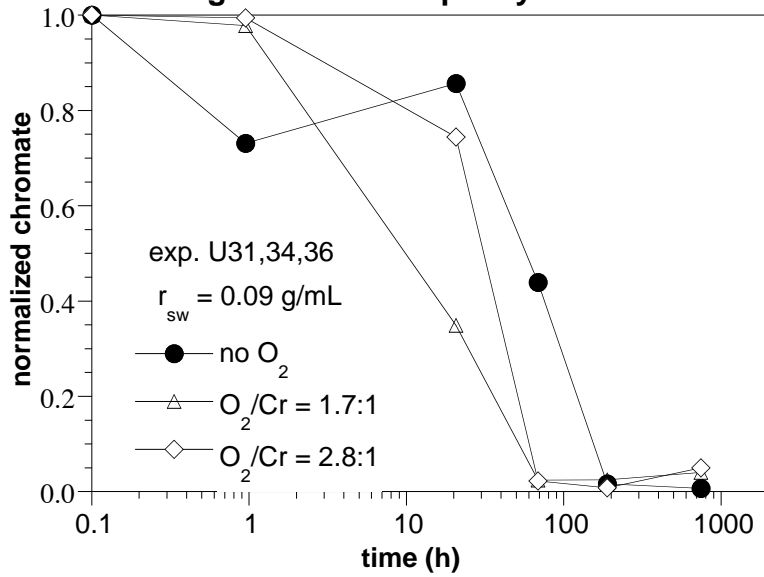
Chromate Natural Reduction w/O₂ (U37)



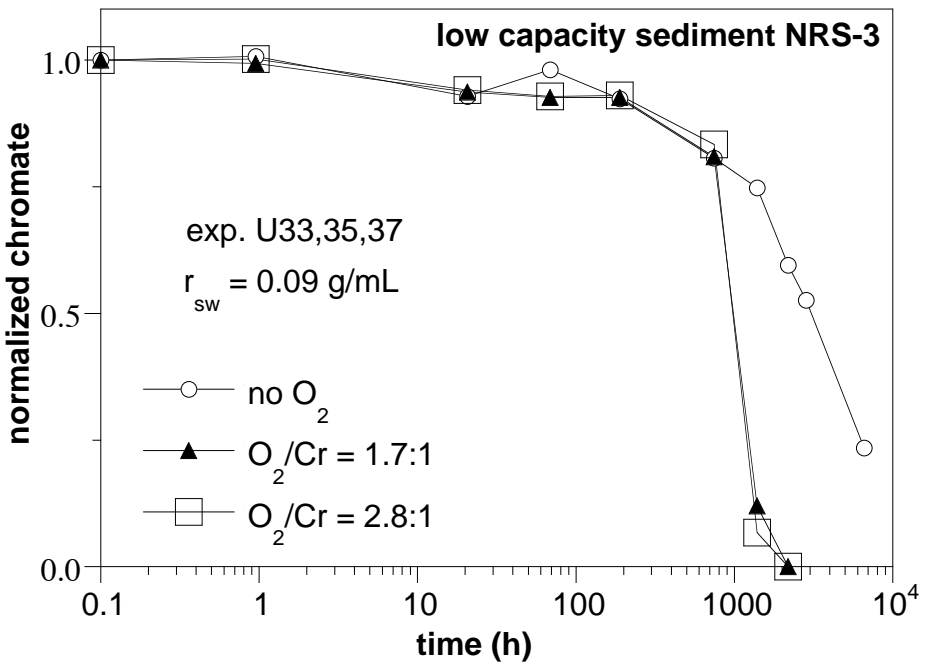
Chromate Natural Reduction with No O₂



Chromate Natural Reduction w/O₂ high reductive capacity sed. NRS3

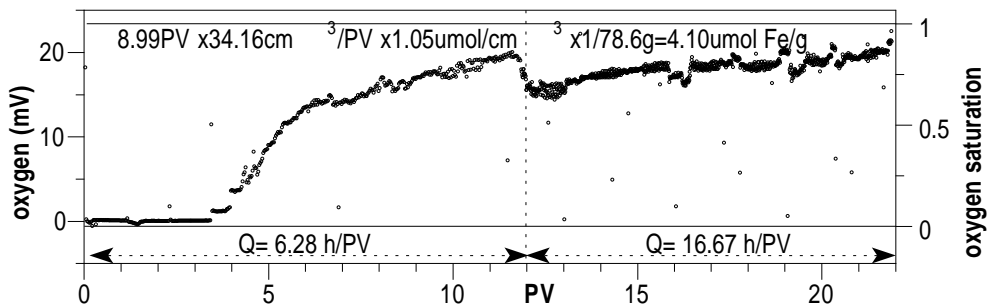


Chromate Natural Reduction w/O₂



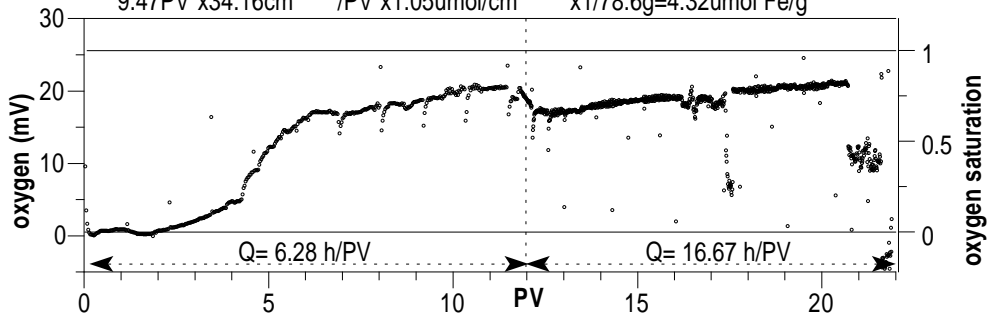
Puchack Sed., Nat. Red. Cap, 1-D flow, MW-36C 151' bgs

U50: Dissolved Oxygen Column, Probe 1

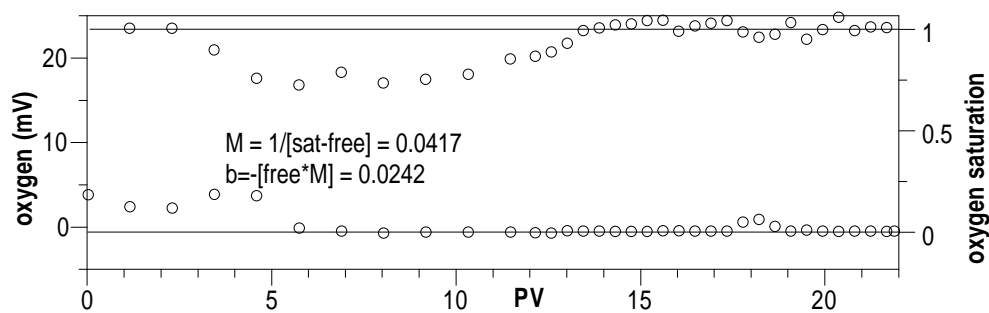


U50: Dissolved Oxygen Standards, Probe 2

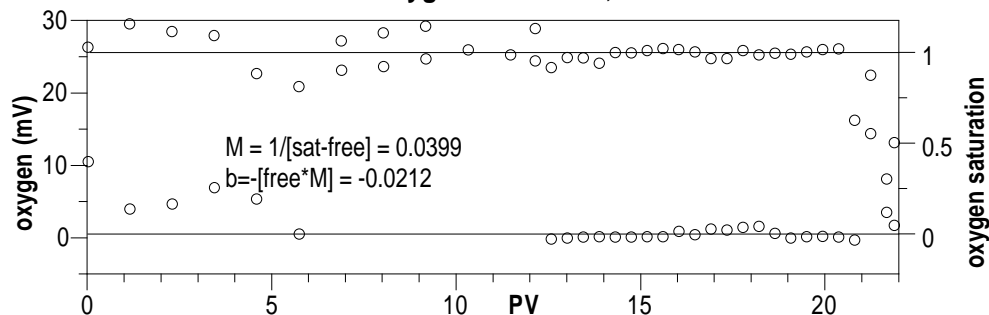
9.47PV x 34.16cm ${}^3/\text{PV} \times 1.05\text{umol/cm}^3$ ${}^3 \times 1/78.6\text{g} = 4.32\text{umol Fe/g}$



U50: Dissolved Oxygen Standards, Probe 1

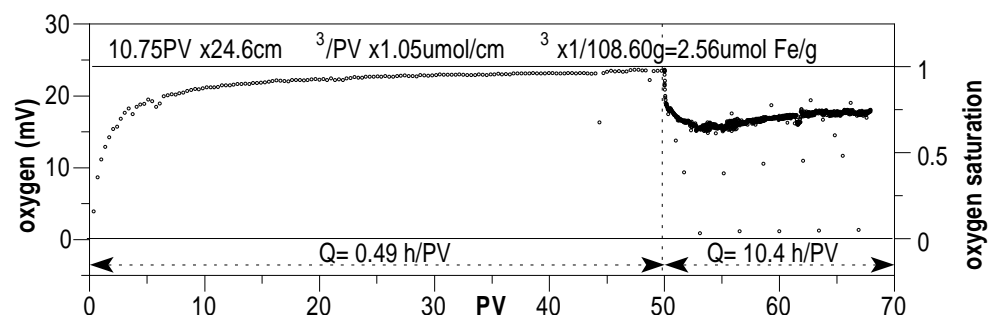


U50: Dissolved Oxygen Standards, Probe 2

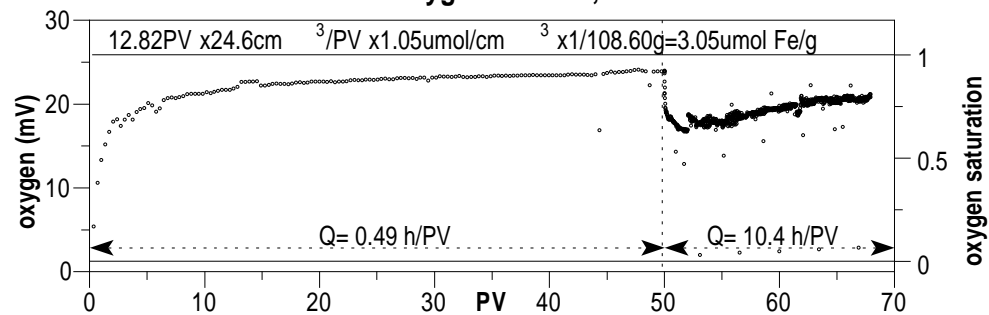


Puchack Sed., Nat. Red. Cap., 1-D flow, MW-37I 199' bgs

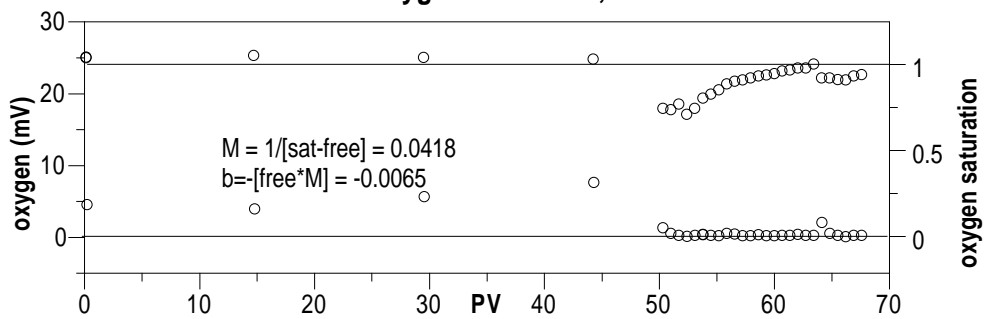
U51: Dissolved Oxygen Column, Probe 1



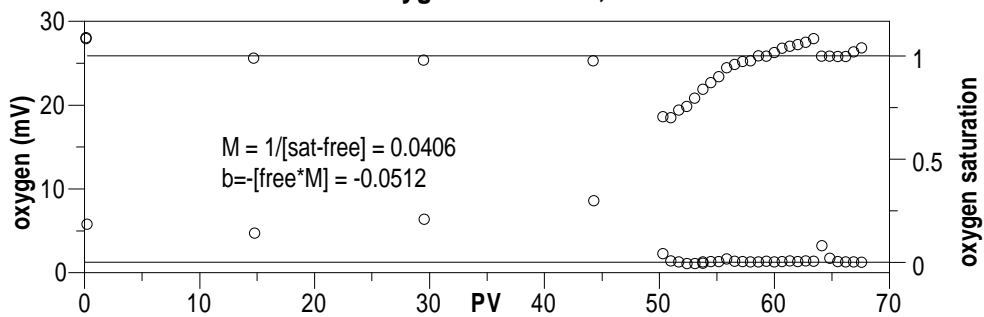
U51: Dissolved Oxygen Column, Probe 2



U51: Dissolved Oxygen Standards, Probe 1

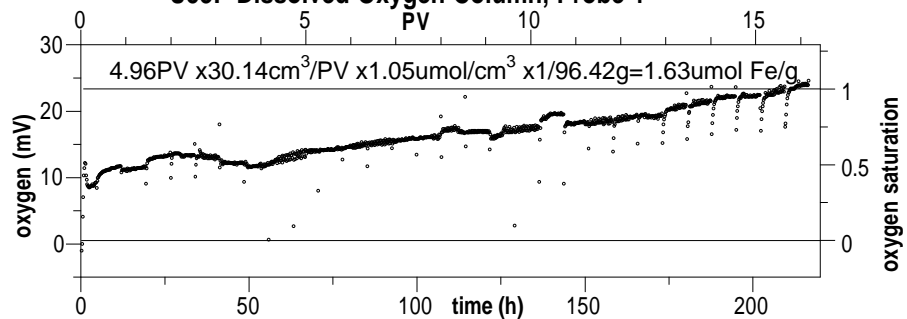


U51: Dissolved Oxygen Standards, Probe 2

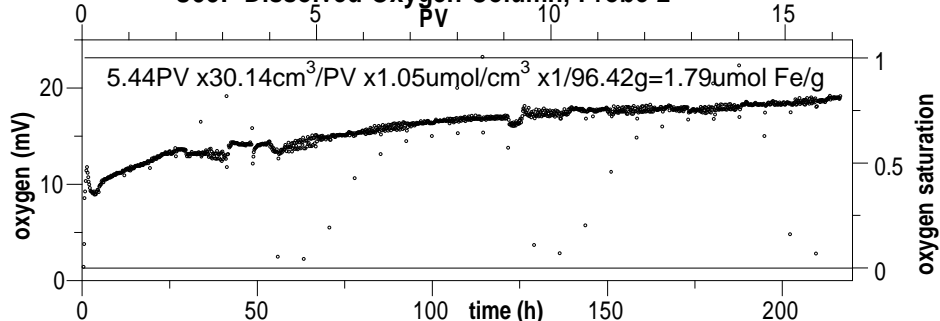


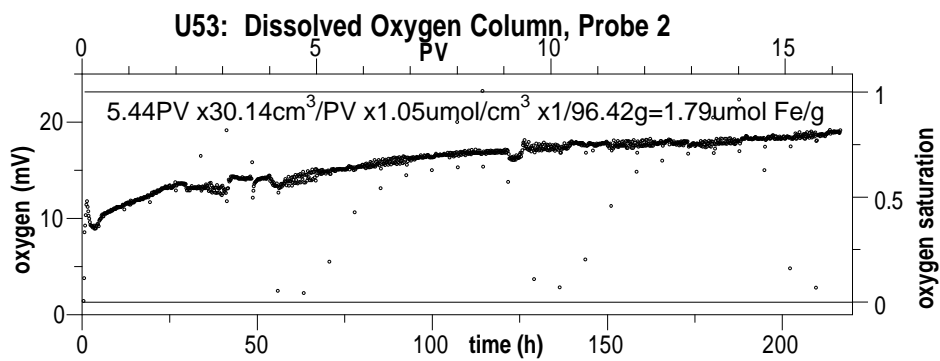
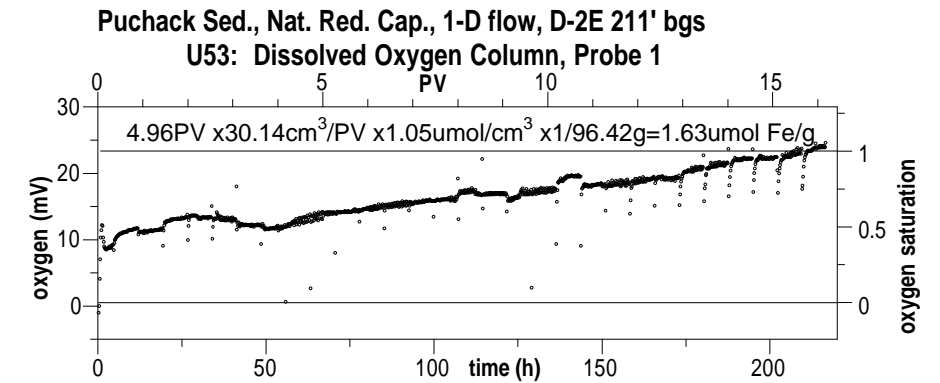
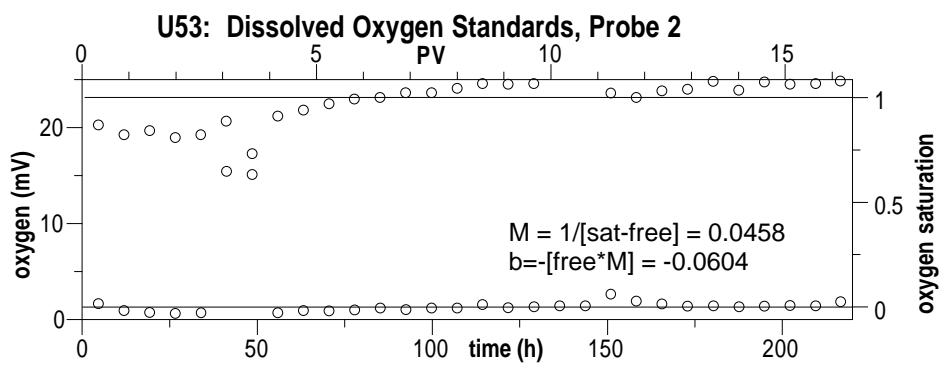
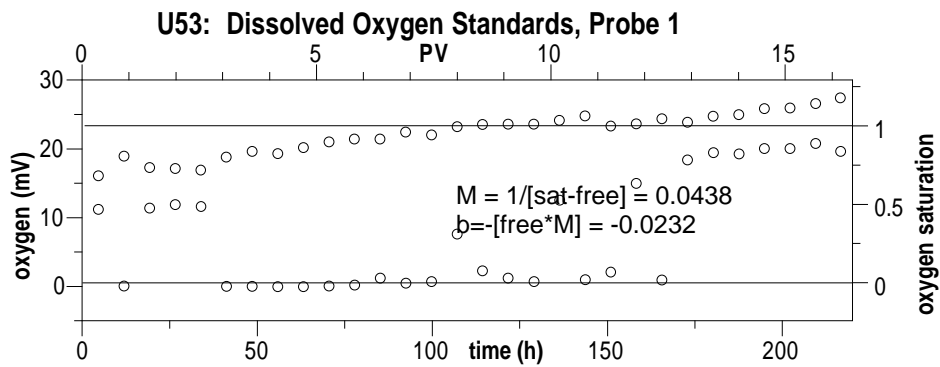
Puchack Sed., Nat. Red. Cap., 1-D flow, D-2E 211' bgs

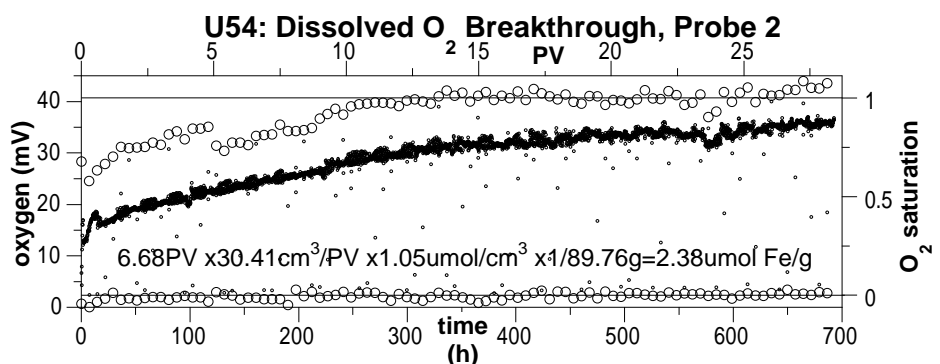
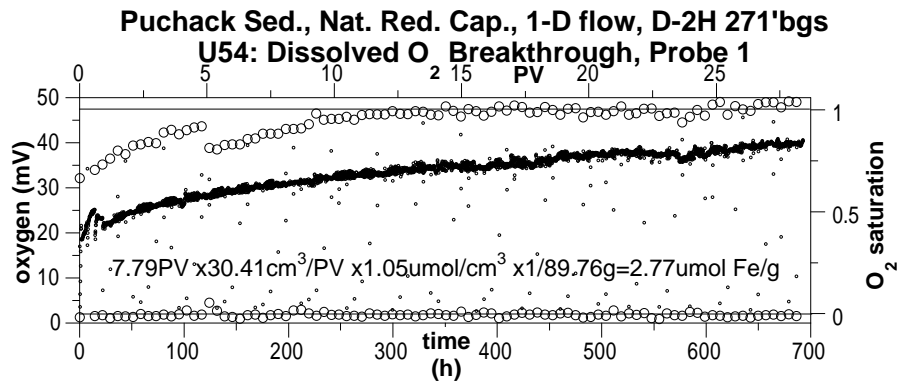
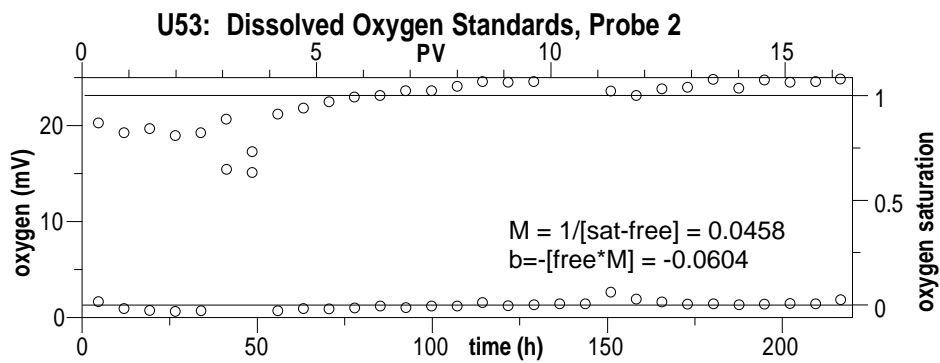
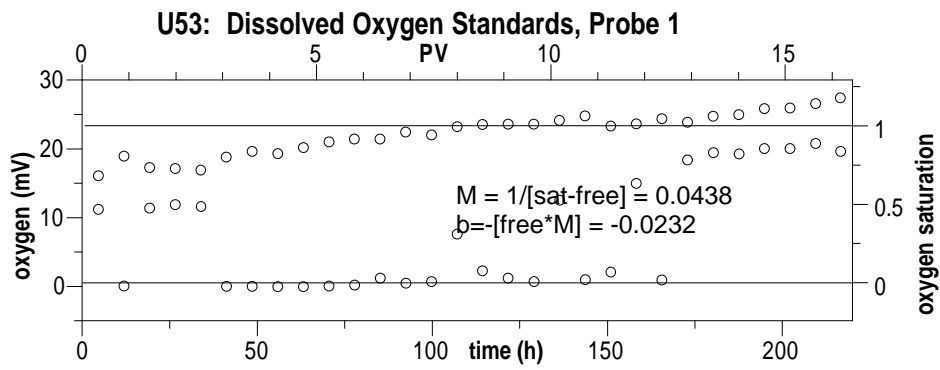
U53: Dissolved Oxygen Column, Probe 1

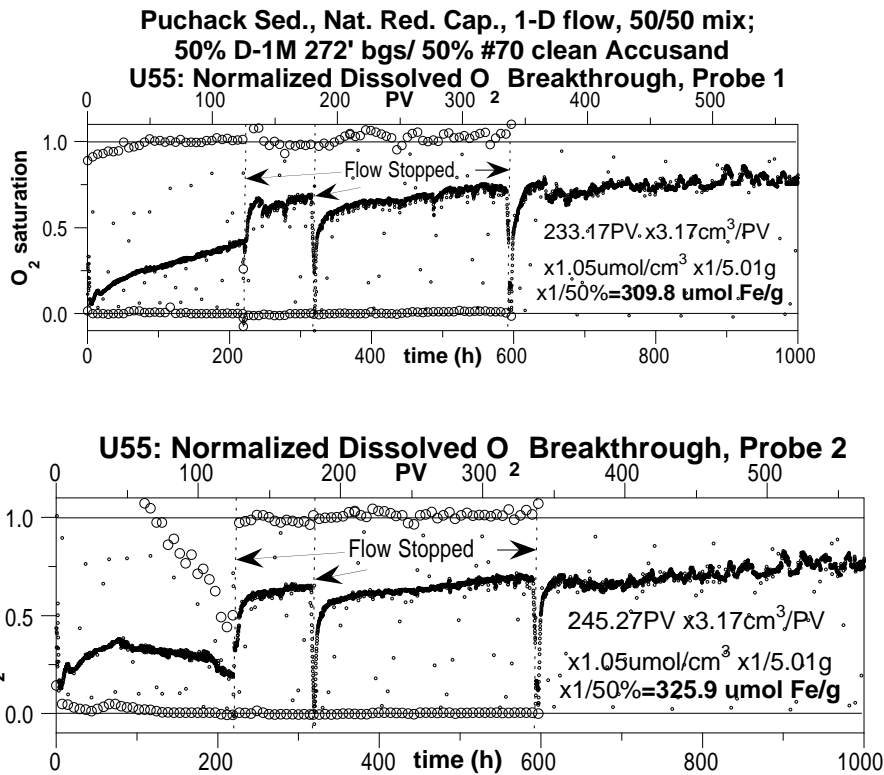


U53: Dissolved Oxygen Column, Probe 2







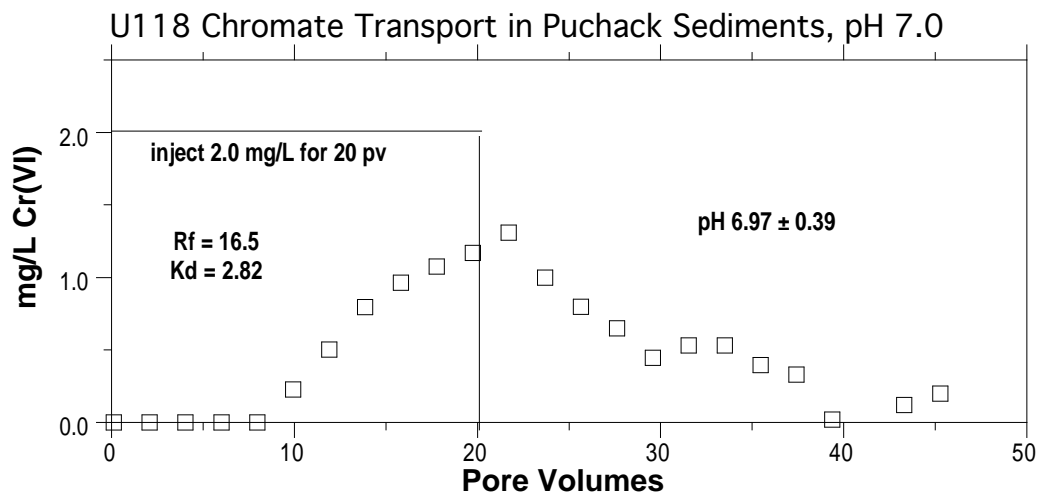
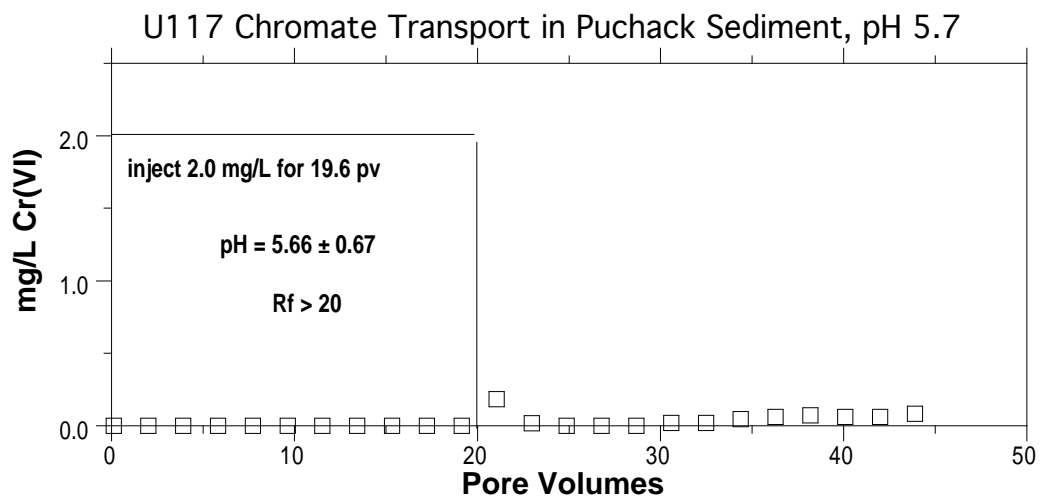
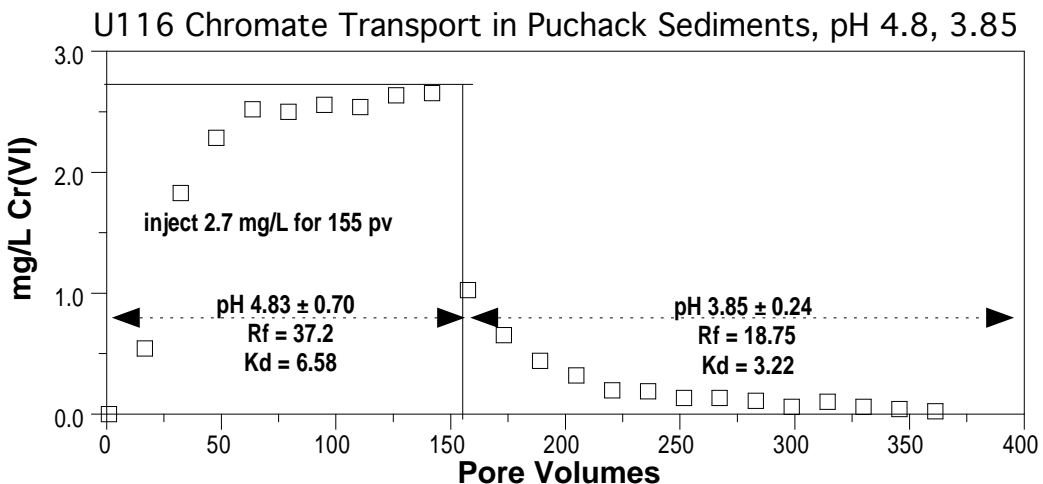


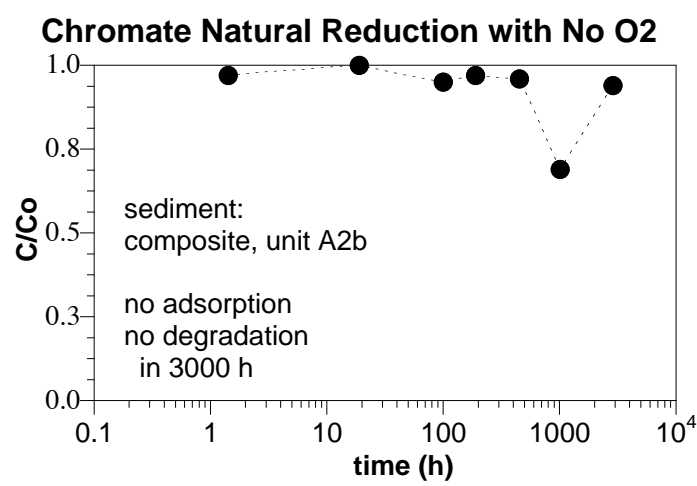
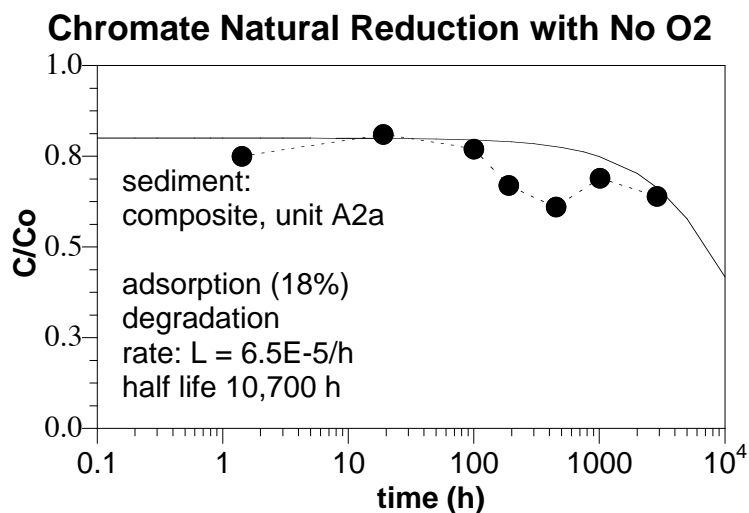
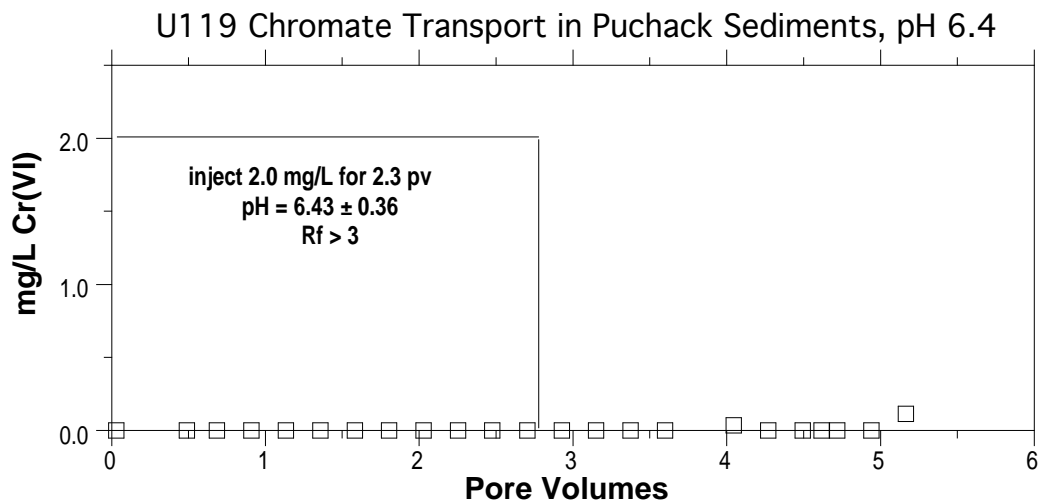
Fe Extraction on Untreated Puchack Sed.

	DCB (U38)	Amm. Oxalate (U39)	5.0M HCl (U40)	0.5M HCl (U41)
Sediment Core	FE(II) ($\mu\text{mol/g}$)	FE(III) ($\mu\text{mol/g}$)	FE(II) ($\mu\text{mol/g}$)	FE(III) ($\mu\text{mol/g}$)
MW-36C	696.24	1069.86	1288.24	631.04
MW-37I	93.90	-16.25	3.64	14.92
D1-H	202.17	-2.13	10.35	16.15
D1-M	246.90	73.18	237.08	8.37
D2-E	100.29	-16.43	2.90	30.54
D2-H	99.83	-11.16	6.01	9.62

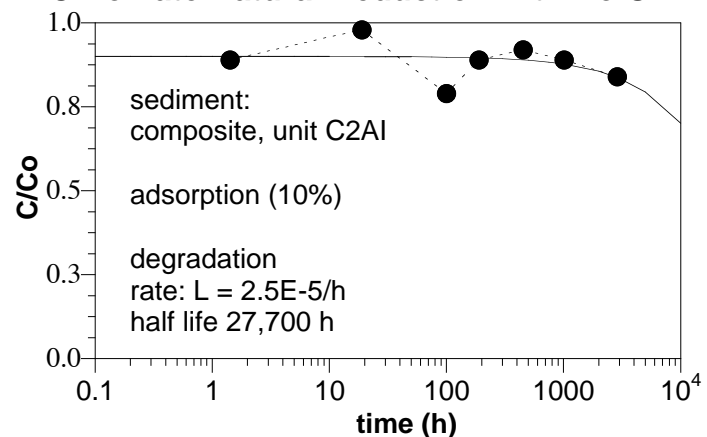
Fe Extractions on Red. Puchack Sed.

Sediment Core	5.0M HCl (U40)		0.5M HCl (U41)
	FE(II) ($\mu\text{mol/g}$)	FE(III) ($\mu\text{mol/g}$)	FE(II) ($\mu\text{mol/g}$)
MW-36C	7.04	535.06	1209.40
MW-36F	21.53	7.47	41.84
MW-36I	35.32	5.29	63.82
MW-36M	2.15	26.72	27.08
MW-37C	2.23	44.32	52.68
MW-37F	2.39	39.51	40.20
MW-37I	2.26	37.48	172.39
D1-H	2.75	142.65	71.23
D2-H	1.16	63.21	50.23

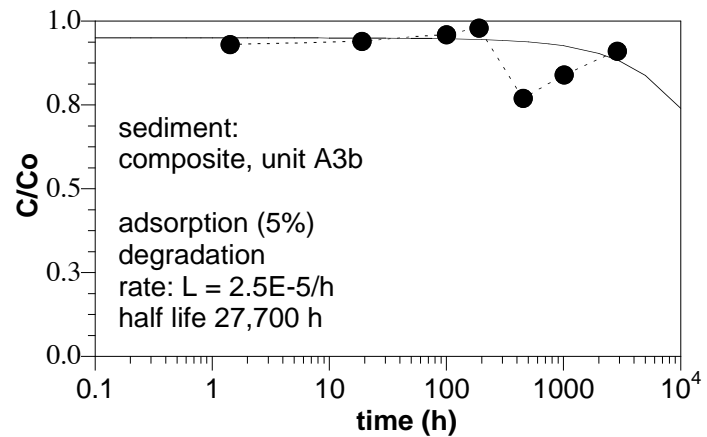




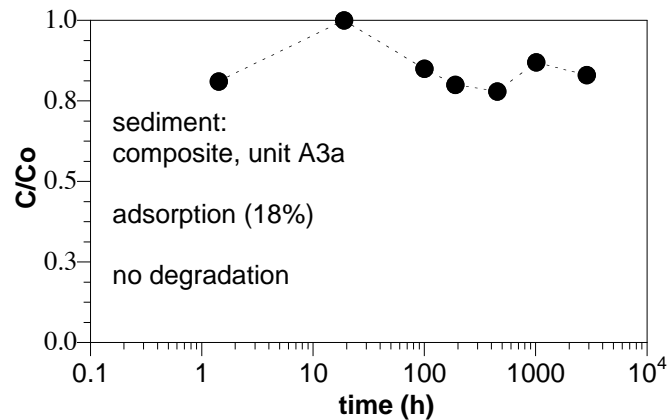
Chromate Natural Reduction with No O₂

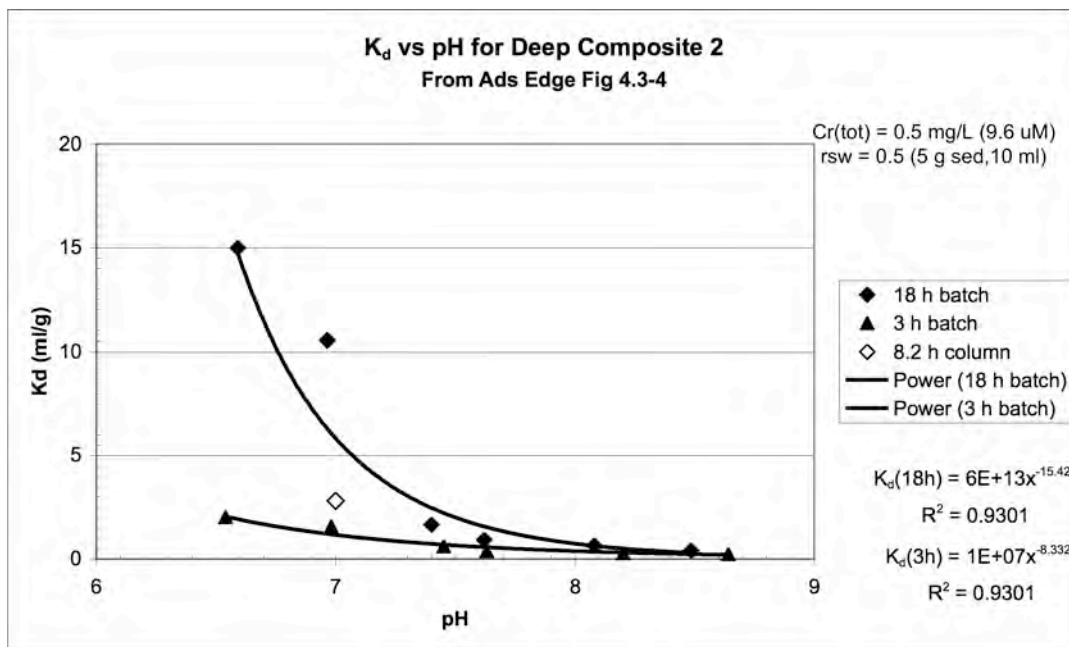
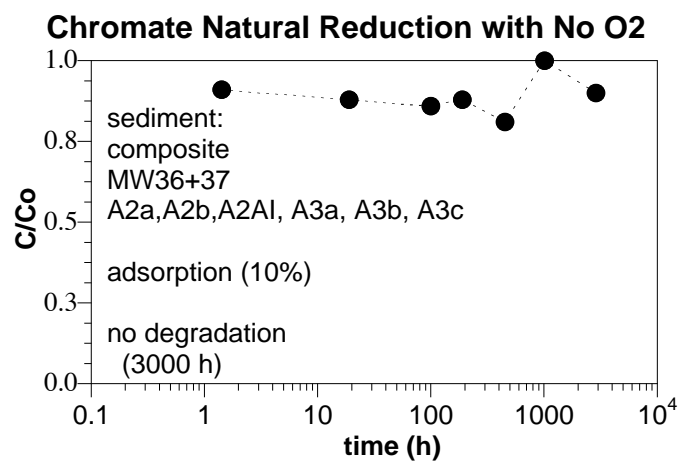
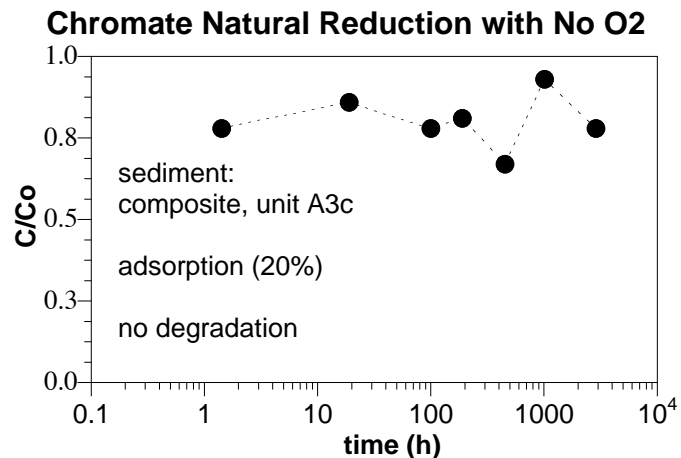


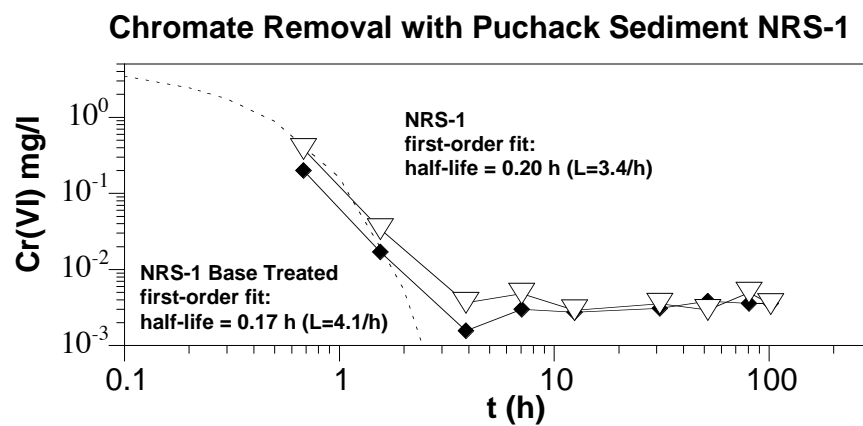
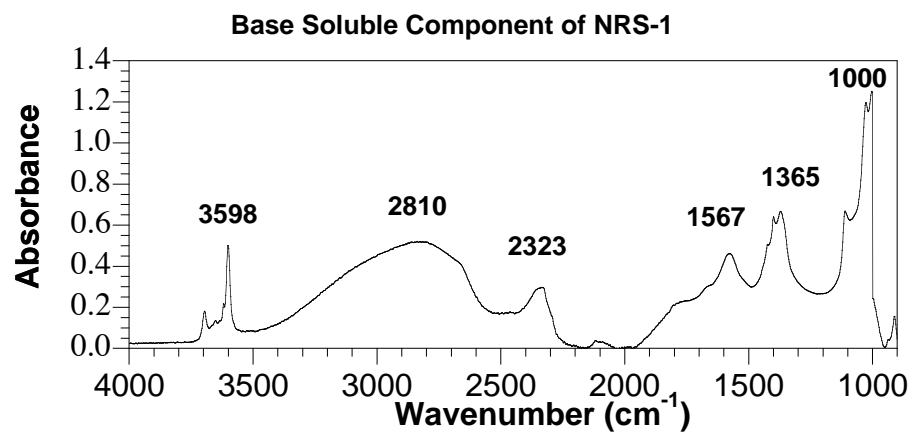
Chromate Natural Reduction with No O₂



Chromate Natural Reduction with No O₂





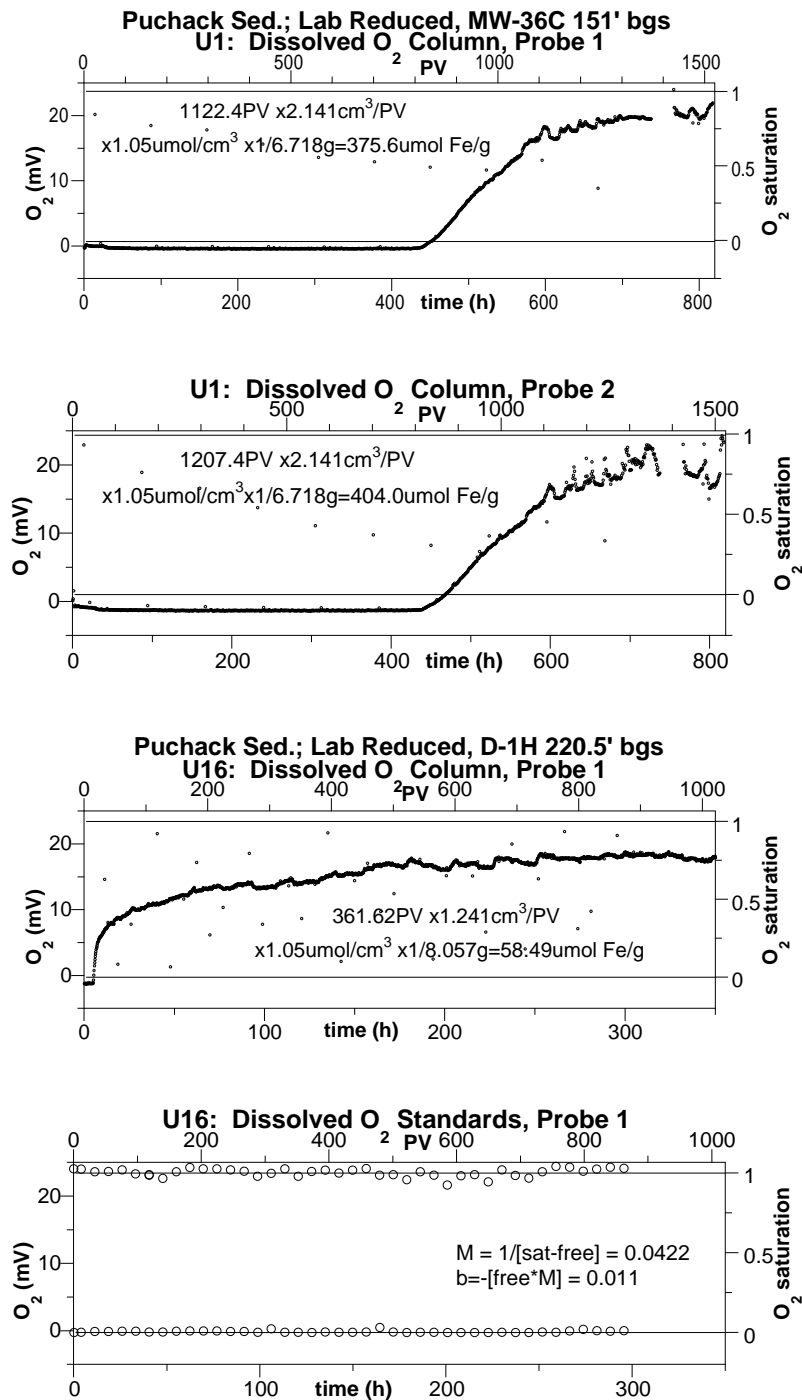


Appendix D

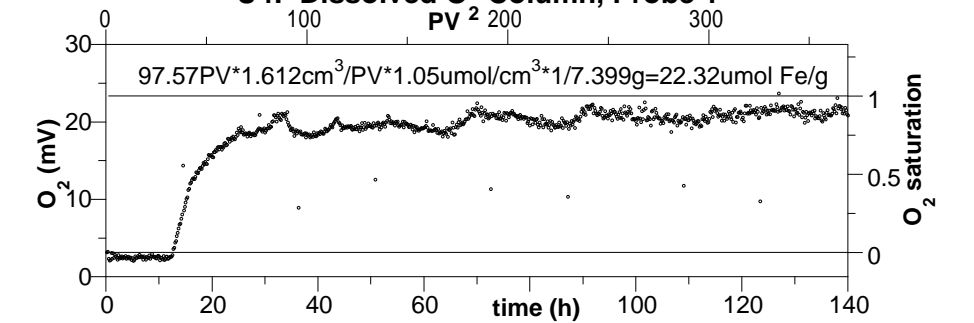
Sediment Reductive Capacity

Appendix D

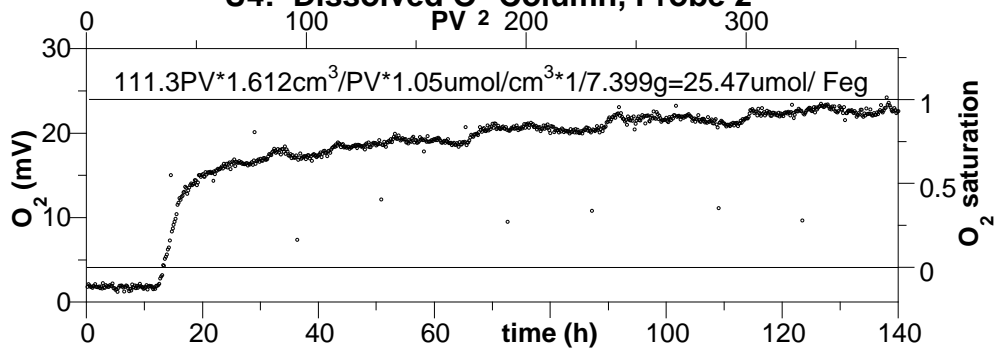
Sediment Reductive Capacity



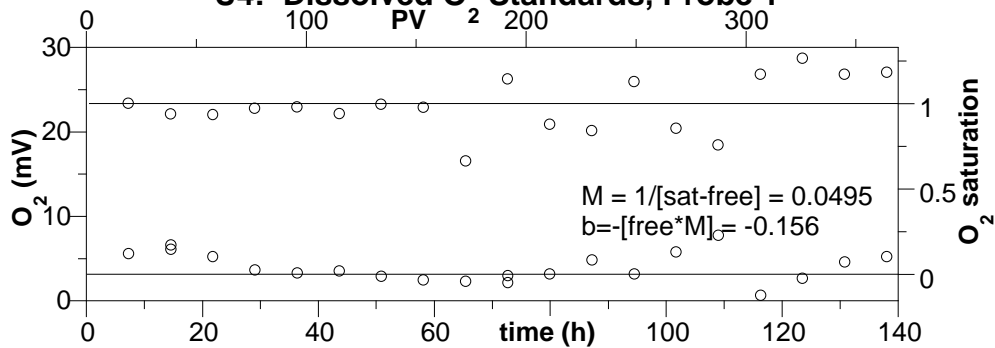
Puchack Sed.; Lab Reduced, MW-36I 197.5' bgs
U4: Dissolved O₂ Column, Probe 1



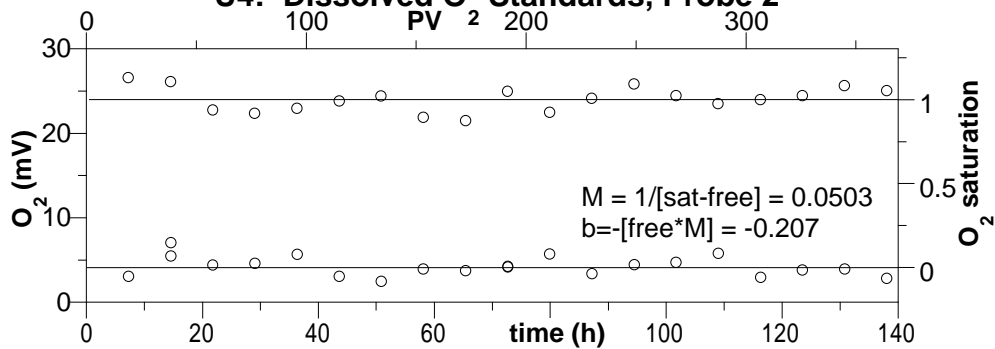
U4: Dissolved O₂ Column, Probe 2



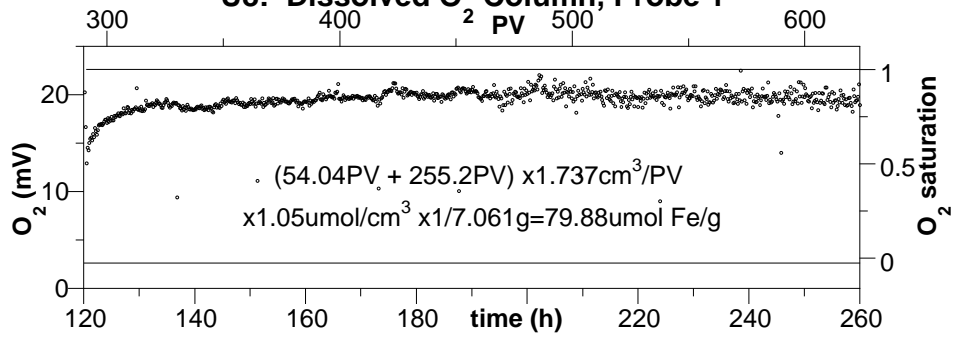
U4: Dissolved O₂ Standards, Probe 1



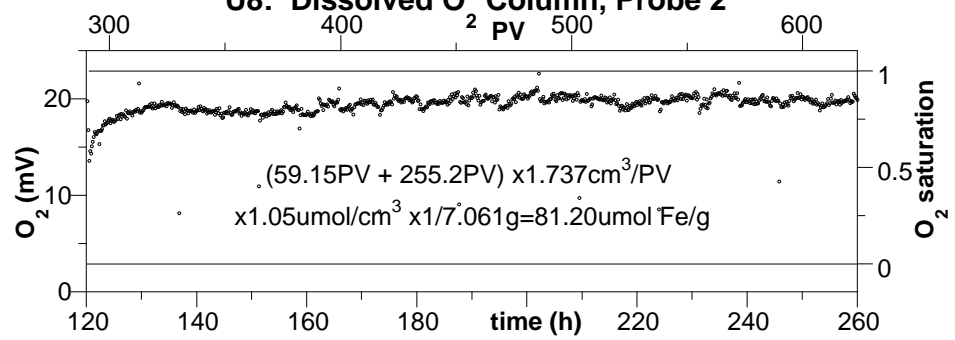
U4: Dissolved O₂ Standards, Probe 2



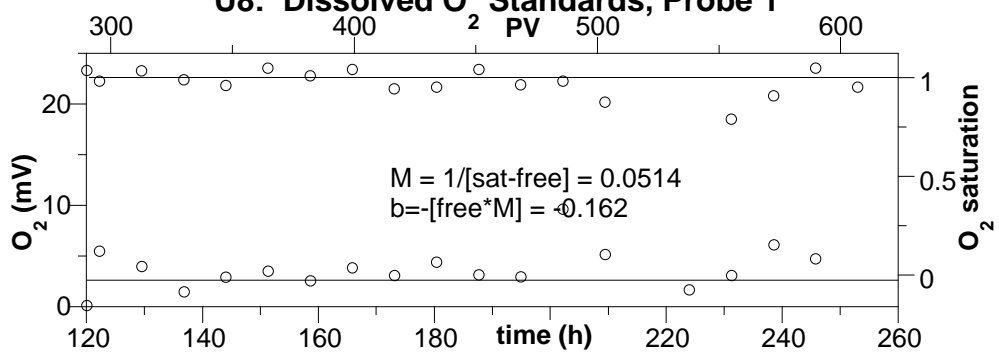
Puchack Sed.; Lab Reduced, MW-37C 154' bgs
U8: Dissolved O₂ Column, Probe 1



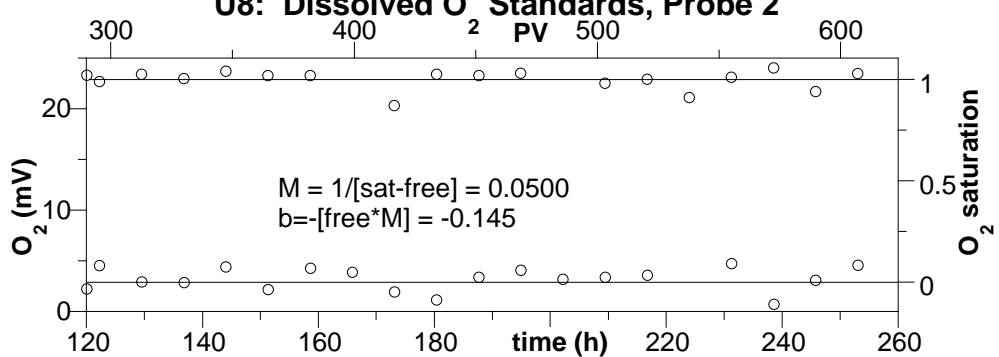
U8: Dissolved O₂ Column, Probe 2



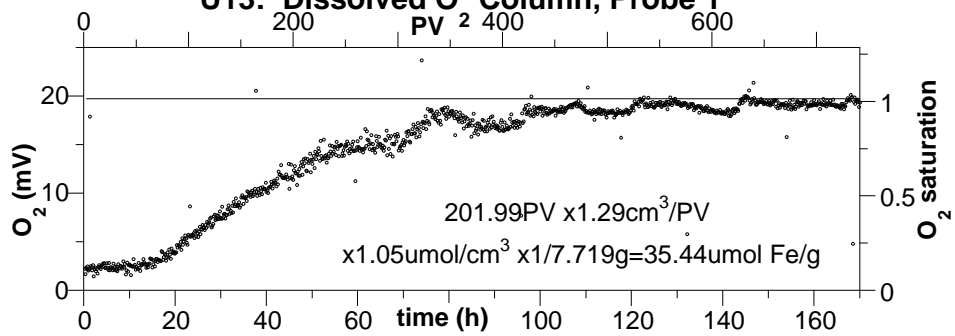
U8: Dissolved O₂ Standards, Probe 1



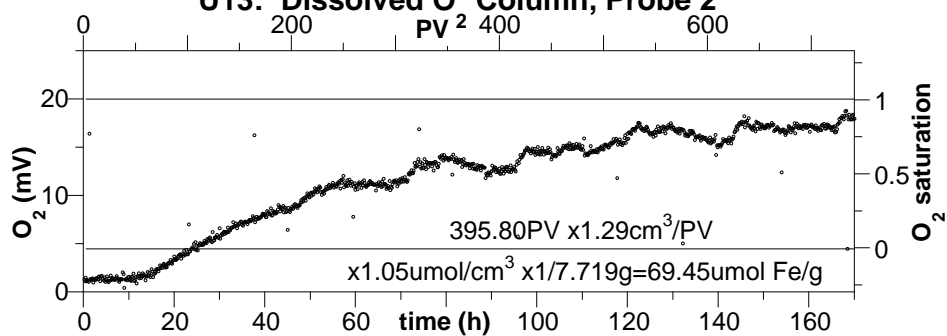
U8: Dissolved O₂ Standards, Probe 2



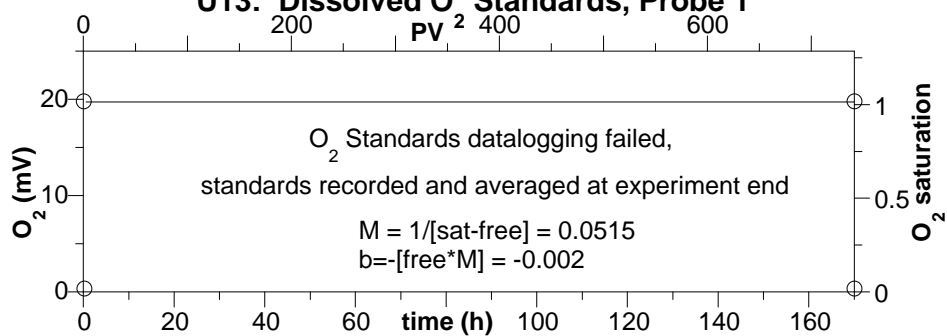
**Puchack Sed.; Lab Reduced, D-1B 106' bgs
U13: Dissolved O Column, Probe 1**



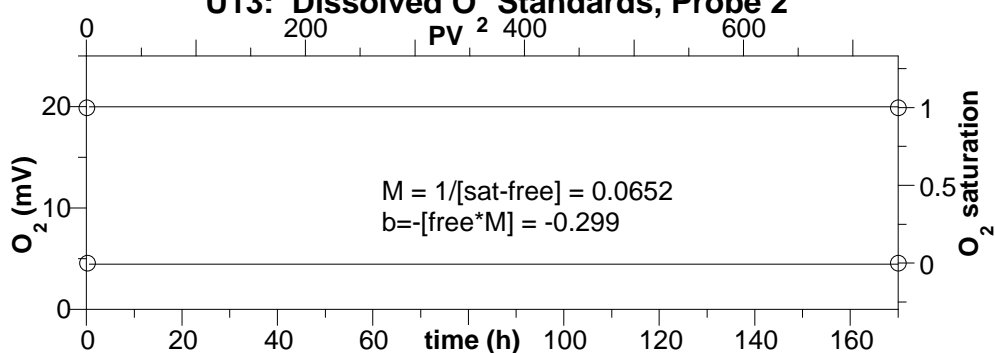
U13: Dissolved O Column, Probe 2



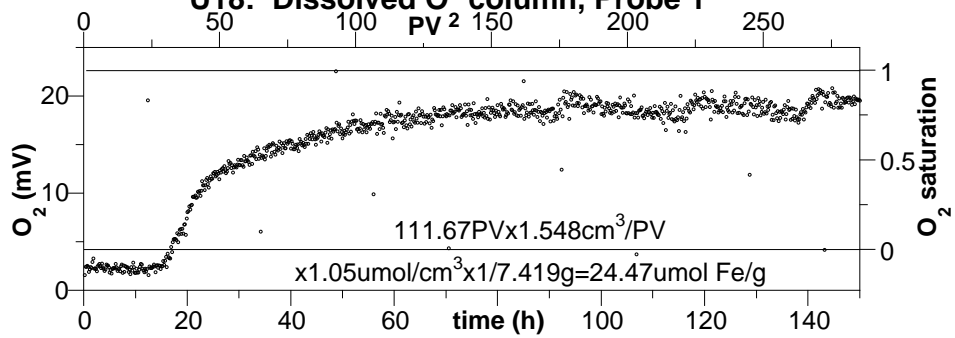
U13: Dissolved O Standards, Probe 1



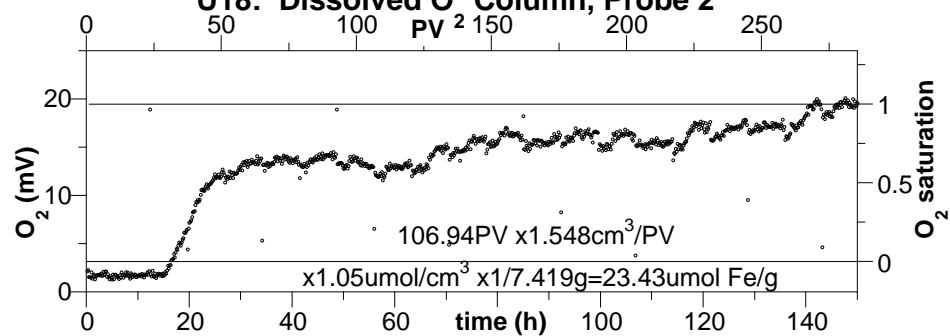
U13: Dissolved O Standards, Probe 2



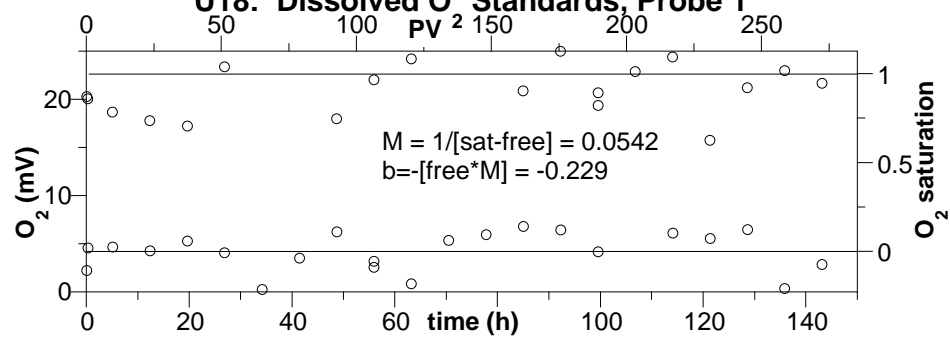
Puchack Sed.; Lab Reduced, D-2C 151' bgs
U18: Dissolved O₂ column, Probe 1



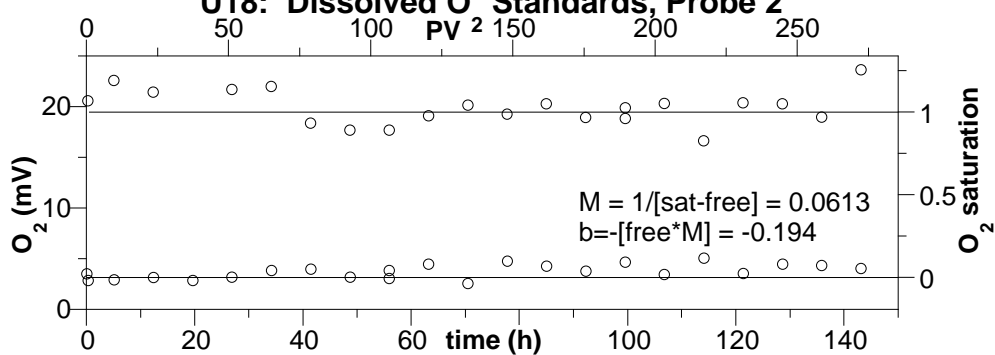
U18: Dissolved O₂ Column, Probe 2



U18: Dissolved O₂ Standards, Probe 1



U18: Dissolved O₂ Standards, Probe 2

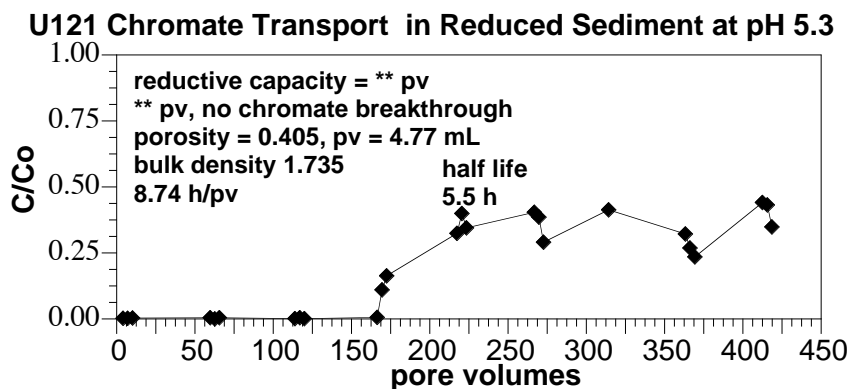
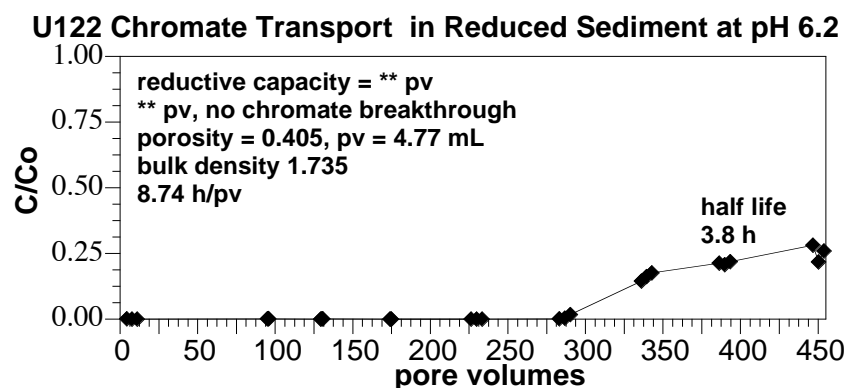
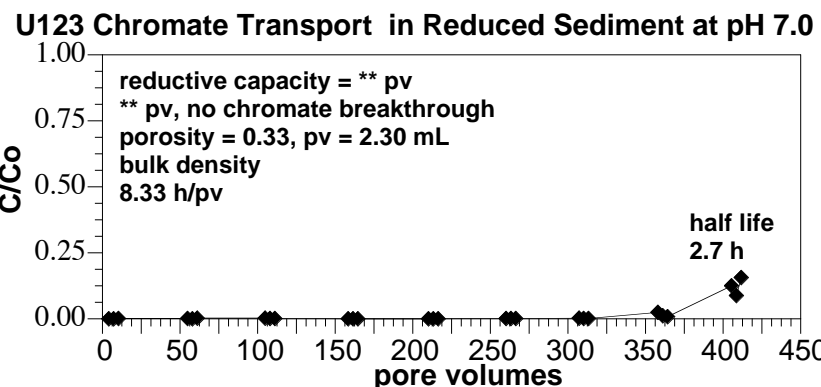


Appendix E

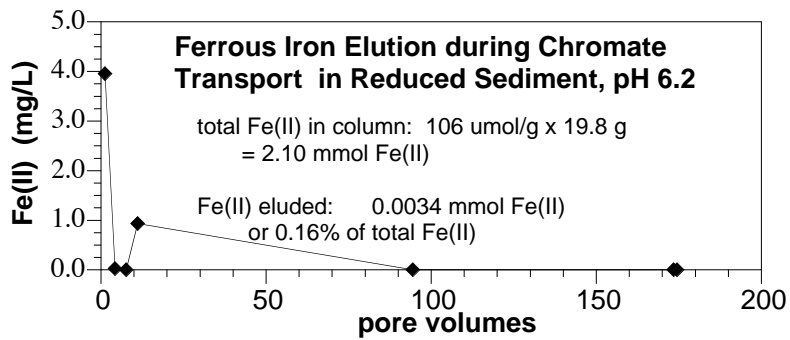
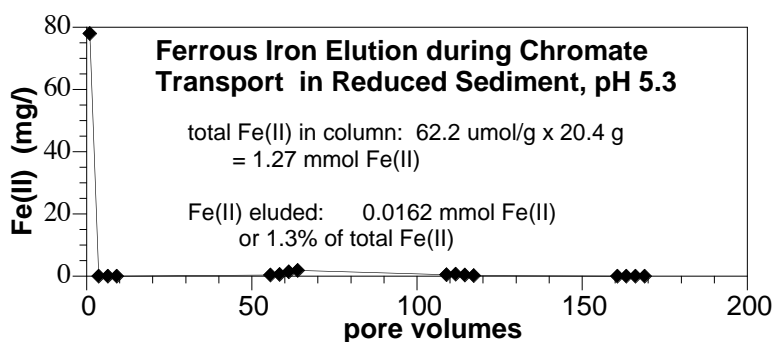
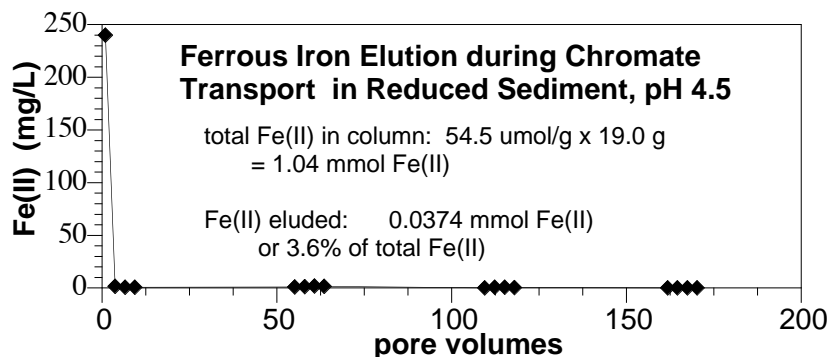
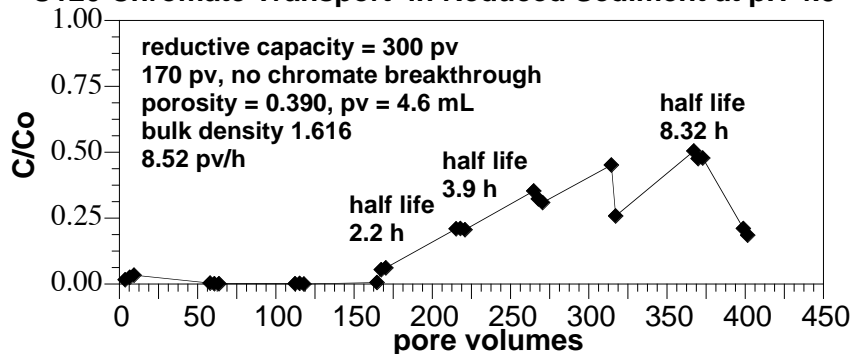
Chromate Transport and Reduction

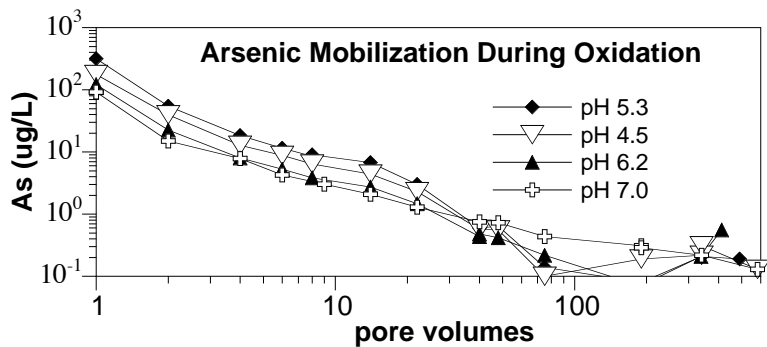
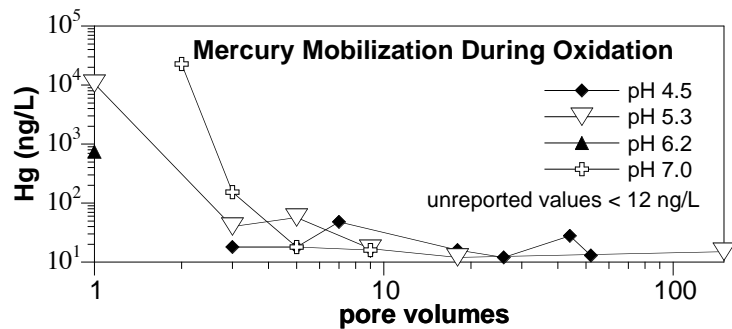
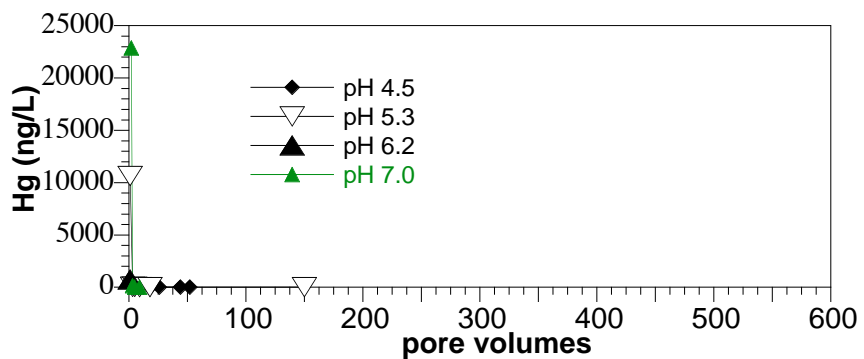
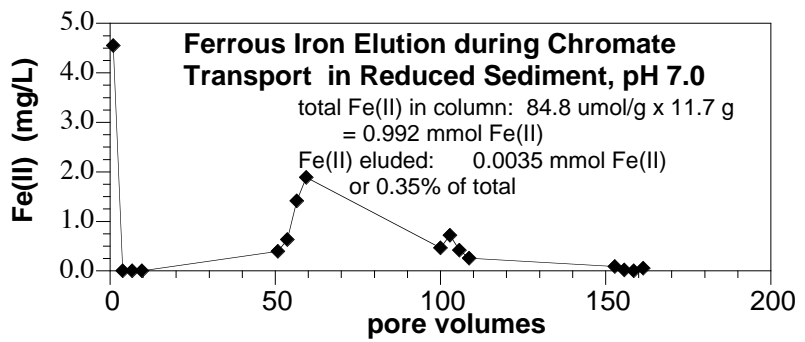
Appendix E

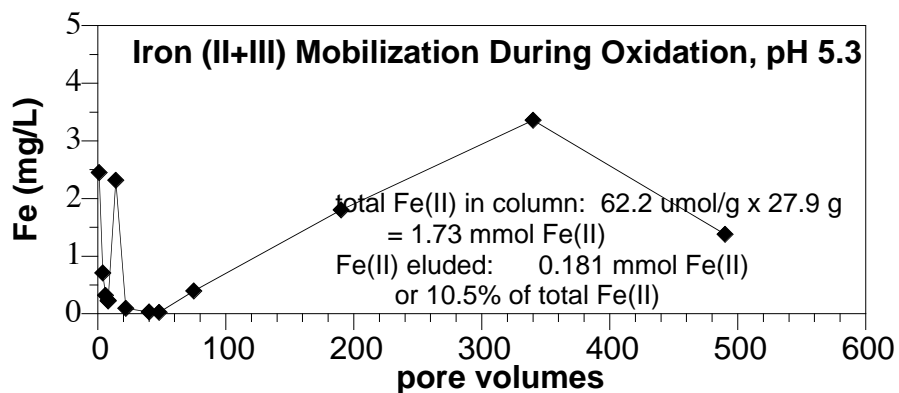
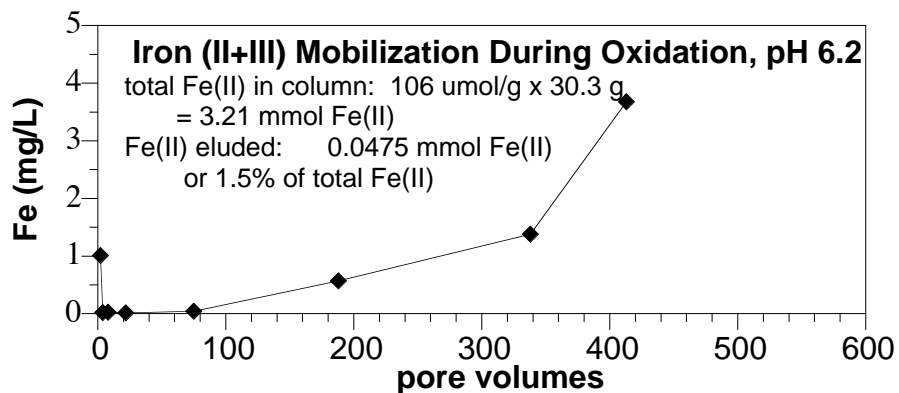
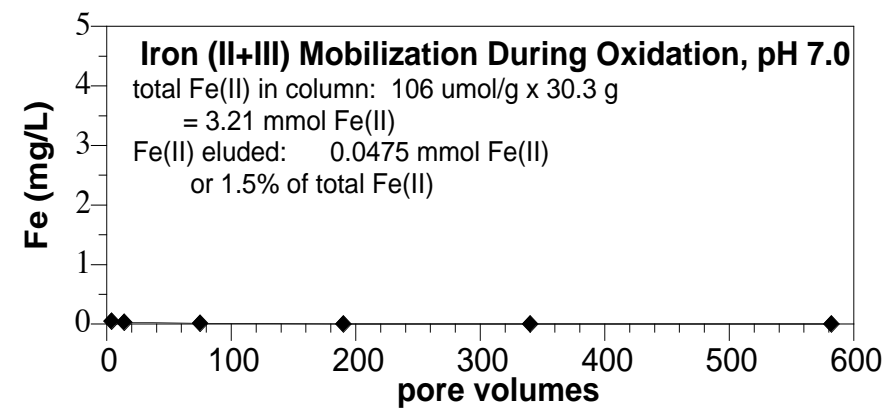
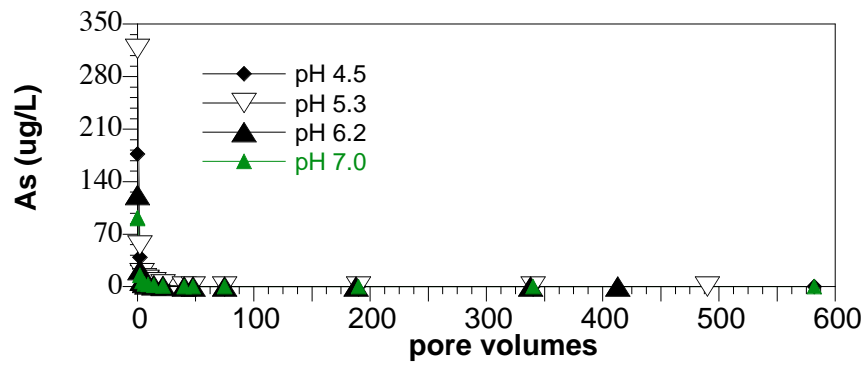
Chromate Transport and Reduction

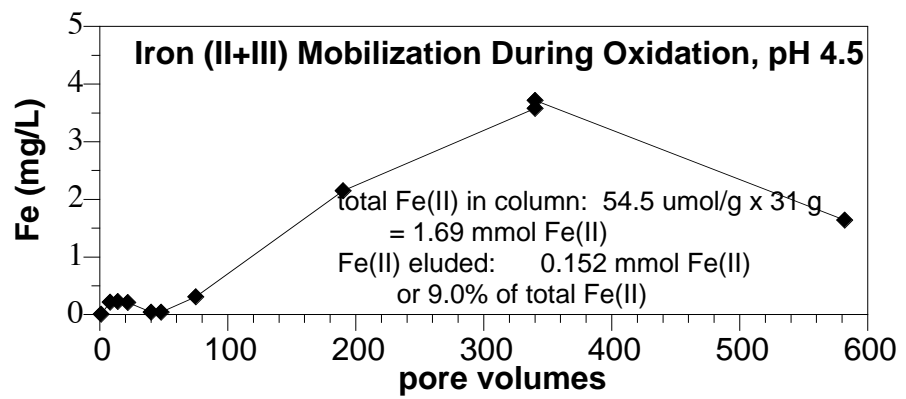


U120 Chromate Transport in Reduced Sediment at pH 4.5





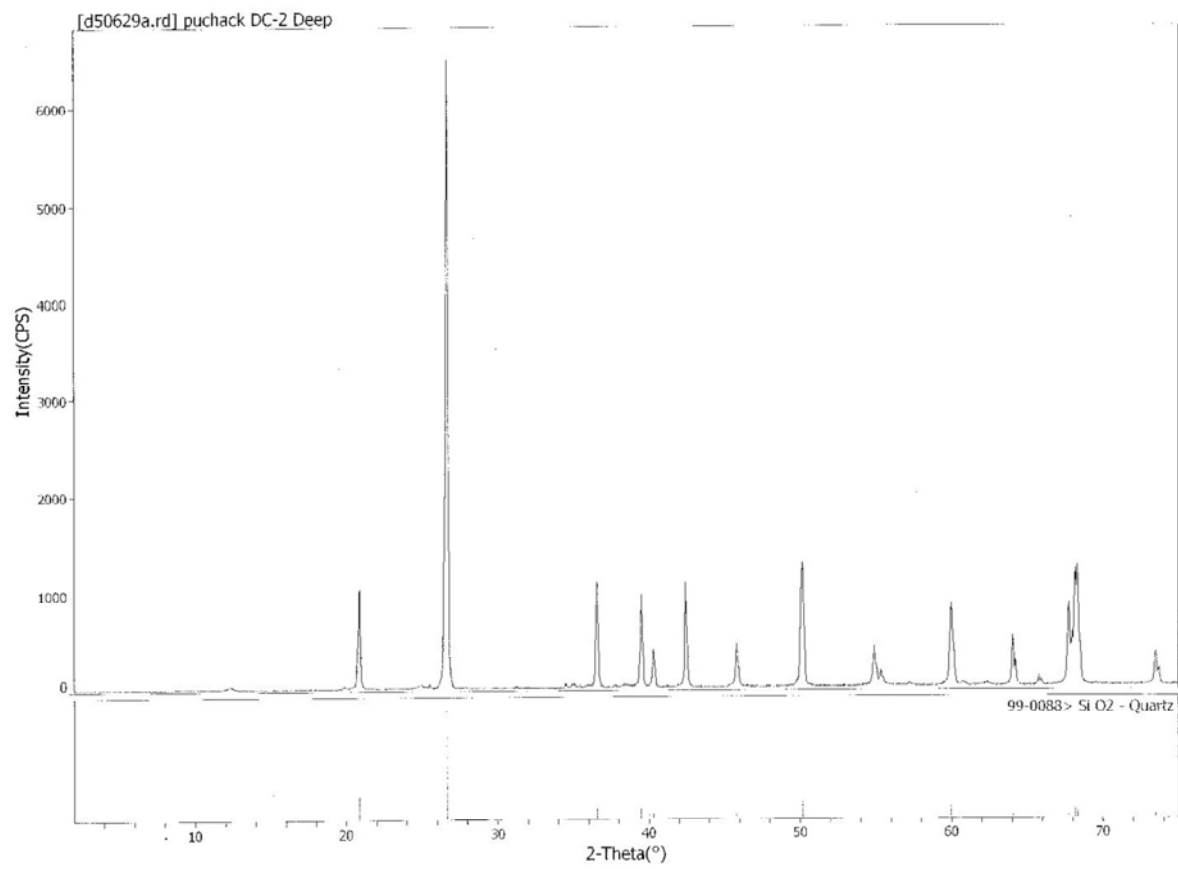


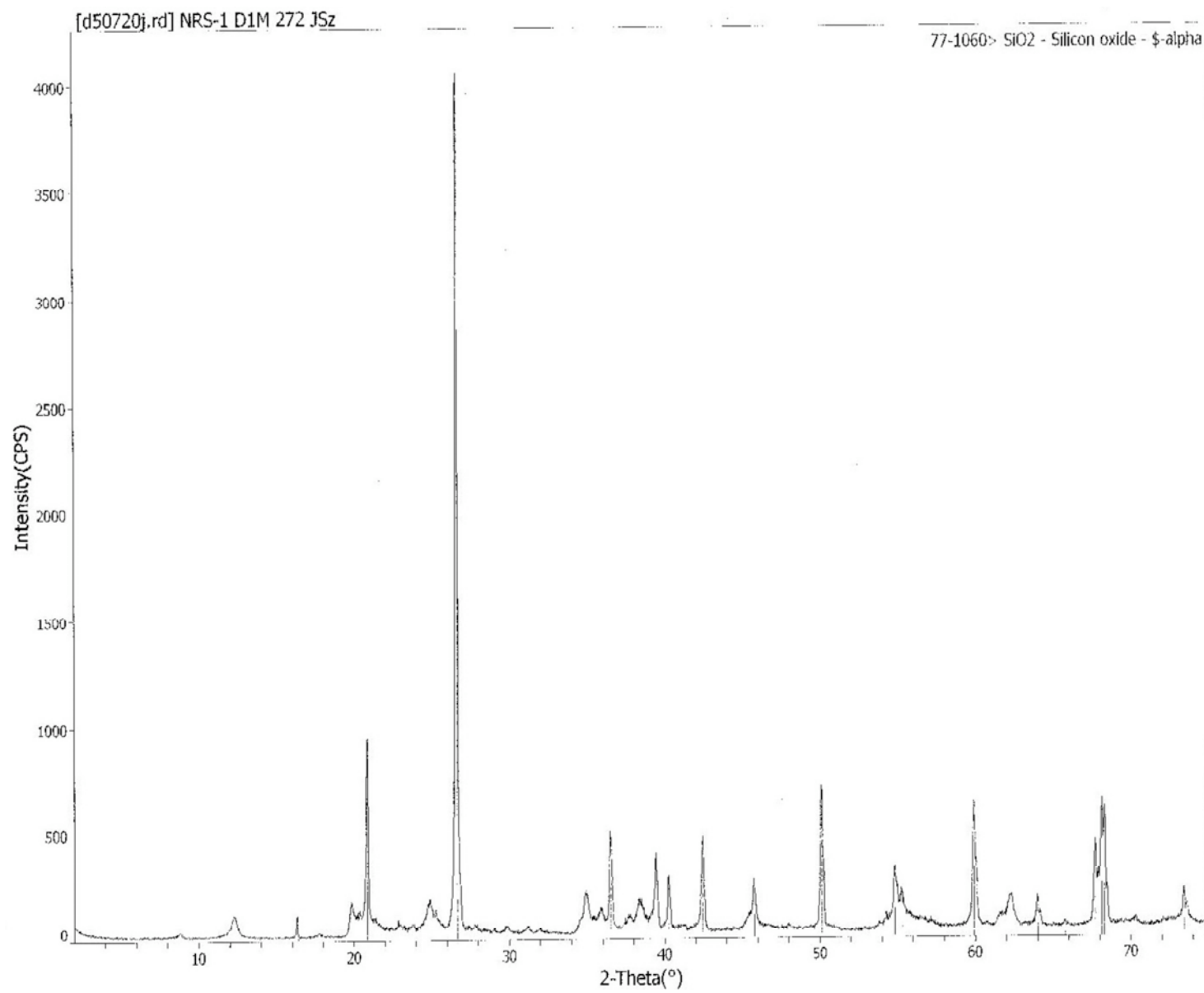


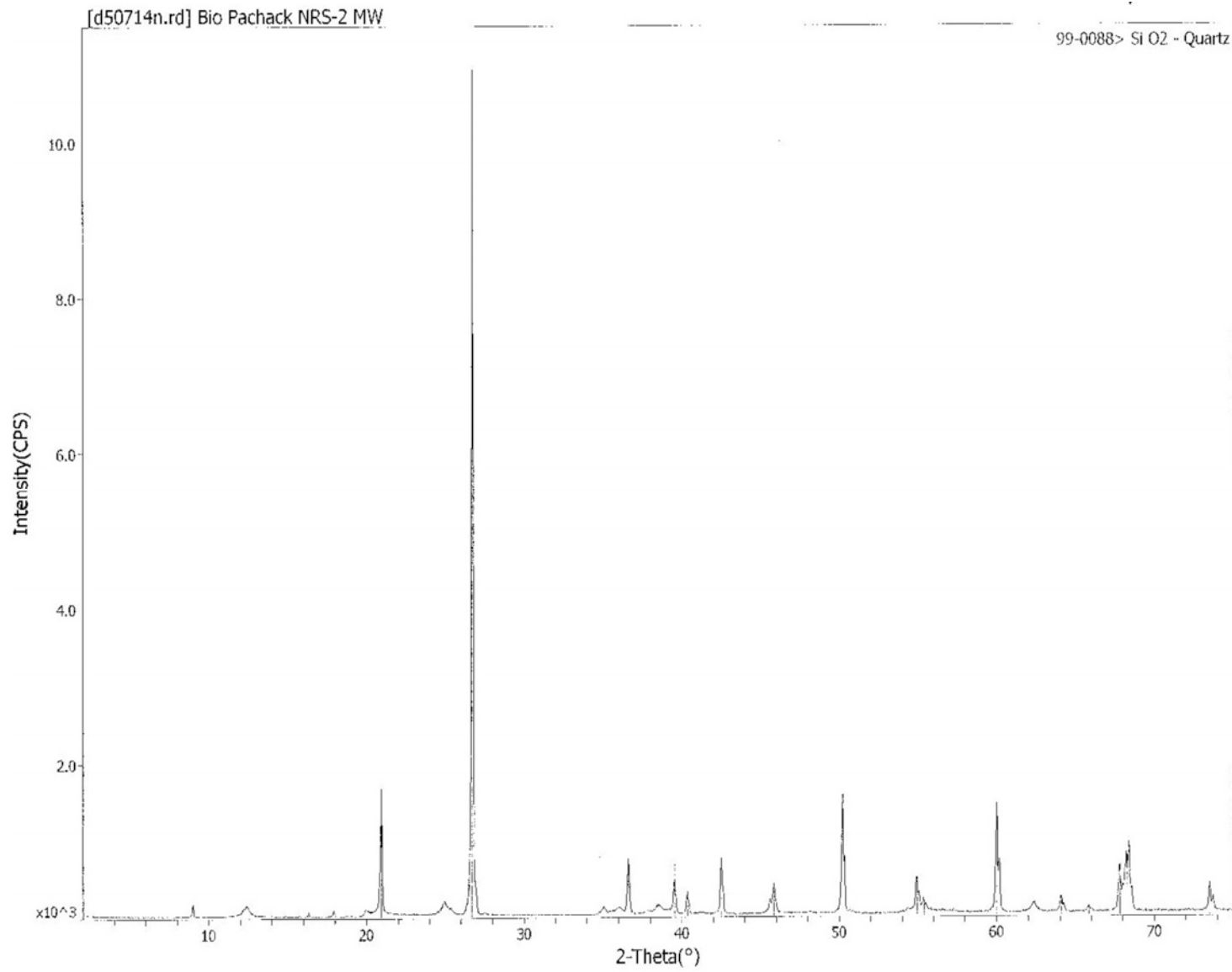
Appendix F

X-Ray Diffraction Spectra

F.I

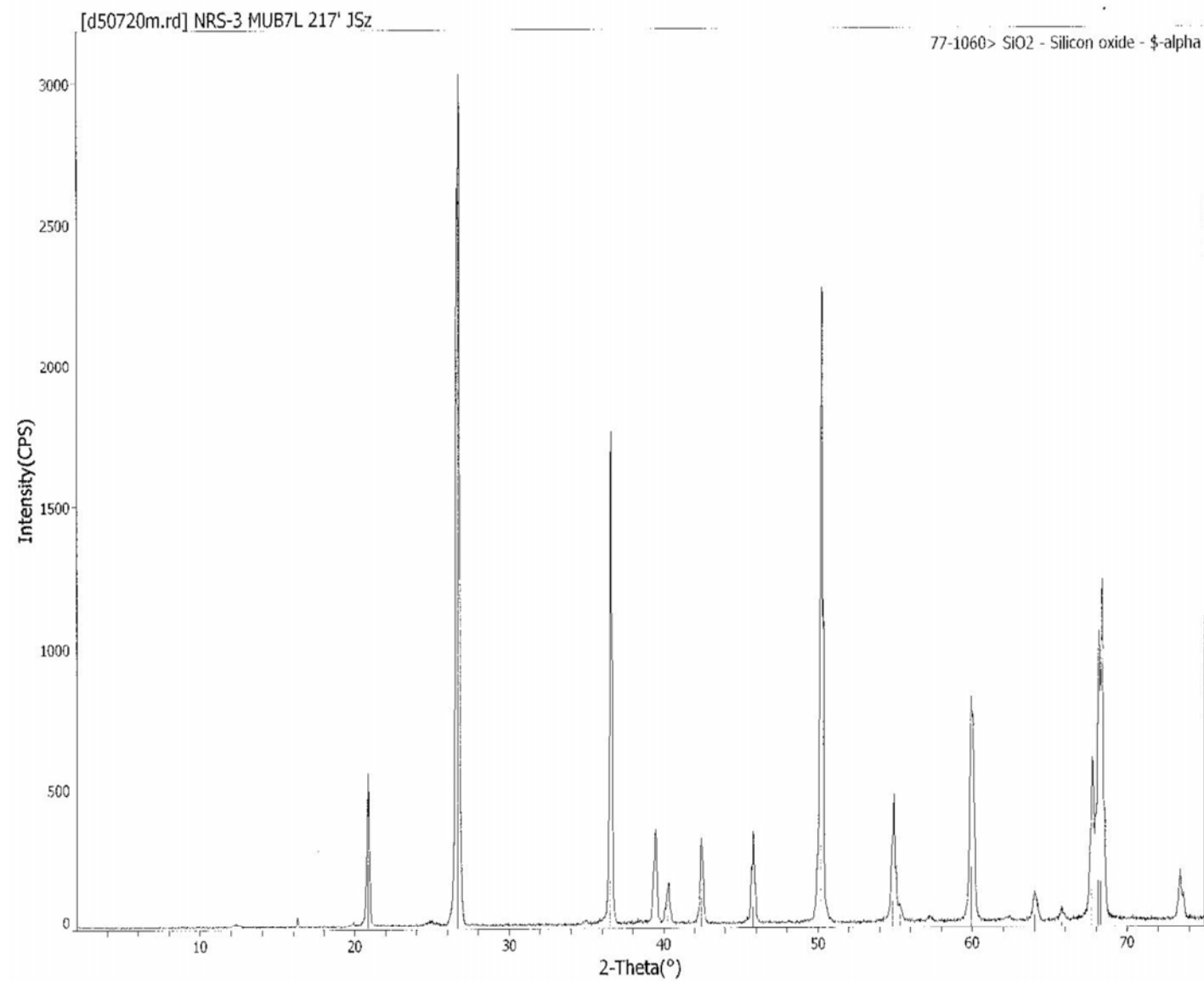






F.3

F.4



Appendix G

Growth Media for Biotic Studies

Appendix G

Growth Media for Biotic Studies

Iron Reducing Medium with 10 mM Fe(III)NTA: per liter

NaHCO ₃	2.5 g
KCl	0.1 g
NH ₄ Cl	1.5 g
NaH ₂ PO ₄	0.6 g
Yeast extract	1.0 g
*Wolfe's vitamin solution	10 ml
**Wolfe's mineral solution	10 ml
Sodium lactate	10 mM
Sodium pyruvate	10 mM
Sodium acetate	10 mM

Equilibrate medium under mixture gas of N₂/CO₂ (80:20 v/v), dispense 10 ml per Balsch tube under same gas phase, stopper with butyl rubber closures, crimp seal, and autoclave. Introduce ***Fe(III)NTA solution to autoclaved medium using anaerobic technique.

***Wolfe's vitamin solution: per liter**

Biotin	2.0 mg
Folic acid	2.0 mg
Pyridoxine HCl	10.0 mg
Thiamine HC	5.0 mg
Riboflavin	5.0 mg
Nicotinic acid	5.0 mg
Calcium D-(+)pantothenate	5.0 mg
Vitamin B12	0.1 mg
P-aminobenzoic acid	5.0 mg
Thioctic acid	5.0 mg

****Wolfe's mineral solution: per liter**

Nitrilotriacetic acid	1.5 g
MgSO ₄ .7H ₂ O	3.0 g
MnSO ₄ . H ₂ O	0.5 g
NaCl	1.0 g
FeSO ₄ .7H ₂ O	0.1 g
CoCl ₂ .6H ₂ O	0.1 g
CaCl ₂	0.1 g
ZnSO ₄ .7H ₂ O	0.1 g
CuSO ₄ .5H ₂ O	0.01 g
AlK(SO ₄) ₂ .12H ₂ O	0.01 g

H_3BO_3	0.01 g
$\text{Na}_2\text{MoO}_4 \cdot 2\text{H}_2\text{O}$	0.01 g

***Fe(III)NTA solution: for 100 mM Fe(III)NTA, dissolve 1.64 g of NaHCO_3 in ~80 ml water. Add 2.56 g trisodiumnitritotriacetic acid. Add 2.7 g $\text{FeCl}_3 \cdot 6\text{H}_2\text{O}$. Bring the solution up to 100 ml, sparge the solution with N_2 , and filter sterilize.

Sulfate Reducing Medium: per liter

KH_2PO_4	0.5 g
NH_4Cl	1.0 g
CaSO_4	1.0 g
$\text{MgSO}_4 \cdot 7\text{H}_2\text{O}$	2.0 g
Yeast extract	1.0 g
Ascorbic acid	0.1 g
Thioglycolic acid	0.1 g
$\text{FeSO}_4 \cdot 7\text{H}_2\text{O}$	0.5 g
*Vitamin solution	1.0 ml
Ethanol	10 mM
Sodium acetate	10 mM
Sodium lactate	10 mM
pH to between 7 and 7.5	

*Vitamin solution: per 100 ml

Biotin	0.002 g
Folicin	0.002 g
B6 (HCl)	0.01 g
Riboflavin	0.01 g
Thiamine (HCl)	0.01 g
Pantothenic acid	0.005 g
Nicotinamide	0.005 g
B12	0.01 g
PABA	0.005 g
Lipoic acid	0.006 g

Phosphate-Buffered-Saline: per liter

$\text{Na}_2\text{HPO}_4 \cdot 7\text{H}_2\text{O}$	2.22 g
$\text{NaH}_2\text{PO}_4 \cdot \text{H}_2\text{O}$	0.223 g
NaCl	8.5 g
pH to 7.0	

Table G.1. Puchack Sediment Cores Selected for Microbiology Studies (sorted by depth)

Station Location	Hydrogeologic Layer ^(a)	Depth, ft	PNNL ID #	Sediment Description	pH	% moisture ^(b)
MW-36S-C	C-2A1	151.5 to 152	5	Yellow clay w. light gray sand	5.6	14.5
MW-37S-A	C-2A1	153.5 to 154	1	Light gray sand	6.4	21.1
MW-36S-D	C-2A1	159 to 159.5	3	Light gray silty sand	6.8	12.4
MW-37S-G	A-3a	190 to 190.5	6	Light gray fine sand	7.1	18.3
MW-37S-H	A-3a	194 to 194.5	2	Beige clay	5.5	17.9
MW-36S-J	A-3a	201 to 201.5	7	Whitish silty fine sand	6.8	17.3
MW-37S-J	A-3a	204 to 204.5	4	Beige clay	5.4	19.3
MW-37S-K	A-3a	210.5 to 211	8	Pale white clay & small gravels	5.5	15.7

(a) C-2A1=Intermediate Sand, A-3a=Lower Aquifer, upper zone
(b) dry weight base

Table G.2. Summary of Iron-Reducing Bacteria Enumeration and Enrichment Results (sorted by depth)

			Treatment				
Sample ID	Depth, ft	PNNL ID#	1g ^(a)	10 ⁻² g to 10 ⁻⁷ g ^(b)	Positive Control: 1g+low cells ^(c)	Positive Control: 1g+med. cells ^(d)	Positive Control: 1g+high cells ^(e)
MW-36S-C C-2A1	151.5 to 152	5	+/+	not done	++/++	+/-	++/++
MW-37S-A C-2A1	153.5 to 154	1	-/-	-/-/-/-	+/+	-/++	+/+
MW-36S-D C-2A1	159 to 159.5	3	-/-	not done	+/+	+/+	+/+
MW-37S-G A-3a	190 to 190.5	6	++/++	not done	++/++	++/++	++/++
MW-37S-H A-3a	194 to 194.5	2	+/+	-/-/-/-	++/+	+/-	++/++
MW-36S-J A-3a	201 to 201.5	7	-/+	not done	+/-	++/-	++/++
MW-37S-J A-3a	204 to 204.5	4	+/+	not done	+/+	++/++	++/++
MW-37S-K A-3a	210.5 to 211	8	+/+	not done	++/++	++/+	+/+

Growth assessment: high growth: ++, medium growth: +, no growth –
(a) 1 g sediments per 10 ml IRB medium, 2 replicates, 4 weeks incubation
(b) MPN, 5 replicates per each of 5 dilutions, 2 replicates per sediments tested, 6 weeks incubation
(c) 1 g sediment plus 2E+3 cells (*G.metallireducens*) per 10 ml IRB medium, 2 replicates, 4 weeks incubation
(d) 1 g sediment plus 2E+5 cells (*G.metallireducens*) per 10 ml IRB medium, 2 replicates, 4 weeks incubation
(e) 1 g sediment plus 2E+7 cells (*G.metallireducens*) per 10 ml IRB medium, 2 replicates, 4 weeks incubation

Table G.3. Summary of Sulfate-Reducing Bacteria Enumeration and Enrichment Results (sorted by depth)

Sample ID	Depth, ft	PNNL ID#	Treatment					
			30 g ^(a)	1 g ^(b)	10 ⁻² g to 10 ⁻⁷ g ^(c)	Positive Control: 1 g+low cells ^(d)	Positive Control: 1 g+med. Cells ^(e)	Positive Control: 1 g+high cells ^(f)
MW-36S-C C-2A1	151.5 to 152	5	-	-/-	not done	+/+	+/+	+/+
MW-37S-A C-2A1	153.5 to 154	1	-	-/-	-/-/-/-	+/+	+/+	+/+
MW-36S-D C-2A1	159 to 159.5	3	-	-/-	not done	+/+	+/+	+/+
MW-37S-G A-3a	190 to 190.5	6	-	-/-	not done	+/+	+/+	+/+
MW-37S-H A-3a	194 to 194.5	2	-	-/-	-/-/-/-	+/+	+/+	+/+
MW-36S-J A-3a	201 to 201.5	7	+	-/-	not done	+/+	+/+	+/+
MW-37S-J A-3a	204 to 204.5	4	-	-/-	not done	+/+	+/+	+/+
MW-37S-K A-3a	210.5 to 211	8	-	-/-	not done	+/+	+/+	+/+
Growth assessment growth: +, no growth: -								
(a) 30 g sediments per 30 ml SRB medium, no replicates, 6 weeks incubation								
(b) 1 g sediments per 10 ml SRB medium, 2 replicates, 4 weeks incubation								
(c) MPN, 5 replicates per each of 5 dilutions, 2 replicates per sediments tested, 6 weeks incubation								
(d) 1 g sediment plus 2E+3 cells (<i>D.vulgaris</i>) per 10 ml SRB medium, 2 replicates, 4 weeks incubation								
(e) 1 g sediment plus 2E+5 cells (<i>D.vulgaris</i>) per 10 ml SRB medium, 2 replicates, 4 weeks incubation								
(f) 1 g sediment plus 2E+7 cells (<i>D.vulgaris</i>) per 10 ml SRB medium, 2 replicates, 4 weeks incubation								

Distribution

(Electronic copy unless otherwise noted.)

<u>No. of Copies</u>	<u>No. of Copies</u>	
OFFSITE		
J. Gorin (3P, 3CD)	B. J. Devary	K3-61
U.S. Environmental Protection Agency	A. E. Fischer (P)	P7-07
Region 2	J. S. Fruchter	K6-96
290 Broadway	T. J Gilmore	K6-96
New York, NY 10007-1866	D. C. Girvin	K3-61
	S-M. W. Li (P)	P7-50
	W. J. Martin	K6-81
	J. L. Phillips	K3-61
	J. E. Szecsody (2P)	K3-61
	M. J. Truex (P)	K6-96
	V. R. Vermeul (3P)	K6-96
	M. D. Williams	K6-96
	Hanford Technical Library (2P)	P8-55
ONSITE		
Pacific Northwest National Laboratory		
C. A. Brandt	K9-04	
C. A. Burns (P)	K3-61	

P = Paper copy.

CD = Compact disk.